The role of Toll-like receptor 9 and ammonia in the development of hepatic encephalopathy, brain oedema and immune dysfunction

Manakkat Vijay, Godhev Kumar

Awarding institution:
King's College London

The role of Toll-like receptor 9 and ammonia in the development of hepatic encephalopathy, brain oedema and immune dysfunction

Godhev Kumar Manakkat Vijay

Thesis submitted to the School of Medicine at King's College London for the degree of Doctor of Philosophy

Institute of Liver Studies

Division of Transplantation Immunology & Mucosal biology

King's College London School of Medicine

September 2016

Abstract

Ammonia plays a central role in the pathogenesis of cerebral oedema in paracetamol-induced acute liver failure (PALF). Infection and inflammation play an important synergistic role in its development. Toll-like receptors (TLRs) sense pathogens and induce inflammation but whether this contributes to the development of cerebral oedema in PALF remains unknown. I postulated that ammonia-induced cerebral oedema and immune dysfunction are mediated by TLR9 and aimed to determine whether this could be prevented in a hyperammonemic TLR9 knockout mouse model.

TLR9 expression on circulating neutrophils and their function in PALF was assessed. To examine the influence of PALF plasma and endogenous DNA on TLR9 expression, healthy neutrophils were incubated with PALF plasma with/without DNase. Ammonium acetate (NH_4-Ac) was injected intraperitoneally in wild type Black6 (WT-B6), $TLR9^{-/-}$ B6 mice and $TLR9^{fl/fl}$ LysCre B6 mice with TLR9 deleted from neutrophils and macrophages. The TLR9 antagonist ODN2088 was also evaluated.

Neutrophil TLR9 correlated with plasma IL-8 and ammonia concentration and increased with severity of hepatic encephalopathy and systemic inflammation. Healthy neutrophil TLR9 expression increased upon stimulation with PALF plasma which was abrogated by pre-incubation with DNase. Following NH_4-Ac stimulation, intracellular cytokine (IFN-γ, TNF-α and IL-6) production of lymphocytes and macrophages were increased in WT-B6 mice compared to controls. This was accompanied by increased brain water however in $TLR9^{-/-}$, cytokine production and brain water content were decreased. This was seen similarly in WT-B6 administered the TLR9 antagonist ODN2088 in conjunction with NH_4-Ac. $TLR9^{fl/fl}$ LysCre mice had decreased cytokine production and brain water compared to the $TLR9^{fl/fl}$ group following NH_4-Ac injection. Total DNA levels were increased in the circulation after NH_4-Ac injection.

In summary, ammonia-induced cerebral oedema and immune dysfunction are mediated through TLR9 and DNA dependent**.** The amelioration of brain oedema and lymphocyte cytokine production by ODN2088 supports exploration of TLR9 antagonism in early PALF to prevent progression to cerebral oedema.

Table of Contents

Table of Figures

List of Tables

Abbreviations

AP-1	Activator protein 1
ALF	Acute liver failure
APACHE	Acute physiology and chronic health evaluation
APC	Allophycocyanin
NH_3	Ammonia
NH_4-Ac	Ammonium acetate
NH_4Cl	Ammonium chloride
BP	Band pass
CXCR	Chemokines
CD	Cluster of differentiation
C.I.	Confidence intervals
CS&T	Cytometer setting and tracking
CBA	Cytometric bead array
DAMPs	Damage associated molecular patterns
DNA	Deoxyribo nucleic acid
DNase-I	Deoxyribonuclease-I
EU/mL	Endotoxin unit / mL
FITC	Fluorescein isothiocyanate
FACS	Fluorescence activated cell sorting
fMLP	Formyl-Methionine-Leucine-Phenylalanine

FSC-A	Forward scatter channel area
G-CSF	Granulocyte colony stimulating factor
HC	Healthy controls
HE	Hepatic encephalopathy
HB	High burst
HMGB-1	High mobility group box -1
IgG	Immunoglobulin G
IACUC	Institutional animal care and use committee
ICU	Intensive care unit
ICAM-1	Intercellular adhesion molecule - 1
IFNs	Interferons
IRF	Interferon regulatory factor
IL	Interleukin
IRAK	Interleukin 1R-associated kinase
ICH	Intracranial hypertension
JNK	Jun amino terminal kinases
KLRG-1	Killer cell lectin like receptor subfamily G 1
LAL	Limulus amoebic lysate
LPS	Lipopolysaccharide
LT	Liver transplantation
LP	Long pass

LB	Low burst
MFI	Mean fluorescence intensity
MLN	Mesenteric lymph nodes
μM	Micromolar
mM	Millimolar
MELD	Model for end-stage liver disease
MOF	Multiple organ failure
MAL	MyD88 adaptor-like
NAC	*N-Acetylcysteine*
NK	Natural killer
NKG2D	Natural killer group 2D
PB	Phagoburst
NPA	Neutrophil phagocytic activity
NMDA	N-methyl D-aspartate
NOD	Non-obese diabetic
NF-κB	Nuclear factor - κB
ODN	Oligodinucleotides
OB	Oxidative burst
PAMPs	Pathogen-associated molecular patterns
PALF	Paracetamol-induced acute liver failure
POD	Paracetamol / Acetaminophen overdose

PerCP	Peridinin chlorophyll protein
PBMC	Peripheral blood mononuclear cells
PMA	Phorbol 12-myristate 13-acetate
PAG	Phosphate–activated glutaminase
PBS	Phosphate-buffered saline
PMT	Photomultiplier tubes
PE	Phycoerythrin
PMNs	Polymorphonuclear neutrophils
PI	Propidium iodide
ROS	Reactive oxygen species
T-regs	Regulatory T cells
RT	Room temperature
RPMI	Rosewell park memorial institute
SOFA	Sequential organ failure assessment
SSC-A	Side scatter channel area
SPF	Specific pathogen-free
SOB	Spontaneous oxidative burst
SIRS	Systemic inflammatory response syndrome
T_H Cells	T helper Cells
TLR	Toll-like Receptor
TIR	Toll/interleukin-1 receptor
TRIF	TIR domain-containing adaptor-inducing IFN-β

TRAM	TRIF-related adaptor molecule
TNF	Tumour necrosis factor
TGF	Tumorogenic growth factor
UK	United Kingdom
USA	United States of America
USDA	United States department of agriculture
WBC	White blood cells
WT	Wild type

Chapter 1. Introduction

1.1. Liver

1.1.1. Anatomy and physiology of the liver

The liver is one of the largest internal organs in the human body situated on the right side of the abdominal cavity beneath the diaphragm. It weighs about 1.2 to 1.5 kg, and consists of two lobes, the right and left lobes, and is further divided into eight segments. Each segment is made up of many smaller units called lobules that comprise a central vein, liver cells (hepatocytes) separated by the sinusoids and portal tracts. The functional unit of the liver is called a hepatic acinus [Figure 1.1]. The liver receives a dual blood supply through the portal vein and hepatic artery carrying nutrient rich blood from the gut and spleen. Among the liver cells, hepatocytes constitute 80% of the population, while the remaining is made up of hepatic stellate cells (1%), endothelial cells (10%) and cells of the immune system (9%). Among the 9% of the immune cells in the liver, Kupffer cells derived from liver macrophages, form the majority and are responsible for 80% of phagocytosis in the system. They are responsible for removal of aged red cells, viruses, bacteria and endotoxin, and can produce inflammatory cytokines that are released into the systemic circulation [1] [Figure 1.2].

1.1.2. Functions of the liver

The liver is a versatile organ and plays a central role in metabolism, synthesis, biotransformation, detoxification and storage of a number of metabolites; it also has a protective function [1] [Figure 1.3]. Since most of the metabolic enzymes are present only in the liver, it plays a vital role in the metabolism of carbohydrates, amino acids and lipids [2]. Metabolism of vitamin-K, an essential factor necessary for the initiation of clotting and excretion of bilirubin, an end product of haeme catabolism, takes places in

the liver. Bilirubin mostly in its unconjugated form requires the liver enzymes for its excretion as stercobilin and urobilin in faeces and urine. An increase in the bilirubin, either conjugated or unconjugated, causes jaundice [1, 3]. Synthesis of proteins including albumin, globulin and fibrinogen and clotting factors – II, VII, IX and X involved in the coagulation cascade also takes place mainly in the liver [1]. Detoxification of certain drugs (e.g. paracetamol) and ammonia into urea and glutamine takes place mainly in the liver. Accumulation of toxic substances may lead to severe liver injury and result in acute hepatitis [1, 4]. Serum bilirubin, albumin and prothrombin time are the most commonly assessed liver function tests and they are robust measures of excretion and liver synthetic function. Abnormalities in the liver function tests may be indicative of hepatic dysfunction [5].

1.1.3. Diseases of the liver

An insult to the liver leads to abnormal liver function and results in acute liver injury or chronic liver disease. Chronic liver disease is the fifth commonest causes of death in United Kingdom (UK) and the mortality rate has increased exponentially over recent years. The three commonest causes of chronic liver disease in the UK include alcohol-related cirrhosis caused by excessive alcohol consumption, non-alcoholic fatty liver disease caused by fat deposition in the liver cells and chronic hepatitis C infection. In acute liver failure, hepatitis or inflammation of the liver occurs within 24 to 72 hours following a liver insult and is most commonly caused by toxicity resulting from drugs e.g. paracetamol or exposure to harmful substances and acute viral infection such as hepatitis B [5, 6].

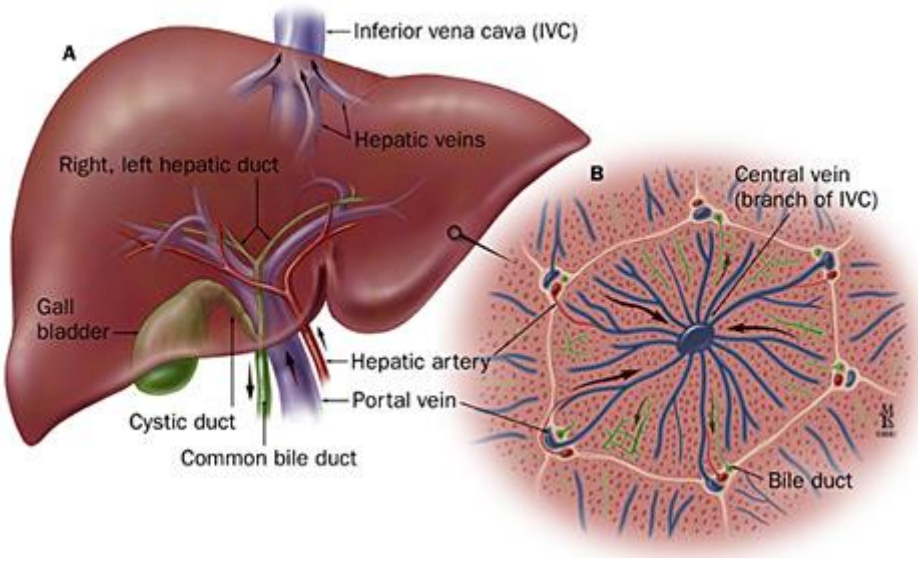

Figure 1.1: Normal anatomy of liver showing an enlarged hepatocyte [7].

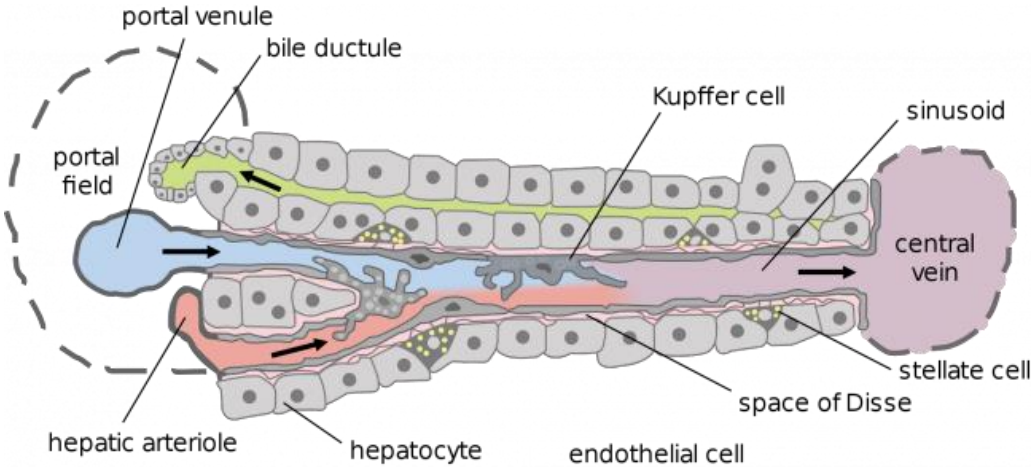

Figure 1.2: Cells present in the liver [8].

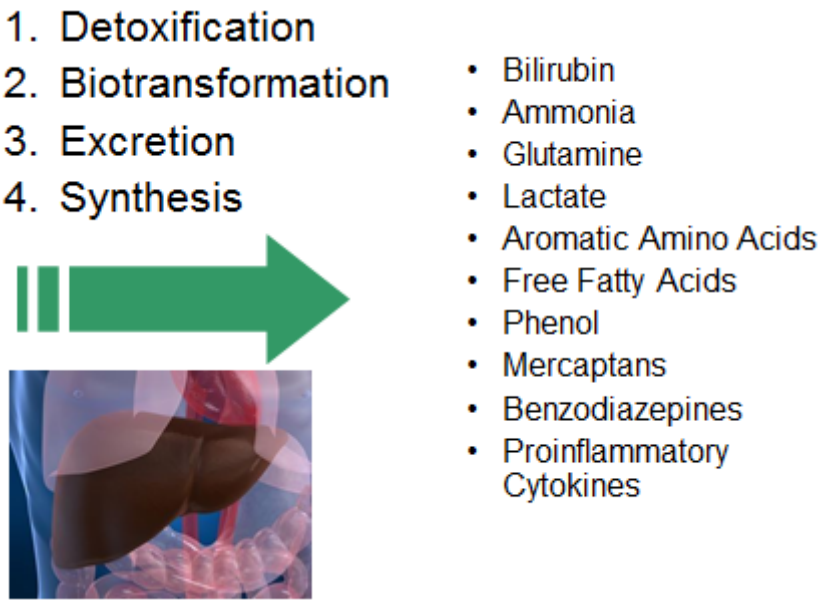

Figure 1.3: Functions of the liver [9].

1.1.3.1. Acute liver failure

Acute liver failure (ALF), or fulminant hepatic failure, as described by Trey and Davidson, is a rare but frequent consequence of severe liver injury and is defined as the onset of hepatic dysfunction with additional complications of coagulopathy and encephalopathy in a patient with no pre-existing liver disease [10]. Subsequently, O'Grady and colleagues at King's College Hospital classified ALF with the prefixes hyper- and sub-acute liver failure, based on the time to the development of encephalopathy from the onset of jaundice. Patients who develop encephalopathy within 7 days are termed as 'hyperacute', patients developing encephalopathy between 5 to 12 weeks are termed as 'subacute', while patients developing encephalopathy between 8 days and 28 days are termed as acute liver failure [Table – 1.1] [11]. ALF is very rare (1 – 6 cases per million) and its presentation is severe and heterogeneous in nature. .

1.1.3.1.1. Causes of acute liver failure

ALF is less common in developed countries compared to the developing countries where it is predominantly caused by viral infections (hepatitis A, B and E) [12]. Although less common in developed countries, ALF occurs more frequently among young adults and middle-aged people and is mainly caused by drug-induced hepatotoxicity. The mortality rate of ALF is high and is the most common cause for an emergency liver transplantation [13]. Paracetamol-induced acute liver injury is the commonest cause of ALF in the western world and culminates in the development of coagulopathy, hepatic encephalopathy (HE) and multiple organ failure (MOF) in less than 7 days. Other causes of ALF include other drug-induced liver injury e.g. ecstasy and cocaine, acute hepatitis B, Wilson's disease and seronegative hepatitis [13] [Table – 1.2].

There was a drastic increase in the number of paracetamol-induced acute liver failure (PALF) cases until a few years ago in the developed western countries, especially in the United Kingdom (UK) and United States of America (USA) but not in the developing countries [13]. In tertiary care centres across USA, approximately 40% of the ALF cases were accounted for paracetamol overdose and one-third of those cases necessitated emergency liver transplantation (LT) [14, 15]. At King's College Hospital in London, one of seven transplant centres in the UK specialising in managing ALF patients, paracetamol toxicity contributed to 57% of all the ALF cases and almost one-third of those patients died or underwent LT [16]. Paracetamol overdose was found to be commonest in people between the ages of 32 and 38, especially in women, and almost half of those cases were intentional (suicidal)[14-16]. Following the legalisation of restriction of paracetamol sales in UK, there has been a decline in the number of cases, mortality and the need for emergency LT following intentional paracetamol overdose [17-19].

1.1.3.1.1.1. Paracetamol and liver injury

Paracetamol is an efficacious analgesic and antipyretic drug, available over the counter at retail stores worldwide [20]. It is safe when paracetamol is taken in recommended doses (4G/day in adults) whilst overdose results in liver and kidney injury in all cases [14]. However it has been shown that aminotransferase levels are elevated after therapeutic doses of paracetamol [21] and factors such as fasting and alcohol have been shown to induce ALF after an unintentional overdose of paracetamol [22-24]. Paracetamol is mainly metabolised by the liver with <5% being excreted in unchanged form [4]. The majority of the paracetamol consumed is excreted through the bile or urine by conjugation of its hydroxyl group with glucuronic acid and sulphate [25]. A small portion of paracetamol is removed along with glutathione to form non-toxic cysteine and mercapturic acid. During

this process an intermediary product *N*-acetyl-*p*-benzoquinoneimine, a reactive metabolite, is formed by the activity of cytochrome P-450s 1A2, 2E1 and 3A4[26-28]. When excessive doses are consumed, more benzoquinoneimine is formed by cytochrome P-450, which depletes the hepatic glutathione stores, since other pathways of detoxification get saturated. An excessive dose of paracetamol causes depletion of protein thiols, and damages the mitochondria by increasing cellular calcium. Furthermore, it increases the formation of peroxynitrite and activates c-Jun N-terminal kinase which leads to mitochondrial permeability transition and necrosis of the liver cell [27, 29, 30] [Figure 1.4].

1.1.3.1.2. Consequences of acute liver failure

In hepatocellular necrosis, the metabolism, synthesis, detoxification and protective functions of the liver are significantly impaired. As a consequence of hepatic dysfunction there is decreased production of essential blood clotting factors causing prolonged bleeding time or prothrombin time, decreased albumin production and increased transaminase levels in the blood. Since the liver is a vital organ, ALF causes dysfunction in the extra hepatic organs too. Acute kidney injury and pancreatitis may be associated with ALF caused by paracetamol toxicity [31]. Some paracetamol overdoses are staggered or inadvertent and may not all be secondary to intentional overdose. ALF also induces cardiovascular, respiratory and adrenal dysfunction [12]. It also induces a sterile systemic inflammatory response syndrome (SIRS) within the body. It also affects the circulating leucocytes causing impaired function and immunoparesis leading to a high risk of sepsis in these patients [12, 13]. Liver dysfunction also leads to decreased ammonia detoxification resulting in hyperammonemia and this may lead to HE [Figure 1.5].

ALF patients may succumb to brain herniation due to brain oedema and intracranial hypertension [32, 33]. Cerebral oedema is mainly caused by increased water content in the brain that results in swelling. The rigid skull bone that protects the brain restricts the swelling of the brain and as a consequence a small increase in fluid can cause a significant increase in intracranial pressure or ICH which in turn leads to decreased cerebral perfusion pressure and capillary blood flow, resulting in ischaemia [34].

Table 1.1: Classification, clinical features and prognosis of the subtypes of ALF [13].

	Hyperacute	Acute	Subacute
Time from jaundice to encephalopathy	0–1 week	1–4 weeks	4–12 weeks
Severity of coagulopathy	+++	++	+
Severity of jaundice	+	++	+++
Degree of intracranial hypertension	++	++	+/–
Survival rate without emergency liver transplantation	Good	Moderate	Poor
Typical cause	Paracetamol, hepatitis A and E	Hepatitis B	Non-paracetamol drug-induced liver injury

Data from O'Grady and colleagues[12] and Ichai and Samuel.[13] +++=high severity. ++=medium severity. +=low severity. +/–=present or absent.

Table 1.2: Distribution and incidence of ALF and its aetiologies [13]

	Drug		Viral			Unknown	Other
	Paracetamol	Non-paracetamol	HAV	HBV	HEV		
Spain 1992–2000[18]	2%	17%	2%	32%	..	35%	12%
Sweden 1994–2003[19]	42%	15%	3%	4%	..	11%	25%
UK 1999–2008[20]	57%	11%	2%	5%	1%	17%	7%
Germany 1996–2005[21]	15%	14%	4%	18%	..	21%	28%
USA 1998–2001[22]	39%	13%	4%	7%	..	18%	19%
Australia 1988–2001[23]	36%	6%	4%	10%	..	34%	10%
Pakistan 2003–05[24]	0%	2%	7%	20%	60%	7%	4%
India 1989–96[25]	0%	1%	2%	15%	44%	31%	7%
Sudan 2003–04[26]	0%	8%	0%	22%	5%	38%	27%

..=not reported. HAV=hepatitis A virus. HBV=hepatitis B virus. HEV=hepatitis E virus.

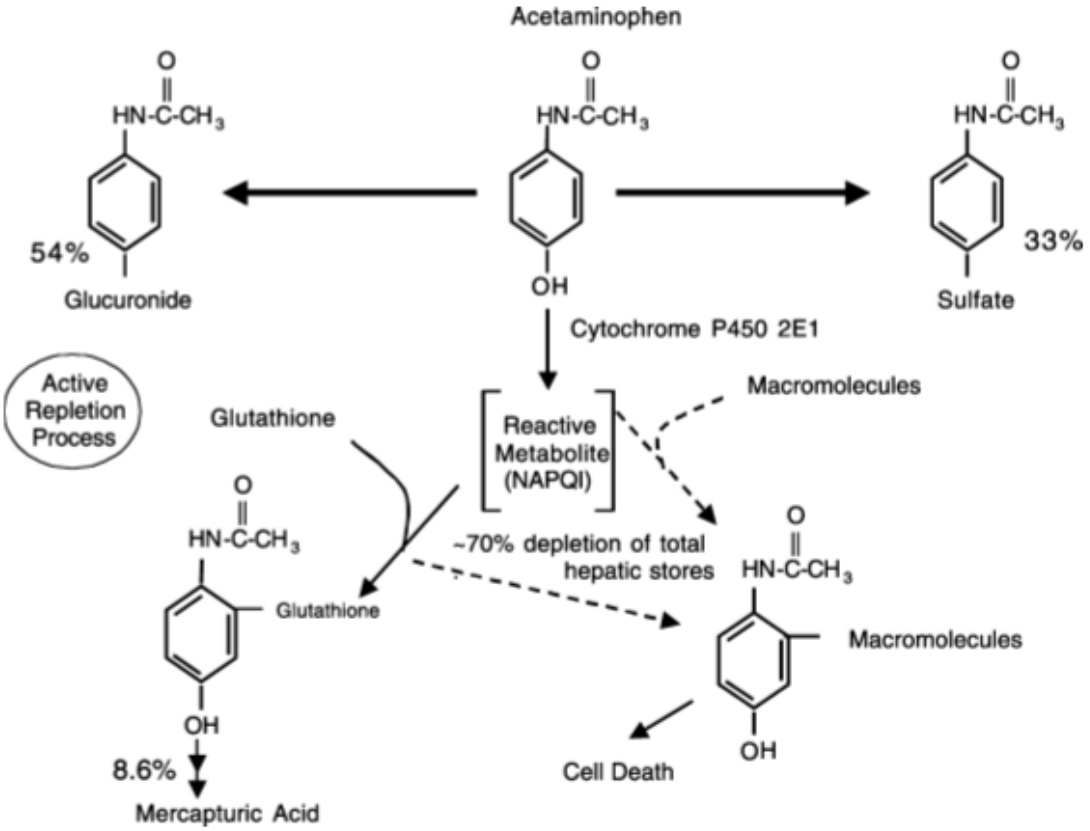

Figure 1.4: Metabolism of paracetamol.

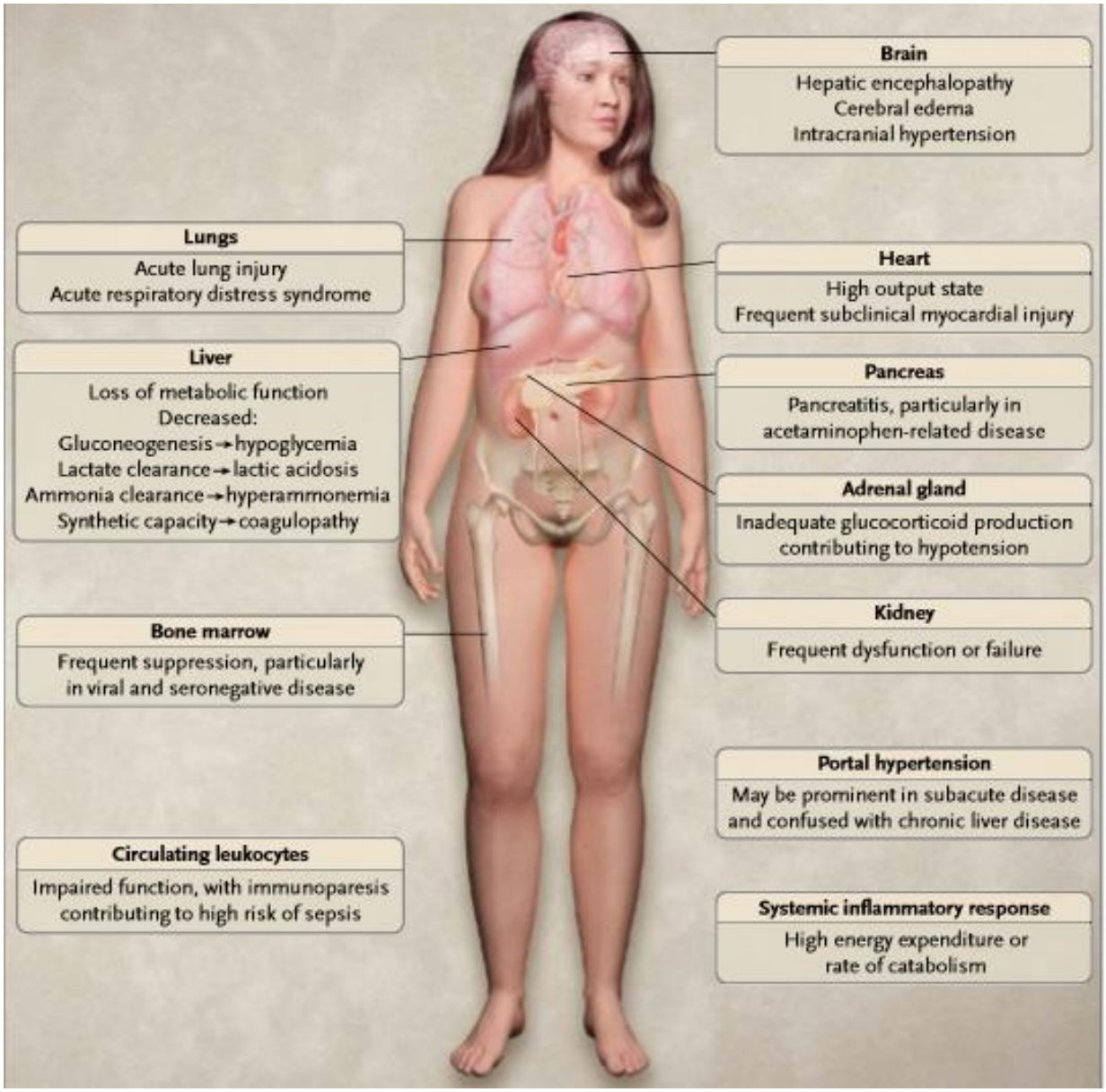

Figure 1.5: Consequences of ALF [35].

1.1.3.1.2.1. Systemic inflammatory response syndrome

Sepsis is defined as the systemic or clinical response arising from an infection. There is an increased risk of morbidity and mortality especially among immunocompromised and critically ill patients who develop sepsis. Sepsis was also reported to be the most common cause for death in non-coronary intensive care units. The term sepsis syndrome was applied to an identical clinical response, which was observed in the non-infectious state. However both these terms, sepsis and sepsis syndrome, led to confusion and a standardisation of terminology was required to eliminate the communication concerning sepsis and its sequelae, especially with the treatment. In 1991, during the American College of Chest Physicians/Society of Critical Care Medicine Consensus Conference, a set of guidelines were introduced to define these terms along with detailed physiological parameters to categorise them. The term sepsis was used to describe the clinical manifestation arising from an infection. A new term 'systemic inflammatory response syndrome (SIRS)' was used to describe the inflammatory process occurring in the absence of an infection, independent of its cause [Figure 1.6] [36].

The term SIRS is used in the presence of 2 or more of the following manifestations, namely body temperature > 38°C or < 36°C; heart rate > 90 beats per minute; tachypnea, respiratory rate > 20 breaths per minute or hyperventilation, as indicated by a $PaCO_2$ of < 32 mm Hg; and alteration in the white blood cell count, > 12000/mm3 or < 4000/mm3, or the presence of more than 10 immature neutrophils. Besides infection, a systemic inflammatory response is also caused by non-infectious pathological causes such as pancreatitis, ischaemia, multiple trauma and tissue injury, immune-mediated organ injury, and the exogenous administration of inflammatory mediators that induce cytokine production. The development of MOF is a frequent complication of SIRS and

this contributes to the mortality of those patients who get admitted to an intensive care unit (ICU) and thereby require the life-support therapy [36].

There is a marked propensity for patients with PALF to develop sepsis which may not only hasten the development of brain oedema, but may further progress to MOF and death [37]. SIRS with or without infection, contributed to the progression of HE in ALF [38]. In addition, SIRS with and without infection, worsened the severity of HE in PALF [39] thereby reducing the chances of transplantation and conferring a poor prognosis.

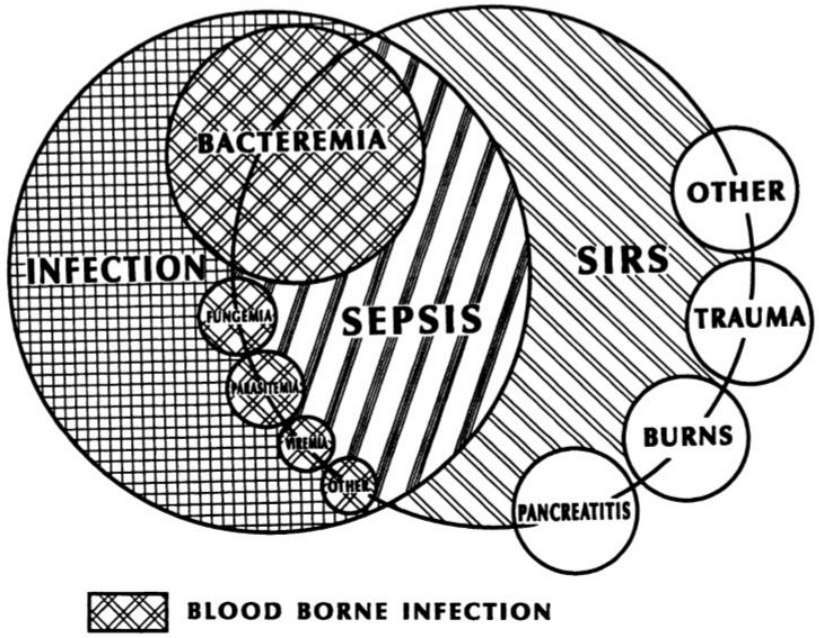

Figure 1.6: The inter-relationship between SIRS, sepsis and infection [36].

1.1.3.1.2.2. Hepatic encephalopathy

Hepatic encephalopathy (HE) is a neuropsychiatric syndrome that is mainly associated with hepatic dysfunction in both acute and chronic liver failure [40]. Symptoms of HE have quantitatively and qualitatively distinct features related to the severity of the acute liver injury. This varies from mild or moderate confusion to coma and seizures. In severe cases of ALF, HE is typically associated with the development of cerebral oedema and in hyperacute cases such as PALF, patients have the highest risk of developing cerebral oedema [41]. Based on the various neurological manifestations that occur in patients with liver disease, HE is quantitatively graded on a scale of 0 to 4 using the West Haven criteria [42] [Table 1.3].

Ammonia has been thought to play an important role in the pathogenesis of HE for the past 125 years [43-45] and when present in high concentrations, has a potential to affect the central nervous system (CNS) by modulating inhibitory and excitatory neurotransmission [46]. In patients with ALF, elevated brain ammonia levels induce swelling of astrocytes leading to cytotoxic brain oedema [47]. There was a significant increase in swelling in cultured astrocytes after they were exposed to high concentrations of ammonia [48]. Ammonia is taken up by astrocytes in the brain and converted to glutamine where it exerts an osmotic effect and induces astrocyte swelling and brain oedema [49]. Therefore it is clear that astrocytes are the main cells involved in the pathogenesis of HE as they have been found to be the cells that are most commonly affected by ammonia [Figure 1.7].

Hyperammonemia plays a definitive role in the development of HE and brain oedema, with up to 25% of patients developing intracranial hypertension (ICH) [33]. In fact arterial

ammonia was found to be at its highest level in patients with ICH [Figure 1.8] [50]. Furthermore, Clemmesen and colleagues showed that mortality was increased in those patients with arterial ammonia >150 μmol/L [Figure 1.9]. Cerebral oedema and increased intracranial pressure may be fatal without access to emergency liver transplantation (LT) [51].

Table 1.3: Clinical features of hepatic encephalopathy classified using the West Haven criteria

Grade using West Haven criteria	Clinical Features
0	No abnormality apparent on clinical examination
1	Short term memory loss, difficulty in concentrating and reverse of sleep wake cycle
2	Lethargy, apathy, confusion, drowsiness, disorientation, inappropriate behaviour
3	Stuporose but rousable, marked confusion, incoherent speech
4	Coma, unresponsive

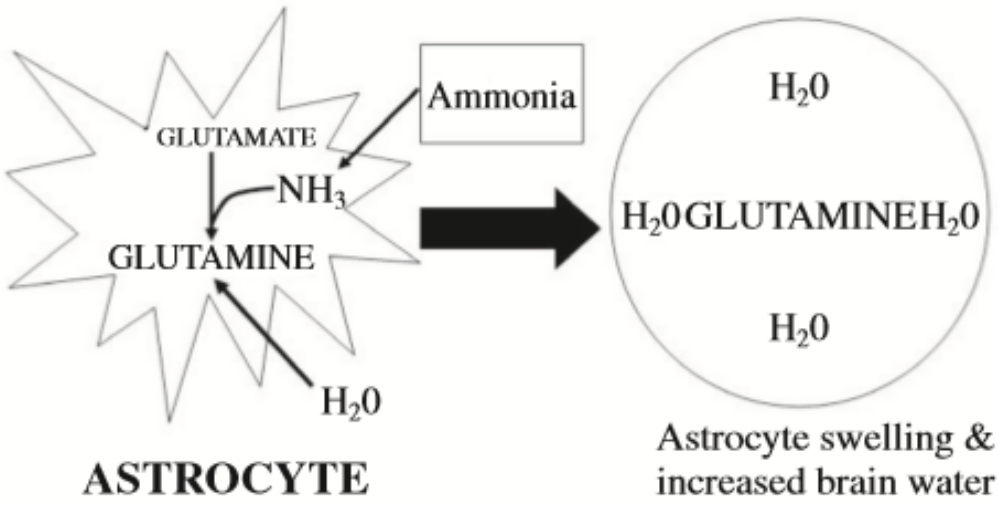

Figure 1.7: Ammonia-glutamine brain swelling hypothesis [49].

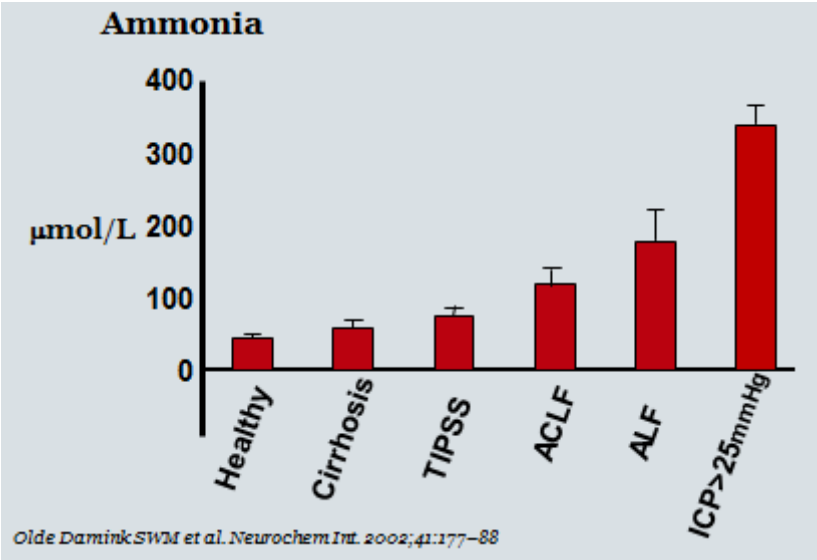

Figure 1.8: Increased arterial ammonia in ALF and patients with intracranial hypertension [50].

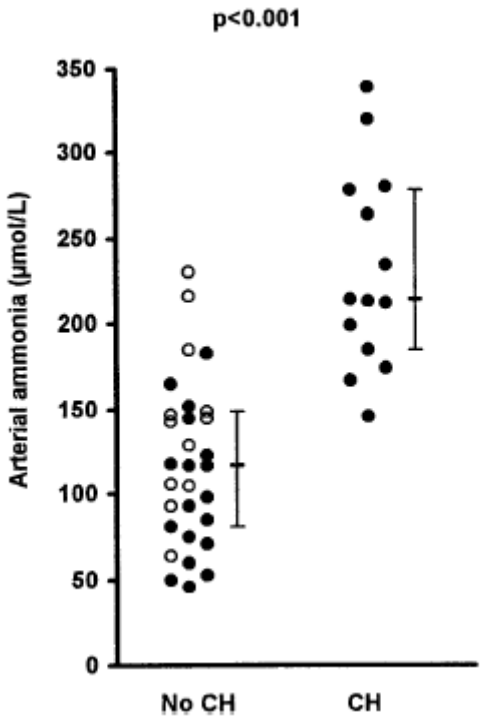

Figure 1.9: Increased arterial ammonia in ALF patients with cerebral herniation [51].

The mortality was increased in patients with cerebral herniation compared to those without cerebral herniation. The black dots are the non-survivors.

1.1.3.1.2.2.1. Ammonia and hepatic encephalopathy

The relationship between ammonia, liver and the brain was discovered in 1890's when Pavlov and his colleagues conducted experiment in dogs and showed the surgical shunting of blood from the portal vein into the vena cava caused increased ammonia in the circulation as the liver was not able to metabolise ammonia into urea [43]. They also observed that the arterial ammonia was increased fourfold and was associated with behavioural disturbances in dogs following a meat protein meal. The researchers concluded that this phenomenon could be due to ammonia following the failure of its conversion to urea in the liver [45]. The similarity between this syndrome and coma induced by hepatic failure stimulated researchers to study the toxicity of ammonia in humans. Measurement of blood and tissue ammonia has become reliable after the development of non-invasive techniques such as $^{13}NH_3$ positron emission tomography and ^{1}H magnetic resonance spectroscopy [52]. In ALF, the concentration of arterial ammonia may go up to 0.45 mM and the magnitude of this increase predicts brain herniation in these patients [51]. The brain to blood ammonia concentration ratios has been shown to be four times greater in ALF [53].

1.1.3.1.2.2.1.1. Ammonia

Ammonia is mainly produced in the gut. Dietary intake of proteins is essential as it is an important source of energy for the body [54]. Proteins are metabolised to amino acids in the liver [54, 55] and they further breakdown into ammonia following deamination [56, 57]. Ammonia is metabolised to less toxic urea so that it can be excreted in the urine. The key enzymes required for the conversion of ammonia to carbamoyl phosphate in the urea cycle is present mainly in the mitochondria of the liver [58, 59]. In paracetamol-induced acute liver injury, the mitochondrial function is impaired [60] and this affects the ammonia

metabolism and results in hyperammonemia. Ammonia is found to have a definitive role in the development of encephalopathy in liver disease [61] and very high values are observed in the patients with coma [62]. Hyperammonemia mainly causes toxicity to the brain and in the patients with acute liver injury it causes neurotransmitter inhibition and excitation [46] which impairs brain energy metabolism [63-66]. It alters the gene expression of proteins involved in brain function [67, 68] and also causes impairment in the auto regulation of cerebral blood flow [69, 70].

1.1.3.1.2.2.1.2. Ammonium salts and brain oedema

Ammonia toxicity have been studied in animals by infusing different ammonium compounds through intravenous, oral, subcutaneous and intraperitoneal routes with an assumption that their toxicities were similar and they induce brain damage. A study on different ammonium compounds shows that the toxicity of those compounds was mainly dependent on their effect on blood pH [71]. This change was related either to the effect of pH on the NH_3/NH_{4+} ratio and the ability of ammonia to cross the blood brain barrier or to a direct effect of pH on the blood brain barrier [72]. However, it has been ammonium acetate ($NH_4CH_3C0_2$) (NH_4-Ac) that has been used in large doses to induce acute ammonia toxicity [71-73]. Injection of a high dose of NH_4-Ac (7 and 12 mM/kg of bodyweight) resulted in the death of mice and rats within a short span of time by depleting the brain ATP and this was mediated through the N-methyl D-aspartate (NMDA) receptors and glutamate binding sites [73, 74]. Acute ammonia toxicity decreased the antioxidants and increased the production of superoxide radicals in liver and brain mitochondria thereby inducing oxidative stress in these animals [75], but by inhibiting the NMDA receptors it was possible to prevent oxidative stress in the brain [76].

1.1.3.1.2.2.1.3. Alternative sources of ammonia

The other alternative source of ammonia is mainly from the intestines. In the colon, bacterial urease produce ammonia by splitting urea and other amino acids [Figure 1.10] [77], while in germ-free mice phosphate–activated glutaminase (PAG) present in the enterocytes breaks down glutamine to produce ammonia [Figure 1.11] [78]. The ammonia produced in the intestine contributes to hyperammonemia-associated neurotoxicity in chronic liver disease or inborn errors of metabolism [79, 80]. Engineering the gut microbes by depleting the pre-existing microbiota and inoculation of altered Schaedler flora, a consortium of bacteria with minimal urease gene content decreased the urease activity in murine models. Transplantation of altered Schaedlar flora decreased the morbidity and mortality in a murine model of hepatic injury [81]. However, in portacaval shunted rats it has been demonstrated that intestinal glutamine uptake does not influence the arterial ammonia concentration [82]. Furthermore, it has been demonstrated that renal glutaminase plays an important role in the excretion of ammonium ions in the urine. In chronic and acute hyperammonemic models there is a mild to marked depletion of renal glutamine uptake which impacts on the net renal ammonia disposal and indicates that glutamine in the kidneys plays an important role in the excretion of ammonia [83].

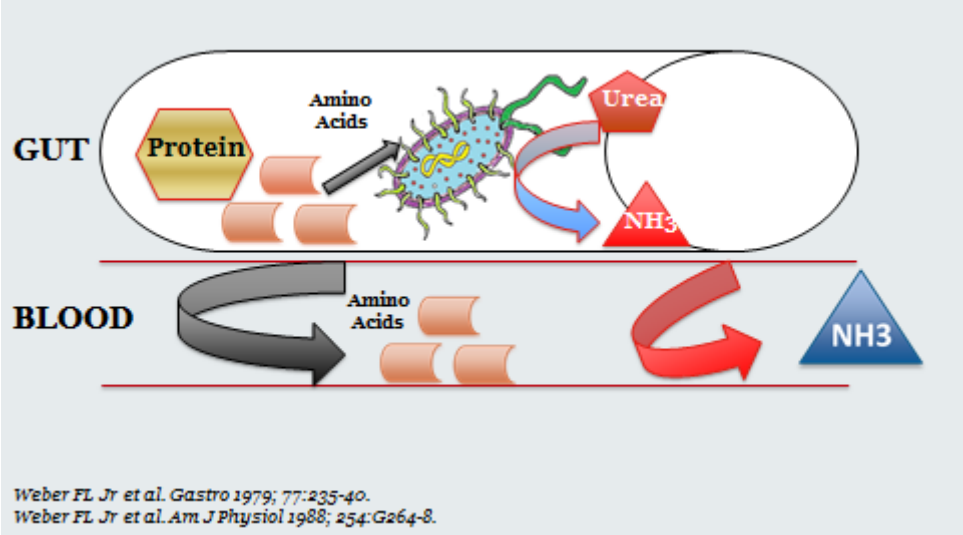

Figure 1.10: Production of ammonia in the colon by bacteria.

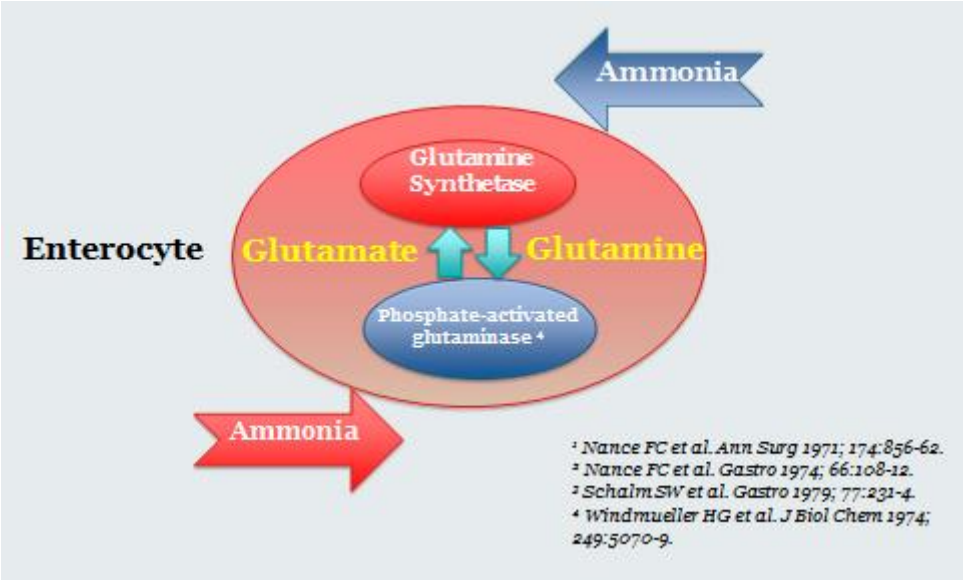

Figure 1.11: Production of ammonia in the enterocytes in germ-free mice by phosphate activated glutaminase.

1.1.3.1.2.2.2. Astrocytes and hepatic encephalopathy

Astrocytes are part of the CNS that also consists of vascular endothelial cells, pericytes and neurons [84]. Astrocytes are star-shaped cells in the brain present in the gray matter and approximately one-third of the brain volume is made up of these cells. They secrete cytokines and neurotrophic factors which activate the neurons and also have many biochemical, neurochemical and regulatory roles [85]. Astrocytes along with endothelial cells help in the formation of the blood brain barrier and astrocyte swelling, a feature of advanced HE in ALF, also affects the function of the blood brain barrier. Astrocyte swelling is the most prominent neuropathological finding in the brain autopsies of ALF patients and animal models of cerebral oedema [Figure 1.12] [47].

Impairment in the astrocyte function can be detrimental to the CNS as it leads to neuronal excitability and dysfunction. Although astrocyte swelling has been associated with increased cerebral blood flow, hyperthermia, by products from the necrotic liver, sepsis, pro-inflammatory cytokines, glutamate and vaso paralysis, the precise mechanism by which the swelling occurs still remains to be determined. Therefore it is assumed that all these factors synergistically induce cytotoxic cell swelling with ammonia playing a central role [85].

In contrast to the concepts regarding the neurotoxic effects of ammonia, it has been recently demonstrated that the neurotoxic effects of ammonia are mainly dependent on the dysfunction of glial and neuronal cells rather than the astrocyte swelling per se. Ammonia impairs astrocyte potassium buffering and the increased extracellular potassium concentration is sufficient to induce neurological dysfunction and seizures in animals. Ammonia along with potassium then promotes the over activation of Na+-K+-

2Cl− cotransporter isoform 1 (NKCC1) in neurones that plays an important role in inhibition of neurotransmission in the cortex [86].

Cerebral oedema is often seen in patients with ALF, and can lead to increased intracranial pressure, brain herniation and death. The exact processes involved are not well defined, but it is a widely held opinion that a cytotoxic process due to the effects of ammonia plays a significant part [87]. At the cellular level, neurones exposed to very high levels of ammonia quickly show extensive degeneration and undergo increased rates of apoptosis and necrosis.

Astrocytes swell in the presence of high ammonia. This is traditionally ascribed to cell hypertonicity from an increase in cellular glutamine. This swelling may contribute to the intracranial hypertension seen in ALF. Arterial ammonia concentrations in ALF have been shown to correlate with the severity of cerebral herniation and death and with severe grades of HE [51]. Patients with ALF who have not progressed to grade 3/4 HE are unlikely to progress to develop intracranial hypertension [33, 87].

In patients with ALF, hyperammonemia increases the glutamine concentration in astrocytes which then produces osmotic stress and astrocyte swelling leading to the development of HE. This is caused by increased synthesis of glutamine and decreased clearance of glutamine from the astrocyte as a result of impaired transport [88, 89]. The ability of the astrocytes to maintain osmotic equilibrium is caused by losing osmolytes such as myo-inositol in response to the increased glutamine, which then decreases the cell volume [90]. However in cirrhotic patients, the buffering capacity of the brain mainly depends on the relative concentrations of myo-inositol and glutamine/glutamate ratio. The decreased concentrations of myo-inositol in cirrhotic patients helps maintain the

cellular osmotic equilibrium in cirrhotic patients caused by increased glutamine [91-93] thereby preventing the osmotic stress and astrocyte swelling.

The ability of the astrocytes to maintain osmotic equilibrium is caused by losing osmolytes such as myo-inositol in response to the increased glutamine, which then decreases the cell volume [90].In patients with chronic liver disease, the buffering capacity of the brain mainly depends on the relative concentrations of myo-inositol and glutamine/glutamate ratio. The decreased concentrations of myo-inositol in patients with cirrhosis helps maintain the cellular osmotic equilibrium caused by increased glutamine [91-93] thereby preventing the osmotic stress and astrocyte swelling. However in ALF, the rapid rise and accumulation of ammonia in the astrocyte overcomes any compensatory buffering mechanism and cerebral oedema is often inevitable.

Taurine is an important amino acid mainly produced in the liver and transported to other organs such as the brain. Taurine mainly stored in the astrocyte plays an important role in the homeostasis of potassium and calcium in the CNS and is also involved in the excitability of neurons. Decreased concentrations of taurine have been reported in ALF and chronic liver disease suggesting that modification of brain taurine concentration could play an important role in the pathogenesis of neurological symptoms that characterise HE [94]. The concentrations of other amino acids are also important as they may influence the outcome of HE in patients with ALF and cirrhosis. In cirrhosis, the concentration of some essential amino acids such as tryptophan, methionine, phenylalanine and non-essential amino acids such as aspartate, glutamate and tyrosine are increased. In ALF, the concentrations of both essential and non-essential amino acids, except for the branched amino acids are markedly increased in the brain and cerebrospinal fluid after hepatic necrosis. Furthermore, the brain to

plasma ratio of the amino acids in patients is similar to those of normal subjects suggesting that the plasma concentration dictates the brain concentration [95, 96]. This indicates the importance of the rate of change of ammonia and the associated astrocyte swelling.

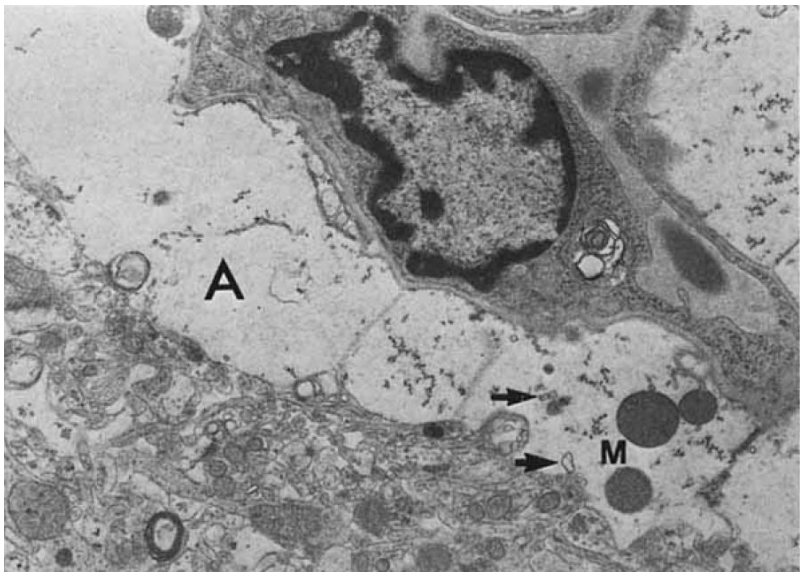

Figure 1.12: Astrocyte swelling in the brain tissue of a patient with PALF [70].

1.1.3.1.2.2.3. Systemic inflammation and hepatic encephalopathy

Although it is very well known that ammonia plays a central role in the development of HE and astrocytes are the key cells involved in this process, there is additional information that inflammation plays a central role in the pathogenesis of HE. Activated microglial cells and astrocytes produce tumour necrosis factor α (TNF-α), a cytokine produced in response to brain injury or inflammation. TNF-α induces the production of cytokines such as interleukin (IL)-1 and IL-6, and they both have the potential to compromise the integrity of blood brain barrier [97-99]. Microglia are bone marrow derived, CNS-resident macrophages that upon activation perform like antigen presenting cells and have proinflammatory effector functions [100]. Brain lactate concentration usually increased following hyperammonemia is solely responsible for the activation of microglial and astroglial cells which in turn produce cytokines such as TNF-α, IL-1β and IL-6. Furthermore, the increased cytokine production in microglial-enriched cultures rather than astroglial-enriched cultures suggest that microglia play an important role in the pathological consequences of hyperammonemia [101].

During infection and inflammation, the peripheral immune system sends signals to the brain to elicit a response. This response involves the expression of pro-inflammatory cytokines such as TNF-α, IL-1β and IL-6, both in circulation and the brain. Cytokines gain a direct entry into the brain by crossing the blood brain barrier through a storable transport mechanism. In patients dying with septic shock, there was apoptosis of neuronal and glial cells within the brain autonomic centres, strongly associated with the iNOS expression in endothelial cells which in turn altered cellular osmotic homeostasis. Cytokines such as TNF-α and IL-6 increase fluid phase permeability and ammonia diffusion in brain endothelial cells which have receptors for TNF-α and IL-1β. Astrocytes

treated with lipopolysaccharide (LPS), ammonia or glutamine separately resulted in the production of free radicals such as nitric oxide and increase in the reactive oxygen species (ROS). In a pig model of ALF, LPS and amatoxin induced more intracranial hypertension than animals given amatoxin alone [49]. Treatment with albumin dialysis reduced the severity of HE in pigs induced with ALF by reducing oxidative stress and restoring nitrogen metabolism [102]. Glutamine synthetase, an enzyme found mainly in the astrocytes, converts ammonia and glutamate into glutamine. Increased glutamine in the brain exerts an osmotic effect, which leads the astrocytes to take in water and cause swelling. Mitochondrial phosphate-activated glutaminase metabolises the glutamine and releases ammonia within mitochondria, which increases the reactive oxygen species [49]. These observations support the role of inflammation in the pathogenesis of HE.

Systemic inflammation contributes to the development of HE in ALF, indicating a possible link between inflammation and HE [38]. Infection and/or the resulting SIRS were shown to be an important factor in the development of HE in patients with PALF [37]. Furthermore, the brain produces pro-inflammatory cytokines such as TNF-α, IL-1β and IL-6 in the advanced stages of HE in ALF [103].

1.1.3.1.3. Management and socio-economic burden of acute liver failure

Intravenous administration of *N-Acetylcysteine* (NAC) is the most common treatment and initial care available for patients with paracetamol-induced hepatotoxicity and is highly efficacious when administered within the first 24 hours [14-16]. NAC has complex antioxidant and immunologic effects that may also benefit other causes of ALF. However an excessive dose of paracetamol, and/or a delay or failure to give NAC therapy increases the risk of MOF developing and culminates in high mortality with the need for emergency LT [104, 105]. A condition specific care is given to ALF patients based on the various organ(s) that fail to function [Table – 1.4].

Following hepatocyte death, necrotic by products such as DNA, ammonia and chemokines are released into the circulation, thereby activating the innate immunity and amplifying the liver injury [106-108]. The SIRS plays an important role in the development of MOF in patients with PALF, thereby increasing the progression to encephalopathy and mortality and prevents them being listed for LT [38]. Therefore in an attempt to remove the necrotic products from circulation, plasma replacement by fresh frozen plasma was considered as an option of treatment. High volume plasma exchange performed in ALF patients as part of a clinical trial reduced the mortality, thereby increasing the transplant free survival in those patients [109]. Necrotic by products such as ammonia, DNA, the neutrophil associated chemokine IL-8 and other pro-inflammatory cytokine released by monocytes were decreased after plasma replacement therapy [109, 110].

Clinical and experimental studies show that hypothermia is beneficial in the treatment of uncontrolled increase of intracranial pressure. Mild hypothermia (33°C – 35°C)

reduced ammonia-induced brain swelling in rats and decreased the toxicity in mice [111, 112], whilst moderate hypothermia (32°C – 33°C) reduced arterial ammonia and cerebral uptake of ammonia thereby decreasing cerebral blood flow in ALF patients [113]. Mild hypothermia improved survival and attenuated liver injury by reducing hepatic congestion in a paracetamol-induced mouse model [114]. In ALF patients, moderate hypothermia restored cerebrovascular autoregulation and vasodilatory response to carbon dioxide [115] and also prevented the cerebral hyperemia in LT [116]. However in a recently concluded multicentre randomized controlled trial, it has been shown that this process is not beneficial, as re-warming has been detrimental to the patients and they cannot be cooled for longer periods [117].

Hospitalisation of these cases causes a huge burden on the economy of the nation's health care system and many cases in the western world are listed for a LT. Although administration of NAC helps to prevent ALF when treated early, there has not been any drug shown to prevent the development of MOF once ALF is established.

Table 1.4: Common management issues and condition-specific elements of care in ALF [13]

Organ System and Common Conditions	Assessment	Specific Elements of Care
Cardiovascular system		
Hypotension	Invasive monitoring for all conditions; echocardiography for low cardiac output and right ventricular failure	
Intravascular volume depletion		Correction of volume depletion
Vasodilatation		Vasopressors
Low cardiac output and right ventricular failure		Inotropic support
Hepatic system		
Evolving hepatic dysfunction	Serial biochemical and coagulation testing	Intravenous acetylcysteine
Respiratory system		
Risk of aspiration pneumonitis	Neurologic observation to monitor level of consciousness	Early tracheal intubation for depressed level of consciousness
Metabolic and renal systems		
Hypoglycemia	Serial biochemical testing	Maintain normoglycemia
Hyponatremia		Active fluid management
Renal dysfunction, lactic acidosis, hyperammonemia		Renal-replacement therapy
Impaired drug metabolism		Review drug administration
Central nervous system		
Progressive encephalopathy	Neurologic observation; monitoring of serum ammonia level; transcranial ultrasonography; consideration of intracranial-pressure monitoring	Treatment of fever and hyponatremia; screening for sepsis High-grade encephalopathy: endotracheal intubation; avoidance of $Paco_2$ of <30 mm Hg or >45 mm Hg; target for serum sodium, 145–150 mmol/liter; risk assessment for intracranial hypertension
Intracranial hypertension		Interventions for pressure surges: osmotherapy (mannitol, hypertonic saline); temperature control; rescue therapies (indomethacin, thiopentone)
Hematologic system		
Coagulopathy	Laboratory coagulation testing	No routine correction of coagulation abnormalities, only for invasive procedures (including platelets and fibrinogen)
Immunologic system		
High risk of sepsis	Clinical evaluation	Antibiotic prophylaxis

1.2. Immunity

In humans and vertebrates, the immune system plays an important role in fighting against infection. To protect the host against any infection, the immune system first detects the presence of an infection and this task is carried out by the white blood cells of the innate immune system. The immune system then contains the infection and eliminates any unwanted microorganisms from the body wherever possible [118]. The immune system also has the ability to memorise the antigens it has previously encountered and activate the immune system quickly in cases of re-infection and this is undertaken by the white blood cells of the adaptive immune system [118, 119]. The immune system consists of two different parts, an early and non-specific innate immunity that takes just a few hours to develop, and a delayed and specific adaptive immunity that takes days rather than hours to develop. The innate and adaptive immune responses depend on the activities of the white blood cells [118] [Figure 1.13].

1.2.1. Innate immunity

Host innate immunity, an immediate and non-specific mechanism, mainly contributes in the initial protection during an infection against all microbes that invade the body. It is an intermediary system that allows the host to develop its specific adaptive immunity. When a microorganism invades the body, it gets detected by certain host receptors that trigger the innate immune system. This results in the activation of other cell types which leads to the release or synthesis of various factors known as 'acute-phase reactants'. The acute-phase reactants are factors that initiate phagocytosis and microbial killing, and are produced mainly in the liver [120]. There are many different types of cells and proteins that are involved in the innate immune system including the phagocytic cells such as

neutrophils, monocytes and macrophages; inflammatory cells such as eosinophils, basophils and mast cells; natural killer (NK) cells; complementary proteins; acute phase proteins and cytokines [121] [122].

1.2.2. Adaptive immunity

Adaptive immunity, a delayed response from the host, involves mainly B and T lymphocytes, which constitute 30 to 40% of the white blood cells and contain unique receptors which are specific in the recognition of pathogens. The important event in adaptive immunity is recognition of pathogens (antigens) by antigen specific cell-surface receptors present on B and T lymphocytes. The lymphocytes also have the ability to memorise the antigens it has previously encountered and activate the immune system quickly in cases of re-infection [119].

1.2.3. Cytokines

Cytokines are soluble proteins that are important in cell signaling and modulate the immune system. They include interferons (IFNs), interleukins (ILs), chemokines (CXCR), tumour necrosis factors (TNF) and colony stimulating factors. They are produced by white blood cells such as neutrophils, lymphocytes, NK cells, macrophages, and other cells such as endothelial cells and fibroblasts. Some cytokines are produced predominantly by helper T cells and macrophages and are secreted by more than one type of cell [123]. Cytokines are classified as either pro-inflammatory or anti-inflammatory, based on their role in inflammation. Pro-inflammatory cytokines promote systemic inflammation and excessive production causes detrimental effects on the body [124] whereas anti-inflammatory cytokines promote healing and reduce inflammation. [125]

Thus a balance between these two classes are required or an imbalance could lead to disease [123].

1.2.4. Inflammasomes

Inflammasomes are receptors expressed mainly in myeloid cells and part of the innate immune system. They are multimeric complexes that assemble in the cytosol after sensing the pathogen-associated molecular patterns (PAMPs) or damage-associated molecular patterns (DAMPs) and leads to the downstream signalling of cytokines. Upon activation, the relevant NOD-like receptors form a caspase-1-activating scaffold which then subsequently cleaves the pro-IL-1β and pro-IL-18 into their active forms and cause inflammatory cell death [126].

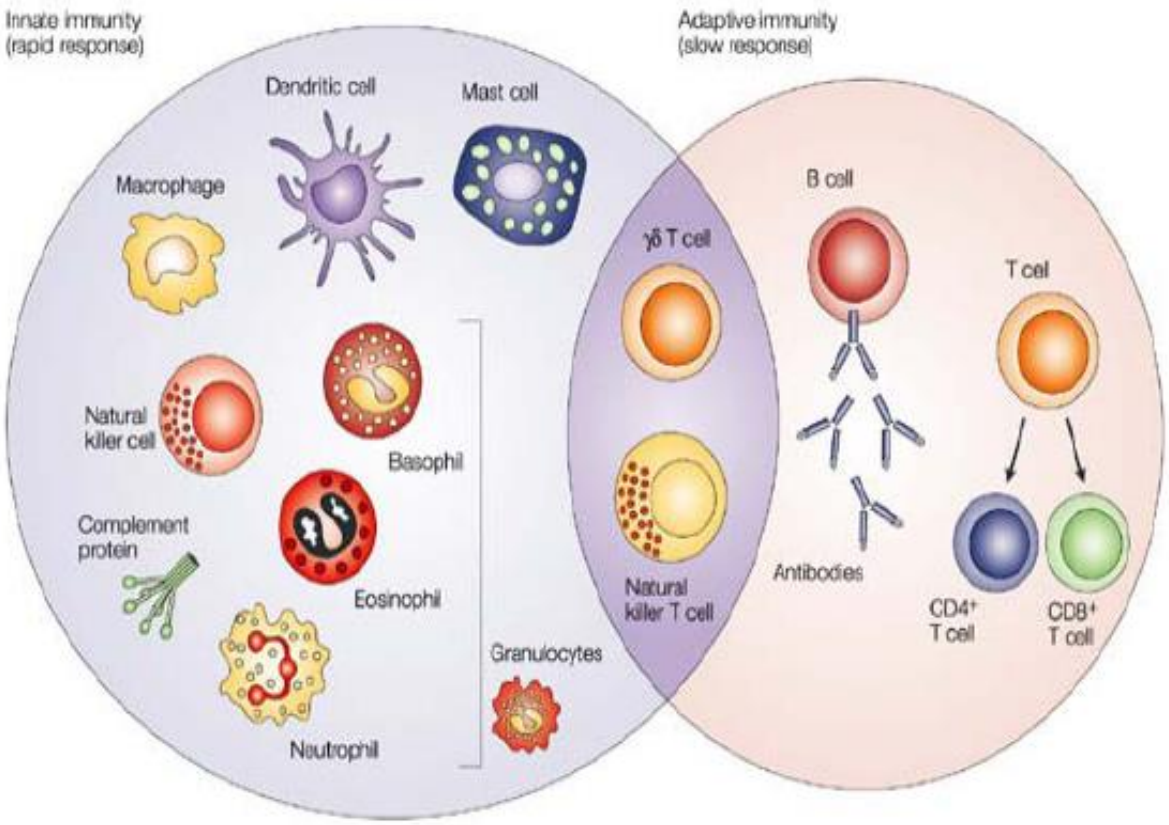

Figure 1.13: Cells of the immune system.

The main cells involved in the innate immunity (rapid response) and in the adaptive immunity (slow response) [127].

1.2.5. White blood cells

White blood cells (WBC) or leukocytes are one of the solid components in the blood along with red blood cells and platelets. Plasma is the liquid part of the blood that carries the solid components and nutrients to different parts of the body. Granulocytes are those white blood cells that contain granules in their cytoplasm such as neutrophils, basophils and eosinophils. Agranulocytes are white blood cells that do not contain any granules and they include lymphocytes and monocytes [118].

1.2.5.1. Neutrophils

Neutrophils form the majority (60 – 70%) of the white blood cells and play a major role in the innate immune system. They are also called polymorphonuclear neutrophils (PMNs) because of the segmentation seen in their nucleus [128]. A normal neutrophil is 10 to 12μM in size, round or spherical shaped and contains a single nucleus which is segmented into 2 to 5 lobes [Figure 1.14] [129]. Under a light microscope, when stained with a Romanowsky stain neutrophils have a pink colour with a purple coloured nucleus and granules in the cytoplasm, and this appearance is due to their acidophilic and basophilic properties [Figure 1.15] [128]. The average life span of a neutrophil is around 5.4 days [130].

1.2.5.1.1. Function of neutrophils

The most important function of the neutrophil is its antimicrobial properties, and it is mainly involved in chemotaxis, phagocytosis and killing of bacteria. In infections and inflammation, neutrophils form the front line of defence and are the first immune cells to migrate to sites of infection or inflammation [118]. The neutrophils are activated through CD16, an IgG molecule with low expression, FcγRIII seen on neutrophils

through a phosphotidylinositol linkage [131]. Neutrophils migrate to the site of infection and adhere to the endothelial wall at the injury site by binding CD11b, the protein integrin alpha M subunit to the intercellular adhesion molecule - 1 (ICAM-1) [132]. Neutrophils form a pseudo pod and slowly surround the bacteria to engulf them (Phagocytosis) [Figure 1.16]. The various antimicrobial substances present within the neutrophil granules such as myeloperoxidase get released upon activation and kill the microorganisms resulting in oxidative burst [Figure 1.17] [133].

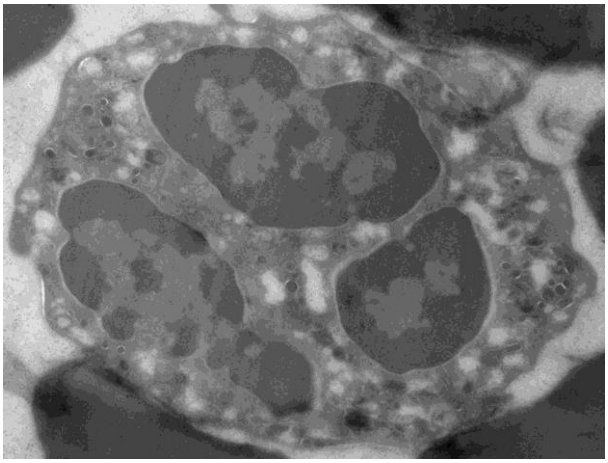

Figure 1.14: Image of a neutrophil under a transmission electron microscope.

This is the image of a neutrophil taken using a transmission electron microscope (4800x magnification).

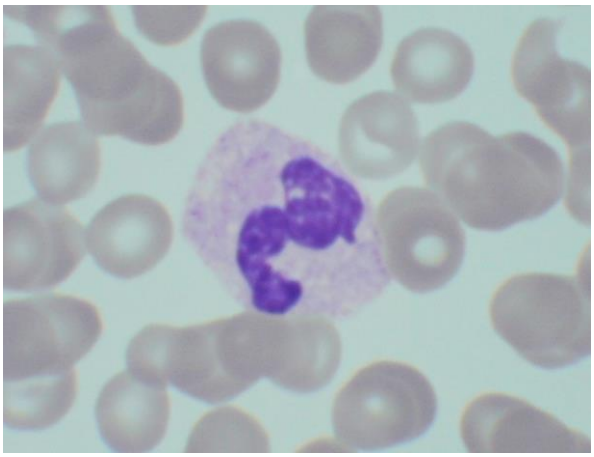

Figure 1.15: Image of a neutrophil under a light microscope.

This is the image of a neutrophil taken using a light microscope (100x magnification).

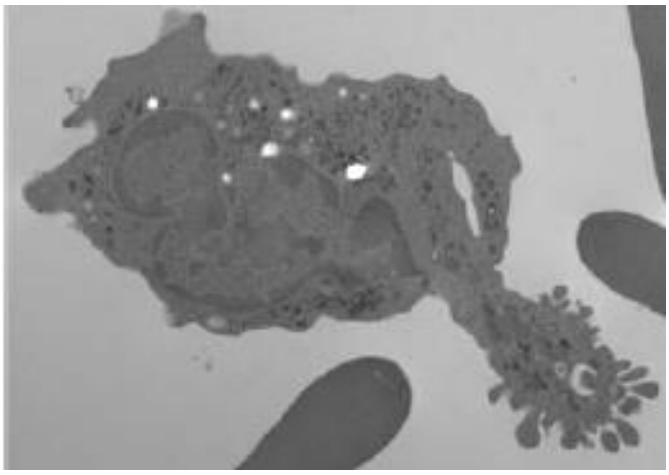

Figure 1.16: Neutrophil engulfing bacteria.

This is the image taken under a TEM (2900x) showing the engulfment of *E. coli* bacteria by pseudo pods of a neutrophil.

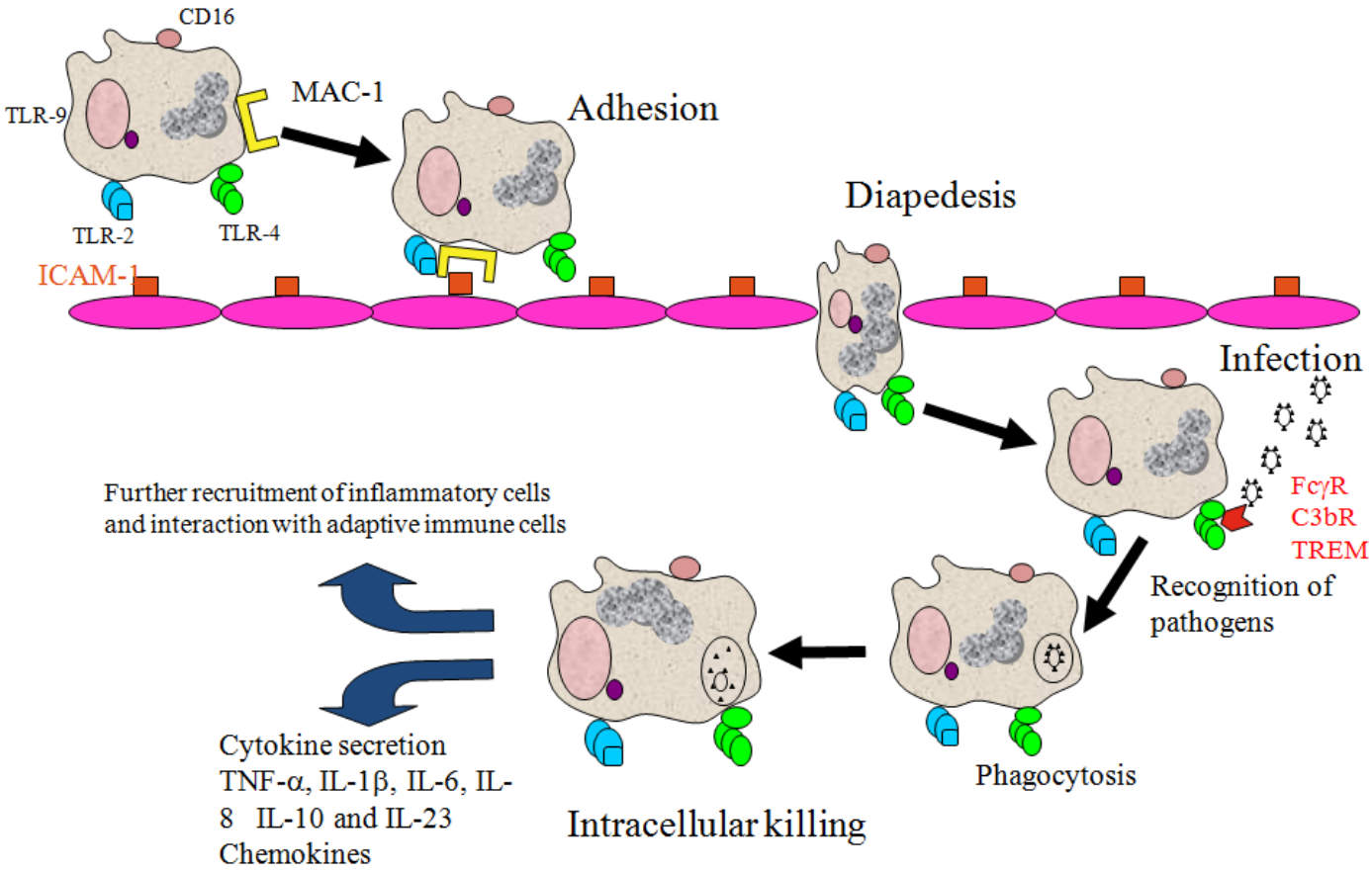

Figure 1.17: Function of neutrophils.

A cartoon illustrating the activation, adhesion, diapedesis, pathogen recognition (by TLRs), phagocytosis and intracellular killing function of the neutrophil.

1.2.5.1.2. Increase and decrease in neutrophil counts

An increase in neutrophil count is termed 'neutrophilia' which is increased in sepsis and inflammatory conditions such as hepatitis. A decrease in neutrophil count is termed 'neutropenia' and it occurs in conditions such as pancytopenia, certain leukaemias and infections. There may also be a decrease in the neutrophil count due to splenic sequestration or as a side effect of certain drugs and chemotherapy [134].

1.2.5.1.3. Neutrophils and acute liver failure

In response to paracetamol hepatotoxicity, neutrophils are rapidly recruited and infiltrated in the liver [135] where they become activated by chemokines such as CXCL8/interleukin-8 (IL-8) [136] and mitochondrial products such as formyl peptides and mitochondrial DNA amplifying hepatocellular damage by release of proteolytic enzymes and reactive oxygen species (ROS) [Figure 1.18] [106]. Neutrophils alongside macrophages also participate in the removal of necrotic cell debris in preparation for tissue repair and resolution of the inflammatory response [137]. Depletion of neutrophils reduced hepatocellular necrosis in paracetamol-induced mouse models indicating that neutrophils play a vital role in the development of acute liver injury [138]. Circulating neutrophils have a decreased phagocytic capacity and increased spontaneous oxidative burst (SOB) in patients with ALF [139]. Moreover, neutrophil function indices are important biomarkers of poor prognosis in ALF and can be implicated as important mediators in the development of cellular and organ dysfunction and the increased susceptibility to developing sepsis [139]. Decreased neutrophil phagocytic activity (NPA) correlates with peak arterial ammonia concentration in patients with ALF and there is growing evidence to suggest that ammonia may be causally implicated in contributing to

neutrophil dysfunction [139, 140]. In paracetamol overdose, neutrophils showed toxic granulation and vacuoles in the cytoplasm, as a result of increased granulocyte colony stimulating factor (G-CSF) production, which is usually seen in sepsis [Figure 1.19] [141].

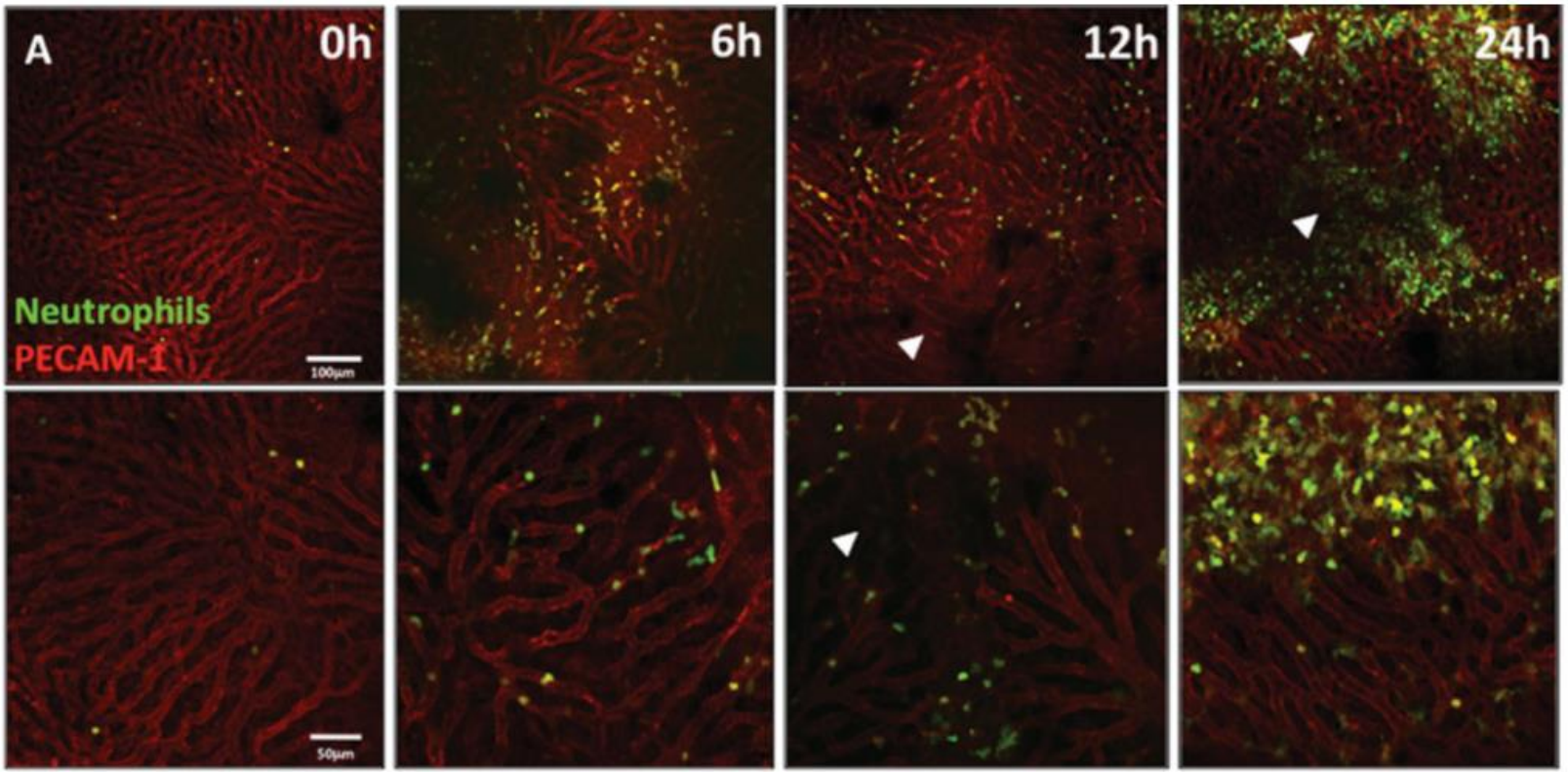

Figure 1.18: Neutrophil infiltration in the liver after paracetamol overdose [106].

This is the image taken under a confocal microscope illustrating the infiltration of neutrophils in the liver after paracetamol overdose in mice with maximum infiltration observed after 24 hours.

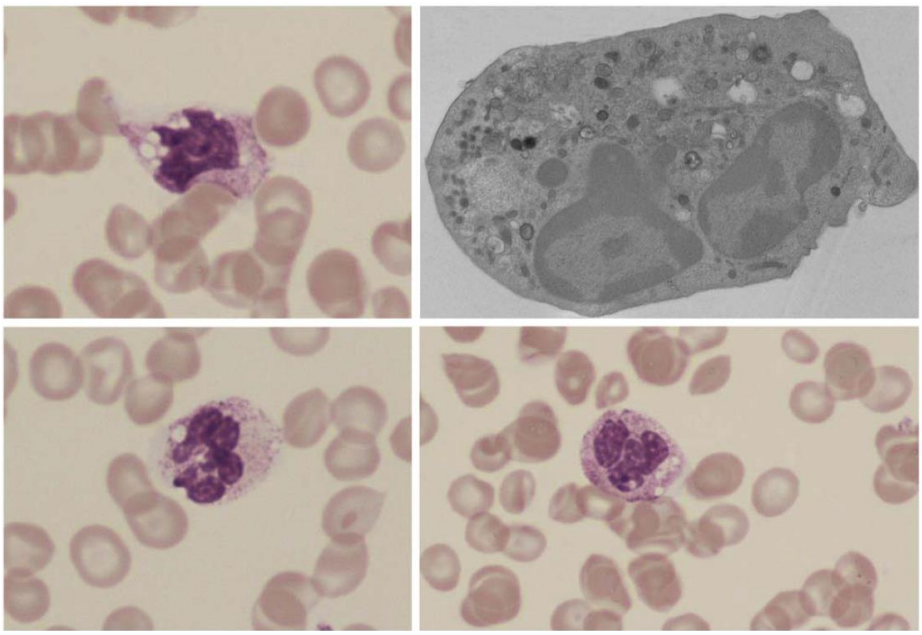

Figure 1.19: Neutrophils in the circulation after paracetamol overdose [141].

These are images taken using a light microscope (100x) and a TEM (4800x) showing toxic granulation, vacuoles and abnormal nucleus to cytoplasm ratio in circulatory neutrophils isolated from a PALF patients.

1.2.5.2. Lymphocytes

Lymphocytes are the second most abundant (20 – 40%) among the white blood cells. A typical lymphocyte is 8 to 10μM in size, round or spherical shaped and contains a single nucleus with a thin rim of cytoplasm [128]. The different types of lymphocytes include T lymphocytes, B lymphocytes and NK cells, where T cells and B cells are part of the adaptive immune system and NK cells are part of the innate immune system. Upon activation by an antigen or during an infection, lymphocytes become effector cells, that are short-lived, along with cytotoxic T cells participate in the host immune defence by producing cytokines and antibodies [118].

1.2.5.2.1. T lymphocytes

As with other immune cell subsets, T lymphocytes (T cells) also originate from haematopoietic stem cells in the bone marrow. However their progenitor cells migrate to the thymus via the blood, where they mature and are named as thymus-dependent lymphocytes or T cells [118]. Initially they develop as immature CD4 and CD8 double-positive cells and mature as single CD4 positive or CD8 positive T cells [142].

CD4+ T cells, also known as T helper (T_H) cells, activate other cell types such as cytotoxic T cells and help in the maturation of B lymphocytes [118]. T helper cells are differentiated into several subsets of effector T cells including T_H1, T_H2, T_H9, T_H17 and regulatory T cells (T-regs) [118]. T helper cells secrete IFN-γ, TNF -α, IL-6, IL-4, IL-10, IL-17, tumorogenic growth factor (TGF) -β and various other cytokines to induce immune responses [123].

CD8+ T cells, also known as cytotoxic T cells, kill target cells by inducing them to undergo apoptosis. The most important function of CD8+ T cells is to kill cancer cells

and virus infected cells. Upon activation, CD8+ T cells, like CD4+ T cells, have the ability to produce cytokines such as IFN-γ and TNF-α. IFN-γ activates the macrophages, recruits them to the site of injury and both act as effector cells and antigen-presenting cells [118].

Memory cells are those T lymphocytes that have the ability to memorise the antigens on exposure to any infection and quickly produce cytokines in cases of re-infection, whereas naive T cells are those cells that have encountered any specific antigen [118]. Memory and naive T cells are seen both in CD4+ and CD8+ T cells [143, 144].

T regs are mainly identified by the transcription factor Fox-P_3 and their main function is to suppress the excessive activity of effector T cells towards the end of an immune reaction [145].

1.2.5.2.2. Natural killer cells

Natural killer (NK) cells are a type of lymphocyte that develop in the bone marrow from the same progenitor cells as B and T lymphocytes. They do not contain any antigen-specific receptors therefore they are identified as part of the innate immune system. They are larger than B and T lymphocytes and contain cytotoxic granules in the cytoplasm. NK cells are responsible for recognising and killing cells infected with tumour and viruses. NK cells are activated by cytokines produced by macrophages. Upon activation NK cells express killer cell lectin-like receptor subfamily G 1 (KLRG-1) and natural killer group 2D (NKG2D) family on their surface, and they also produce cytokines such as IFN-γ [118].

1.2.5.2.3. Macrophages

Macrophages are the mature form of monocytes that are present mainly in tissues. Macrophages along with neutrophils mainly participate in the initial defence mechanism and in the adaptive immune mechanism. During the innate immune phase, macrophages participate in microbial killing by phagocytising invading pathogens, whilst in the adaptive immune phase they are involved in clearing the dead cells targeted by effector cells and producing cytokines such as IFN-γ, TNF-α, and IL-6. They also induce inflammation and secrete cytokines that activate other immune cells and recruit them to the site of injury [118].

1.2.6. Toll-like receptors

Toll like receptors (TLRs) or pattern-recognition receptors are type I transmembrane receptors that detect pathogens based on specific molecular patterns [146]. In the year 1989, Charles Alderson Janeway Jr, a famous immunobiologist at Yale University, predicted that innate immunity is responsible for the activation of the adaptive immune system. He also proposed the theory of innate pattern recognition and their links to adaptive immunity [147]. This prediction paved the way for further research in this field and many researchers around the globe including him confirmed this theory in the subsequent years [148].

Hoffmann observed that mutations in *Drosophila melanogaster* prevented them from making a protective immune response against *Aspergillus fumigates*. By analysing the genes that caused this mutation, Hoffmann showed that this was dependent on the activation of a particular factor called dorsal related immune factor [149]. Following this, Charles Janeway Jr and Ruslan Medzhitov showed that a homologue of the dorsal related factor were present in humans, which are now termed as Toll like receptors (TLRs) [150]. They also showed that activation of these receptors on certain white blood cells induced cytokine production and activated the adaptive immune system [150, 151]. However, the importance of this TLR family was not fully accepted, until Bruce Beutler showed that activation of TLRs and the resultant cytokine production was based on a specific recognition pattern. He found that mice defective of a particular gene (TLR4) did not induce any inflammatory response and this receptor (TLR4) was essential for the identification of lipopolysaccharide (LPS) and subsequent cytokine production [152].

Later on a similar set of genes, in a large family consisting of 10 members (TLRs 1, 2, 3, 4, 5, 6, 7, 8, 9 and 10) were identified in humans and other species [153]. Among those, TLRs 1, 2, 4, 5 and 6 are present on the surface of cells and are specialized in the recognition of bacterial products, while TLRs 3, 7, 8 and 9 are intracellular and specialized in the detection of viral products and nucleic acids [Figure 1.20] [118, 154].

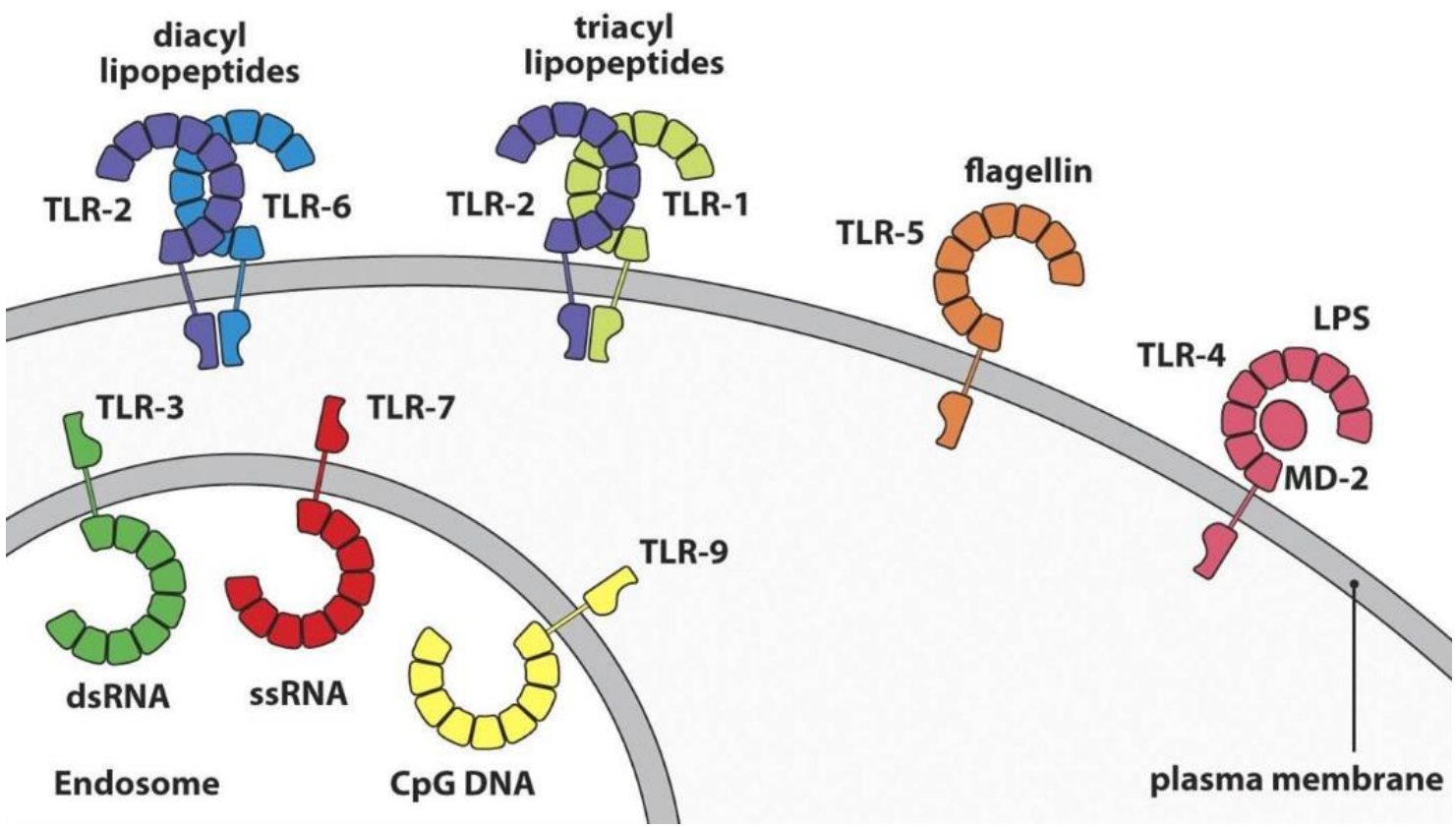

Figure 1.20: Position of TLRs and their ligands.

This picture illustrates the position of the different human TLRs in a cell, whether they are present on the surface or intracellular organelle (endosomes). It also illustrates the ligands that bind to the different TLRs.

1.2.6.1. TLR signaling pathways

When stimulated by microbial components, TLRs present on various cell types induce intracellular responses that result in the production of inflammatory cytokines, chemotactic factors and antiviral type I interferons. Cytokines are produced by activating the different transcription factors such as nuclear factor - κB (NF-κB), interferon regulatory factor (IRF) and activator protein 1 (AP-1) in different signaling pathways. NF-κB and AP-1 act to induce the production of pro-inflammatory cytokines and chemotactic factors, whereas IRF factors induce the production of antiviral type I interferons [118].

1.2.6.1.1. Myeloid differentiation factor 88 dependent pathway

The different signaling pathways are activated by the ligand-induced dimerization of two TLR ectodomains, which brings the Toll/interleukin-1 receptor (TIR) domains in the cytoplasm close together so that they can interact with the TIR domains of the adaptor molecules that initiate intracellular signaling. There are four different adaptors in mammalian TLRs and they are myeloid differentiation factor 88 (MyD88), MyD88 adaptor-like (MAL), TIR domain-containing adaptor-inducing IFN-β (TRIF) and TRIF-related adaptor molecule (TRAM). It is important that different TLRs interact with different combinations of these adaptors to induce cytokine production [118] [Figure 1.21].

To activate the signaling pathways, TLR5, -7 and -9 interact only with the MyD88 molecule; TLR3 interacts only with TRIF; while the rest either use MyD88 paired with MAL, or TRIF paired with TRAM [118]. The MyD88 is a protein that interacts with the TLR and IL-1R and it contains a TIR domain in its C-terminal protein and a death domain in its N-terminal portion. MyD88 upon stimulation recruits the IL-1R-associated kinase

(IRAK), which gets phosphorylated and associates itself with TRAF-6, leading to activation of two important signalling pathways, jun amino terminal kinases (JNK) and NF-κB. This in turn causes the production of cytokines and activation of other cells [155].

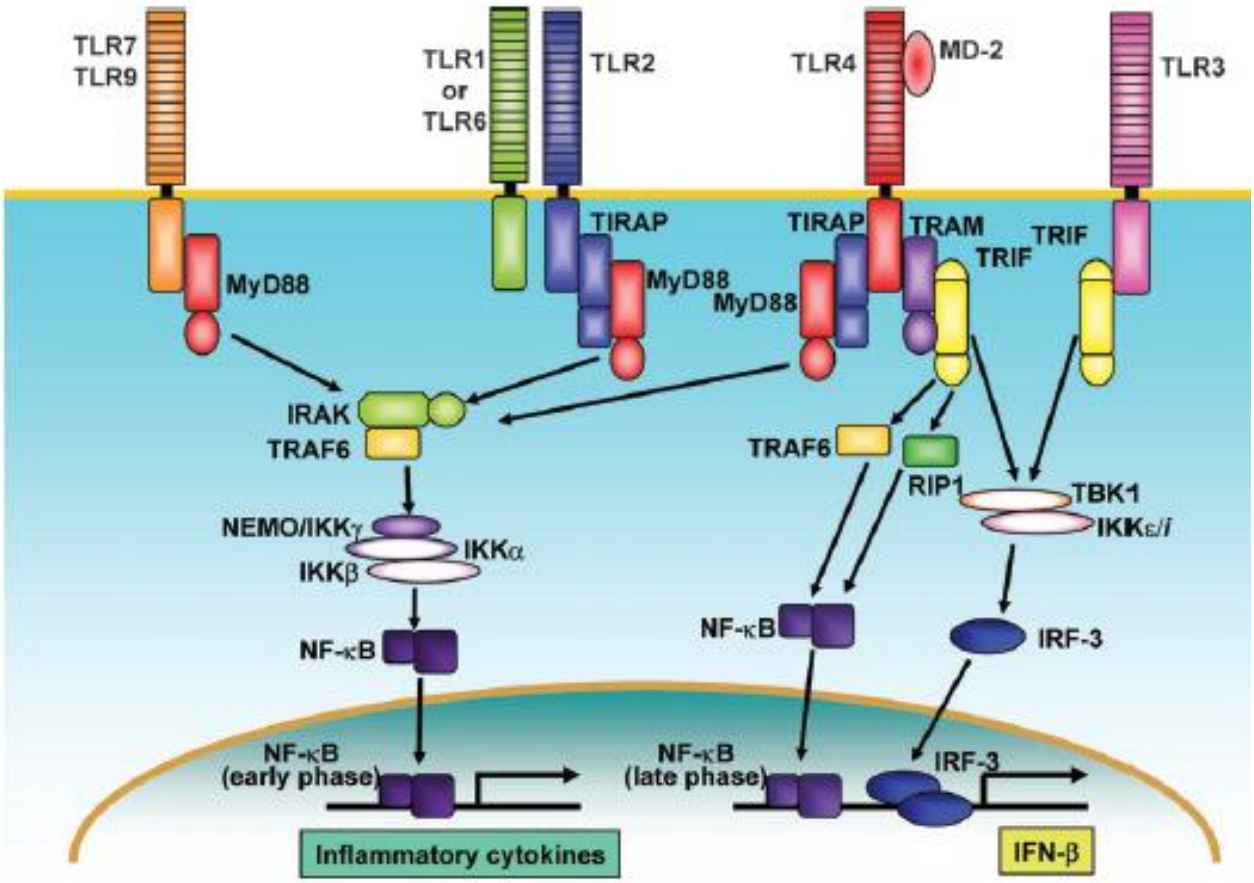

Figure 1.21: TLR signalling pathways, MyD88-dependent and MyD88-independent.

This picture shows the signalling pathways of TLR2, TLR4 and TLR9 which require the common adaptor MyD88 for cytokine activation by signalling the NF-κB pathway. It also shows the cytokine activation by TLR4 through the NF-κB pathway, without the common adaptor MyD88, resulting in a delayed response [155].

1.2.6.2. TLRs role in phagocytosis and adaptive immunity

There is impairment in bacterial phagocytosis including *Escherichia coli, Salmonella typhimurium* and *Staphylococcus aureus* due to the impaired maturation of the phagosome in the absence of MyD88. It has also been demonstrated that TLRs induce phagosome maturation through activation of p38 in the MyD88 pathway. Phagocytosis, an important process during the host defence against microbes, causes degradation of those microbes and its subsequent presentation of pathogen-derived peptide antigen. Recognition of pathogens by TLRs is also known to induce the production of genes coding for inflammatory cytokines and co-stimulatory molecules. The phagocytosis-mediated antigen presentation and TLR-gene production causes the development of antigen specific adaptive immunity in the host [155].

Among all TLRs, TLR2, 4 and 9 are the most common receptors on neutrophils and have been studied mostly in relation to liver disease. They can be easily detected using antibody detection methods, while the expression of other TLRs involves molecular techniques.

1.2.6.3. TLR2

TLR2 recognises a broad spectrum of microbial components like lipopeptides, peptidoglycan from gram-positive bacteria mainly [156], and also has high affinity towards some of the products from *Mycobacterium, Trypanosoma cruzi, Staphylococcus epidermidis, Treponema maltophilum* and fungi. TLR2 recognises a wide spectrum of microbial components, mainly because it forms heterophilic dimers with TLR1 and TLR6, and is also involved in the recognition of various components of fungi. TLR2

expressed on the cell surface can be identified by staining the cell surface using specific monoclonal antibodies [155, 157].

1.2.6.4. TLR4

TLR4, an important receptor for LPS, requires an extracellular protein MD-2 to detect the LPS [156]. It also recognises endogenous ligands, such as heat shock proteins (HSP60 and HSP70), fibronectin, hyaluronic acid, heparan sulfate and fibrinogen. TLR4 gets activated by endogenous ligands only at higher concentrations, whilst exposure to minimal quantities of LPS is sufficient for its activation. TLR4, which is also expressed on the cell surface can be identified by staining the cell surface using specific monoclonal antibodies [155, 157].

1.2.6.5. TLR9

Shizuo Akira from Japan, developed a TLR9 deficient ($TLR9^{-/-}$) mouse and showed that TLR9 recognises the unmethylated CpG motif of bacterial DNA. [158]. CpG DNA are of two types and are termed as A/D-type CpG DNA and B/K-type CpG DNA, which induces the production of inflammatory cytokines such as IL-6, IL-12, TNF-α and IFN-α [155]. Lethal doses of CpG DNA did not cause any harm or induce any inflammation in $TLR9^{-/-}$ mice [158]. TLR9 is presumed to be involved in the pathogenesis of autoimmune disorders such as diabetes [159], in addition to recognising viral and bacterial products [155, 157].

Apart from the above mentioned molecules, TLR2 and TLR4 are activated by damage-associated molecular patterns (DAMPs) such as heat shock proteins including HSP22, -70 and -72 and Gp96, high-mobility group box-1 (HMGB-1) protein, fibrinogen and antiphospholipid antibodies, whilst TLR9 is activated by IgG-chromatin complexes [160].

1.2.6.6. TLRs and neutrophils

Human neutrophils also contain TLRs, and they express all of them other than TLR3. The neutrophils are not only a target, but also act as a source of activation for cytokines. Pro-inflammatory cytokines mediated through various mechanisms of the TLR pathway stimulate the neutrophils and activate their antimicrobial functions. The neutrophils also release and synthesize various other pro-inflammatory cytokines that activate other immune cells (e.g. monocytes) and direct them towards the site of infection and initiate the adaptive immune system in the host [153]. TLRs are also known to have various other activities on neutrophils apart from phagocytosis and cytokine production, including ROS generation, receptor expression and priming of neutrophils.

TLRs activate neutrophils by pathogen-associated molecular patterns (PAMPs) and endogenous molecules known as damage associated molecular patterns (DAMPs) produced by tissues in response to infection and injury [161]. Several studies have determined TLR activation on neutrophils. Studies show that *Helicobacter pylori* activates TLR2 and TLR4 expression in neutrophils and blocking these receptors has resulted in an inhibitory effect on pro-inflammatory cytokine production [162].

1.2.6.7. TLRs and liver disease

The liver is an organ that is particularly important to the immune system because it produces acute-phase reactants, and thus in patients with liver disease, the immune system can be severely compromised. Thus, by gaining a greater understanding of the dysfunction of the immune system observed in patients with liver disease, it is hoped that better therapeutic targets will emerge in order to treat patients with liver disease.

Stimulation by LPS causes SIRS and septic shock resulting in MOF and death. In D-Galactosamine treated mice, LPS activity was greatly increased resulting in hepatocyte cell death causing acute liver injury. This was mainly activated by TLR4 resulting in the production of various inflammatory cytokines that are detrimental in the case of liver injury [163]. When CpG DNA is induced in D-Galactosamine mice, TLR9 activation also results in acute liver injury mediated by the mitochondrial apoptotic pathway. TLR9 is activated through the MyD88 pathway similar to LPS activation [164]. Unlike TLR4, the activation of TLR9 results only in liver damage and does not cause problems in other organs [165]. Although there is no direct involvement of TLRs in the recognition of hepatitis B and C viruses, studies show there is indirect activation of some TLRs in relation to these viruses. Since TLRs are involved in many diseases related to the liver, blocking TLRs has been the focus of novel therapeutic strategies[163].

1.2.6.8. TLRs and microglia

Microglia express TLRs 1-9 and upon activation by various TLR agonists such as LPS, peptidoglycan and CpG DNA they upregulate unique patterns of innate and effector immune cytokines and chemokines at the mRNA and protein level [100]. Activation of TLR4 in the microglia by ammonia and LPS result in the release of reactive oxygen species, nitric oxide and cytokines that ultimately contribute to astrocyte swelling [166] indicating that microglia plays a critical role in the development of brain oedema in ALF.

1.2.6.9. TLRs and paracetamol-induced acute liver injury

In a paracetamol-induced mouse model, TLR9 plays a significant role in the development of acute liver injury and survival upon activation of free DNA released by the apoptotic hepatocytes. TLR9 along with Nalp3 inflammasome, activates caspase-1,

an enzyme required for the maturation of pro-inflammatory cytokines, IL-1β and IL-18 [108]. In another mouse model, it has been shown that TLR4 plays an important role in the development of MOF including increased brain water content after paracetamol overdose, and using an inhibitor of TLR4 or mice deficient of TLR4 prevented the development of brain oedema [165].

1.3. Summary

Paracetamol-induced hepatocellular necrosis is the commonest cause of ALF in the western world and culminates in the development of coagulopathy, encephalopathy and MOF in less than 7 days. The loss of hepatocellular synthetic function leads to decreased ammonia detoxification capacity resulting in hyperammonemia. Hyperammonemia plays a definitive role in the development of HE and brain oedema, with up to 25% of patients developing ICH. Cerebral oedema and increased intracranial pressure may be fatal without access to emergency LT. There is a marked propensity for patients with PALF to develop sepsis which may not only hasten the development of brain oedema, but may further progress to MOF and death. The SIRS contributes to the progression of HE in ALF, however the mechanism by which this occurs remains unclear.

In response to paracetamol hepatotoxicity, neutrophils are rapidly recruited and infiltrate the liver where they become activated by chemokines such as CXCL8/ IL-8 and mitochondrial products such as formyl peptides and mitochondrial DNA amplifying hepatocellular damage by release of proteolytic enzymes ROS. Neutrophils alongside macrophages also participate in the removal of necrotic cell debris in preparation for tissue repair and resolution of the inflammatory response. Circulating neutrophils have a decreased phagocytic capacity and increased SOB in patients with ALF. Moreover, neutrophil function indices are important biomarkers of poor prognosis in ALF and can be implicated as important mediators in the development of cellular and organ dysfunction and the increased susceptibility to developing sepsis. Decreased neutrophil phagocytic activity (NPA) correlates with peak arterial ammonia concentration in patients with ALF and there is growing evidence to suggest that ammonia may be causally implicated in contributing to neutrophil dysfunction.

TLRs are innate pattern recognition receptors that detect microorganisms based on a specific molecular pattern. TLR9 is an intracellular receptor that has high affinity towards the oligodinucleotides (CpG motif of bacterial DNA), whilst TLR2 and TLR4 are surface receptors that detect PAMPs from gram-positive and gram-negative bacteria (LPS), respectively. Downstream signalling of TLRs activates the NF-κB pathway thereby upregulating the production of pro-inflammatory cytokines and chemokines, and recruiting key components of the adaptive immune system. Neutrophil TLRs are able to sense PAMPS and induce inflammatory responses but whether this is protective or detrimental in patients with PALF remains unknown. TLR2, -4 and -9 are the most prevalent TLRs on neutrophils and activation of TLRs in an *in vitro* experiment in healthy human neutrophils resulted in increased phagocytic capacity, superoxide generation, L-selectin shedding, and inhibition of chemotaxis and also triggered cytokine release. This has not been examined in patients with PALF although a TLR9 antagonist was recently demonstrated to have a protective effect against developing liver injury in a mouse model of PALF.

Although the evidence base supporting the relationship between ammonia, inflammation and brain oedema is robust, there is a paucity of data characterising the specific pathogenic mechanisms entailed. Prof Roger F. Butterworth, an eminent researcher in the field of hepatic encephalopathy, once stated that "the prevention of central pro-inflammatory processes will undoubtedly herald a new chapter in the development of agents for the prevention and treatment of the CNS complications of the liver failure" [40]. The aim of this study is to open a new chapter within that area of research.

1.4. Hypothesis

Ammonia and inflammation are increased in paracetamol-induced acute liver injury and they play an important role in the progression towards hepatic encephalopathy. There is a robust evidence base to support the role of TLR9 in the pathogenesis of neutrophil-mediated liver injury and systemic inflammation in paracetamol-induced ALF.

I therefore postulate that ammonia induces systemic inflammation and contributes to the development of brain oedema through a TLR9-mediated pathway.

To better understand how ammonia and inflammation contribute towards the progression to hepatic encephalopathy in human PALF, the following hypotheses were formulated:

1. Circulating neutrophil TLR9 expression is increased in PALF patients with advanced hepatic encephalopathy and SIRS resulting from the release of necrotic hepatocyte products, ammonia, DNA and IL-8 into the circulation [Figure 1.22, Q1].

2. Ammonia induces inflammation by activating neutrophils through a TLR9-mediated mechanism which then triggers the adaptive immune system culminating in pro-inflammatory cytokine production by effector T cells, cytotoxic T cells, NK cells and macrophages [Figure 1.22, Q2]; the activation of TLR9 is dependent on DNA [Figure 1.22 Q3].

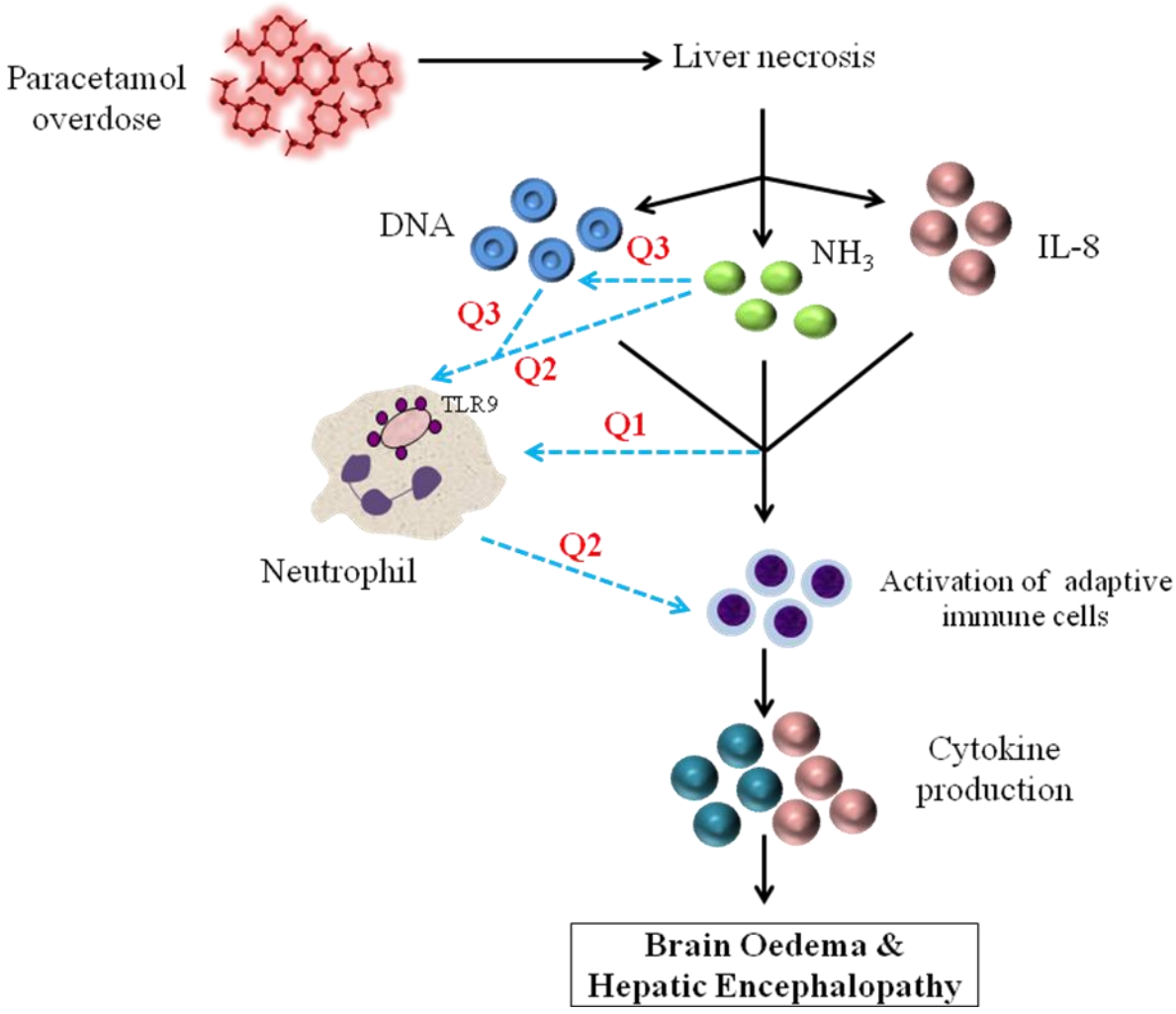

Figure 1.22: Hypothesis figure.

It is well established that paracetamol overdose causes necrosis in the liver and the resulting necrotic byproducts such as ammonia IL-8 and DNA are released into the circulation. This leads to systemic inflammation and as a result cytokines are produced by various cells. Ammonia and cytokines enter the brain through the cerebrospinal fluid and induce brain oedema. In my hypothesis (shown as ---->), I postulate that ammonia-induced inflammation and subsequent brain oedema is influenced through a neutrophil-TLR9 mediated pathway.

1.5. Aims and objectives

1. To prospectively characterise circulating neutrophil function and TLR2, -4 and -9 phenotype in healthy controls (HC) and in patients presenting with PALF, based upon the severity of SIRS and HE.

2. To study the neutrophil TLR9 expression and cytokine production at baseline, and following *ex-vivo* stimulation with oligodinucleotides, ammonium chloride (NH_4Cl) and LPS.

3. To analyse healthy neutrophil TLR9 expression and cytokine production at baseline, and following *ex-vivo* stimulation with IL-8 and/or NH_4Cl.

4. To determine whether activation of TLR9 is a DNA dependent or DNA independent mechanism by examining the influence of PALF plasma and endogenous mitochondrial DNA on neutrophil TLR9 expression by incubating healthy neutrophils with PALF plasma with and without deoxyribonuclease-I (DNase-I) [Figure 22, Q4].

5. To determine whether innate immune cells such as neutrophils and/or macrophages can propagate systemic and organ TLR9 expression.

A key objective would be to also determine if neutrophil TLR9 expression is increased by ammonia and systemic inflammation synergistically in human PALF.

Chapter 2. Materials and methods

My PhD study comprised of two different models, human and mouse, the former was performed at the Institute of Liver Studies in King's College Hospital, London, United Kingdom (UK), while the latter was performed at Li Wen's laboratory in the Department of Endocrinology, School of Medicine at Yale University, United States of America (USA). The materials which were purchased at both the sites from those companies which are universal have been listed under general consumables while the rest have been listed under specific headings.

2.1. Materials

2.1.1. General consumables

Rosewell Park Memorial Institute (RPMI) medium [Sigma-Aldrich, United Kingdom (UK)]; Flow cytometer tubes – 5mL [Becton Dickinson (BD), UK] [Corning Science, Mexico]; Falcon tubes / Cellstar tubes - 15 and 50 mL [Starlabs, UK] [Greiner bio one, USA]; Lysing solution [BD]; Polymorphprep™ solution [Axis Shield, Norway]; DNAse-I [Sigma-Aldrich]; Phosphate buffered saline (PBS) [Sigma-Aldrich]; Cytofix/cytoperm solution [BD]; Permwash buffer [BD]

Flow cytometry Antibodies: Detailed information given in appendix tables.

Instruments: Flow cytometer – BD Fluorescence activated cell sorting (FACS) machine Canto II and LSRII [BD, San Jose, California, USA]

Analysis softwares: BD FACS DIVA software V6.0 [BD, San Jose, California, USA]; FCAP array software V1.0.1 [BD, San Jose, California, USA]; SPSS 20.0 [IBM statistics, UK]; GraphPad Prism V6.0 [UK]

2.1.2. Human study

Stimulants: Lipopolysaccharide (LPS) [Sigma-Aldrich, UK]; Ammonium chloride (NH_4Cl) [Sigma-Aldrich, UK]; Oligodinucleotides (ODN) 2395 [Innaxon, UK]; IL-8 [R&D, UK]

Kits: Neutrophil function kit – Phagotest™ and Burst Test™ [Orpegen Pharma, Germany]; Cytometric bead array [BD, UK] – Human Soluble Protein Master Buffer Kit; Human Soluble Protein Flex Sets – IL-6, IL-8, IL-10 and TNF-α

Instruments: Centrifuge [Rotina, Germany]; Water bath [Grant, UK]

2.1.3. Animal study

In-vivo **Stimulation:** Ammonium acetate (NH_4-Ac) [J.T. Baker, USA]; Sodium Chloride [J.T. Baker, USA]; ODN2088 [Invivogen, USA]

In-vitro **stimulation:** Phorbol 12-myristate 13-acetate (PMA) [Invivogen, USA]; Ionomycin [Invivogen, USA]; Golgi plug [BD, USA]

Other materials: Tris pH-8.0 [American Bioanalytical, USA]; EDTA [American Bioanalytical, USA]; SDS [American Bioanalytical, USA]; Pronase [Roche, USA]; Ethanol [Dacon Laboratories, USA]; Iso-fluorane [Butler Schein Animal Health, USA]; Iso-propanol [Sigma-Aldrich, USA]; Pronase [Roche, USA]; 25G needle [BD, USA]; 1mL, 3mL and 5mL syringes [BD, USA]; collagenase-IV [Worthington, USA]

Kits: Quant-iT ™ PicoGreen® dsDNA (Life Technologies, USA); DNA plate reader – Bio Tek, USA

Instruments: Centrifuge [Corning, USA]; Water bath [Precision, USA]

2.2. Human study design

A prospective cohort study was performed on patients presenting with PALF. Circulating neutrophil function and TLR phenotype were determined and compared to HC. Blood samples were collected from patients with PALF within 24 hours of admission to the intensive care unit (ICU) [day 1] and followed longitudinally (days 4 and 7) until recovery, death or LT. HCs were only studied on day 1 as we have previously shown that HC variability is negligible over 7 days.

2.3. Patients

Twenty four consecutive patients with PALF were recruited on admission to the liver ICU at King's College Hospital between January 2011 and December 2013. PALF was defined by the onset of hepatocellular dysfunction in the absence of pre-existing liver disease characterised by coagulopathy and encephalopathy following an intentional or unintentional overdose of paracetamol [167].

2.4. Inclusion and exclusion criteria

Patients with PALF were included aged 18-75 years. Healthy age and sex-matched non-smoking volunteers with no history of liver disease were used as HC. The HC alcohol intake was <20g/day and they had not drunk alcohol or exercised excessively, 72-hours prior to blood being drawn.

Patients were excluded if they had evidence of sepsis on clinical examination, radiological or laboratory evidence of infection, malignancy and any coexisting history of immunodeficiency including HIV and glycogen storage disease. Patients who had an

alcohol intake of >20g/day prior to the paracetamol overdose or who were treated with immunosuppressant drugs were also excluded.

2.5. Consent and data collection

The study was performed in accordance with the declaration of Helsinki and ethical permission was granted from the North East London Research Ethics Committee (Ref 08/H0702/52) and King's College Hospital Local Research Ethics Committee (Ref 01-04-005). After obtaining fully informed consent or declaration by an appropriate consultee, clinical, biochemical and physiological data were collected. The information included tobacco and alcohol use, arterial ammonia (μmol/L), sodium (mmol/L) and differential leucocyte count ($x10^9$). The grade of encephalopathy according to the West-Haven criteria [42], admission SIRS score [36], Sequential Organ Failure Assessment (SOFA) score [168] and the Acute Physiology and Chronic Health Evaluation (APACHE) II score [169] were also calculated. Length of ICU stay, survival and number of days requiring vasopressors, ventilation or renal replacement therapy were also recorded.

Antibiotic use and immunomodulatory therapies such as corticosteroids, hypothermia, haemofiltration and plasmapheresis were recorded. None of the patients were treated with albumin dialysis or biological liver support devices but one patient underwent plasmapheresis. The occurrence of bacterial, fungal and viral infection was noted along with other relevant patient outcomes including the development of MOF.

2.6. Sample collection and storage

All experiments were performed within 1 hour of blood being drawn. Twenty millilitres of venous blood was collected into heparinised pyrogen-free tubes. Neutrophil function

and TLR phenotyping were performed and plasma was obtained by centrifugation of whole blood at 4750g for 10 minutes at 4°C and stored at -80°C for subsequent cytokine determination by cytometric bead array (CBA).

2.7. Measurement of blood ammonia

Arterial blood was collected from all patients soon after admission in pre-heparinised syringes from indwelling catheters. Ammonia was measured using the Ammonia Test Kit II for the PocketChem BA device (Arkay, Inc., Kyoto, Japan) with 20 μL of blood sample applied to a reagent strip. The continuous measurement range is 7–286 μmol/L and the normal blood ammonia level for healthy adults in this device was < 54 μmol/L. The device was maintained in accordance with the manufacturer's specification, with daily internal and monthly external calibration. The device was located within the ICU and testing was performed by trained technical staff immediately after collection so the delay in processing the sample was never more than 5 min from collection [170]. Since blood ammonia was measured in the ICU as part of standard care, it was deemed unethical and a poor use of resources to repeat testing in the laboratory. Therefore I was not able undertake a comparison of blood ammonia with the plasma ammonia.

2.8. Flow cytometry

In humans and mice, the expression [mean fluorescence intensity (MFI) and frequency] of various surface and intracellular receptors present on the white blood cells were analysed using a flow cytometer. After white blood cells were isolated from whole blood using Polymorphprep™ solution or red blood cell lysis method, they were stained for flow cytometry.

2.9. Isolation of white blood cells after lysis of red cells

To stain the cells for flow cytometry, 100 µL of whole blood was placed in 5 mL tubes and 1 mL of lysis solution [<15% formaldehyde and <50% di-ethylene glycol] was added. The lysate was mixed gently and left at room temperature (RT) for 15 minutes. The reaction was stopped by adding 2 mL of phosphate-buffered saline (PBS). The solution was centrifuged at 600g for 5 minutes at 18°C and the supernatant was discarded leaving the cell pellet at the bottom of the tube. The cells were then re-suspended in 100 µL of PBS before staining for flow cytometry.

Alternatively red blood cells were also lysed using distilled water. To lyse the red blood cells in whole blood or immune cells isolated from animal tissues, cells were gently suspended and 900 µL of de-ionised water was added and mixed well for ten seconds. The reaction was stopped immediately using 100 µL of 10x PBS and 5 mL of 1x PBS and the tissue debris were removed. Cells were centrifuged at 600g for 5 minutes at 18°C and the supernatant was discarded. The lysis of red blood cells using water was not used in the human study since water can affect neutrophil function.

2.10. Isolation of white blood cells using Polymorphprep™ solution

Polymorphprep™ solution is a density gradient solution which separates white blood cells and other blood components based on their density. To isolate the white blood cells using Polymorphprep™ solution, 20 mL of heparinised blood was collected and processed under aseptic conditions in a bio-safety cabinet. Whole blood was layered over 15 mL of Polymorphprep™ solution in a 50 mL falcon tube. The tubes were balanced and centrifuged at 800g for 35 minutes at 18°C, with least acceleration and zero brakes. After centrifugation the tubes were placed carefully in the safety cabinet to

avoid mixing of separated cells. The separated blood contained peripheral blood mononuclear cells (PBMC) on top, granulocytes in the middle and red blood cells at the bottom [Figure 2.1]. PBMC and granulocytes were isolated in two different sterile 50 mL falcon tubes. Granulocytes were washed twice with PBS and centrifuged at 800g for 10 minutes at 18°C with brakes. When there was red blood cell contamination in the granulocytes, red blood cells were lysed and washed as above.

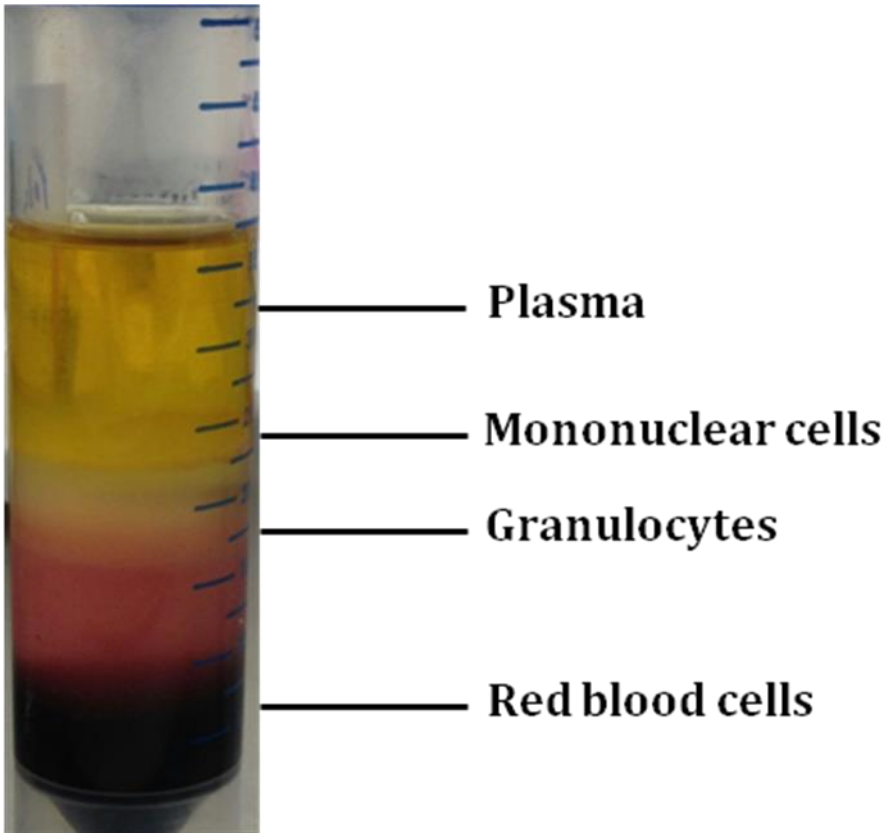

Figure 2.1: Separation of white blood cells using a density gradient Polymorphprep™ solution.

2.11. Cell count

The granulocytes or PBMCs were suspended with PBS and diluted (1/10) with Trypan Blue solution. Cells were counted using a Neubauer haemocytometer and up to 1 million ($1x10^6$) viable cells were re-suspended with 100 µL of PBS in a single tube for flow cytometry staining.

The total number (no.) of cells in the PBS (isolated from a single sample) was calculated as follows:

$$\text{Total no. of cells} = \frac{\text{Cells counted x dilution factor x depth factor x } 10^3 \text{ x volume of PBS}}{\text{Area counted}}$$

$$= \frac{\text{Cells counted x 10 x 10 x } 10^3 \text{ x volume of PBS}}{4}$$

Cells counted – number of cells counted in the haemocytometer

Dilution factor – the dilution of cells with trypan blue (1 in 10 dilution – 5 µL cells with 45 µL of trypan blue)

Depth factor – the distance between the cytometer and cover slip (0.1 mm - 10)

10^3 – for the conversion of per mL

Volume of PBS – 5 mL of PBS in which the cells were suspended

Area counted – four, the 16 small squares in the areas 1, 2, 3 and 4 of the haemocytometer were counted as shown below in figure 2.2.

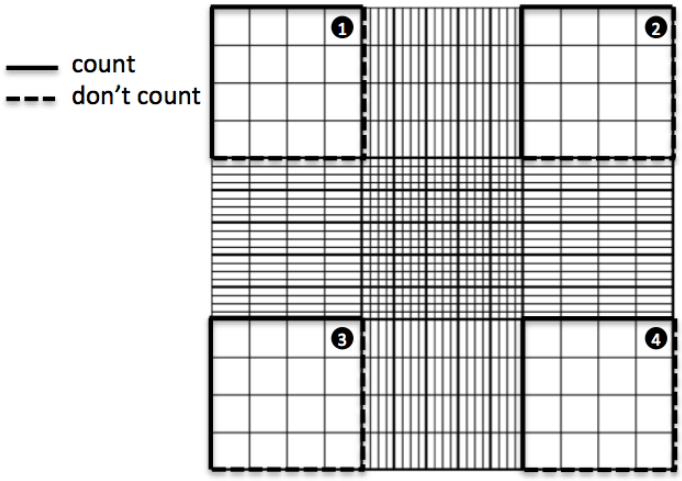

Figure 2.2: Image of the areas used for counting white blood cells in a haemocytometer.

2.12. Staining of cells for flow cytometry

For flow cytometry, up to 1 million (1 x 10^6) white blood cells were re-suspended in 100 µL of staining buffer and stained with fluorochrome conjugated antibodies in one tube. To stain for receptors present on cell surface, monoclonal antibodies conjugated with fluorochromes were added to the white blood cells, mixed and incubated at RT in darkness for 30 minutes. Following this the cells were washed with 1 mL of sterile PBS, centrifuged at 600g for 5 minutes at 18 °C and the supernatant was discarded. To prepare the cells for intracellular staining, 100 µL of cytofix/cytoperm solution was added to the cell pellet after surface stain, mixed gently and left at RT for 20 minutes. The cells were washed with 1 mL of BD permeabilisation wash buffer, centrifuged at 600g for 5 minutes at 18°C and the supernatant was discarded. To prepare the cells for intranuclear staining, 1 mL of Tonbo's transcription factor fix/perm buffer (1x) was added to the cell pellet after surface stain, mixed gently and left at RT for 1 hour. The cells were washed with 1 mL of Tonbo's permwash buffer, centrifuged at 600g for 5 minutes at 18C and the supernatant was discarded. The cells were then stained with intracellular or intranuclear antibodies and incubated at RT in darkness for 30 minutes. The cells were washed again with 1 mL of permeabilisation buffer, centrifuged at 600g for 5 minutes at 18°C and the supernatant was discarded. The cells were then re-suspended in 300 µL of PBS and analysed using a flow cytometer.

For the human study, all antibodies were titrated by staining them with blood samples collected from HC to determine the right concentration of antibody required to be added to the cells. The stock antibodies were diluted with PBS and those dilutions which expressed maximum mean fluorescence intensity (MFI) were chosen for the experiment.

The final concentration and detailed information of all the antibodies used for the human study are given in the appendix. For the animal study, the appropriate amount of antibody added to the cells was based on the protocols followed at Li Wen's laboratory in Yale University. The concentration of all the antibodies were calculated and optimised using immune cells isolated from spleen.

2.13. Stimulation of intracellular cytokine production

To determine the intracellular cytokine production of PBMCs, up to 5.0 x 10^6 cells per mL were stimulated with phorbol 12-myristate 13-acetate (PMA) (50 ng) and ionomycin (500 pg) in complete media with Golgi plug (1 µL) and incubated at 37°C for 5 hours in the presence of 5% CO_2. At the end of 5 hours, stimulated cells were centrifuged at 600g for 5 minutes at 18°C, and supernatants were discarded. The cells were first stained with surface antibodies and then with intracellular cytokine antibodies and analysed using flow cytometry.

2.14. Flow cytometer

Cytometry is a process by which physical and chemical characteristics of a single cell are measured. Flow cytometry is a technique mainly used for analysing multiple characteristics of single cells that pass through a single apparatus in a fluid stream [171, 172]. The first flow cytometer was patented by Wallace coulter in 1953 based on the disturbances particles exert when moving in an electric field and the fluorescence-based flow cytometer was patented by Wolfgang Gohde in 1968. Although Coulter counters are still widely used in clinical practice, it was fluorescence activated cell sorter (FACS) machine that transformed the understanding of cellular immunology.

Flow cytometry is used for immunophenotyping of cells from various specimens including whole blood, body fluids and bone marrow [173]. The optical and fluorescence characteristics of single cells are measured in a flow cytometer to determine its size, DNA or RNA content, cytoplasmic complexity, and proteins expressed in the surface and intracellular region. The size and internal complexity of cells are measured using the light scattered by forward angle and right angle respectively. The nucleic acid contents and the protein expression are determined by measuring the fluorescent dyes conjugated to antibodies that bind to them. When cells are labelled with different fluorochromes and are passed through a light source, they get excited to a high energy state. When they return to their resting state, these fluorochromes emit light at different wavelengths and are measured simultaneously. The most common dyes used are fluorescein isothiocyanate (FITC), phycoerythrin (PE), Peridinin chlorophyll protein (PerCP) and propidium iodide (PI) and allophycocyanin (APC). To produce dyes of longer wavelengths and more colours, tandem dyes with internal fluorescence resonance energy transfer (PE-Cy5, PE-Cy7, APC-Cy7 & PerCP-Cy5.5) are used [171].

2.14.1. Acquisition of samples in the flow cytometer

The samples were acquired in a BD FACSCanto II ™ instrument consisting of 2-lasers and 6-colours at King's College Hospital [Figure 2.4], whilst the samples at Yale University were acquired in a BD LSRII instrument which consisted of 4-lasers and 13-colours. The flow cytometer was connected to a fluidic cart containing the sheath and cleaning solutions necessary for running the machine smoothly and the instrument was operated using the BD FACS Diva software 6.1.2 installed in a computer.

2.14.1.1. Setting up an experiment

A new experiment was created and compensation settings were applied to the experiment. In a new global worksheet, a dot plot was created to display the cells. Cells were identified in the forward scatter channel area (FSC-A) and side scatter channel area (SSC-A) of the dot plot based on their size and internal complexity. With the increase in size and internal composition, cells lie away from zero in the FSC-A and SSC-A, respectively. The FSC-A and SSC-A are measured on a linear scale and the fluorochrome expression was measured on a logarithmic scale in a dot plot.

2.14.1.2. Identification of white blood cells and the different subsets

In the global worksheet, a dot plot with FSC-A/SSC-A was created. To display the human or mouse white blood cells in the dot plot, PMT voltages for FSC and SSC were usually set between 250 - 400V. The population close to the X-& Y-axis were considered as lymphocytes since they are the small cells among the white blood cells without granules. The population observed further along the X-axis were considered as monocytes since they are the large cells among the white blood cells without granules. The large population found above were identified as granulocytes, since they are present in the

majority amongst the white blood cell and contain granules in their cytoplasm [Figure 2.5].

After classifying the white blood cells in the cell suspension based on FSC-A/SSC-A characteristics, the different types of white blood cells were identified by staining for the key receptors expressed on those cells using fluorochrome conjugated antibodies.

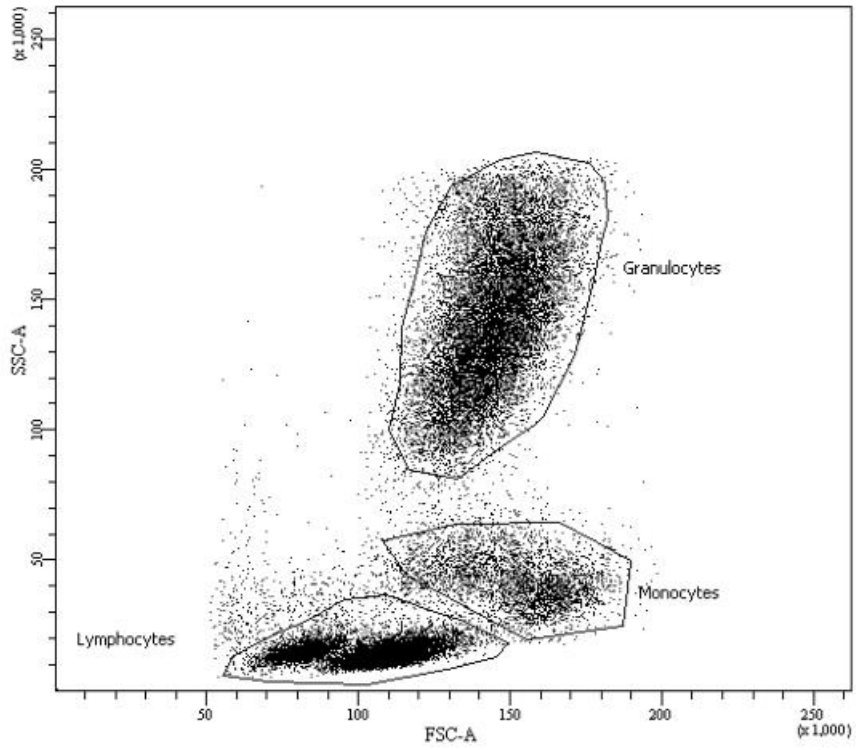

Figure 2.3: Flow cytometry image of human white blood cells (leucocytes) showing the position of granulocytes, lymphocytes and monocytes on a FSC-A/SSC-A dot plot.

2.14.1.3. Identification and characterisation of neutrophils

In humans, CD16, CD11b and CD62L have been shown to be useful markers for the identification of neutrophils. Depending on the experimental set up these markers were used as an individual marker or in different combinations to identify the neutrophils. CD16, an FcγRIII molecule, is an important receptor present on the cell surface which helps in the activation of neutrophils. CD11b is an ICAM-1 molecule which binds to the integrin present on the surface of neutrophils that helps in the adhesion of neutrophils to endothelial cells and other cells. CD62L or L-selectin is an adhesion molecule present on the surface of neutrophils.

In humans, baseline neutrophil phenotype was characterised by determining the expression of CD16, CD11b, CD282, TLR4 and TLR9 in granulocytes isolated from whole blood after red blood cell lysis. The panel of antibodies used for characterising neutrophil phenotype are given in *appendix table – 1*. The panel of antibodies used for characterising the expression of IL-8 in neutrophils are given in *appendix table – 2.*

Lys6-G and CD11b are the best markers for the identification of neutrophils in mice. Lys6-G, also known as Gr-1 is a protein expressed by the myeloid lineage and this is mainly present on the surface of peripheral neutrophils. Expression of extracellular myeloperoxidase was also measured in the neutrophils (*appendix table – 3)*.

2.14.1.4. Identification and characterisation of T cells

The different subsets of lymphocytes were identified using their specific markers. T cells were identified using CD3 an important receptor present on the surface of T cells that helps in its activation. Following that, CD4 and CD8 markers were used to characterise the different subsets of T cells. Frequency (%) of activated cells (CD69+), memory cells

(CD44+/CD62L-) and naive cells (CD44-/CD62L+) were characterised further amongst the different T cell subsets (*appendix table – 4)*. In mice, the memory and naive cells are usually characterised using CD44 and CD62L compared to the CD45RA and CD45RO isoforms found only in humans. Intracellular cytokine production [IL-6, IFN-γ, TNF-α and IL-17] were determined in the CD4+ and CD8+ T cell subsets (*appendix table – 5 and 6)*.

2.14.1.5. Identification and characterisation of NK cells

NK cells were identified primarily using DX-5 also known as CD49b which is expressed on the surface of NK cells along with CD122. Activation marker KLRG-1 was used to characterise the frequency (%) of KLRG-1^{pos} amongst the NK cells (*appendix table – 7)*. Cytokine production of IFN-γ and TNF-α were determined in the KLRG-1 activated NK cells (*appendix table – 8 and 9)*.

2.14.1.6. Identification and characterisation of macrophages

Macrophages in mice were identified mainly using F4/80 and CD11b markers. Intracellular cytokine production [IL-6, IFN-γ and TNF-α] was determined in the F4/80 and CD11b+ macrophage (*appendix table – 10)*.

2.15. *Ex-vivo* neutrophil TLR9 stimulation with LPS, NH_4Cl and ODN2395

Whole blood was incubated at 37°C with Roswell Park Memorial Institute (RPMI)-1640 media and stimulated with either LPS (*E. coli* 0111:B4) (200ng/mL) or NH_4Cl (400μM) or ODN 2395 (oligodinucleotides) (0.25μM) or with PBS in controls for 2 hours (unstimulated). The stimulated cells were then stained and analysed by flow cytometry

as mentioned previously. The panel of antibodies used for characterising neutrophil phenotype and the expression of IL-8 in neutrophils are given in *appendix table – 1 and 2,* respectively. The supernatant was collected for defining cytokine profiles. The time and concentration of the stimulants used for the *ex-vivo* studies were optimised after performing sequential assays using different concentrations of stimuli with healthy blood.

2.15.1. RPMI and incubation time

This was performed to calculate the amount of RPMI medium and the duration of incubation at 37°C, required for *ex-vivo* stimulation. For this purpose, 100µL of whole blood from healthy controls were incubated at 37°C from 0 hour to 3 hours, with different concentrations of RPMI. The incubation period and the amount of RPMI required for the experiment were calculated by determining the maximum percentage of granulocyte population in the concentration that maintained cell viability. There was maximum cell viability with 400µL of RPMI and 2 hours of incubation.

2.15.2. Lipopolysaccharide

According to the manufacturer's instruction, the concentration of lipopolysaccharide (LPS) stock solution was 1 mg/mL and the optimal concentration of LPS for in-vitro experiments was 0.05 to 1 µg/mL. The optimal concentration of LPS for this experiment was determined by measuring the changes in neutrophil TLR4. For this experiment, the whole blood from healthy controls was stimulated with different concentrations of LPS, ranging from 0 to 400 ng/mL. For a concentration of zero, PBS was used instead of LPS. Based on the results, the final concentration of 200 ng/mL LPS was determined to be the appropriate concentration required for stimulation of neutrophils in the experiment [Figure 2.6].

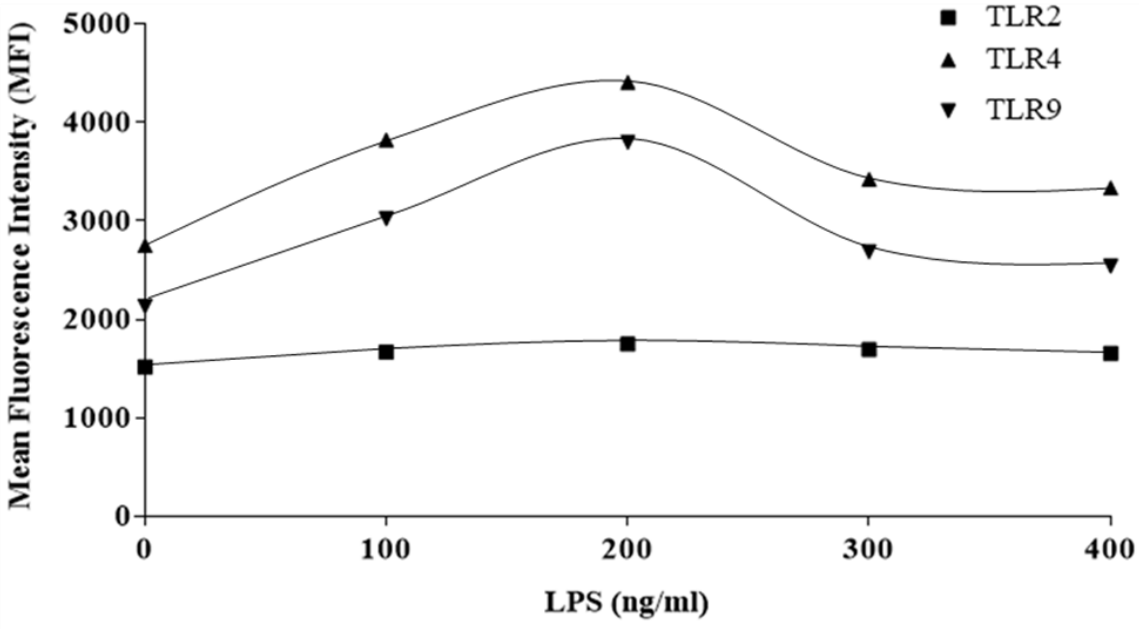

Figure 2.4: Titration curve of LPS used for determining the dose required for ex-vivo stimulation of neutrophil TLRs.

2.15.3. Ammonium chloride

A 1M (53.49 g/litre) ammonium chloride (NH_4Cl) was freshly prepared by dissolving the salt in de-ionised water. The optimal concentration of NH_4Cl was determined by measuring the changes in neutrophil TLR4 and TLR9. For this experiment, the whole blood from healthy controls was stimulated with different concentrations of NH_4Cl, ranging from 0 to 800µM. For a concentration of zero, PBS was used instead of NH_4Cl. Based on the results, the final concentration of 400µM NH_4Cl was determined to be the appropriate concentration required for stimulation of neutrophils in the experiment [Figure 2.7]. Although the highest concentration of ammonia amongst the PALF patients in this study was 234 µM, it was higher than the detectable range >286 µM in two patients, suggesting that the 400µM NH_4Cl used in the *ex vivo* studies would be representative of the pathophysiological levels observed in ALF. Following the two-hour incubation NH_4Cl did not change the pH and osmolality of the incubation medium. It was also reflected in the colour of the incubation media, which remained the same.

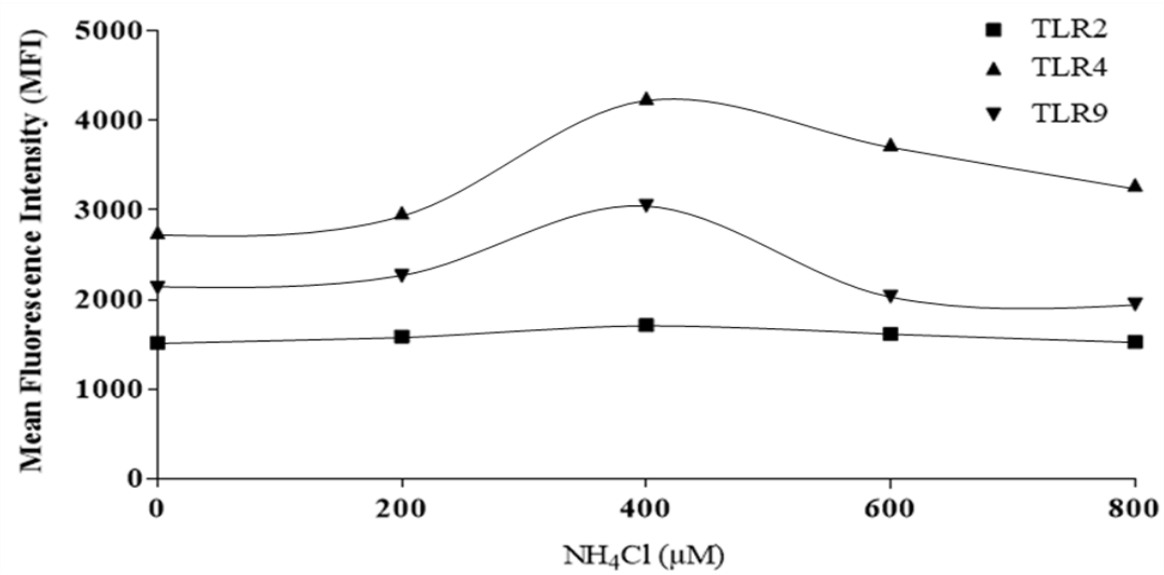

Figure 2.5: Titration curve of NH_4Cl used for determining the dose required for ex-vivo stimulation of neutrophil TLRs.

2.15.4. Oligodinucleotide 2395

According to the manufacturer's instruction, the concentration of oligodinucleotide (ODN) 2395 stock solution was 100 µM and the optimal concentration of ODN 2395 for *in-vitro* experiments was 0.1 to 1 µM. The optimal concentration of ODN 2395 for this experiment was determined by measuring the changes in neutrophil intracellular IL-8 and TLR9. The whole blood from healthy controls was stimulated with different concentrations of ODN 2395 ranging from 0 to 1 µM (0 – 1000 nM). For a concentration of zero, PBS was used instead of ODN 2395. Based on the results, the final concentration of 0.25µM (250 nM) ODN 2395 was determined to be the appropriate concentration required for stimulation of neutrophils in the experiment [Figure 2.8].

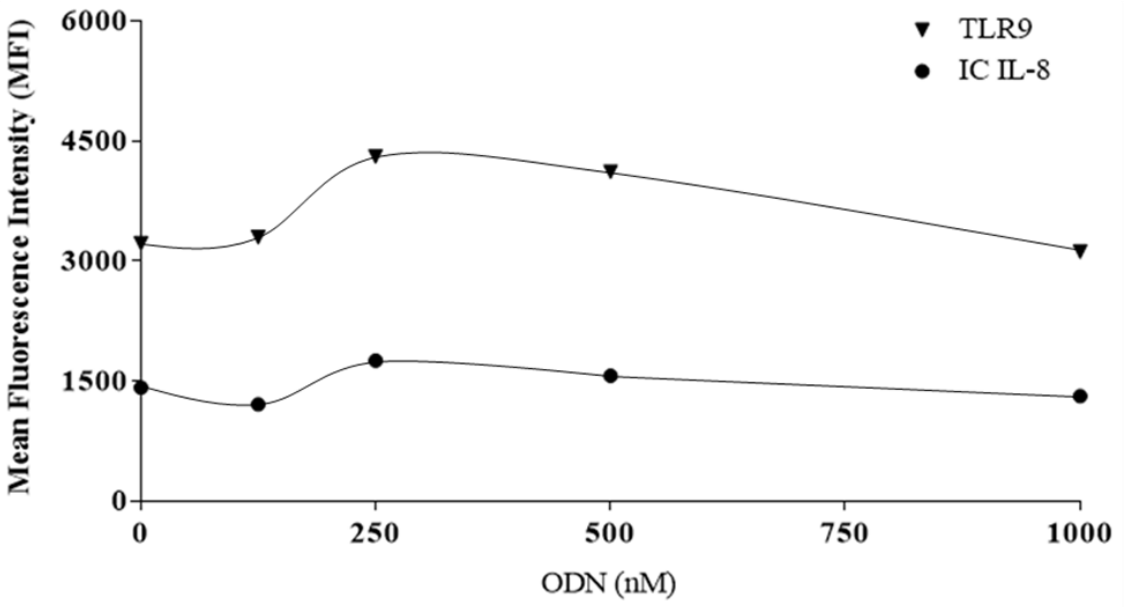

Figure 2.6: Titration curve of ODN2395 used for determining the dose required for ex-vivo stimulation of neutrophil TLR9 and IL-8.

2.16. *Ex-vivo* stimulation of neutrophils with IL-8 and NH_4Cl

To examine the effect of IL-8 and ammonia on TLR9 expression, healthy neutrophils were incubated at 37°C with RPMI and stimulated either with different concentrations of recombinant IL-8 (125, 250 and 500 pg/mL) or in combination with NH_4Cl (400µM) for 2 hours; PBS was used as a control. These IL-8 concentrations were chosen to reflect the levels of IL-8 measured in patients with PALF; the highest levels being observed in those with high-grade SIRS. For the purposes of this study, the SIRS score of patients with PALF has been classified as either low SIRS score (0 – 1) or high SIRS score (2 – 4). Futhermore, the HE of PALF patients have been classified as either mild HE (grade 0 – 2) or advanced HE (grade 3/4). The different concentrations of IL-8 and/or NH_4Cl used to stimulate 100 µL of whole blood and 380 µL of RPMI are given in table – 2.1.

Table 2.1: Stimulation of healthy neutrophils with various concentrations of IL-8 and NH_4Cl

Tubes	Whole blood	RPMI	PBS	IL-8	NH_4Cl
Tube – 1	100 µL	380 µL	25 µL	--	--
Tube – 2	100 µL	380 µL	--	--	400 µM
Tube – 3	100 µL	395 µL	--	125 pg/mL	--
Tube – 4	100 µL	375 µL	--	125 pg/mL	400 µM
Tube – 5	100 µL	395 µL	--	250 pg/mL	--
Tube – 6	100 µL	375 µL	--	250 pg/mL	400 µM
Tube – 7	100 µL	395 µL	--	500 pg/mL	--
Tube – 8	100 µL	375 µL	--	500 pg/mL	400 µM

After two hours of incubation, the whole blood treated with different kinds of IL-8 and NH_4Cl were centrifuged at 600g for 5 minutes at 18°C and the supernatant was discarded leaving the cell pellet at the bottom of the tube. The red blood cells were then lysed and white blood cells were stained for flow cytometry. The panel of antibodies used for characterising neutrophil phenotype after stimulation with IL-8 and NH_4Cl are given in *appendix table – 2*.

2.17. *Ex-vivo* neutrophil TLR9 stimulation with patient plasma

To examine the influence of PALF plasma and endogenous DNA on TLR9 expression, healthy neutrophils were isolated and incubated with different PALF patient plasma samples for 2 hours, with and without pre-treatment of DNAse-I (5µg). The cells were then analysed by flow cytometry. To examine the effect of patient plasma on healthy neutrophils, whole blood was collected from HC; 750, 000 ($7.5x\ 10^5$) neutrophils were isolated and incubated at 37°C with 100 µL of patient plasma for 2 hours. Granulocytes were isolated from whole blood using Polymorphprep™ solution as mentioned previously. The ratio of neutrophils and patient plasma was determined by calculating the average neutrophil count in PALF patients. To determine the influence of endogenous DNA on neutrophil TLR9, patient plasma was pre-treated with DNAse-I (5µg) for 30 minutes at 37°C before incubating them with healthy neutrophils separately. The time and concentration of DNAse-I enzyme were optimised based on the assays performed in the lab. Following the 2 hour incubation, cells were washed with PBS and stained with antibodies and analysed by flow cytometry. The panel of antibodies used for characterising neutrophil phenotype and IL-8 expression in neutrophils are given in *appendix table – 2*.

2.18. Cytokine level determination

Pro- and anti-inflammatory cytokines [CXCR-8/IL-8, IL-6, IL-10 and TNF-α] levels were determined from previously stored plasma and supernatant samples using cytometric bead array (CBA). Cytokine levels were quantified using the capture and detection beads from different Human Soluble Protein Flex Sets and a Master Buffer Kit. The advantage of using a CBA is it measures multiple cytokines with fewer sample dilutions in a short time. There was no variability between the experiments, since all the samples were analysed in a single batch.

2.18.1. Preparation of standards

CBA top standards are lyophilised standard spheres which were reconstituted and serially diluted and prepared fresh just before the experiment. A lyophilised standard sphere from the flex set of each cytokine to be tested, IL-6, IL-8, IL-10 and TNF-α were pooled into one 15 mL polypropylene tube and reconstituted with assay diluent. The reconstituted standards were allowed to equilibrate for 15 minutes at RT followed by gentle mixing using a pipette. A serial dilution was performed by transferring 500 µL of top standard with equal volume of assay diluent to 1:2 dilution and then further up to 1:256. Assay diluent was used to serve as the 0-pg/mL.

2.18.2. Preparation of capture and detection beads

Based on the instruction manual provided by the manufacturer, equal volumes (50µL) of capture bead and detection bead were used for testing the plasma or supernatants and the beads were 50x concentration. After optimising this experiment in our laboratory, I found that the capture and detection beads yield a good result when diluted 100 times. All the beads were mixed using a vortex for 15 seconds just before use.

2.18.2.1. Capture bead

The procedure for capture beads preparation was different for supernatant samples compared to the plasma, therefore the total bead volume was calculated based on the number of samples (including standards) and cytokines measured for each experiment.
For plasma samples:

The appropriate amount of capture beads (as shown below) from the stock vials of each Human Soluble Protein Flex Set were pooled into a 15-mL polypropylene tube and 0.5 mL of wash buffer was added to them. The tube was then centrifuged at 200 g for 5 minutes and the supernatant was discarded by carefully aspirating it without disturbing the bead pellet. The bead pellet was then re-suspended in capture bead diluent to a final concentration of 50 µL / test.

An example calculation:
No. of tests – 50; Volume of capture beads from each flex set – 25 µL; No. of flex sets (cytokine beads) – 4; final concentration – 50 µL
Therefore Total bead volume = 50 No. of tests x 50 µL of final concentration = 2500 µL

For supernatants:

The appropriate amount of capture beads (as shown below) from the stock vials of each Human Soluble Protein Flex Set were pooled into a 15-mL polypropylene tube and mixed with capture bead diluent. The final concentration of capture bead volume was 50 µL / test. The volume of the capture bead diluent was calculated by subtracting the volume for each bead tested from the total bead volume required for the assay.

An example calculation:

No. of tests – 50; volume of capture beads from each flex set – 25 µL; final concentration – 50 µL; No of flex sets (cytokine beads) – 4

Total bead volume = No. of tests – 50 x Final concentration – 50 µL = 2500 µL

So when 4 cytokines were tested, diluent volume = 2500 µL – (25 µL x 4) = 2400 µL

2.18.2.2. Detection bead

The procedure for detection bead preparation was the same for supernatant samples and plasma. Therefore the appropriate amount of detection beads (as shown below) from the stock vials of each Human Soluble Protein Flex Set were pooled into a 15-mL polypropylene tube and mixed with detection bead diluent. The final concentration of detection bead volume was 50 µL/test. The volume of the detection bead diluent was calculated by subtracting the volume for each bead tested from the total bead volume required for the assay.

An example calculation:

No. of tests – 50; Volume of detection beads from each flex set – 25 µL; No of flex sets (cytokine beads) – 4; Final concentration – 50 µL

Total bead volume = No. of tests – 50 x Final concentration – 50 µL = 2500 µL

When 4 cytokines were tested, diluent volume = 2500 µL – (25 µL x 4) = 2400 µL

2.18.3. Assay procedure

The assay was performed on tubes and 50 µL of flex standards starting from 0 to 2000 pg/mL (top standard) and plasma and supernatant samples were placed in FACS tubes. The mixed capture beads were vortexed for at least 5 seconds and 50 µL was added to

the standards and samples. The tubes were mixed gently and incubated at RT in darkness. After an hour, the mixed PE detection reagent was vortexed for at least 5 seconds and 50 µL was added to all the tubes. The tubes were mixed gently and left to incubate at RT in darkness. After two hours of incubation, 1 mL of wash buffer was added to all the tubes and centrifuged at 200g for 5 minutes. The supernatant was discarded carefully and the beads were re-suspended in 300 µL of wash buffer for flow cytometry analysis.

2.18.4. Sample acquisition and analysis

All samples were acquired in the BD FACS CantoII flow cytometer using the BD FACS DIVA software. Compensation was performed using the instrument setup beads provided along with the Master Buffer Kit, to avoid spectral overlap. Standards were acquired starting from negative or 0-pg/mL to top standard or 2000 pg/mL followed by the plasma or supernatant samples. Files were saved as FCS 3.0 and the results were analysed using the FCAP array software.

2.19. Neutrophil function

2.19.1. Neutrophil phagocytic activity

2.19.1.1. Principle and assay procedure

Neutrophil phagocytic activity (NPA) was determined using a Phagotest kit, using FITC-labelled opsonised *E. coli* bacteria. For this experiment, 100 µL of whole blood was incubated in a water bath at 37°C in darkness for 20 minutes with 20 µL of FITC labelled opsonized *E. coli* along with a control (PBS). Ice cold trypan blue was added to all the tubes and left at RT for 20 minutes to quench the fluorescence of bacteria attached to the

cell surface. Cells were washed with PBS by gently mixing with a pipette, centrifuged at 600g for 5 minutes and the supernatant was discarded. Red blood cells were lysed using a lysis buffer as mentioned previously. Four µL of fluorochrome conjugated antibody CD16 (PE) was added to the tube containing *FITC E. coli* and the control tube incubated at RT in darkness for 30 minutes. Cells were washed with 2 mL of PBS, centrifuged at 600g for 5 minutes and the supernatant was discarded to remove the excess antibody. Three hundred µL of PBS was added to all the tubes and acquired in a flow cytometer. A negative control tube (100 µL of whole blood) was treated in similar conditions without the addition of FITC-labelled *E. coli* and CD16-PE. An overview of the NPA experiment is summarised in Table – 2.2.

Table 2.2: Stimulation of neutrophils with *E. coli* to determine NPA.

	Negative	Tube – 1	Tube – 2
Whole blood	100 µL	100 µL	100 µL
FITC-labelled *E. coli*	--	--	20 µL
PBS	20 µL	20 µL	--
All tubes were incubated at 37°C in a water bath for 20 minutes			
Trypan blue (Quenching soln.)	100 µL	100 µL	100 µL
All tubes were left at RT in darkness for 20 minutes			
Red blood cell Lyse solution	1.5 mL	1.5 mL	1.5 mL
CD16 (PE)	--	4 µL	4 µL
PBS	4 µL	--	--

2.19.1.2. Flow cytometer set up for NPA experiment

In the DIVA software, a new experiment was created and the specimen tubes were labelled as negative, tube – 1 and tube – 2. In the inspector, settings were adjusted to show FSC-A, SSC-A, FITC and PE in the panel. In the global worksheet, a dot plot with FSC-A (X-axis) and SSC-A (Y-axis) was created. Cells in the negative tube were acquired and the FSC/SSC voltages were adjusted between 250 - 400 V to identify the white blood cells in the dot plot. The large population in the dot plot was identified as granulocytes [Figure 2.9]. Another dot plot with CD16-PE (X-axis) and SSC-A (Y-axis) were created showing the granulocytes. While cells from tube – 1 (without FITC *E. coli*) were acquired, granulocytes expressing CD16+ were gated and identified as CD16+ neutrophils. A histogram with FITC *E. coli* showing CD16+ neutrophils was created and voltages in the FITC channel were adjusted to show the CD16+ neutrophils over 10^2 in the FITC-histogram plot or CD16+ neutrophils showing an MFI of 100 ± 10 in the statistics view. In the histogram, an interval gate was fixed next to the population to identify the cells undergoing phagocytosis [Figure 2.10]. Cells from tube – 2 were acquired with the voltages adjusted based on tube – 1 to identify the neutrophils undergoing phagocytosis (%) [Figure 2.11].

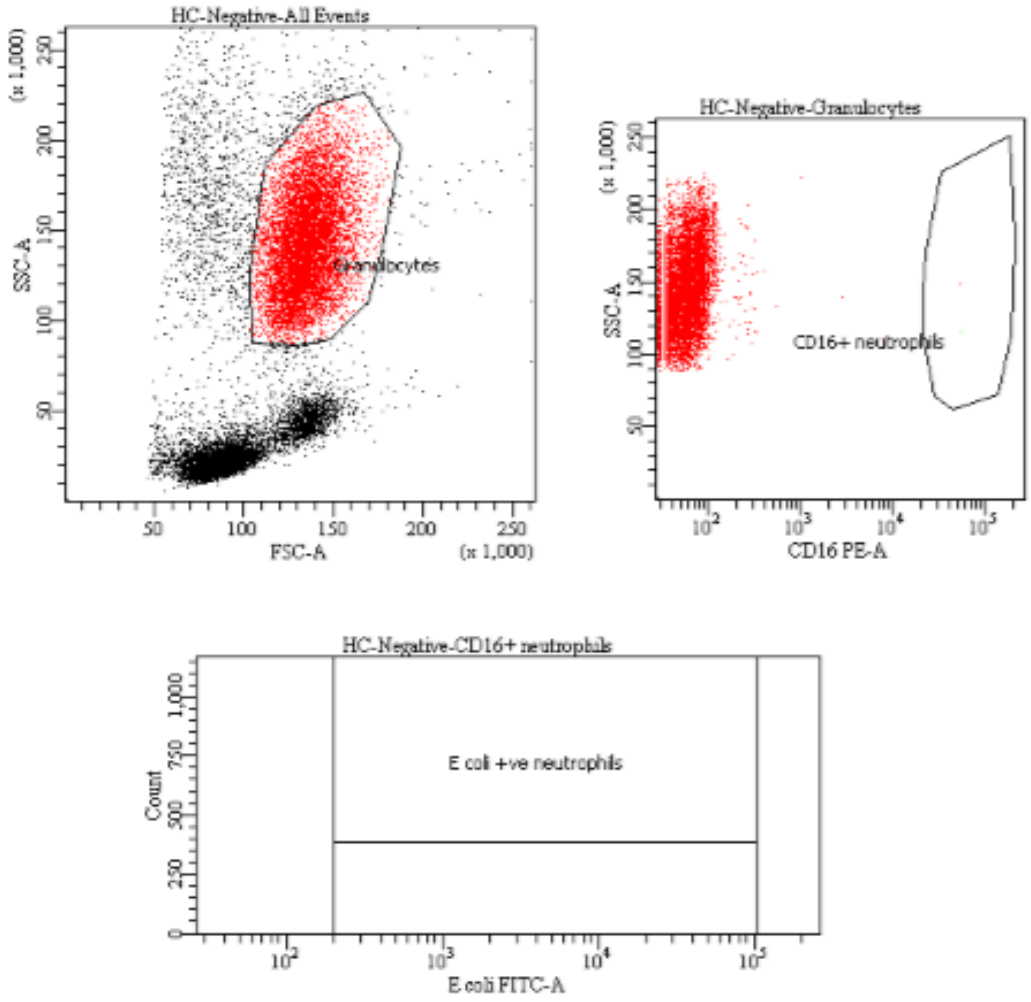

Figure 2.7: Image of dot plots and histogram from negative tube in NPA.

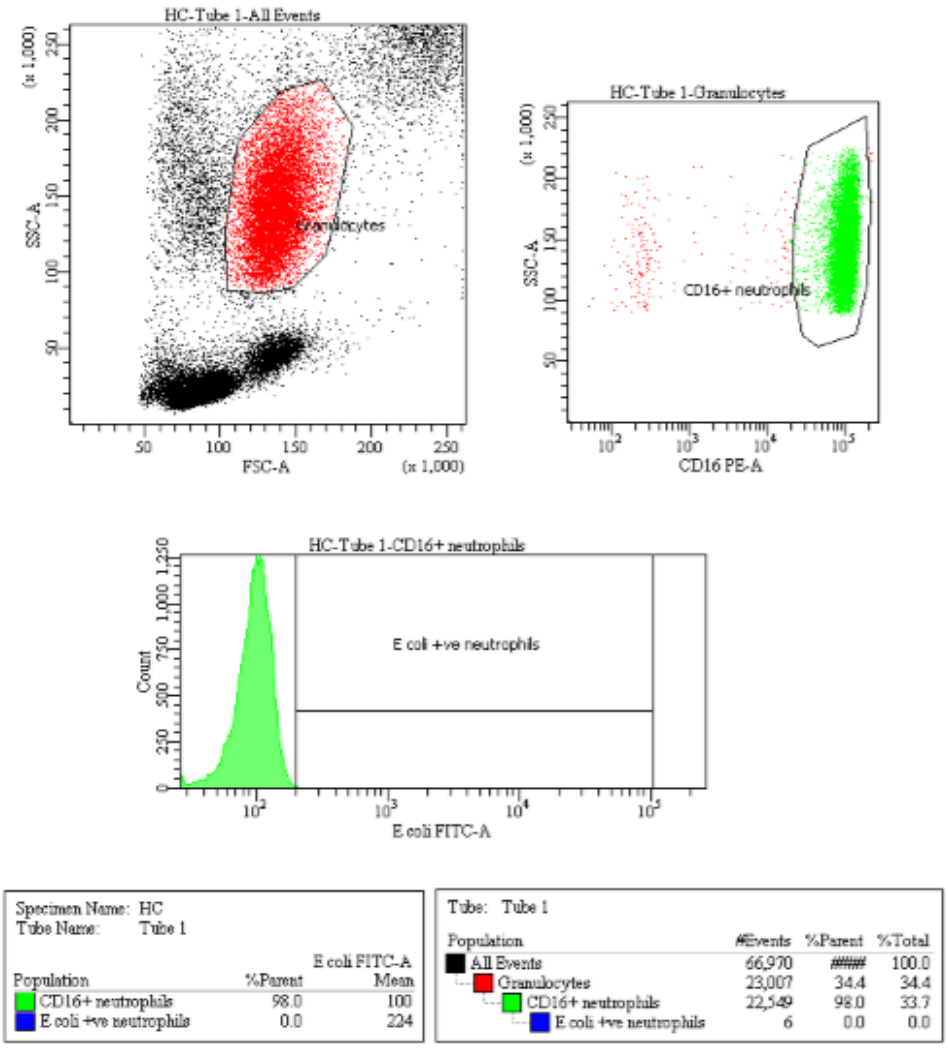

Figure 2.8: Image of dot plots and histogram from tube – 1 in NPA.

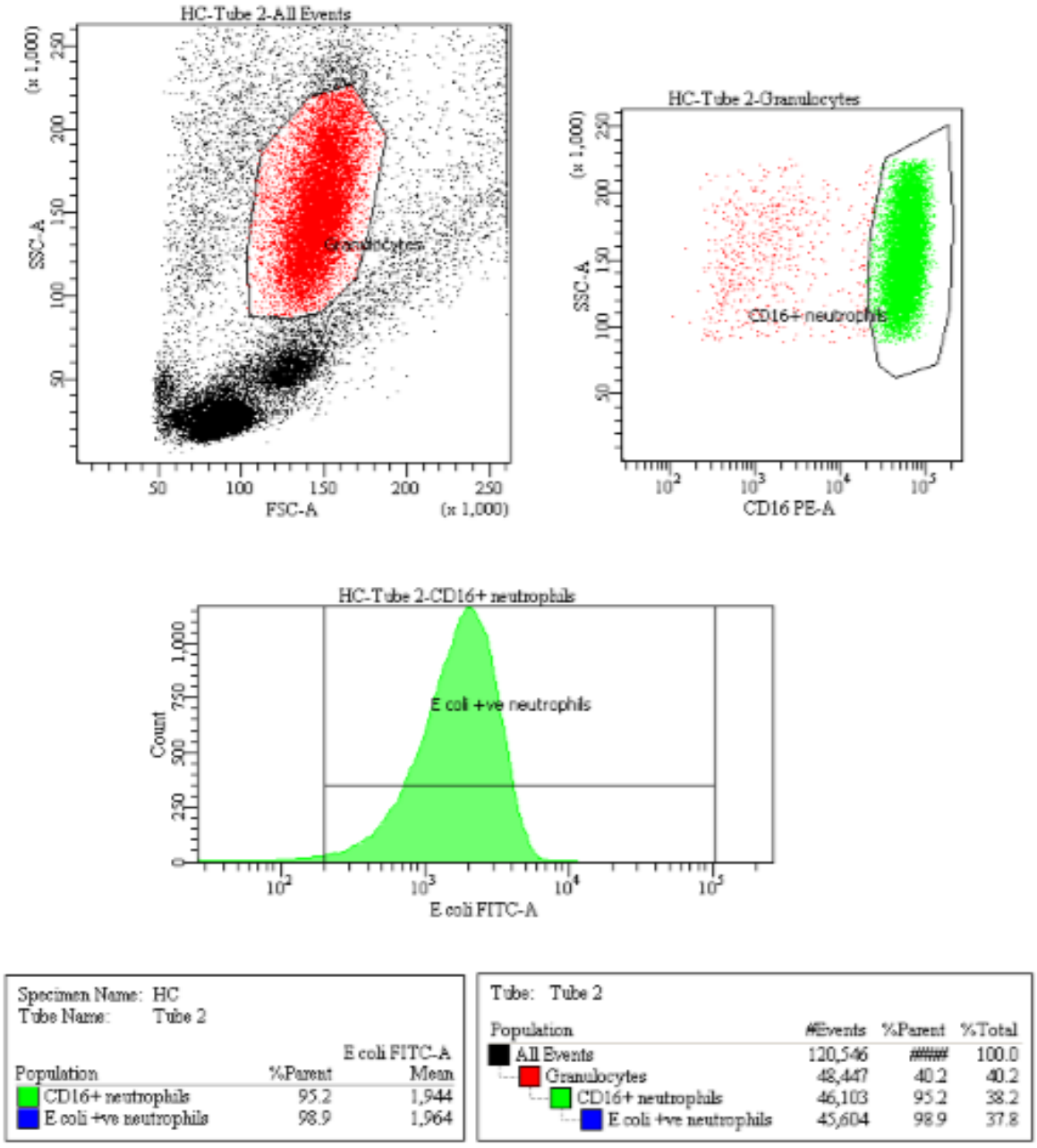

Figure 2.9: Image of dot plots and histogram from tube – 2 in NPA.

2.19.2. Phagoburst assay

2.19.2.1. Principle and assay procedure

Neutrophil oxidative burst (OB) was determined with a Burst kit using different stimulants and dihydrorhodamine as fluorogenic substrate. Reactive oxygen species (ROS) produced by phagocytic neutrophils convert dihydrorhodamine to rhodamine, therefore oxidative burst of neutrophils was determined by measuring the converted rhodamine using a flow cytometer indirectly.

Neutrophil low burst (LB) was assessed by stimulating the whole blood using 20 µL of chemotactic synthetic peptide, formyl-Met-Leu-Phe (fMLP) (0.2µM) and high burst (HB) was assessed by stimulating whole blood using 20 µL of PMA (0.2µM), a protein kinase C activator. Neutrophil phagoburst (PB) was assessed by stimulating the whole blood with 20 µL of *E. coli* ($2x10^7$) while spontaneous oxidative burst (SOB) was assessed by adding 20 µL of PBS to the whole blood. To measure the ROS production, 20 µL of dihydrorhodamine was added to all the tubes and incubated in a water bath at 37°C in darkness for 20 minutes. Whole blood without dihydrorhodamine was added to a tube separately as a control. Cells were washed with 1 mL of PBS by gently mixing with a pipette, centrifuged at 600g for 5 minutes and the supernatant was discarded. Red blood cells were lysed using a lysis solution as mentioned previously. Four µL of fluorochrome conjugated antibody CD16 (PE) was added to all the tubes and incubated at RT in darkness for 30 minutes. Cells were washed with 2 mL of PBS, centrifuged at 600g for 5 minutes and the supernatant was discarded to remove the excess antibody. Three hundred µL of PBS was added to all the tubes and acquired in a flow cytometer. A negative control (100 µL of whole blood) was treated in similar conditions without the

addition of dihydrorhodamine and CD16-PE. An overview of the neutrophil OB experiment is summarised in Table – 2.3.

Table 2.3: Stimulation with fMLP, PMA and *E. coli* to determine Neutrophil OB.

	Negative	Tube – 1	Tube – 2	Tube – 3	Tube – 4	Tube – 5
Whole blood	100 µL	100 µL	100 µL	100 µL	100 µL	100 µL
PBS	20 µL	20 µL	20 µL	--	--	--
fMLP	--	--	--	20 µL	--	--
PMA	--	--	--	--	20 µL	--
E. coli	--	--	--	--	--	20 µL
All tubes were incubated at 37°C in a water bath for 20 minutes						
Dihydrorhodamine	--	--	20 µL	20 µL	20 µL	20 µL
All tubes were incubated at 37°C in a water bath for 20 minutes						
Red blood cell Lyse solution	1.5 mL	1.5 mL	1.5 mL	1.5 mL	1.5 mL	1.5 mL
CD16 (PE)	--	4 µL	4 µL	4 µL	4 µL	4 µL

2.19.2.2. Flow cytometer set up for neutrophil oxidative burst experiment

In the DIVA software, a new experiment was created and the specimen tubes were labelled as negative, tube – 1, 2, 3, 4 and 5. In the inspector, settings were adjusted to show FSC-A, SSC-A, rhodamine and PE in the panel. In the global worksheet, a dot plot with FSC-A (X-axis) and SSC-A (Y-axis) was created. Cells in the negative tube were acquired and the FSC/SSC voltages were adjusted between 250 - 400 V to identify the white blood cells in the dot plot. The large population in the dot plot was identified as granulocytes. Another dot plot with CD16-PE (X-axis) and SSC-A (Y-axis) were created showing the granulocytes [Figure 2.12]. While cells from tube – 1 (without rhodamine) were acquired, granulocytes expressing CD16+ were gated and identified as CD16+ neutrophils. A histogram with rhodamine showing CD16+ neutrophils was created and voltages in the rhodamine channel were adjusted to show the CD16+ neutrophils over 10^2 in the rhodamine-histogram plot or CD16+ neutrophils showing an MFI of 100 ± 10 in the statistics view. In the histogram, an interval gate was fixed next to the population to identify the cells undergoing phagocytosis [Figure 2.13]. Cells from tube – 2 were acquired with the voltages adjusted based on tube – 1 to identify the neutrophils producing ROS (%) [Figure 2.14].

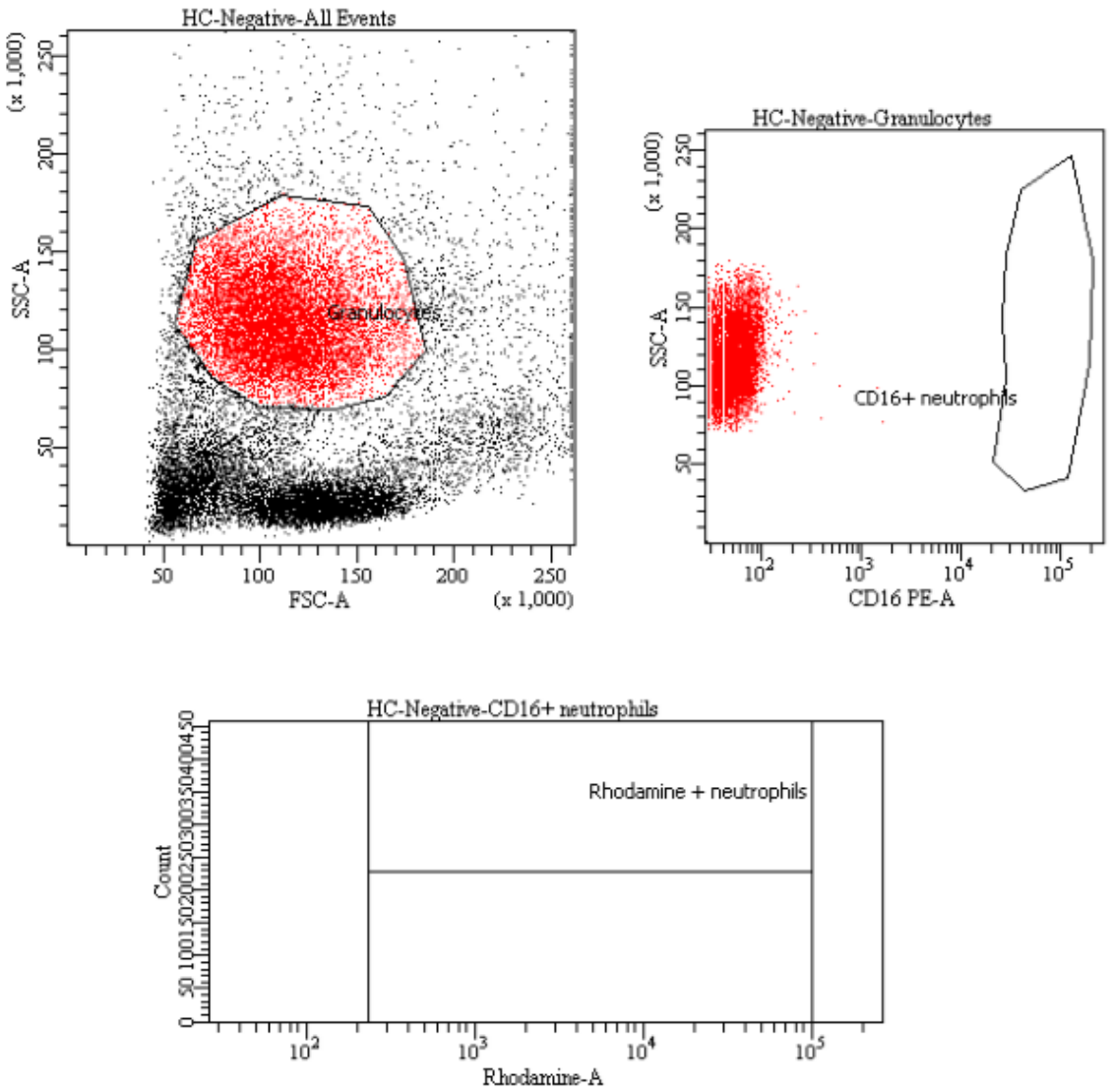

Figure 2.10: Image of dot plots and histogram from negative tube in Neutrophil OB.

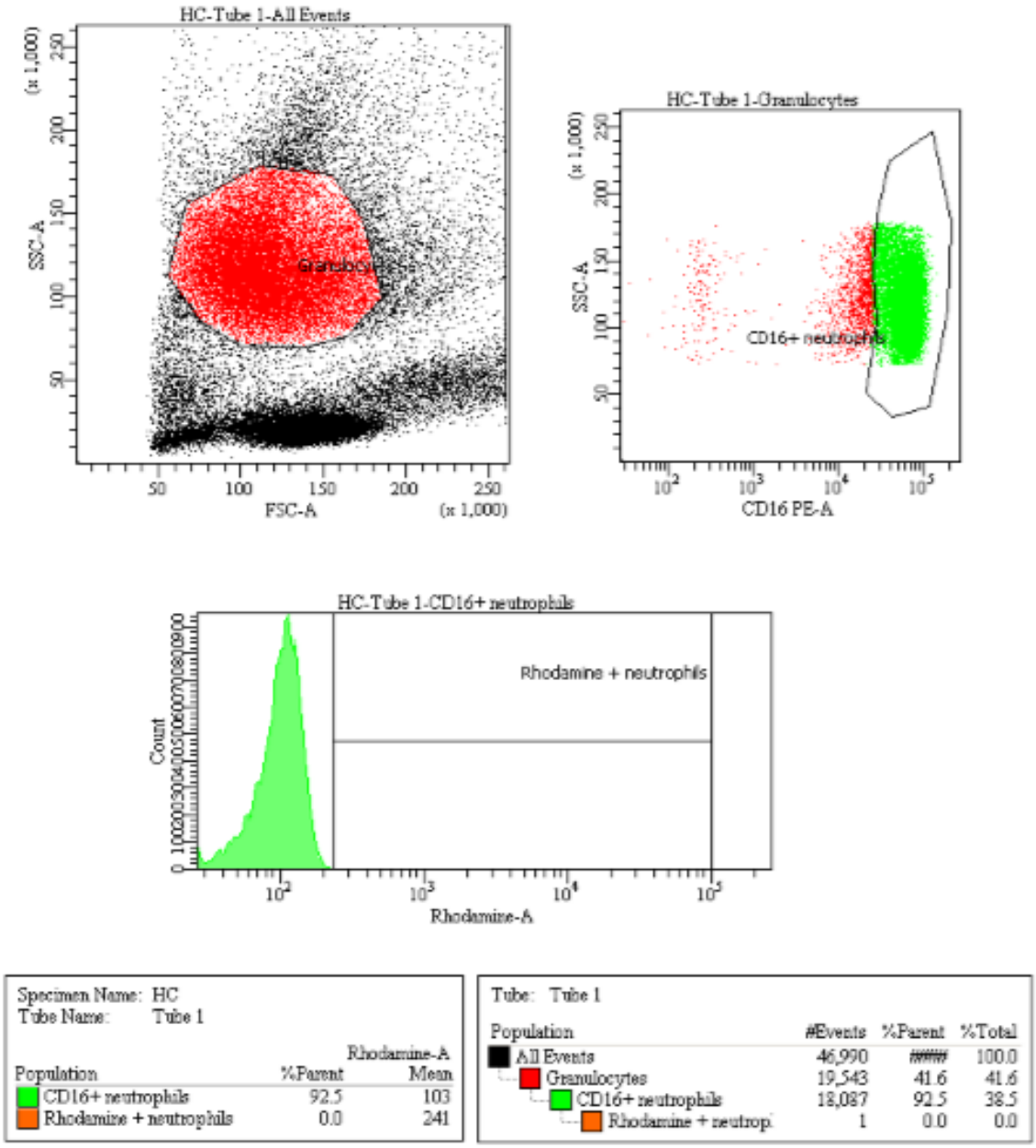

Figure 2.11: Image of dot plots and histogram from tube – 1 in Neutrophil OB.

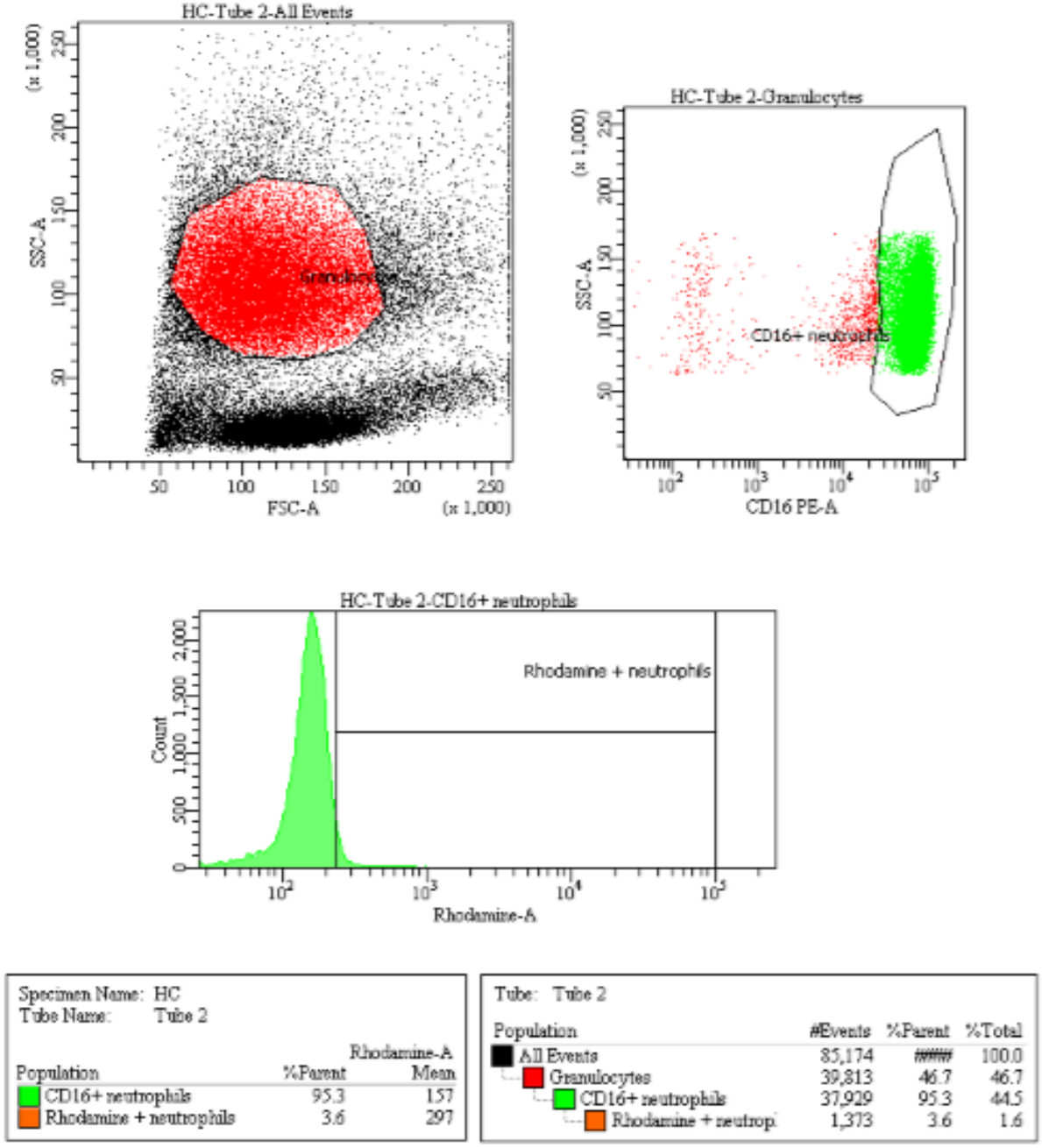

Figure 2.12: Image of dot plots and histogram from tube – 2 in Neutrophil OB.

2.20. Endotoxin measurement

Endotoxin levels were measured in the plasma samples stored at -80°C, using the Toxisensor Chromogenic Limulus Amoebic Lysate (LAL) Endotoxin Assay (Genscript, UK). This method detects endotoxin based on a chromogen using a modified LAL and a synthetic substrate. This kit is very sensitive and can measure from 0.005 to 1 endotoxin unit / mL (EU/mL). This assay was performed based on the protocol booklet provided along with the kit.

2.21. Animals used for *in-vivo* experiments

All the animals used for this experiment were bred and maintained at the animal facility in Yale University, USA. The animals used for this study were categorised under United States Department of Agriculture (USDA) category E of pain and distress. The experiments were performed and animals were sacrificed after obtaining the approval of the Institutional Animal Care and Use Committee (IACUC) at Yale University. All the animals were sacrificed under anaesthesia *(appendix table – 11)* and treated with minimal or no pain and distress.

For *in-vivo* experiments, C57/Black 6 (C57/B6) mice between seven to nine weeks of age were used. Four different strains, wild type (WT), $TLR9^{-/-}$, TLR9flox/flox LysCre ($TLR9^{fl/fl}$ LysCre) and TLR9flox/flox ($TLR9^{fl/fl}$) mice were used for this experiment. WT B6 mice were purchased from Jackson Laboratory (Bar Harbor, Maine, USA) and have been breeding and maintained by Li Wen's laboratory at the animal facility in Yale University for more than eight years. The original $TLR9^{-/-}$ B6 mice were obtained from Shizuo Akira, Japan, who originally developed this strain and the mice used for this experiment have been breeding and maintained by Li Wen's laboratory for more than 10

years. The original TLR9$^{fl/fl}$ B6 mice and TLR9$^{fl/fl}$ LysCre B6 mice were obtained from Prof Mark Schlomchik's laboratory at Pittsburgh University and the mice used for this experiment have been breeding and maintained at Li Wen's laboratory for more than 2 years.

2.22. Breeding and maintenance conditions

All animals were bred in specific pathogen-free (SPF) conditions and were fed on a regular chow diet with no other special needs. For breeding any particular strain, one male and two females were left in a separate cage until a female mouse became pregnant. The pregnant mother was then left in the same cage whilst the others were changed to a different cage. The mice used for breeding were not used for any experiment. The newborn pups were left with the mother until they were three weeks old. After three weeks of birth, mice were separated as male and females and left in different cages until the time of experiment. Only male mice were used for the experiment.

2.23. Mouse genotyping

Mice genotyping was usually performed within seven days of birth to identify the strain of each mouse. Since these strains have been maintained for a long time and many generations have been raised by this group, genotyping was performed only in the breeders. This was usually performed by an animal care technician on a regular basis; I performed this on some of the animals to learn this technique and also at other times when the technician was absent.

2.23.1. Isolation of DNA from the mouse tail

To perform genotyping, mice tails (~1cm) were clipped and placed in a 1.5 mL Eppendorf. The tail was then mixed with digesting buffer (500 µL) *(appendix table – 14)* and pronase (450 µg) and left in a 55°C water bath for overnight incubation. Saturated sodium chloride (1 litre) was added to the samples incubated overnight and mixed well after they were cooled in 4°C. Samples were then centrifuged at 16000g for 15 minutes at 4°C and the nucleic acid containing supernatant was transferred to another 1.5 mL tube. The tube was then filled with 100% ethanol and mixed by inverting the tube several times and the DNA was seen like a hair ball structure in the tube. The tubes were then centrifuged at 16000g for 15 minutes at 4°C and the supernatant was discarded. The DNA pellet was re-suspended with 70% ethanol (500 µL) and centrifuged at 16000g for 5 minutes at 4°C. The supernatant was discarded and the DNA pellet was left at RT until it was completely dry. The pellet was then re-suspended with 100 µL of de-ionised water and incubated in a water bath at 37°C for overnight and stored in 4°C.

2.23.2. Molecular genotyping

A PCR master mix comprising de-ionised water, buffer (1x), primers (100µM), dNTPs (10mM) and Taq DNA polymerase was prepared and placed in a 96-well PCR plate and added to the DNA extracted from the mice tail clipping. After mixing it by gentle pipetting, 10ul of the sample was loaded onto a 1% agarose gel with the respective positive and negative controls loaded on separate wells. The 1% agarose gel was prepared earlier by dissolving one gram of agar in 100 mL of de-ionised water by heating, 3 µL of ethidium bromide was added to the agar solution after it was cooled and poured on a tray and solidified. After running the samples for 20 minutes using

electrophoresis, a photograph of the gel was taken using a gel document. The samples positive for a particular genotype expressed a band similar to the positive control in the gel [Figure 2.15].

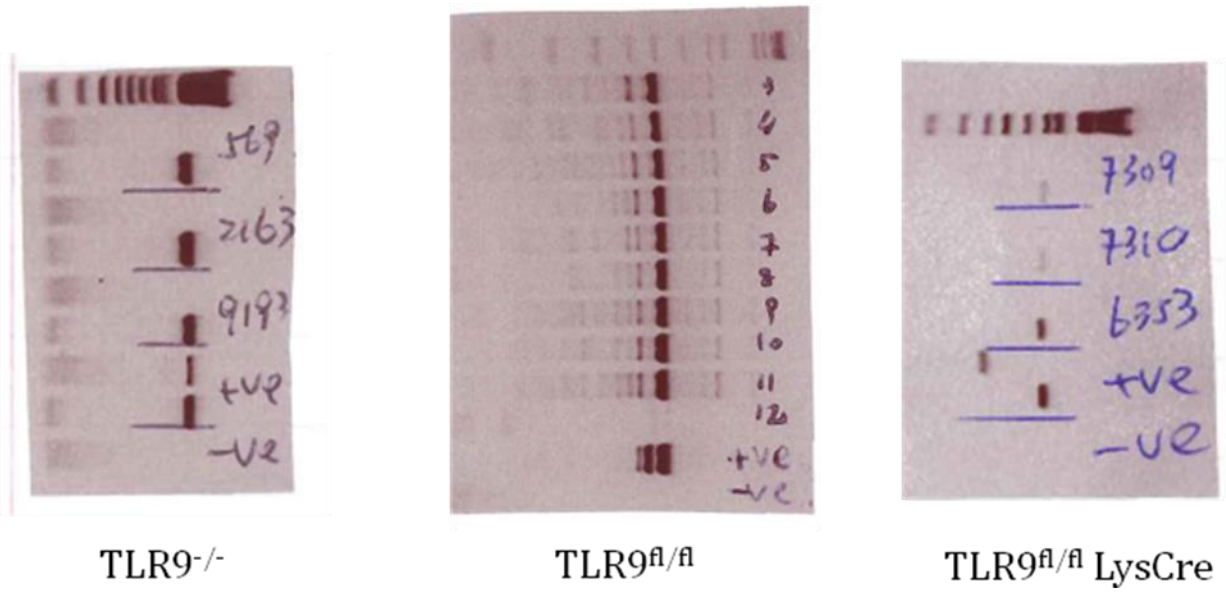

Figure 2.13: Gel images of TLR9$^{-/-}$ B6 mice, TLR9$^{fl/fl}$ B6 mice and TLR9$^{fl/fl}$ LysCre B6 mice to identify their genotype.

2.24. Stimulation with ammonium acetate

Stimulation with 12mmol/kg of ammonium acetate (NH_4COONH_3) (NH_4-Ac) in the mice resulted in severe convulsions and death. To determine whether TLR9 plays a role in the brain oedema in the mice, ammonium acetate (NH_4-Ac) (4 mmol/kg of bodyweight) was injected intraperitoneally and stimulated for six hours in wild type (WT) B6 mice, TLR9$^{-/-}$ B6 mice, TLR9flox/flox LysCre (TLR9$^{fl/fl}$ LysCre) mice and TLR9flox/flox (TLR9$^{fl/fl}$) mice.

2.24.1. Optimisation of ammonium acetate

Stimulation with 12 mM/kg of NH_4-Ac resulted in seizure and death of the WT-B6 mice, whereas 7 mM/kg caused immune cell death within 15 minutes. Therefore to optimise the concentration and time of NH_4-Ac required for *in-vivo* stimulation, different concentrations of NH_4-Ac between 1 and 4 mM/kg were injected intraperitoneally in WT-B6 mice. Changes in neutrophil phenotype [TLR9] were measured using flow cytometry to determine the influence of NH_4-Ac at different time points up until 24 hours following the stimulation in those mice. There was no difference in pH in the plasma and urine samples collected before and after the stimulation of NH_4-Ac.

There was an increasing trend in the neutrophil TLR9 expression as measured by mean fluorescent intensity (MFI) following the stimulation of 1, 2, 3 and 4 mM/kg of NH_4-Ac with time until 6 hours and this returned to baseline after 8-hour time point. There was no difference in the neutrophil TLR9 expression between these concentrations [Figure 2.16]. Based on the results, 4 mM/kg of bodyweight of NH_4-Ac for 6 hours was used for the experiments. There was a decreasing trend in the neutrophil TLR4 expression as measured by mean fluorescent intensity (MFI) following the stimulation of 1, 2, 3 and 4

mM/kg of NH_4-Ac with time until 6 hours and this returned to baseline after 8-hour time point. There was no difference in the neutrophil TLR4 expression between these concentrations [data not shown].

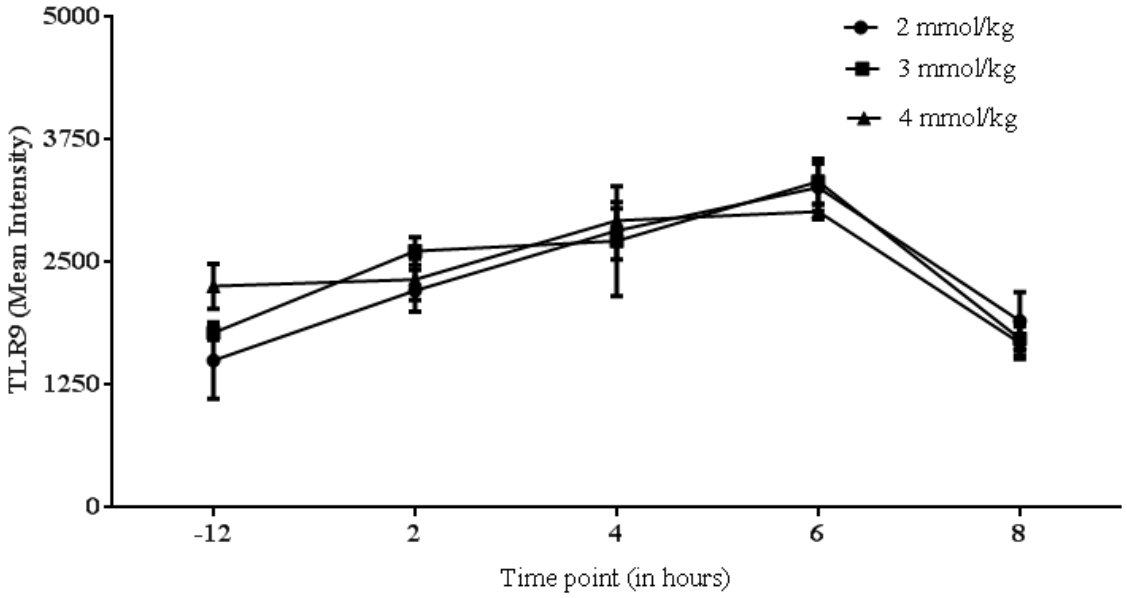

Figure 2.14: Titration curve showing the changes in neutrophil TLR9 MFI in mice following escalating doses of NH_4-Ac stimulation at different time points.

2.25. Stimulation with sodium acetate

To determine whether the brain oedema and inflammation were induced by ammonia per se and not influenced by acetate or changes in pH, sodium acetate (CH_3COONa) (Na-Ac) (4 mmol/kg of bodyweight) was injected intraperitoneally and stimulated for six hours in wild type (WT) B6 mice.

2.26. Blood collection and tissue harvesting

Six hours after the NH_4-Ac stimulation, mice were anaesthetised according to the guidelines. Blood was collected from the retro-orbital region using a heparinised blood tube and was stored at 4°C and cervical dislocation was performed after blood collection to ensure the animals were dead before the tissues were harvested. This method was performed mainly because this was easier for me and also this allowed me to harvest the brain used for the measurement of water content without containing any blood. Immediately after the mouse death the circulatory blood clots, therefore the liver was quickly injected with PBS (1x) using a 5 mL syringe and 25G needle through the portal vein to remove any circulating immune cells. The injected PBS was flushed from circulation by puncturing the systemic vein using a needle. Liver weight was measured using an electronic balance and the tissue was placed in ice-cold media (RPMI 1640), until they were processed further. Spleen and mesenteric lymph nodes (MLN) were harvested next and placed in ice-cold media, until they were processed further. Femur and tibia bones of the mice were collected and placed in ice-cold media, until they were processed further. The head of the mouse was cut separately from the body and placed in a petri dish at RT to harvest the brain.

2.26.1. Storage of plasma

Plasma was collected from the mouse blood and stored in a 1.5 mL Eppendorf at -80°C as mentioned previously.

2.26.2. Isolation of immune cells from tissues

2.26.2.1. Homogenisation and isolation of immune cells from liver

Liver tissue was homogenised using a plunge through a wire mesh. The homogenised tissue was then incubated with liver digestion solution *(appendix table 11)* for 45 minutes at 37°C in a water bath. The digested tissue was centrifuged at 600g for 5 minutes at 18°C and the supernatant was stored in -80°C. The sedimented pellet was mixed with 3 mL of 40% Polymorphprep™ solution *(appendix table 11)* and layered over 3 mL of 70% Polymorphprep™ solution *(appendix table 11)* in a 15 mL falcon tube. The tubes were then centrifuged at 1000g for 20 minutes at 18°C. The immune cells that formed a layer at the interface of the two density-gradient solutions were carefully isolated using a pipette. The isolated cells were then washed with 10 mL of PBS and centrifuged at 600g for 5 minutes at 18°C. The supernatant was discarded and cells were suspended in PBS (1x) and the viable cells were counted using Trypan blue as mentioned previously. The immune cells were then stained to determine the phenotype and intracellular cytokine production of T cells.

2.26.2.2. Homogenisation and isolation of immune cells from spleen

The spleen was cut into small pieces and the tissue was homogenised using the rough-edge of two grinding slides. The homogenised cells were centrifuged at 600g for 5 minutes at 18°C and the supernatant was discarded. The sedimented cell pellet was re-suspended and red blood cells were lysed using distilled water as mentioned previously. The cells were suspended in PBS (1x) and the viable cells were counted using Trypan blue. The immune cells were then stained with flow cytometry antibodies to determine

the phenotype and intracellular cytokine production of T cells, NK cells and macrophages.

2.26.2.3. Homogenisation and isolation of immune cells from MLN

The MLN were homogenised using the rough-edge of two grinding slides. The homogenised cells were centrifuged at 600g for 5 minutes at 18°C and the supernatant was discarded. Cells were re-suspended in PBS (1x) and the viable cells were counted using Trypan blue. The immune cells were then stained with flow cytometry antibodies to determine the phenotype and intracellular cytokine production of T cells.

2.26.2.4. Homogenisation and isolation of immune cells from bone marrow

To isolate the immune cells from bone marrow, the femur and tibia bones were flushed with PBS (1x) using a 3 mL syringe and 30G needle and the cells were then homogenised by mixing them using a syringe. The homogenised cells were centrifuged at 600g for 5 minutes at 18°C and the supernatant was discarded. The sedimented cell pellet was re-suspended and red blood cells were lysed using distilled water as mentioned before. The cells were suspended in PBS (1x) and the viable cells were counted using Trypan blue. The immune cells were then stained with flow cytometry antibodies to determine the phenotype of T cells and NK cells.

2.26.2.5. Processing of brain tissue

After removing the skin over the head, the skull was opened and the whole brain was carefully removed without any damage. The brain is divided into regions and the water content is assessed from different areas of the brain. Since I did not have the training to

handle the brain tissue, I chose to examine the whole brain. The entire brain was weighed immediately using an electronic balance to determine the wet weight. The brain was then dried in an oven at 100°C for 24 hours to obtain the dry weight. The brain water content was then calculated according to the formula:

$$\text{Brain water content (\%)} = \frac{\text{Wet weight} - \text{Dry weight}}{\text{Wet weight}} \times 100$$

2.26.2.6. Preservation of tissues for histopathological examination

For histopathological examination of animal tissues, the mice were anaesthetised and the abdomen was cut open from the neck to the intestine region. To remove the systemic blood, PBS (1x) was injected through the left ventricle and flushed by puncturing the right atrium. When the liver and lungs turned from red to pale, it was an indicator that the organs were flushed and were devoid of any blood. Ten percent formalin was injected through the left ventricle for ten minutes and the animal was left on the table for 30 minutes for the tissues to be fixed properly. Brain and liver were harvested and stored in a container with 10% formalin at RT. This method was performed to mainly isolate the brain tissues without any damage for histopathological examination. Specimens were then processed routinely, embedded in paraffin and stained with haematoxylin and eosin (H & E).

Immunohistochemistry for detection of TLR9 in astrocytes was performed using anti-TLR9 and S-100 (for astrocytes) antibodies.

2.27. Total DNA estimation

Total DNA was measured from the plasma samples stored in -80°C using the Quant-iT ™ PicoGreen® dsDNA quantitation assay according to the manufacturer instructions.

Each sample was analyzed by mixing the plasma in a black microtitre plate with the reagents provided in the kit. The plates were then read in a plate reader at emission wavelength of 520 nm and excitation wavelength of 480 nm.

2.28. TLR9 antagonist injection

To determine whether an inhibitor of TLR9 offers protective effect against NH_4-Ac stimulation, a TLR9 antagonist (ODN2088) (50 μG/mouse), or PBS, were injected intraperitoneally in WT-B6 mice immediately following NH_4-Ac injection, and 6 hours after the stimulation blood was collected and organs were harvested as mentioned previously. The time and concentration of ODN2088 were used based on the recently established mouse model of paracetamol hepatotoxicity [108].

2.29. Statistics

Patient demographics are expressed as median (inter-quartile range), frequency (percentage) as appropriate. Student t-test and Friedman's with Conover's multiple comparison tests are used for hypothesis testing. Mean and 95% confidence intervals are reported. Pearson's and Spearman's correlations were used for parametric and non-parametric data, respectively. In the animal studies, for comparisons between NH_4-Ac stimulated and control group or between two NH_4-Ac stimulated groups independent t-test or Mann-Whitney U test was used; for comparisons between three groups One-way ANOVA or Kruskal Wallis with Dunn's multiple comparison test was used based on the normal distribution of the data. All the results are reported as mean or median differences with 95% confidence intervals (C.I.). Hypothesis testing was two-tailed at an alpha level 0.05. All statistical analyses were performed using SPSS 20.0 for windows; $p<0.05$ was considered as statistically significant.

Chapter 3. Neutrophil TLR9 expression and the systemic inflammatory response in paracetamol-induced acute liver failure

This chapter aims to test the first hypothesis that circulating neutrophil TLR9 expression is increased in PALF patients with advanced hepatic encephalopathy and SIRS resulting from the release of necrotic hepatocyte products, ammonia, DNA and IL-8 into the circulation.

3.1. Basic study design

3.1.1. Patient demographics and clinical parameters

Twenty four patients with PALF were recruited and their baseline demographics, biochemical and physiological parameters are detailed in Tables 3.1 and 3.2. Amongst the PALF cohort seven patients (29%) fulfilled King's College Hospital criteria for poor prognosis [174], of whom five underwent successful LT, two died (one died two-days post-LT) and one recovered spontaneously following plasmapheresis. All patients were profoundly unwell with MOF and this was reflected by high organ failure scores. There was a significant decrease in arterial ammonia and Model for End-stage Liver Disease (MELD) score in PALF patients on days 4 and 7 compared to day 1. There was no difference in the ammonia concentrations and other biochemistry parameters in the patients based upon severity of HE or SIRS score. Even though microbial cultures were negative, all patients were treated empirically on admission with tazocin (piperacillin and tazobactam) 4.5 grams every 8 hours (substituted for meropenem 1 gram every 8 hours if penicillin allergic) and fluconazole 400mg once daily. All PALF patients were also treated with a continuous infusion of N-acetyl cysteine following ICU admission for up to 72 hours and managed as per published evidence-based guidelines [175].

Table 3.1: Demographic and clinical data for patients with PALF and HC

Number	HC (n=10)	PALF Day 1 (n=24)	PALF Day 4 (n=20)	PALF Day 7 (n=17)
Median Age (range)	29.5 (23.5 – 41)	36 (33 – 45)	35.5 (32.5 – 46)	35.5 (32.5 – 46)
Female (%)	3 (30%)	13 (54%)	11 (55%)	9 (53%)
Transplant-free 90 day survival (%)	-	22 (92%)	20 (100%)	17 (100%)
Met King's Criteria for LT (%) [a]	-	7 (29%)	1 (5%)	0
Declined LT due to co-morbidity (%)	-	0	0	0
Underwent LT (%)	-	5 (21%)	1 (5%)	0
Listed for LT but died before graft became available (%)	-	0	0	0
Listed but survived without LT	-	1 (4%)	1 (5%)	1 (5%)
Died (%)	-	2 (8%) [b]	0	0
Grade of encephalopathy (%) Grade 0-2 Grade 3-4	-	 12 (50%) 12 (50%)	 9 (45%) 11 (55%)	 9 (53%) 8 (47%)
SIRS score (%) Score: 0-1 Score: 2-4	-	 11 (46%) 13 (54%)	 11 (55%) 9 (45%)	 8 (47%) 9 (53%)

Number requiring ventilation (%)	-	18 (75%)	11 (55%)	9 (53%)
Number requiring vasopressors (%)	-	18 (75%)	10 (50%)	9 (53%)
Number requiring hemofiltration (%)	-	21 (88%)	13 (65%)	11 (65%)

a - Fulfilled King's College Hospital Criteria for poor prognosis, b - one patient died post-LT

Abbreviations: Paracetamol-induced acute liver failure: PALF; Liver transplantation: LT

Table 3.2: Biochemical and organ failure parameters for patients with PALF.

Parameters **Median (Interquartile range)**	**PALF Day 1** **(n=24)**	**PALF Day 4** **(n=20)**	**PALF Day 7** **(n=17)**
Bilirubin (3-20 µmol/L)	78 (39.8 – 104)	133 (45.5 – 172)	141 (45.5 – 192.5) *
Albumin (35-50 g/L)	27 (24 – 30.8)	28 (25 – 29)	27 (24 – 28.5)
INR (0.9-1.2 Ratio)	6.7 (3.4 – 8.9)	1.7 (1.4 – 2) ****	1.2 (1.1 – 1.4) $$
Creatinine (45-120 µmol/L)	152.5 (80.3 – 232.5)	122 (70.5 – 176.5)	118 (90 – 201)
Sodium (135-145 mmol/L)	140 (137 – 146)	140 (138 – 145)	138 (136 – 140) *
C-reactive Protein (<5.0 mg/L)	10.8 (8.2 – 17.1)	31 (17.6 – 60.4)	46.5 (28.6 – 85.3) **
Aspartate aminotransaminase (10-50 IU/L)	5696 (3955 – 9289)	390 (167 – 521) ****	88 (71 – 124)
Arterial ammonia (<54 µmol/L)	111 (66 – 139)	69 (55 – 102) **	51 (19 – 56)
Total white blood cell count (4.0-11.0 x 10^9/L)	9.2 (5.4 – 11.7)	7.1 (4 – 9.4)	9.4 (6.5 – 14.4)
Neutrophil count (2.2-6.3 x 10^9/L)	8.8 (4.8 – 10.1)	5.7 (2.7 – 6.9)	7.3 (5.2 – 11.6)
Lymphocyte count (1.3-4.0 x 10^9/L)	0.4 (0.2 – 0.8)	0.9 (0.6 – 1.3) *	1.2 (0.9 – 1.6)
Lactate (0.5-2.2 mmol/L)	3 (2.3 – 4.3)	1.6 (1.1 – 2) *	1 (0.7 – 1.5) $

Arterial pH (7.38-7.42)	7.4 (7.35 – 7.45)	7.43 (7.39 – 7.45)	7.45 (7.4 – 7.48)
SIRS Score [36]	2 (1 – 2.75)	1 (1 – 2)	2 (0 – 3)
MELD Score [176]	37.9 (31.6 – 42)	23.7 (18.7 – 27.5) ****	19.1 (13.8 – 25.6) $
SOFA Score [168]	12 (10 – 15)	15 (10 – 18)	16 (13 – 16)
APACHE II Score [169]	19 (15 – 24)	21 (15 -24)	18 (14 – 20)

* - indicates the difference between PALF patients on day 4 compared to day 1. $ - indicates the difference between PALF patients on day 7 compared to day 4. *, $ - $p<0.05$; **, $$ - $p<0.01$; **** - $p<0.0001$

Abbreviations: Paracetamol-induced acute liver failure: PALF; Acute Physiology and Chronic Health Evaluation: APACHE; International Normalised Ratio: INR; Model for End-stage Liver Disease: MELD; Sequential Organ Failure Assessment: SOFA; Systemic inflammatory response syndrome: SIRS.

3.2. Neutrophil phenotype

In PALF, baseline neutrophil surface receptor expression of the FcγRIII molecule CD16 and the β-integrin CD11b (C3bi), which binds to the surface of opsonised microbes along with TLR2, -4 and -9 was determined on days 1, 4 and 7 and compared to HC. CD16 and TLR4 expression were significantly decreased in PALF patients on day 1 compared to HC ($p<0.0001$). There was no difference in CD16 expression between PALF patients on days 1, 4 and 7 [Figure 3.1]. There was no difference in CD11b expression in PALF patients compared to HC [Figure 3.2] [Method – 2.14.4.6].

Baseline neutrophil TLR4 expression was significantly decreased in PALF patients on day 1 compared to HC ($p<0.0001$). There was no difference in TLR4 expression between PALF patients on days 1, 4 and 7 [Figure 3.3]. Baseline neutrophil TLR9 expression was significantly increased in PALF patients on day 1 compared to HC ($p=0.0002$). There was no difference in TLR9 expression between PALF patients on days 1, 4 and 7 [Figure 3.4]. There was no difference in the baseline neutrophil TLR2 expression in PALF patients compared to HC [Figure 3.5].

3.3. Plasma endotoxin and cytokines

Cytokine levels were increased in PALF patients compared to HC. Plasma IL-8 ($p<0.0001$), IL-6 ($p<0.0001$) and IL-10 ($p=0.04$) were significantly increased in PALF patients on day 1 compared to HC. There was no difference in the cytokine levels between ALF patients on days 1, 4 and 7 [Figures 3.6 – 3.8] [Method- 2.18]. There was no association of cytokines with the recovery in patients with PALF on days 4 and 7. Endotoxin levels in sera of all PALF patients and HC were <0.01 EU/ml, the detectable limit set up by the manufacturer (data not shown) [Method – 2.20].

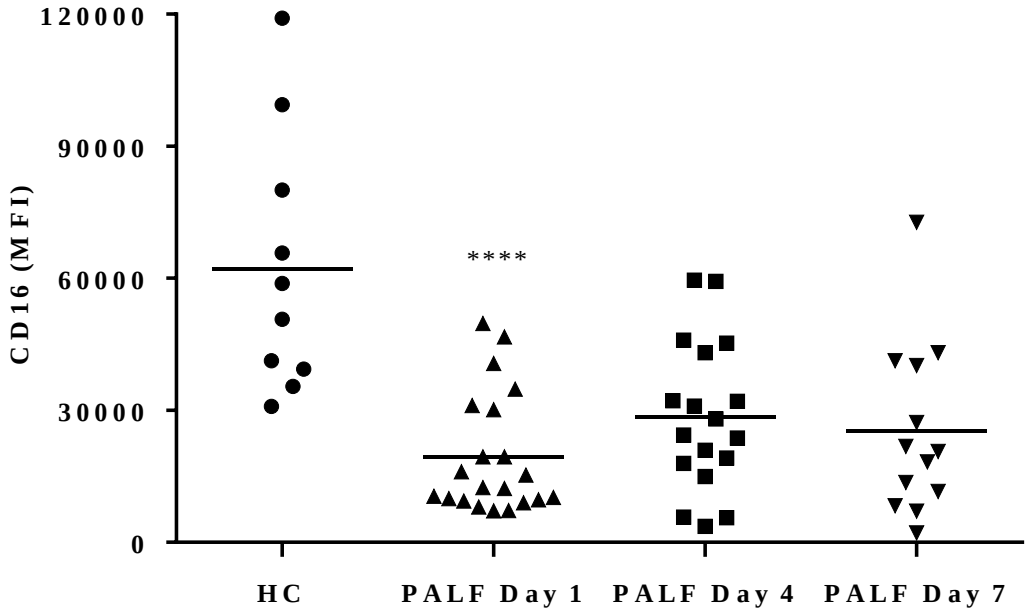

Figure 3.1: Decreased circulating neutrophil CD16 receptor expression in patients with PALF on day 1 compared to HC.

CD16 was significantly decreased in PALF on day 1 (n=21) compared to HC (n=10) (* - compared to HC; **** - $p<0.0001$) [mean: -42589; 95% C.I.: -58223 to -26594 and r^2-0.52]. There was no difference in the CD16 expression in PALF between days 1, 4 and 7. Normality assumptions were checked; $p<0.05$ were considered statistically significant. Student t-test (HC Vs PALF day 1) (normal data) and Friedman's with multiple Conover's testing (PALF day 1 Vs day 4 Vs day 7) (normal data) were used to analyse the data.

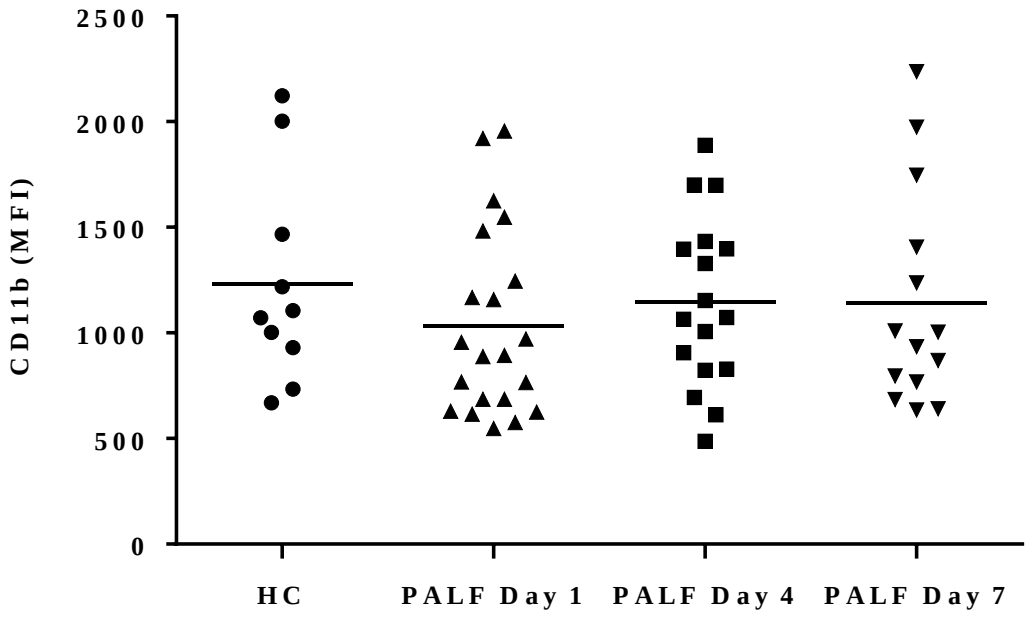

Figure 3.2: Circulating neutrophil CD11b receptor expression in patients with PALF on day 1 compared to HC.

There was no difference in the CD11b expression in patients with PALF on day 1 (n=21) compared to HC (n=10). Normality assumptions were checked; $p<0.05$ were considered statistically significant. Student t-test (HC Vs PALF day 1) (normal data) was used to analyse the data.

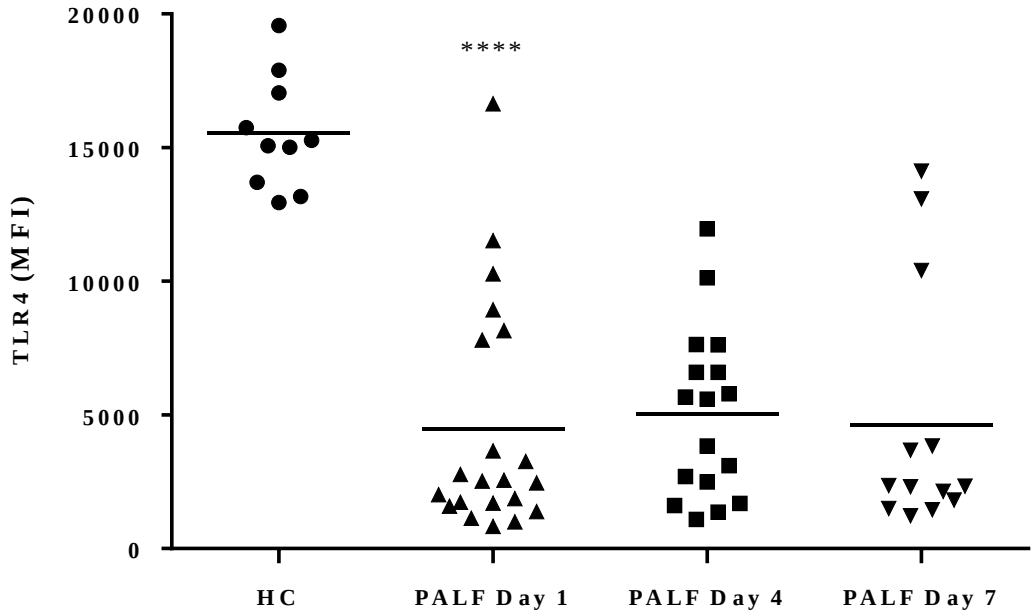

Figure 3.3: Decreased circulating neutrophil TLR4 expression in patients with PALF on day 1 compared to HC.

Neutrophil TLR4 was significantly decreased in PALF on day 1 (n=21) compared to HC (n=10) (* - compared to HC; **** - $p<0.0001$) [mean: -11075; 95% C.I.: -14047 to -8102 and r^2-0.67]. There was no difference in the TLR4 expression in PALF between days 1, 4 and 7. Normality assumptions were checked; $p<0.05$ were considered statistically significant. Student t-test (HC Vs PALF day 1) (normal data) and Friedman's with multiple Conover's testing (PALF day 1 Vs day 4 Vs day 7) (normal data) were used to analyse the data.

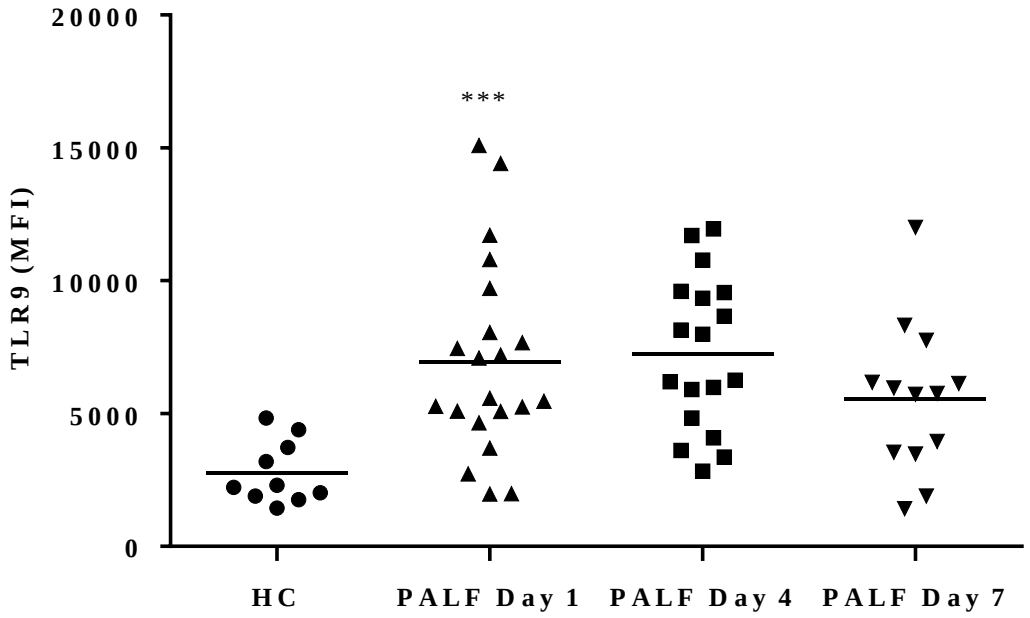

Figure 3.4: Increased circulating neutrophil TLR9 expression in patients with PALF on day 1 compared to HC.

Neutrophil TLR9 was significantly increased in PALF on day 1 (n=21) compared to HC (n=10) (* - compared to HC; *** - p=0.0002) [mean: 4176; 95% C.I.: 1727 to 6625 and r^2-0.3]. Normality assumptions were checked; $p<0.05$ were considered statistically significant. Student t-test (HC Vs PALF day 1) (normal data) and Friedman's with multiple Conover's testing (PALF day 1 Vs day 4 Vs day 7) (normal data) were used to analyse the data.

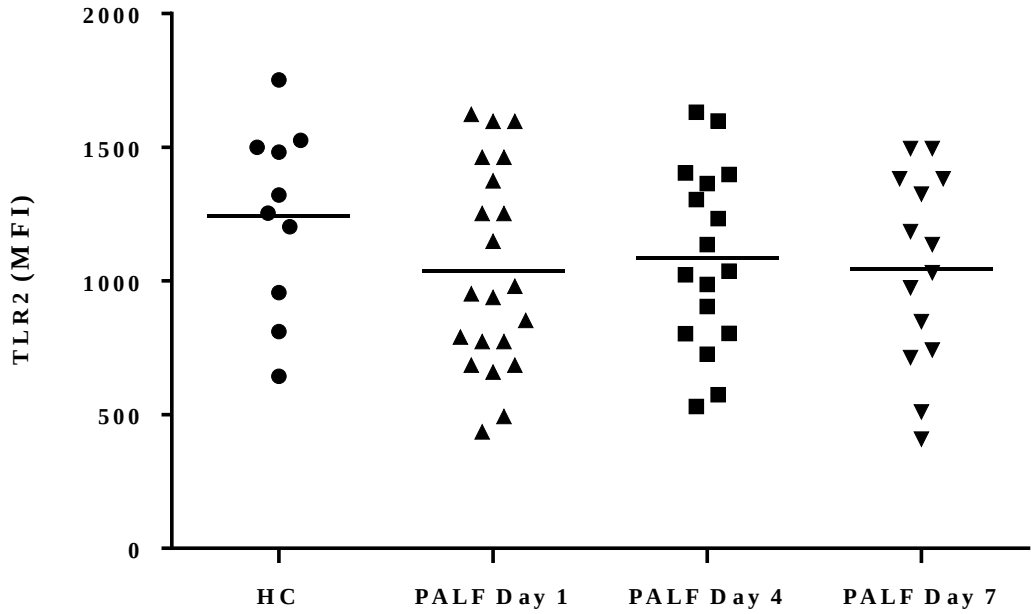

Figure 3.5: Circulating neutrophil TLR2 expression in patients with PALF on day 1 compared to HC.

There was no difference in the neutrophil TLR2 expression in patients with PALF on day 1 (n=21) compared to HC (n=10). Normality assumptions were checked; $p<0.05$ were considered statistically significant. Student t-test (HC Vs PALF day 1) (normal data) was used to analyse the data.

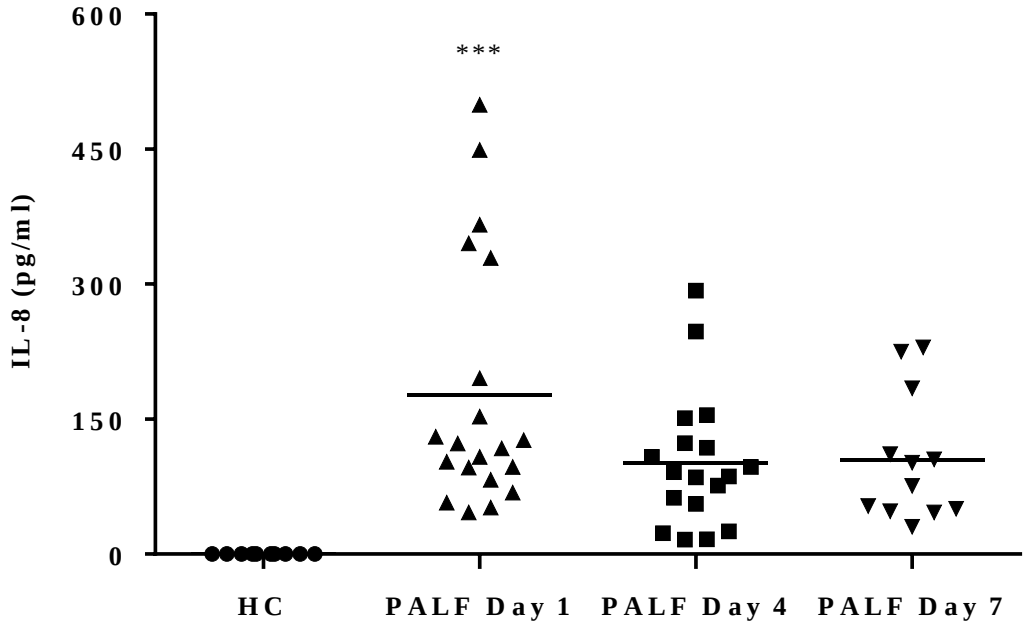

Figure 3.6: Increased circulating IL-8 in patients with PALF compared to HC.

Plasma IL-8 (pg/ml) measured using CBA was significantly increased in PALF on day 1 (n=21) compared to HC (n=10) (* - compared to HC; *** - p=0.0004) [mean: 177; 95% C.I.: 86 to 268 and r^2-0.36]. There was no difference in the plasma IL-8 level in PALF between days 1, 4 and 7. Normality assumptions were checked; $p<0.05$ were considered statistically significant. Student t-test (HC Vs PALF day 1) (normal data) and Friedman's with multiple Conover's testing (PALF day 1 Vs day 4 Vs day 7) (normal data) were used to analyse the data.

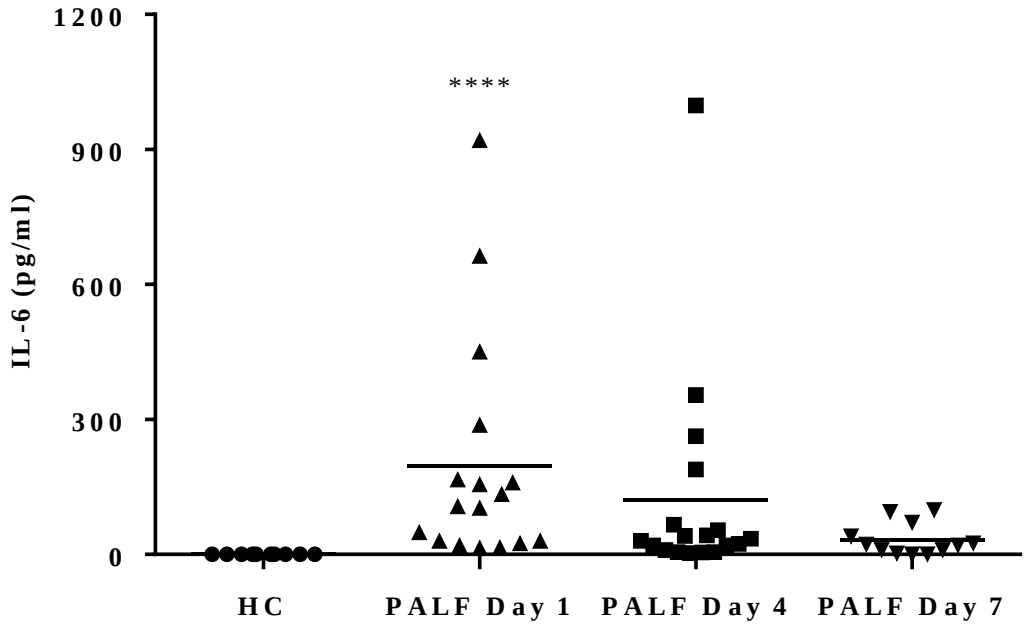

Figure 3.7: Increased IL-6 production in patients with PALF compared to HC.

Plasma IL-6 (pg/ml) measured using CBA was significantly increased in PALF on day 1 (n=21) compared to HC (n=10) ($p<0.0001$; * - compared to HC) [mean: 186; 95% C.I.: 21 to 351 and r^2-0.2]. There was no difference in the plasma IL-6 level in PALF between days 1, 4 and 7. Normality assumptions were checked; $p<0.05$ were considered statistically significant. Student t-test (HC Vs PALF day 1) (normal data) and Friedman's with multiple Conover's testing (PALF day 1 Vs day 4 Vs day 7) (normal data) were used to analyse the data.

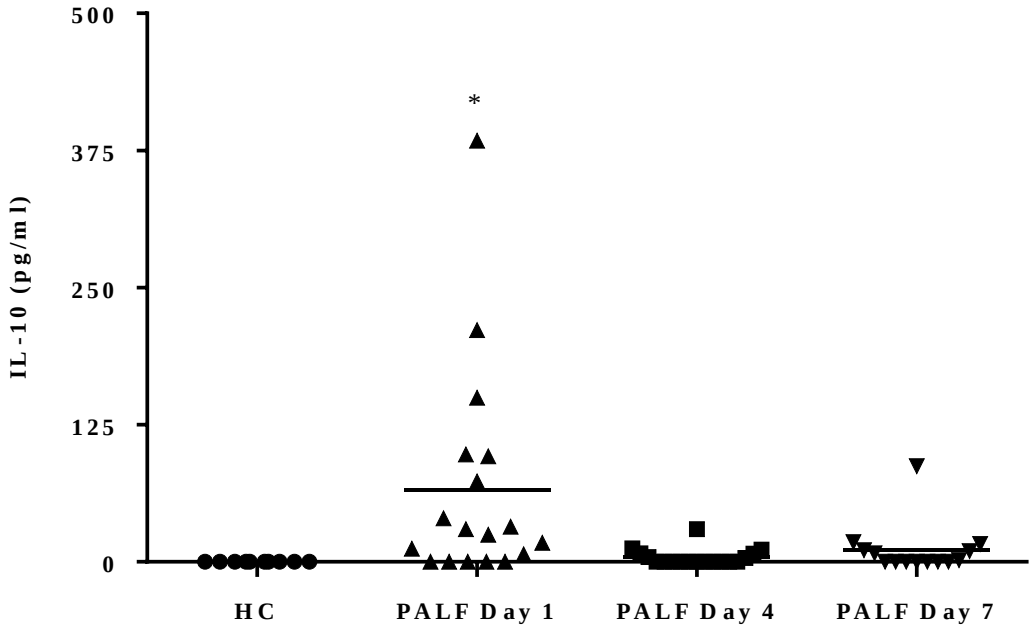

Figure 3.8: Increased IL-10 production in patients with PALF compared to HC.

Plasma IL-10 (pg/ml) measured using CBA was significantly increased in PALF on day 1 (n=21) compared to HC (n=10) (* - compared to HC; * - p=0.04) [mean: 65; 95% C.I.: 0.5 to 130 and r^2-0.15]. There was no difference in the plasma IL-10 level in PALF between days 1, 4 and 7. Normality assumptions were checked; $p<0.05$ were considered statistically significant. Student t-test (HC Vs PALF day 1) (normal data) and Friedman's with multiple Conover's testing (PALF day 1 Vs day 4 Vs day 7) (normal data) were used to analyse the data.

3.4. Relationship of TLR9 with ammonia and IL-8

There was a positive correlation between peak arterial ammonia and neutrophil TLR9 expression in patients with PALF on day 1 (r=0.63; p=0.005) [Figure 3.9]. There was also a positive correlation between plasma IL-8 and TLR9 in patients with PALF on day 1 (r=0.6; p=0.012) [Figure 3.10]. There was no significant correlation between neutrophil TLR4 expression and arterial ammonia or plasma IL-8 [Figures 3.11 and 3.12]. There was no correlation between arterial ammonia and plasma IL-8 levels (data not shown). As one patient underwent plasmapheresis before sampling and three patient's pre-haemofiltration ammonia level was not available, TLR9 expression in these patients was excluded from the analysis.

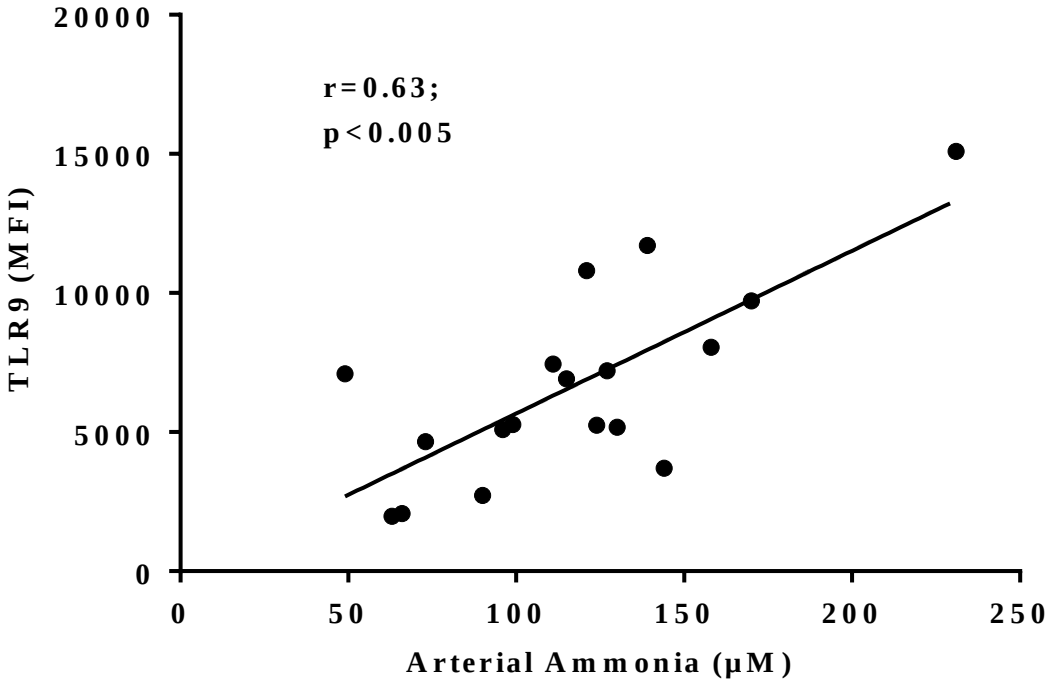

Figure 3.9: Correlation between neutrophil TLR9 expression and peak arterial ammonia in patients with PALF on day 1.

There was a direct correlation between peak arterial ammonia and TLR9 MFI in the PALF patients on day 1 (r=0.63; p=0.005) (Spearman's correlation) (non-normal data).

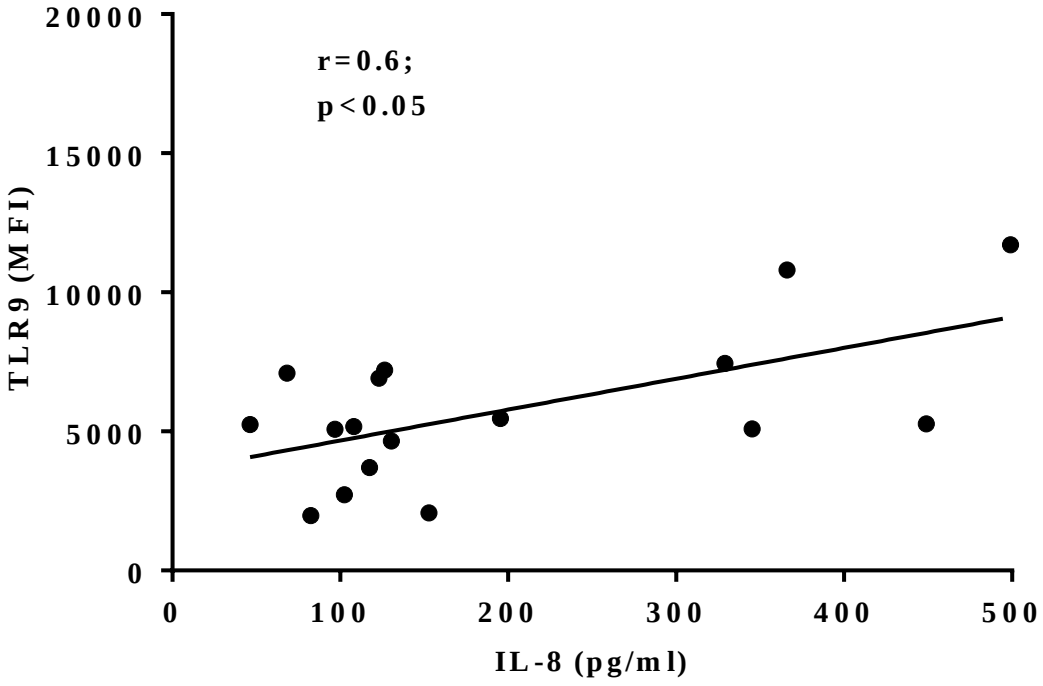

Figure 3.10: Correlation between neutrophil TLR9 expression and plasma IL-8 in patients with PALF on day 1.

There was a direct correlation between plasma IL-8 and neutrophil TLR9 MFI in PALF on day 1 (r=0.6; p=0.012) (Pearson's correlation) (normal data).

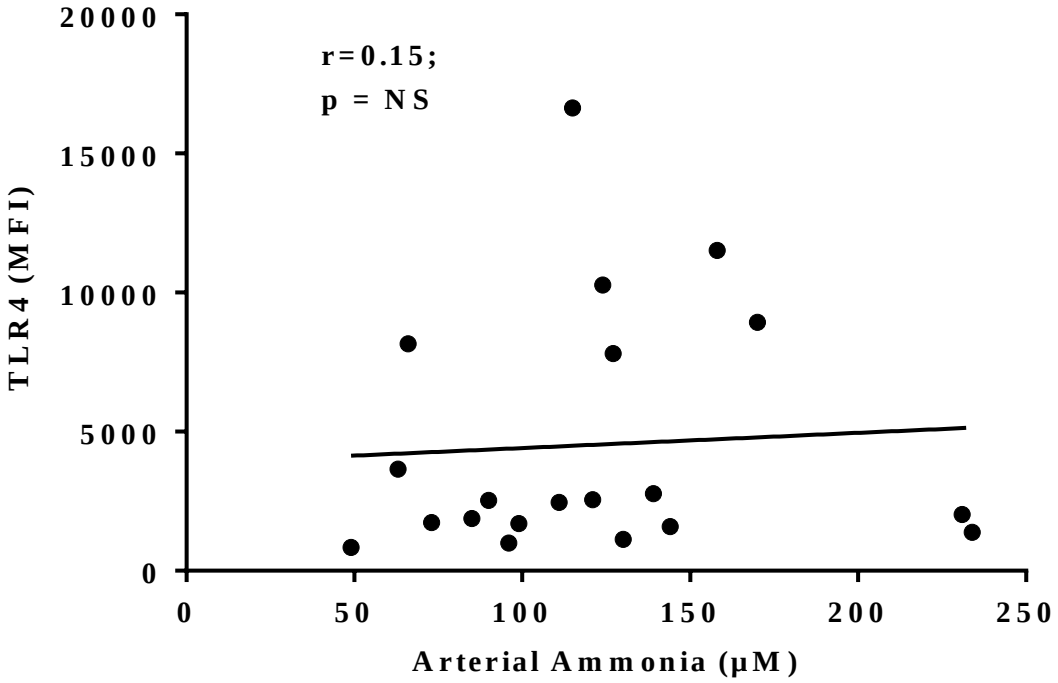

Figure 3.11: Relation between neutrophil TLR4 expression and peak arterial ammonia in patients with PALF.

There was no significant correlation between arterial ammonia and neutrophil TLR4 MFI in PALF on day 1.

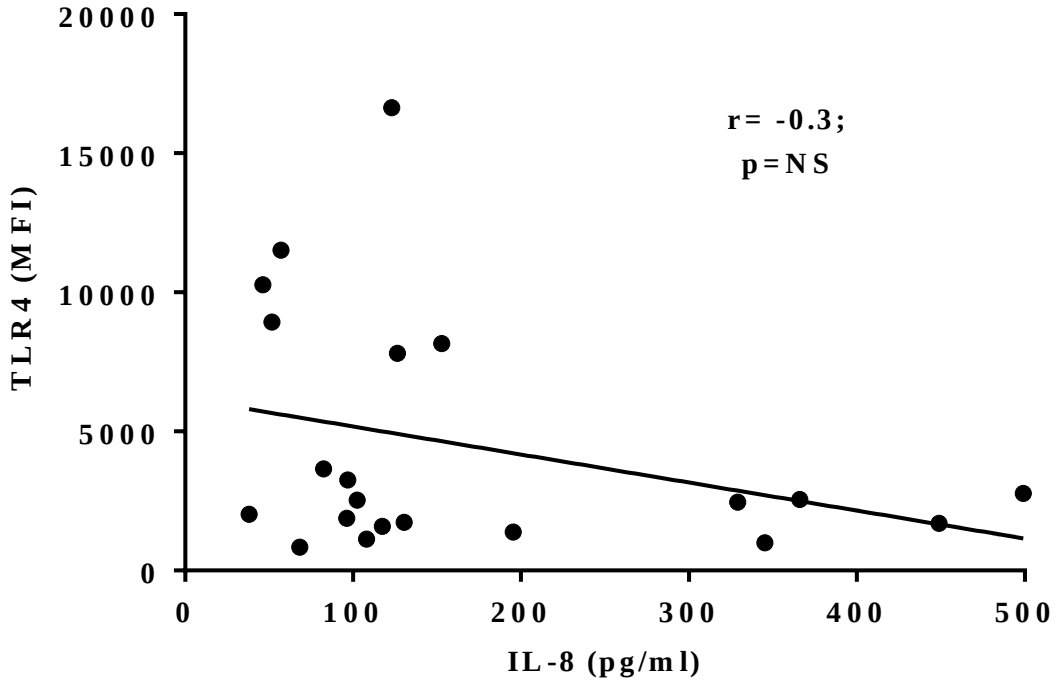

Figure 3.12: Relation between neutrophil TLR4 expression and plasma IL-8 in patients with PALF on day 1.

There was no significant correlation between plasma IL-8 and neutrophil TLR4 MFI in PALF on day 1.

3.5. Neutrophil TLR9 and IL-8 expression and severity of HE and SIRS score

The correlation between TLR9 and arterial ammonia and plasma IL-8 in PALF led us to investigate the association between severity of SIRS (scores: 0-1 versus 2-4) and (i) neutrophil TLR9 expression and (ii) plasma IL-8 concentration. Neutrophil TLR9 expression was significantly higher in patients with high SIRS score (2-4) on day 1 ($p=0.04$) and 7 ($p=0.007$), compared to those with low SIRS score (0-1) [Figure 3.13]. Neutrophil TLR9 expression was then compared amongst PALF patients cohorted based upon HE grade (grades: 0-2 versus 3/4). On day 1, TLR9 was significantly higher in patients with advanced (grade 3/4) HE compared to those with milder (grade 0-2) HE ($p=0.006$) [Figures 3.14 and 3.15]. Neutrophil TLR9 expression in relation to both SIRS score and HE grade was reflected in the plasma IL-8 levels. On day 1, plasma IL-8 was significantly higher in patients with SIRS score 2-4 or advanced HE (grade 3/4) compared to those with SIRS score 0-1 ($p=0.004$) or milder HE (grade 0-2) ($p=0.03$) [Figures 3.16 and 3.17]. There was no difference observed in other cytokines based upon SIRS score or HE grade. Amongst the PALF day 1 patients, 72.3% of those with low SIRS score developed mild HE and 75% of those with high SIRS score developed advanced HE [data not shown].

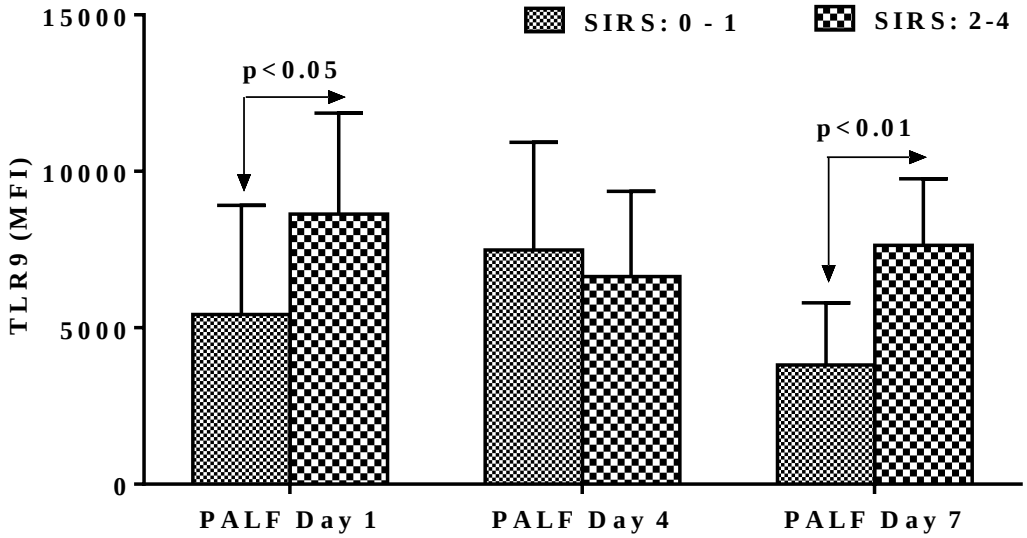

Figure 3.13: High SIRS score (2-4) was associated with increased neutrophil TLR9 expression in patients with PALF.

Neutrophil TLR9 expression was significantly increased in PALF patients with high SIRS score (2-4) on days 1 (n=11) (p=0.04) [mean: 3206; 95% C.I.: 129 to 6284 and r^2-0.2] and -7 (p=0.007), compared to low SIRS score (0-1) (n=11). Normality assumptions were checked and the data are expressed as mean with S.D.; p<0.05 were considered statistically significant. Student t-test (SIRS: 0 - 1 Vs SIRS: 2 - 4) (normal data) was used to analyse the difference.

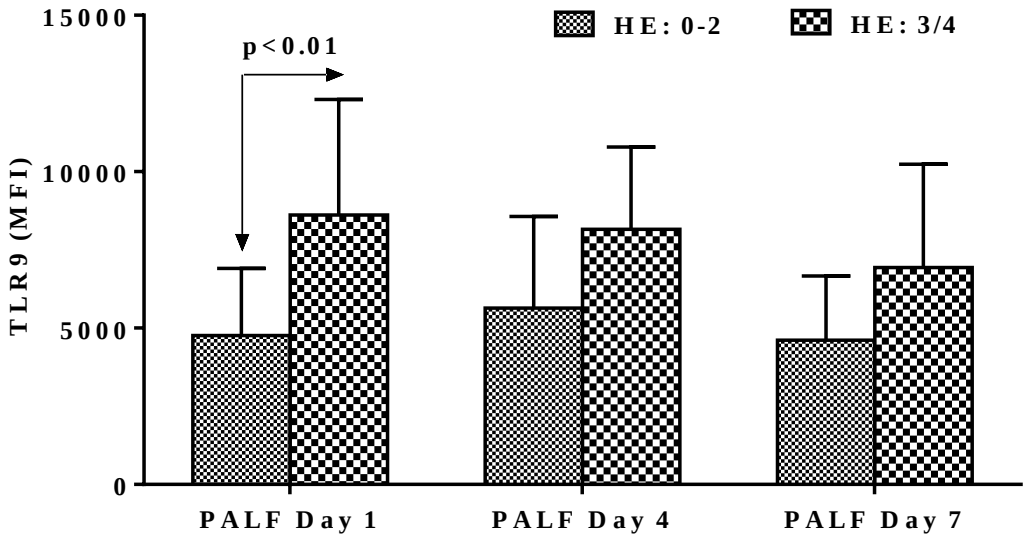

Figure 3.14: Advanced HE (grade 3/4) was associated with increased neutrophil TLR9 expression in patients with PALF.

Neutrophil TLR9 expression was significantly increased in patients with PALF on day 1 with advanced HE (grade 3/4) (n=12) compared to milder HE (grade 0-2) (n=10) ($p=0.006$) [mean: 3818; 95% C.I.: 1284 to 6352 and r^2-0.5]. Normality assumptions were checked and the data are expressed as mean with S.D.; $p<0.05$ were considered statistically significant. Student t-test (HE: 0 - 2 Vs HE: 3 - 4) (normal data)was used to analyse the difference.

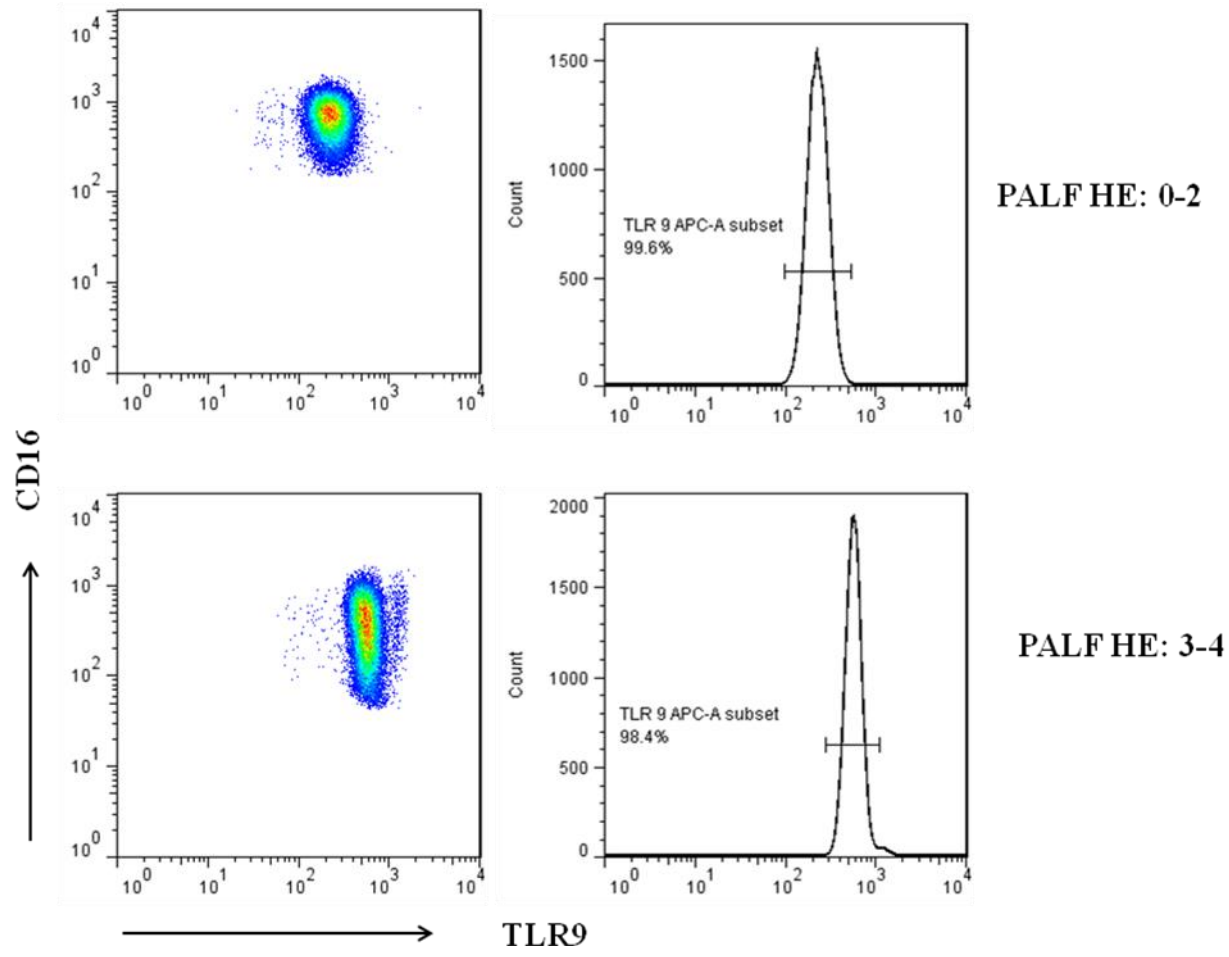

Figure 3.15: Representative FACS plots and histograms of neutrophil TLR9 expression amongst PALF patients on day 1.

These are the FACS plots (left panels) and histograms (right panels) of TLR9 in neutrophils showing increased expression in PALF patients with HE: 3 – 4 (bottom panels) compared to PALF patients with HE: 0 – 2 (top panels). TLR9 expression was measured from neutrophils gated based on CD16 and CD11b positive expression.

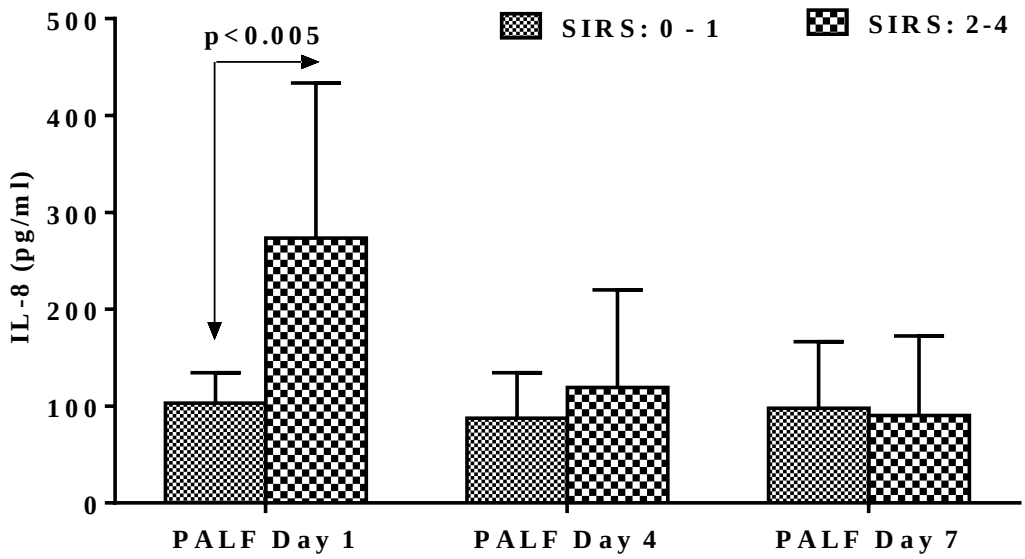

Figure 3.16: High SIRS score (2-4) was associated with increased plasma IL-8 in patients with PALF.

Plasma IL-8 was significantly higher in PALF on day 1 in those with high SIRS score (2-4) (n=11) compared to low SIRS score (0-1) (n=11) (p=0.004) [mean: 170; 95% C.I.: 61.5 to 279 and r^2-0.39]. Normality assumptions were checked and the data are expressed as mean with S.D.; $p<0.05$ were considered statistically significant. Student t-test (SIRS: 0 - 1 Vs SIRS: 2 - 4) (normal data) was used to analyse the difference.

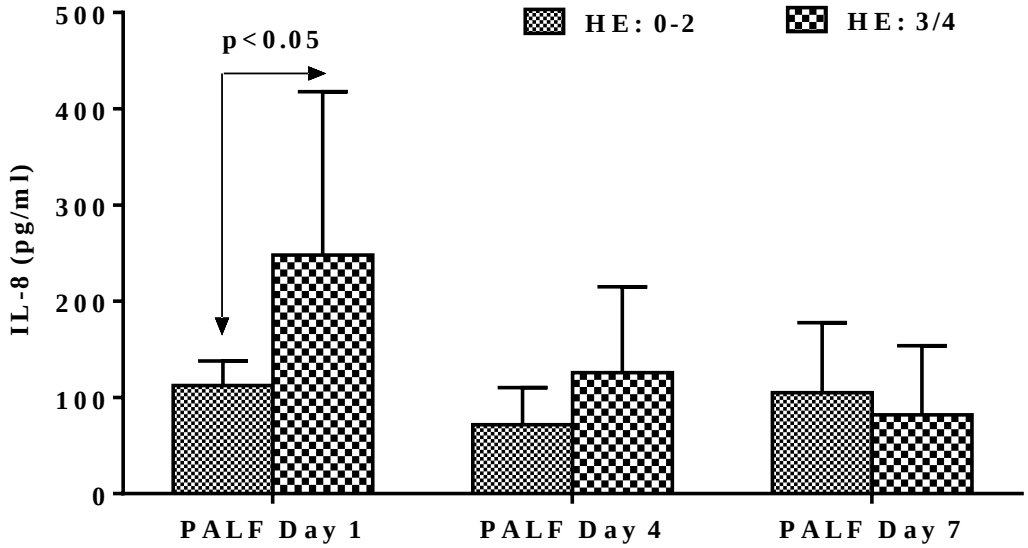

Figure 3.17: Advanced HE (grade 3/4) was associated with increased plasma IL-8 in patients with PALF.

Plasma IL-8 was significantly increased in PALF on day 1 in those with advanced HE (grade 3/4) (n=12) compared to milder HE (grade 0-2) (n=10) (p=0.03) [mean: 136; 95% C.I.: 15 to 257 and r^2-0.25]. Normality assumptions were checked and the data are expressed as mean with S.D.; $p<0.05$ were considered statistically significant. Student t-test (HE: 0 - 2 Vs HE: 3 - 4) (normal data) was used to analyse the difference.

3.6. Neutrophil response to IL-8 and NH_4Cl stimulation and patients' plasma

When HC neutrophils were stimulated with either IL-8 or NH_4Cl no change in TLR9 expression was observed. However TLR9 expression was significantly increased when the neutrophils were co-stimulated with NH_4Cl and IL-8 at 125 and 250 pg/ml, compared to baseline ($p<0.05$), stimulation with IL-8 at 125 pg/ml alone ($p<0.05$) and NH_4Cl alone ($p<0.05$) [Figure 3.18] [Method – 2.16].

There was a significant increase in TLR9 expression when HC neutrophils were incubated with PALF plasma compared to unstimulated cells ($p=0.01$) and there was a significant decrease in TLR9 expression when those plasma samples were pre-incubated with DNase-I ($p=0.0003$) [Figure 3.19]. The changes in TLR9 reflected neutrophil intracellular IL-8 expression [Figure 3.20] [Method – 2.17].

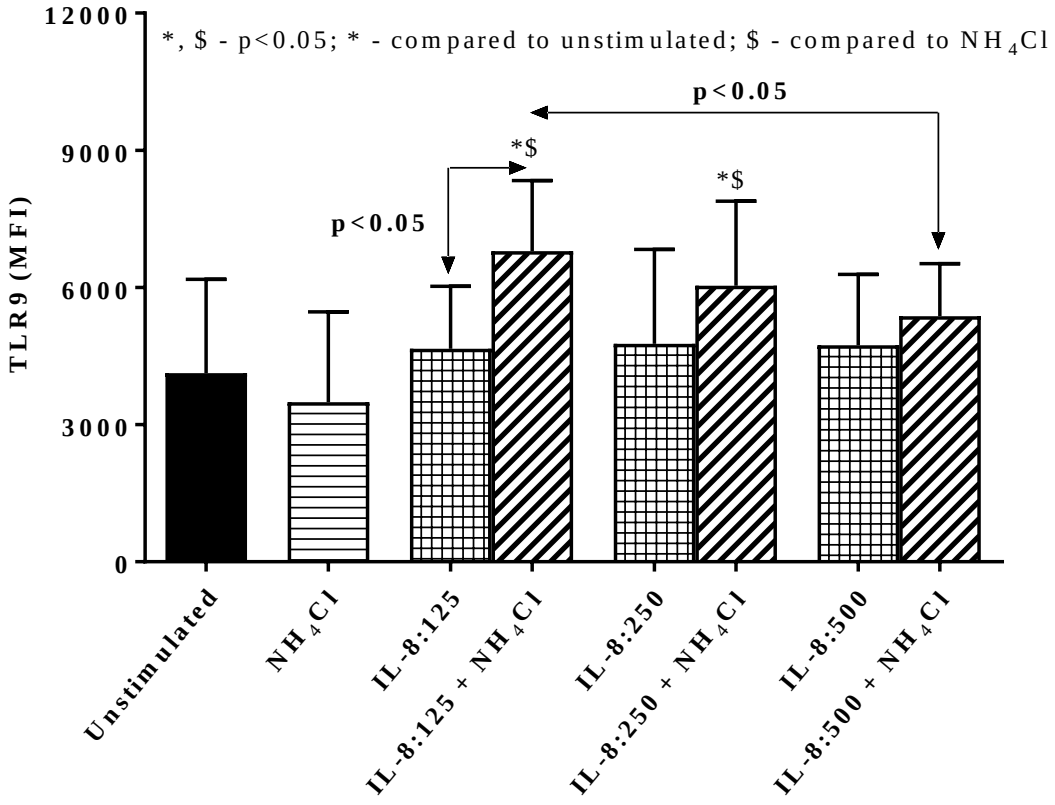

Figure 3.18: Upregulation of TLR9 in healthy neutrophils following stimulation with NH_4Cl and IL-8.

Neutrophil TLR9 expression was significantly increased following co-stimulation with IL-8:125 and NH_4Cl compared to unstimulated (p=0.03) [mean: 2667; 95% C.I.: 423.2 to 4911 and r^2-0.73], NH_4Cl alone (p=0.01) [mean: 3303; 95% C.I.: 1256 to 5350 and r^2-0.83] and IL-8:125 alone (p=0.016) [mean: 2134; 95% C.I.: 662 to 3606 and r^2-0.8]. Neutrophil TLR9 expression was also significantly increased following co-stimulation with IL-8:250 and NH_4Cl compared to unstimulated (p=0.015) [mean: 1915; 95% C.I.: 618 to 3213 and r^2-0.8], NH_4Cl alone (p=0.03) [mean: 2551; 95% C.I.: 457 to 4645 and r^2-0.74] and IL-8:250 alone (p=0.03) [mean: 1749; 95% C.I.: 284 to 3214 and r^2-0.8]. Normality assumptions were checked and the data are expressed as mean with S.D.; p<0.05 were considered statistically significant. Student t-test was used to analyse the differences between two groups (normal data).

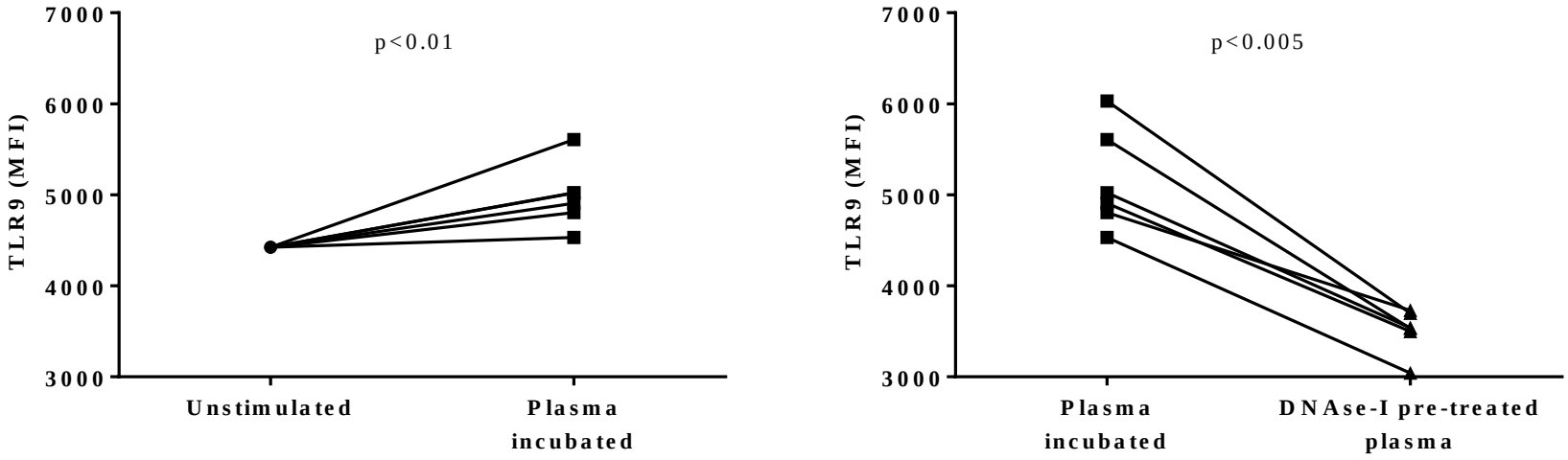

Figure 3.19: Upregulation of TLR9 in healthy neutrophils following stimulation with PALF plasma.

(a) Neutrophil TLR9 expression was significantly increased when neutrophils from a HC were incubated with PALF plasma (patients who fulfilled King's criteria for liver transplantation, n=6) compared to unstimulated cells (p=0.01) [mean: 559; 95% C.I.: 186 to 932 and r^2-0.74]. (b) Neutrophil TLR9 expression was significantly decreased when neutrophils from a HC were incubated with PALF plasma pre-incubated with DNase-I (p=0.0003) [mean: 1644; 95% C.I.: -2133 to -1155 and r^2-0.94]. Normality assumptions were checked; $p<0.05$ were considered statistically significant. Paired t-test was used to analyse the difference (normal data).

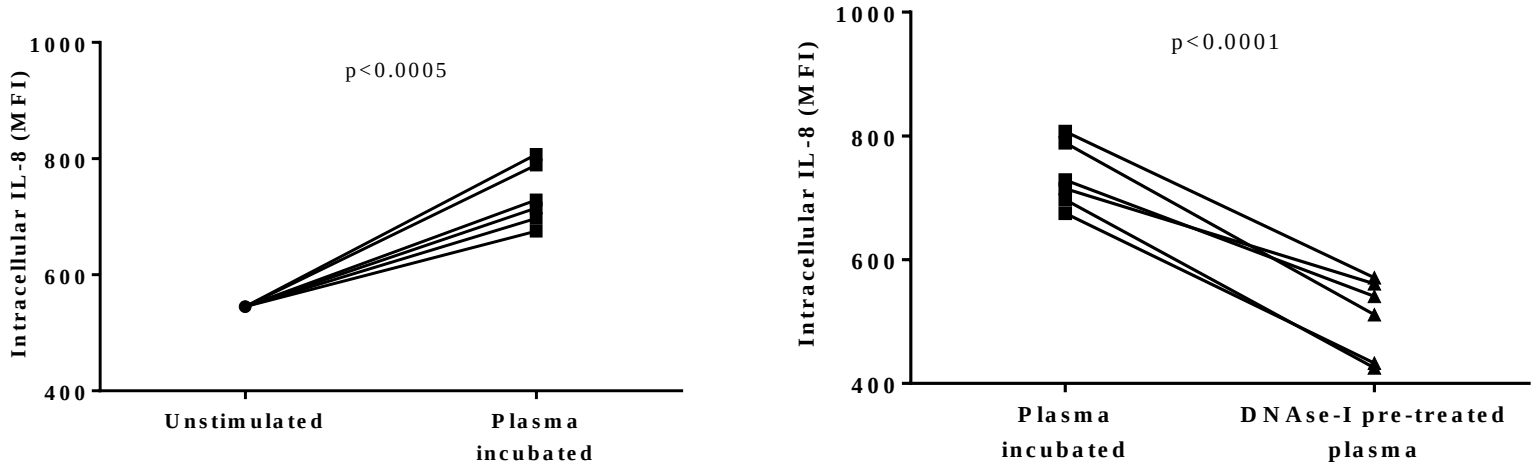

Figure 3.20: Changes in intracellular IL-8 in healthy neutrophils following exposure to PALF plasma.

(a) Neutrophil intracellular IL-8 expression was significantly increased when neutrophils from a HC were incubated with PALF plasma (patients who fulfilled King's criteria for liver transplantation, n=6) compared to unstimulated cells (p=0.0003) [mean: 190; 95% C.I.: 136 to 245 and r^2-0.94]; (b) Neutrophil intracellular IL-8 expression was significantly decreased when neutrophils from a HC were incubated with PALF plasma pre-incubated with DNase-I enzyme (p<0.0001) [mean: -228; 95% C.I.: -279 to -177 and r^2-0.96]. Normality assumptions were checked; p<0.05 were considered statistically significant. Paired t-test was used to analyse the difference (normal data).

3.7. *Ex-vivo* stimulation of neutrophils with LPS, NH_4Cl and ODN 2395

Following NH_4Cl or LPS stimulation, neutrophil TLR9 expression remained unchanged in HC and PALF patients with low SIRS score (0-1) on day 1 compared to unstimulated cells. Whereas neutrophil TLR9 expression was downregulated significantly in PALF patients with high SIRS score (2-4) on day 1 ($p<0.05$) compared to unstimulated cells [Figure 3.21] [Methods – 2.15.2 and 2.15.3].

Following NH_4Cl or LPS stimulation, neutrophil TLR9 expression remained unchanged in HC and PALF patients with mild HE (grade 0-2) on day 1 compared to unstimulated cells. Whereas neutrophil TLR9 expression was downregulated significantly in PALF patients with advanced HE (grade 3/4) on day 1 ($p<0.05$) compared to unstimulated cells [Figures 3.22 and 3.23].

Neutrophil TLR9 expression was not changed by stimulation with ODN 2395 [oligodinucleotides] in both HC and PALF patients [Figure 3.24] [Method – 2.15.4].

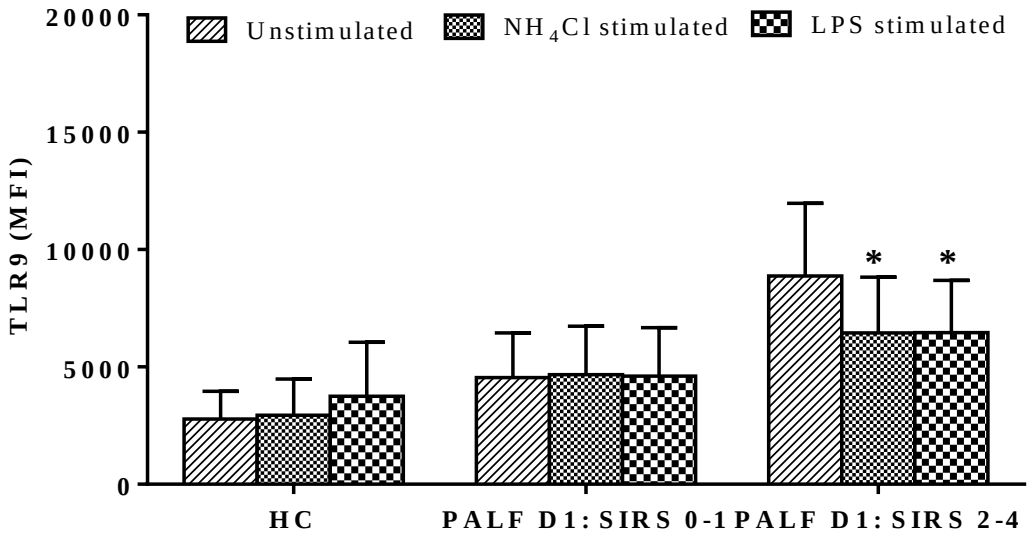

Figure 3.21: Changes in neutrophil TLR9 expression in PALF patients with high SIRS score (2-4) following *ex-vivo* stimulation with LPS and NH_4Cl.

Neutrophil TLR9 was significantly downregulated in PALF patients with high SIRS score (2-4) on day 1 (n=11) in response to NH_4Cl [mean: -2728; 95% C.I.: -4712 to -745 and r^2-0.48] and LPS [mean: -4757; 95% C.I.: -9513 to -1.5 and r^2-0.65] stimulation compared to unstimulated cells ($p<0.05$; *- compared to unstimulated). There was no change in PALF patients with low SIRS score (0-1) on day 1 (n=11) or in HC (n=10) following NH_4Cl and LPS stimulation. Normality assumptions were checked and the data are expressed as mean with S.D.; $p<0.05$ were considered statistically significant. Paired t-test was used to analyse the pre- and post-stimulation data (normal data).

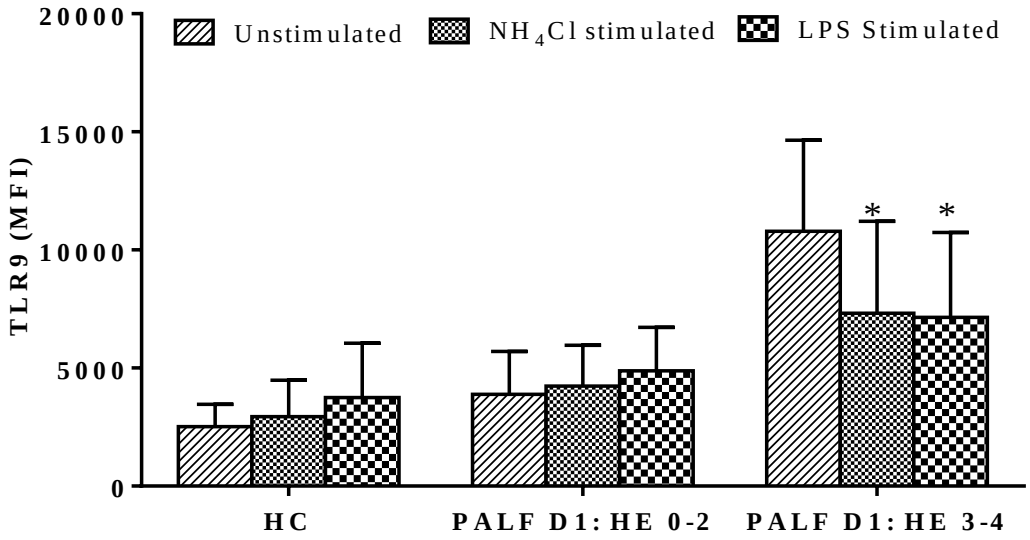

Figure 3.22: Changes in neutrophil TLR9 expression and cytokine production in PALF patients with advanced HE (grade 3/4) following *ex-vivo* stimulation with LPS and NH_4Cl.

Neutrophil TLR9 was significantly downregulated in PALF patients with high HE score (3/4) on day 1 (n=12) in response to NH_4Cl [mean: -3469; 95% C.I.: -6919 to -19 and r^2-0.57] and LPS [mean: -3648; 95% C.I.: -9256 to -142 and r^2-0.64] stimulation compared to unstimulated cells ($p<0.05$; *- compared to unstimulated). There was no change in PALF patients with milder HE score (0-2) on day 1 (n=10) nor in HC (n=10) following NH_4Cl and LPS stimulation. Normality assumptions were checked and the data are expressed as mean with S.D.; $p<0.05$ were considered statistically significant. Paired t-test was used to analyse the pre- and post-stimulation data (normal data).

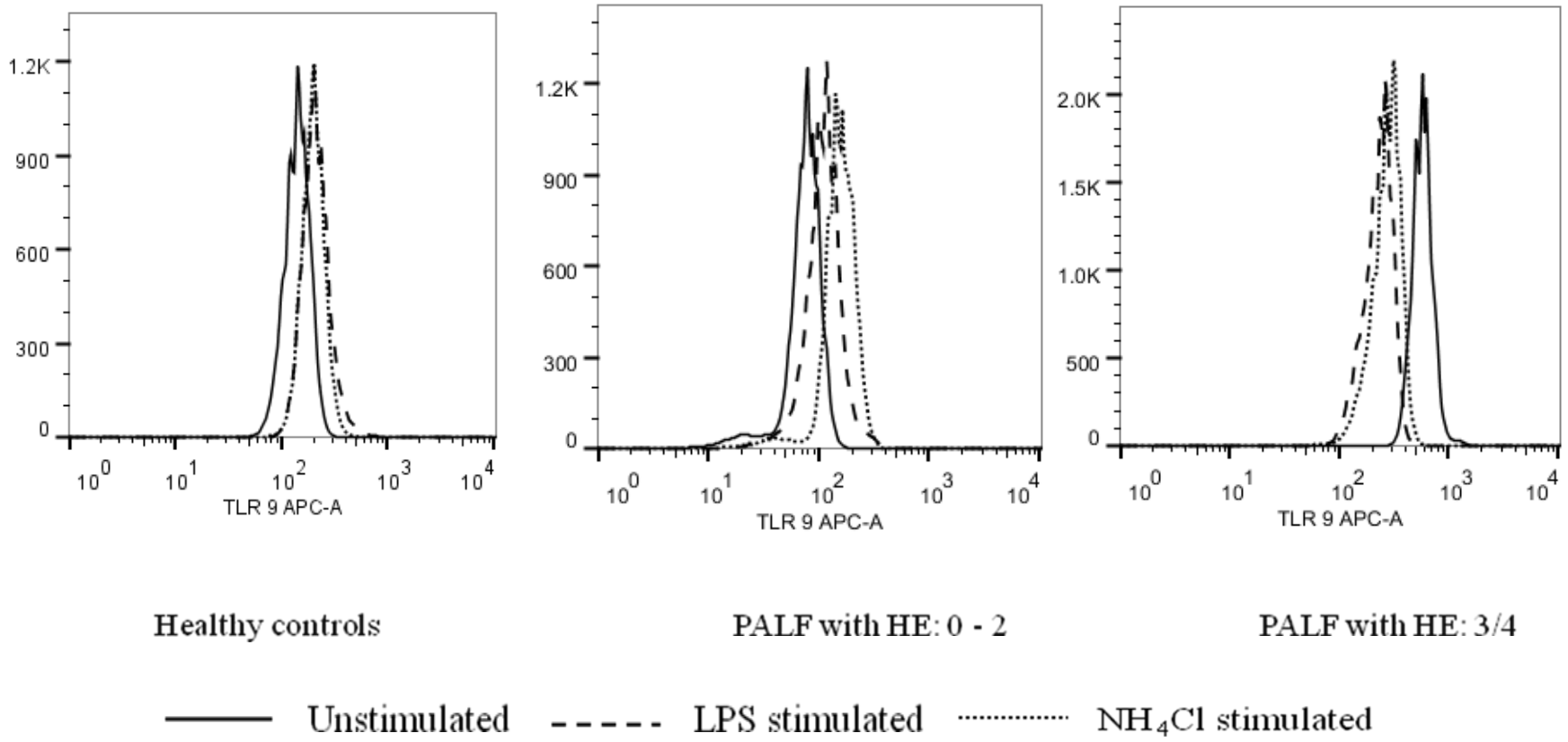

Figure 3.23: Histograms illustrating the TLR9 expression in neutrophils in patients with PALF and HC before and after LPS or NH_4Cl stimulation.

These histograms show that neutrophil TLR9 expression is downregulated in PALF patients with HE: grade 3/4 after LPS or NH_4Cl stimulation but not in PALF patients with HE: grade 0 – 2 and HC compared to its unstimulated counterparts.

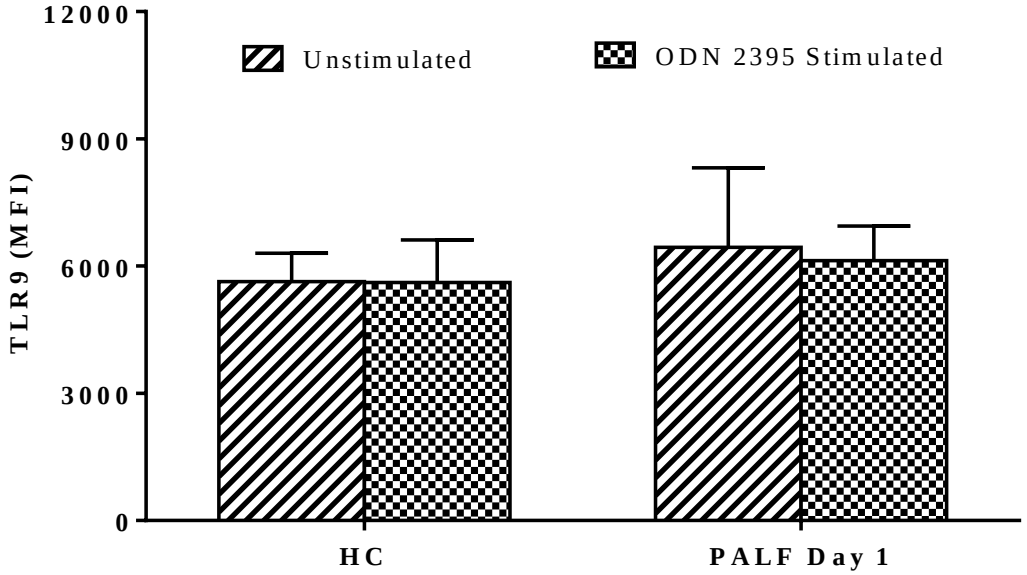

Figure 3.24: Neutrophil TLR9 expression following *ex-vivo* stimulation with ODN 2395.

Neutrophil TLR9 remained unchanged in PALF patients (n=8) and HCs (n=10) on day 1 in response to ODN 2395 stimulation compared to unstimulated cells. Normality assumptions were checked and the data are expressed as mean with S.D.; $p<0.05$ were considered statistically significant. Paired t-test was used to analyse the pre- and post-stimulation data.

3.8. Neutrophil cytokine production in response to stimulation

Cytokines were measured in the supernatants collected from cells stimulated by NH_4Cl and/or LPS and compared to unstimulated cells from both HC and PALF patients. There was a 400-800 fold increase in TNF-α and IL-8 production following LPS stimulation in HC compared to their unstimulated counterparts ($p<0.0001$). In PALF patients with low SIRS score (0-1) on day 1, the cytokine production was increased 40-60 fold compared to unstimulated cells ($p<0.05$). However in PALF patients with high SIRS score (2-4) there was no change or a maximum two fold increase in the cytokine production compared to their unstimulated counterparts on day 1 [Figure 3.25]. A similar trend was observed in the cytokine production following NH_4Cl stimulation even though it was not in manifold increase [Figure 3.26].

Following ODN 2395 stimulation, IL-8 and TNF-α were significantly increased in the supernatants in PALF patients on day 1 ($p<0.05$) compared to HC which were unchanged [Figure 3.27]. Intracellular IL-8 expression remained unchanged in PALF patients on day 1 compared to HC which were significantly increased ($p<0.05$) [Figure 3.28]. Baseline intracellular IL-8 expression was significantly increased in PALF patients on day 1 compared to HC [Figure 3.29]. These data are indicative that neutrophils in PALF become primed following hepatic necrosis and over react to stimulation.

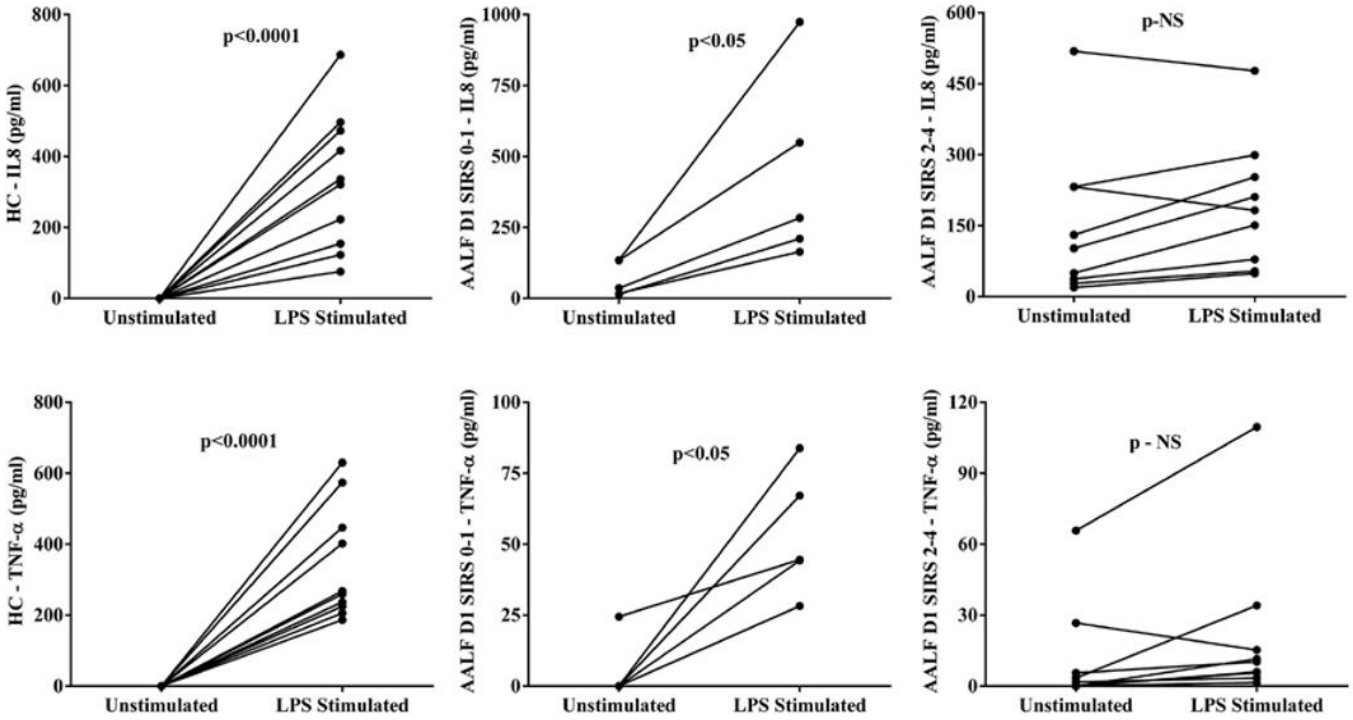

Figure 3.25: Changes in cytokine production in PALF patients following *ex-vivo* stimulation with LPS.

IL-8 and TNF-α production was increased 200 to 600 fold following LPS stimulation (both $p<0.0001$) in HC and increased 40 to 60 fold in PALF patients with low SIRS score (0-1) (both $p<0.05$). There was only a maximum of a two-fold increase in IL-8 and TNF-α production in PALF patients with high SIRS score (2-4) on day 1 following the NH_4Cl or LPS stimulation. Normality assumptions were checked; $p<0.05$ were considered statistically significant. Paired t-test was used to analyse the pre- and post-stimulation data.

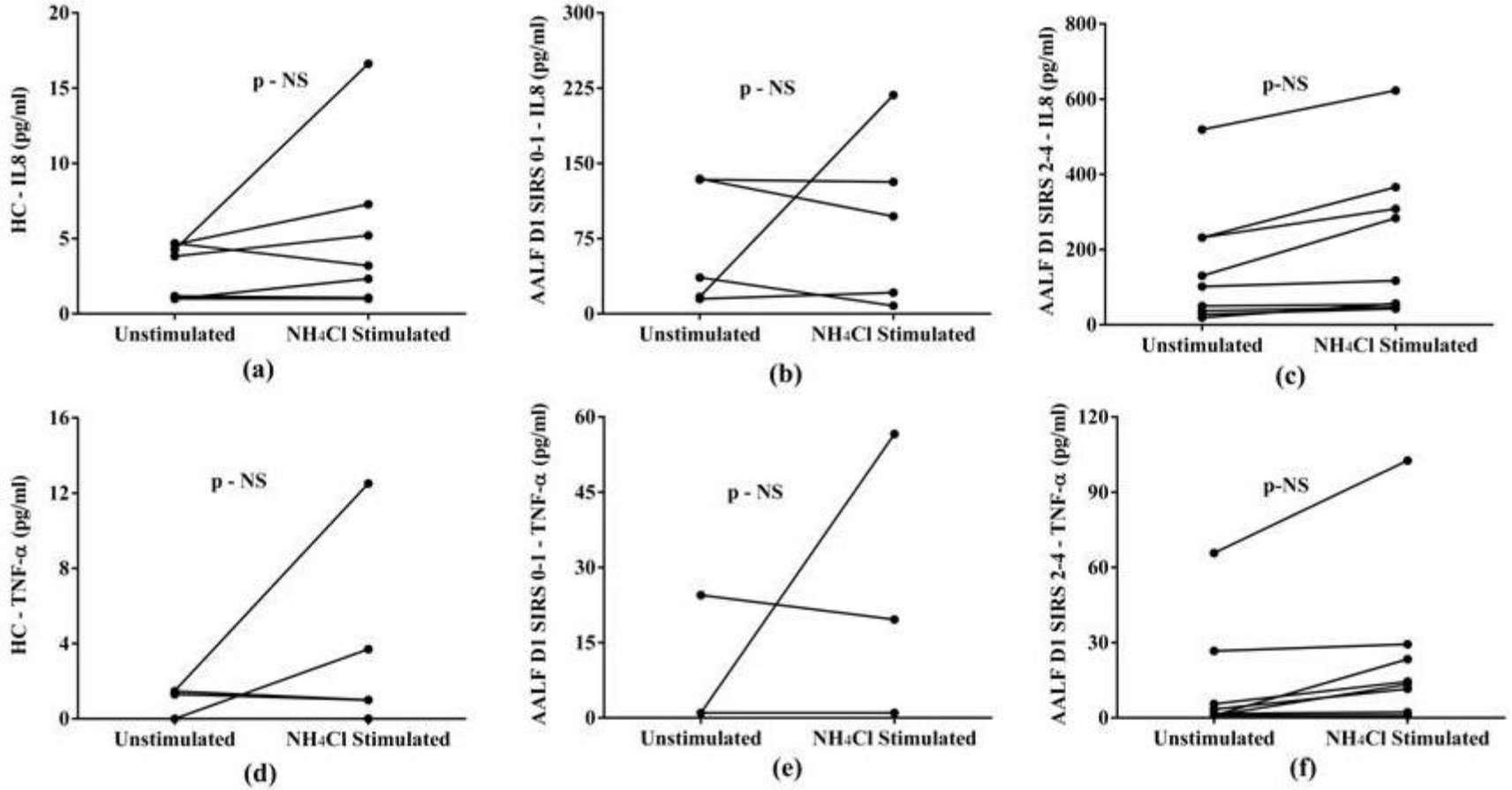

Figure 3.26: IL-8 and TNF-α were increased following *ex-vivo* stimulation with NH_4Cl in the neutrophil supernatants of HC and PALF patients with low SIRS score (0-1) but not in PALF patients with high SIRS score (2-4).

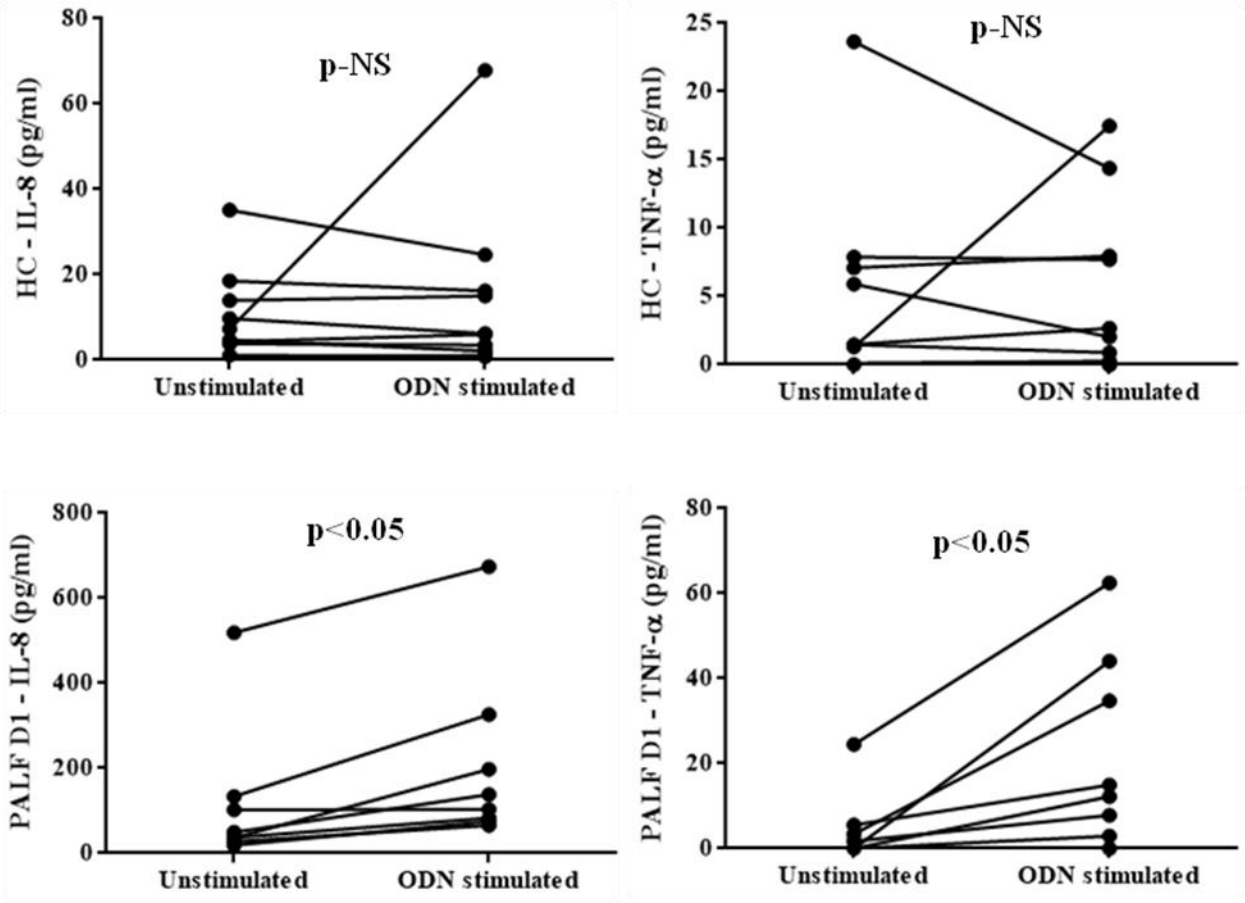

Figure 3.27: Changes in supernatant cytokines in PALF patients following *ex-vivo* stimulation with ODN 2395.

Following ODN 2395 stimulation, IL-8 and TNF-α remained unchanged in HC supernatants but were significantly increased in PALF supernatants ($p<0.05$). Normality assumptions were checked; $p<0.05$ were considered statistically significant..Paired t-test was used to analyse the pre- and post-stimulation data.

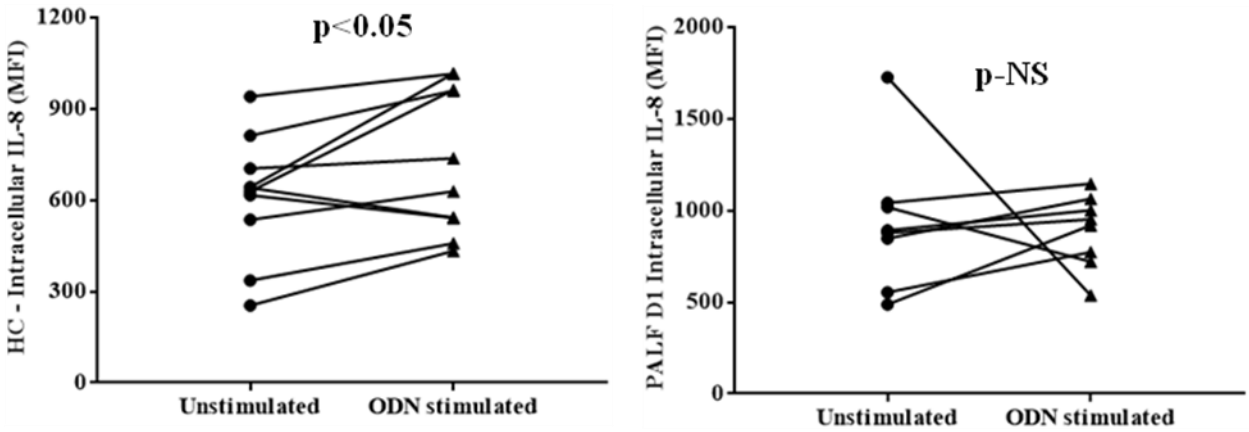

Figure 3.28: Changes in intracellular neutrophil IL-8 expression following *ex-vivo* stimulation with ODN 2395.

Following ODN 2395 stimulation, intracellular IL-8 was significantly increased compared to unstimulated ($p<0.05$) but remained unchanged in PALF patients on day 1 compared to its unstimulated counterpart. Normality assumptions were checked; $p<0.05$ were considered statistically significant.. Paired t-test was used to analyse the pre- and post-stimulation data.

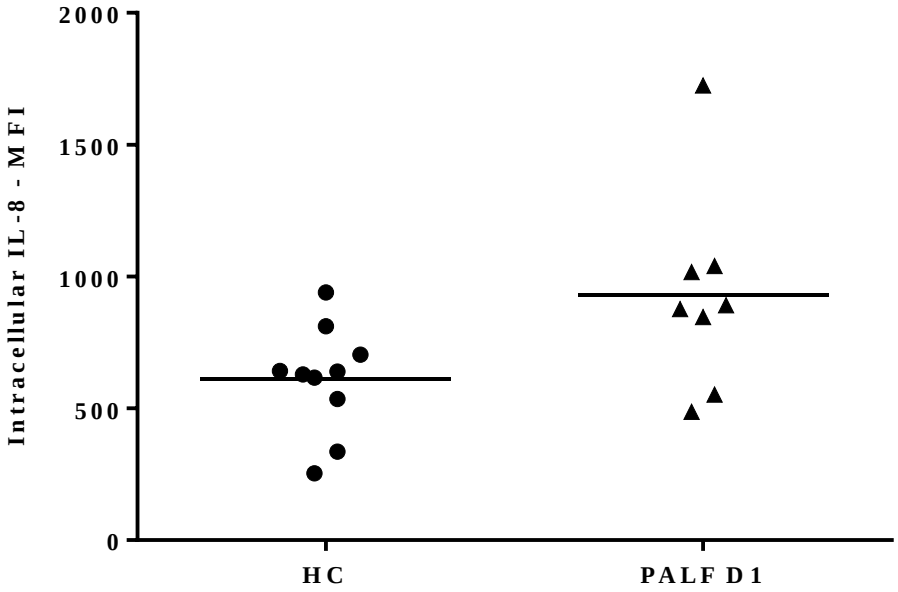

Figure 3.29: Increased intracellular IL-8 in PALF patients on day 1 compared to HC.

Baseline intracellular IL-8 was significantly increased in PALF patients on day 1 (n=8) compared to HC (n=10) ($p<0.05$) [mean: 319; 95% C.I.: 25 to -613 and r^2-0.25]. The data are normally distributed and $p<0.05$ were considered statistically significant. Student t-test was used to analyse the difference between two groups.

3.9. Neutrophil function

Neutrophil dysfunction has been previously studied in PALF patients by our group [139]. To confirm these findings amongst the patients recruited for my study, NPA and oxidative burst of neutrophils were studied amongst a small cohort of PALF patients at a later stage in the study. NPA was significantly decreased in PALF on day 1 compared to HC ($p<0.0001$) significantly improving on days 4 and 7 compared to day 1 ($p<0.005$) (Figure 3.30). Neutrophil SOB was significantly increased in PALF on day 1 compared to HC ($p<0.0001$). There was no difference in the neutrophil SOB between PALF patients on days 1, 4 and 7 (Figure 3.31). Neutrophil low burst (LB) and high burst (HB) induced by fMLP and PMA respectively was also significantly increased in PALF on day 1 compared to HC ($p<0.05$). There was no difference in the neutrophil LB and HB between PALF patients on days 1, 4 and 7 (Figures 3.32 – 3.33). There was no difference in the neutrophil PB in patients with PALF compared to HC (Figures 3.34) [Methods – 2.19.1 and 2.19.2].

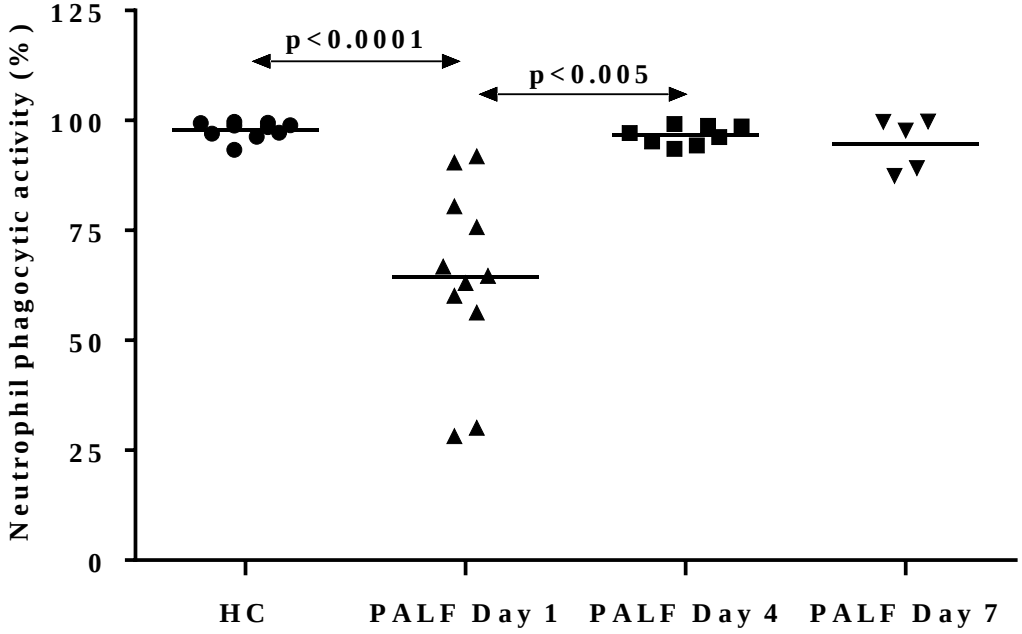

Figure 3.30: Impaired neutrophil phagocytosis in patients with PALF.

(a) NPA (percentage of neutrophils undergoing phagocytosis) was significantly decreased in PALF patients on day 1 (n=11) compared to HC (n=10) ($p<0.0001$) [mean: -33.5; 95% C.I.: -47.5 to -19.6 and r^2-0.57]. NPA increased in PALF patients on day-4 compared to day 1 ($p<0.005$). Normality assumptions were checked; $p<0.05$ were considered statistically significant. Student t-test (HC Vs PALF day 1) (normal data) and Friedman's with multiple Conover's testing (PALF day 1 Vs day 4 Vs day 7) (normal data) were used to analyse the data.

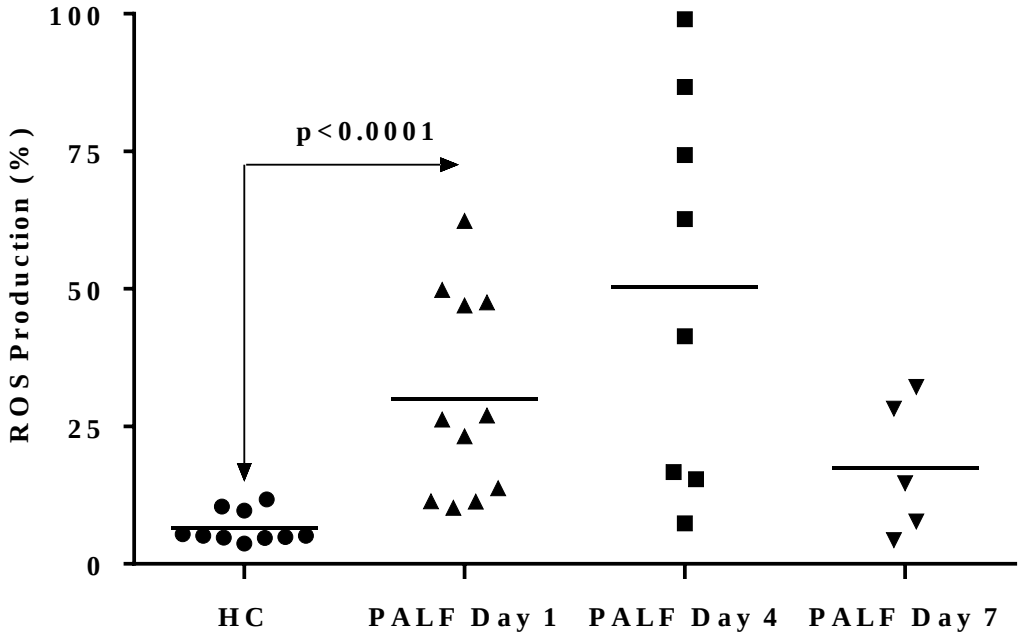

Figure 3.31: Impaired neutrophil spontaneous oxidative burst in patients with PALF.

Neutrophil SOB was significantly increased in PALF patients on day 1 (n=11) compared to HC (n=10) ($p<0.0001$) [mean: 23.4; 95% C.I.: 11 to 35.9 and r^2-0.45]. There was no difference in the neutrophil SOB in PALF patients on days-4 and 7 compared to day 1. Normality assumptions were checked; $p<0.05$ were considered statistically significant. Student t-test (HC Vs PALF day 1) (normal data) and Friedman's with multiple Conover's testing (PALF day 1 Vs day 4 Vs day 7) (normal data) were used to analyse the data.

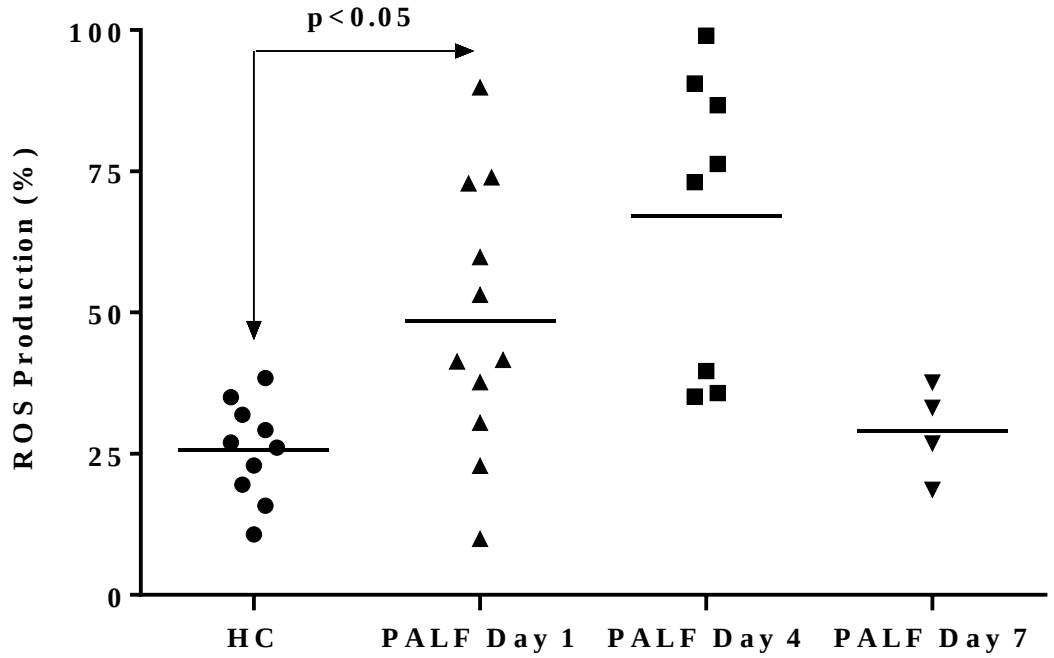

Figure 3.32: Impaired neutrophil oxidative low burst (LB) in patients with PALF.

Neutrophil LB was significantly increased in PALF patients on day 1 (n=11) compared to HC (n=10) ($p<0.05$) [mean: 23.4; 95% C.I.: 11 to 35.9 and r^2-0.45]. There was no difference in the neutrophil LB in PALF patients on days-4 and 7 compared to day 1. Normality assumptions were checked; $p<0.05$ were considered statistically significant. Student t-test (HC Vs PALF day 1) (normal data) and Friedman's with multiple Conover's testing (PALF day 1 Vs day 4 Vs day 7) (normal data) were used to analyse the data.

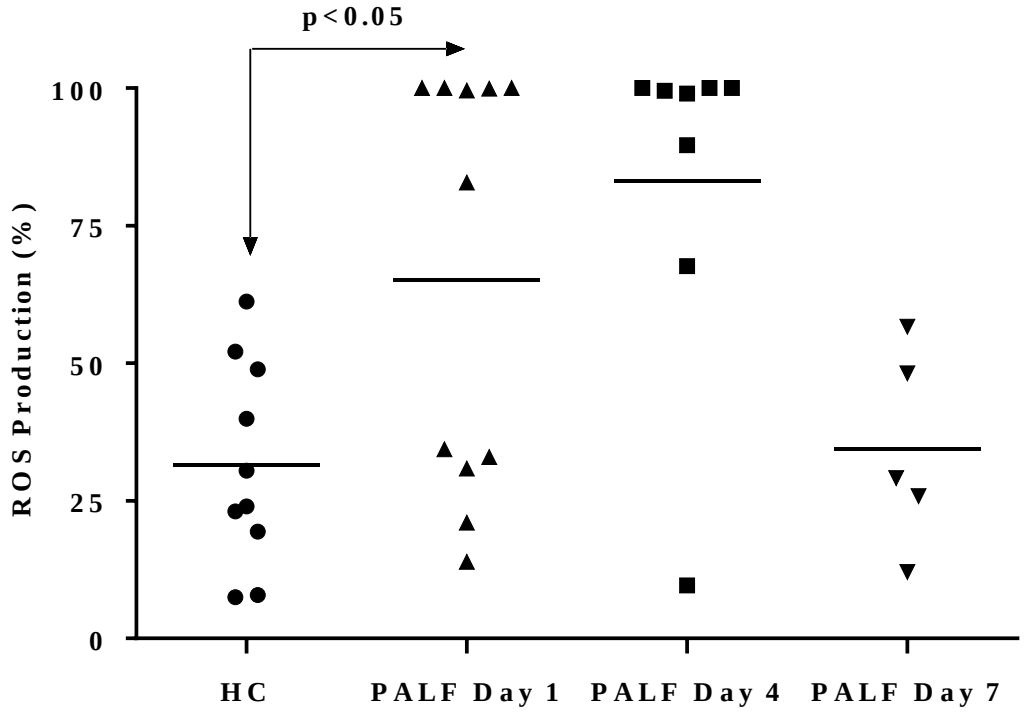

Figure 3.33: Impaired neutrophil oxidative high burst (HB) in patients with PALF.

Neutrophil HB was significantly increased in PALF patients on day 1 (n=11) compared to HC (n=10) ($p<0.05$) [mean: 23.4; 95% C.I.: 11 to 35.9 and r^2-0.45]. There was no difference in the neutrophil HB in PALF patients on days 4 and 7 compared to day 1. Normality assumptions were checked; $p<0.05$ were considered statistically significant. Student t-test (HC Vs PALF day 1) (normal data) and Friedman's with multiple Conover's testing (PALF day 1 Vs day 4 Vs day 7) (normal data) were used to analyse the data.

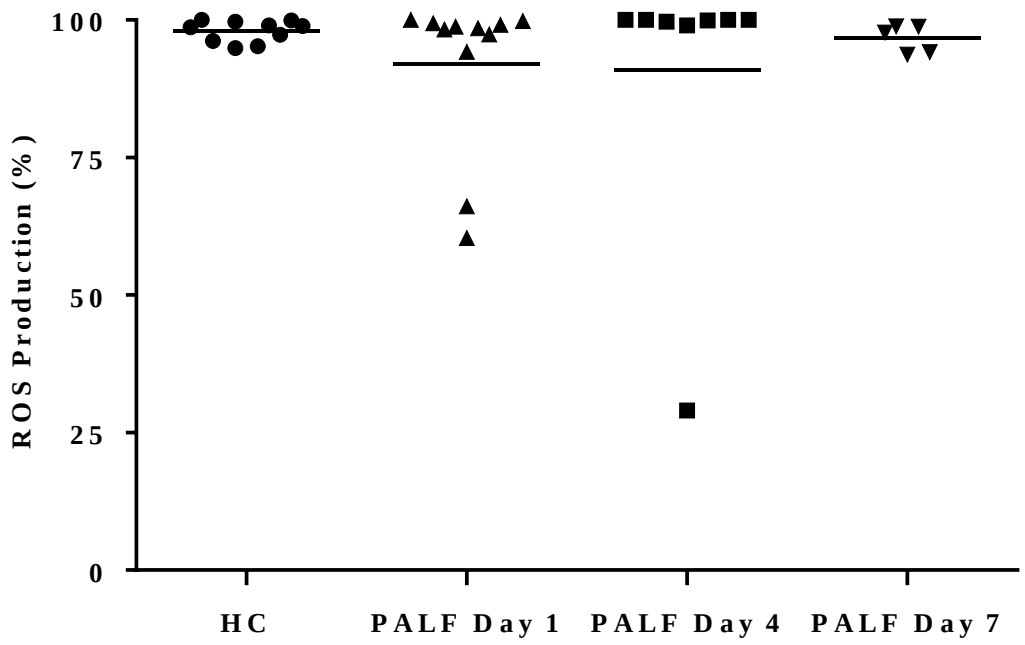

Figure 3.34: Neutrophil phagoburst in patients with PALF and HC.

There was no difference in neutrophil PB in PALF patients on day 1(n=11) compared to HC (n=10). There was no difference in the neutrophil PB in PALF patients on days 4 and 7 compared to day 1. Normality assumptions were checked; $p<0.05$ were considered statistically significant. Student t-test (HC Vs PALF day 1) and Friedman's with multiple Conover's testing (PALF day 1 Vs day 4 Vs day 7) were used to analyse the data.

3.10. Discussion

In this study, a robust correlation between neutrophil TLR9 expression and arterial ammonia concentration and plasma IL-8 in PALF has been demonstrated. Neutrophil TLR9 expression and IL-8 were highest in those with severe SIRS and advanced HE which is consistent with the pro-inflammatory state observed in patients with PALF. Neutrophil function was impaired with reduced phagocytic activity and increased SOB.

This led me to postulate that in addition to the release of pro-inflammatory cytokines such as IL-6 and IL-8 following paracetamol-induced hepatic necrosis, the resulting reduced hepatocyte mass (with less capacity to incorporate nitrogen species into urea) results in an elevation in arterial ammonia inducing neutrophil TLR9 expression. Indeed, it has been shown that the necrotic liver releases DNA into the systemic circulation [106, 108] where upon exposure, TLR9 along with the Nalp3 inflammasome and caspase-1 activates the cell signaling cascade of pro-inflammatory cytokines IL-1β and IL-18 [108]. This is supported by my observation that there was a significant increase in TLR9 expression when healthy neutrophils were incubated with PALF plasma which was abrogated by pre-incubating with DNase-I. It has been shown that TLR9 receptor activation stimulates IL-8 production by activating the p38 – mitogen activated protein kinase (MAPK) and downstream NF-κB pathways in haematopoietic stem cells [177] and endothelial cells [178] which is reflected in our observation that TLR9 expression reflected neutrophil intracellular IL-8 expression.

In this study it has been demonstrated that neutrophil TLR9 is synergistically induced by ammonia and IL-8. Furthermore, the pre-treatment of PALF plasma with DNAse-I edIt has been well established that TLR9 is mainly activated by the DNA released from

the necrotic liver induced by paracetamol overdose [108, 179]. This led me to postulate that DNA could be increased in the circulation in paracetamol-induced liver injury as a result of hyperammonemia in addition to DNA released by apoptotic hepatocytes. However this warrants further investigation as there has been no direct evidence so far associating hyperammonemia with release of DNA into the circulation.

It has previously been reported that astrocyte swelling is reduced in TLR4 silenced brain endothelium exposed to ammonia, cytokines and LPS [180] and brain oedema is abrogated in acute HE TLR4 knockout mice models [180]. TLR4 antagonists administered to a paracetamol-induced mice have also been shown to be protective with a reduction in the brain water volume [165] implicating TLR4 as playing a major role in the development of HE. However the decrease in circulating neutrophil TLR4 expression observed in this study in the context of no detectable systemic endotoxin suggests that neutrophil TLR4 does not play as significant a role as TLR9 in the development of SIRS in PALF. The distinct effects of ALF caused by paracetamol and TLR sub-type changes in mice versus patients could be due to the fact that mice and humans behave differently.

The neutrophils from patients with PALF and high SIRS failed to upregulate TLR9 in response to LPS and NH_4Cl challenge and paradoxically downregulated which may result from a negative feedback mechanism. They were also unable to produce the pro-inflammatory cytokines TNF-α and IL-8 compared to those with PALF and lower SIRS implying that exposure to high levels of the potent neutrophil chemokine IL-8 in early PALF may lead to circulating neutrophil exhaustion. Furthermore, stimulation with oligodinucleotides failed to upregulate intracellular IL-8 expression in patients with PALF explaining why patients with PALF and severe SIRS are so susceptible to developing bacterial and fungal infections [181].

Upregulation of TLR9 in HC following co-stimulation with NH_4Cl and IL-8 but not with IL-8 or NH_4Cl alone suggests that inflammation and ammonia act synergistically to increase TLR9 expression in PALF. Moreover, increased intracellular IL-8 production in healthy neutrophils following stimulation with NH_4Cl (or oligodinucleotides) suggests that ammonia and circulating DAMPs can potentially trigger production of this potent neutrophil attracting chemokine. LPS also activates the production of IL-8 in human neutrophils [182] with IL-15 inducing this process by activating the NF-κB pathway [183]. The increased neutrophil TLR9 expression observed following ex-*vivo* stimulation with IL-8 and NH_4Cl in healthy neutrophils is similar in magnitude to the TLR9 expression observed in PALF patients on presentation and may be representative of the circulating inflammatory milieu which develops in PALF. However the mechanistic pathway through which TLR9 responds to these stimuli would require further interrogation in these patients.

Although the phagocytic activity of neutrophils improved on days 4 and 7 in PALF patients compared to the baseline, there was no change in the production of ROS on days 4 and 7. The overproduction of ROS is detrimental to PALF patients as it leads to tissue damage and apoptosis of hepatocytes in paracetamol overdose [184]. Furthermore, in an azoxymethane acute liver injury model it has been demonstrated that TNF-α plays an important role in the pathogenesis of ALF and HE. Etanercept, an antagonist of TNF-α, neutralized TNF-α and attenuated systemic inflammation, hepatic damage, oxidative stress and neuroinflammation [185]. Whilst it has been demonstrated that etanercept inhibits the cytokine production and reduces hepatocyte necrosis, the influence of etanercept on TLRs remains to be determined. The expression of CXCR-4 is increased in aged neutrophils and this receptor plays an essential role in the neutrophil homeostasis

in bone marrow [186, 187]. Therefore measuring the CXCR4 expression would have helped identify exhausted neutrophils and their function in PALF patients.

These data may put into context why studies have revealed that high arterial ammonia concentration is central in the development of ICH in those with advanced HE [51] and go some way to explaining why there is progression to more severe grades of HE in patients with ALF who have significant systemic inflammation [37]. Indeed, we have demonstrated that patients with PALF and high SIRS score (2-4) and advanced HE (grade 3/4) had higher baseline plasma IL-8 concentration and circulating neutrophil TLR9 expression than those with low SIRS (score 0-1) and milder HE (grade 0-2) which supports the validity of this concept. These circulating neutrophils are integral in the development of SIRS and advanced HE but may also amplify liver injury as neutrophil depleted mice with paracetamol hepatotoxicity have evidence of reduced hepatocellular necrosis. Furthermore, blocking CXCR-2 and formyl peptides protected against the development of SIRS and remote lung injury [106].

3.11. Conclusion

Neutrophil TLR9 expression in PALF is mediated both by circulating endogenous DNA as well as ammonia and IL-8 in a synergistic fashion inducing systemic inflammation, neutrophil exhaustion and exacerbating HE [Figure 3.35]. The findings of this study taken with the important observation by Imaeda and colleagues that paracetamol-induced hepatotoxicity in wild type and Nalp3 deficient mice is dependent on TLR9 and the Nalp3 inflammasome resulting from DNA released from the apoptotic hepatocytes [108] implies that TLR9 antagonists may be of therapeutic value in PALF, particularly in those with high SIRS and advanced HE on presentation.

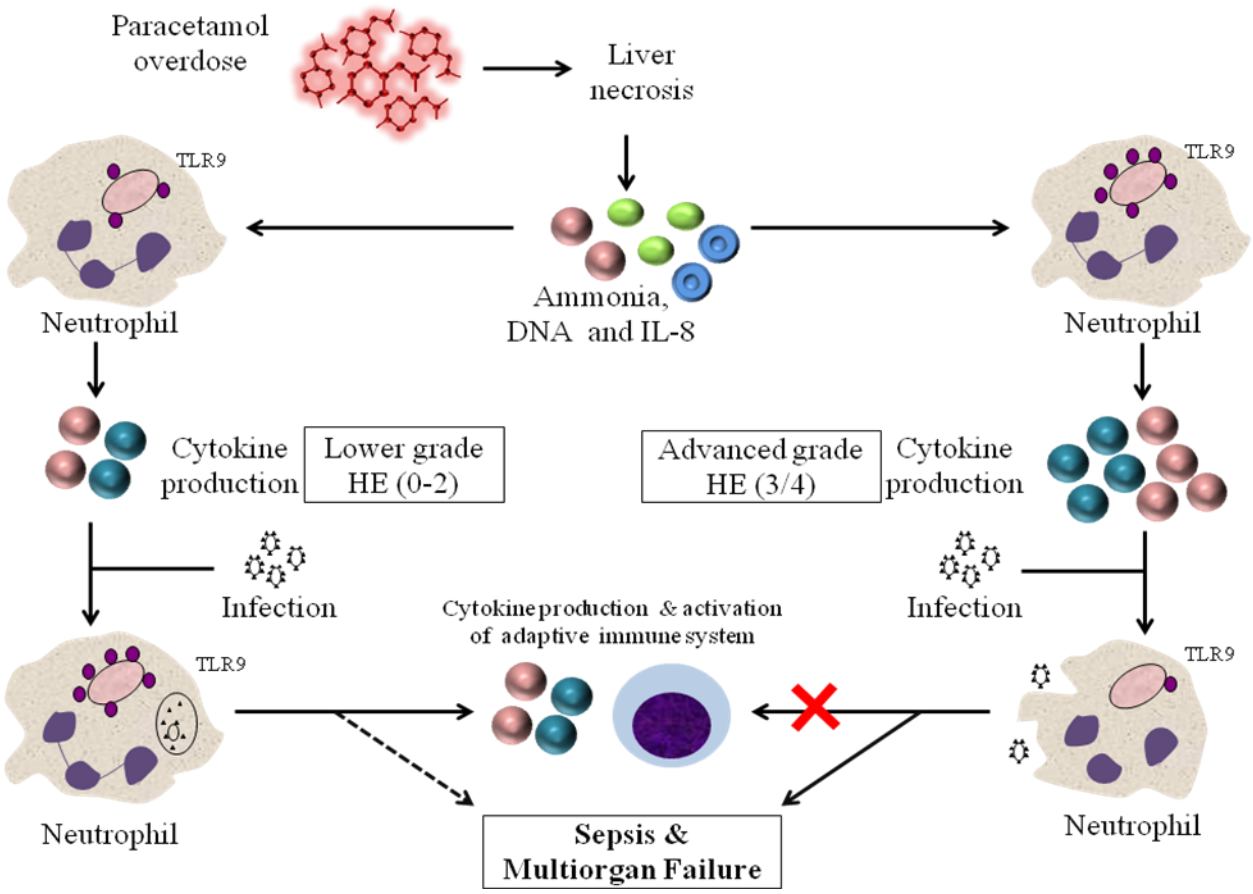

Figure 3.35: Illustration demonstrating the mechanism by which paracetamol hepatotoxicity might lead to MOF.

Paracetamol overdose causes necrosis of the liver leading to reduced ammonia detoxification capability and increased IL-8 production. Ammonia and IL-8 act synergistically to induce increased neutrophil TLR9 expression and cytokine production in PALF patients with advanced grade HE (3/4) compared to lower grade HE (0-2). When there is an infectious stimulus, neutrophils of the patients with lower grade HE (0-2) are more likely to be able to respond resulting in cytokine production and recruitment of the adaptive immune system. In patients with advanced grade HE the increased neutrophil TLR9 expression and cytokine production culminates in neutrophil exhaustion and failure to respond to an infectious stimulus resulting in sepsis and MOF. Patients with lower grade HE (0-2) still have a tendency towards developing sepsis and MOF however this is less marked compared to patients with advanced grade HE (3/4).

Chapter 4. Ammonia-induced brain oedema and immune dysfunction is mediated by TLR9

In the previous chapter, it has been demonstrated that ammonia, IL-8 and DNA together contribute to upregulating neutrophil TLR9 expression with the highest values of TLR9 being associated both with high SIRS score and advanced HE grade. Therefore the next question was to determine whether TLR9 plays a central role in the development of brain oedema in HE. However it has been previously reported in paracetamol hepatotoxicity that inhibition of TLR9 using genetically altered mice and neutralizing antibodies abrogates the inflammatory responses and protects the mice against acute liver injury [108]. Therefore it is not possible to determine the role of TLR9 in the development of brain oedema in a paracetamol mouse model. Therefore to test my hypothesis, ammonium acetate (NH_4-Ac) was used as a stimulant to induce brain oedema in mice deficient of TLR9 ($TLR9^{-/-}$ B6) and compared to WT-B6 along with controls (NH_4-Ac untreated).

4.1. Ammonia-induced brain oedema and changes in the liver were dependent on TLR9

Ammonia is increased in the blood in PALF and it crosses the blood brain barrier resulting in astrocyte swelling and brain oedema thereby increasing the water content in the brain [51, 188]. Increased ammonia also causes hepatocyte swelling and changes to the liver [189, 190]. Since 12 mM/kg of NH_4-Ac induced mortality and 7 mM of NH_4-Ac induced cell death, a lower concentration was used after optimisation experiments to induce inflammation and brain oedema [Method 2.24.1]. To determine whether TLR9 influenced the ammonia-induced brain oedema the differences in the brain water content of WT-B6 and $TLR9^{-/-}$ B6 mice was determined six hours after a single low dose

of NH_4-Ac administration (I.P., 4 mM) and compared to controls (untreated) [Method-2.24.4.5].

Following NH_4-Ac stimulation (4 mM), there was a significant increase in the brain water content in WT-B6 mice (n=11) compared to controls (n=12) (NH_4-Ac untreated) ($p<0.0001$); there was no difference in the brain water content in $TLR9^{-/-}$ B6 mice (n=10) compared to controls (n=12). There was a significant decrease in the brain water content in $TLR9^{-/-}$ B6 mice compared to WT-B6 mice ($p<0.01$) following NH_4-Ac stimulation (4 mM) [Figure 4.1]. These findings were consistent with the recently published data from Shah et al. that demonstrated the development of brain oedema in a paracetamol-induced mouse model [165].

Since brain oedema was decreased in $TLR9^{-/-}$ B6 mice and astrocyte swelling is an important consequence of brain oedema in the pathogenesis of HE, immunohistochemistry staining was performed on the brain sections to identify whether there are changes in the expression of TLR9 in astrocytes following NH_4-Ac stimulation. This technique was not successful as the TLR9 antibodies were raised from mouse and did not yield good results. The availability of TLR9 antibodies raised from other species, which are reactive with mouse and could be used for immunohistochemistry/immunofluorescence, were limited.

To determine whether the water content in the brain was associated with the changes in the liver, the histology and liver bodyweight ratio were also assessed in these groups [Method-2.24.2].

4.1.1. Changes in the liver bodyweight ratio

Following low dose of NH_4-Ac stimulation (4 mM), there was a significant increase in the liver bodyweight ratio in WT-B6 mice (n=16) compared to controls (n=13) ($p<0.0001$); there was no difference in the liver bodyweight ratio in $TLR9^{-/-}$ B6 mice (n=11) compared to controls (n=14). There was a significant decrease in the liver bodyweight ratio in $TLR9^{-/-}$ B6 mice compared to WT-B6 mice following NH_4-Ac stimulation (4 mM) ($p<0.0001$) [Figure 4.2].

4.1.2. Changes in the liver histology

Following NH_4-Ac stimulation (4 mM), there was hepatocyte swelling in the histology sections of WT-B6 mice liver compared to controls (H&E staining). Hepatocyte swelling was decreased in $TLR9^{-/-}$ B6 mice compared to WT-B6 mice following NH_4-Ac stimulation (4 mM) [Figure 4.3].

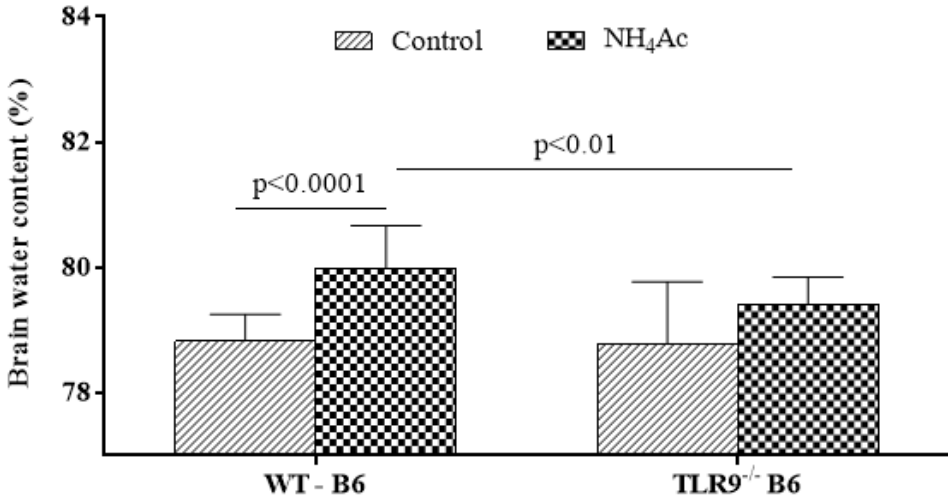

Figure 4.1: Brain water content in WT-B6 and TLR9$^{-/-}$ B6 mice following NH_4-Ac stimulation.

Following NH_4-Ac stimulation (4 mM), there was a significant increase in the brain water content in WT-B6 mice compared to controls ($p<0.0001$) [mean difference: 1.35; 95% C.I.: 0.9 to 1.8], which was ameliorated in TLR9$^{-/-}$ B6 mice compared to WT-B6 mice ($p<0.01$) [mean difference: -0.9; 95% C.I.: -1.4 to -0.39]. [WT-B6 mice (n=11) & controls (n=12); TLR9$^{-/-}$ B6 mice (n=10) & controls (n=12)]. Normality assumptions were checked and the data are expressed as mean with S.D.; $p<0.05$ were considered statistically significant. Student t-test was used to analyse the differences between parametric data sets.

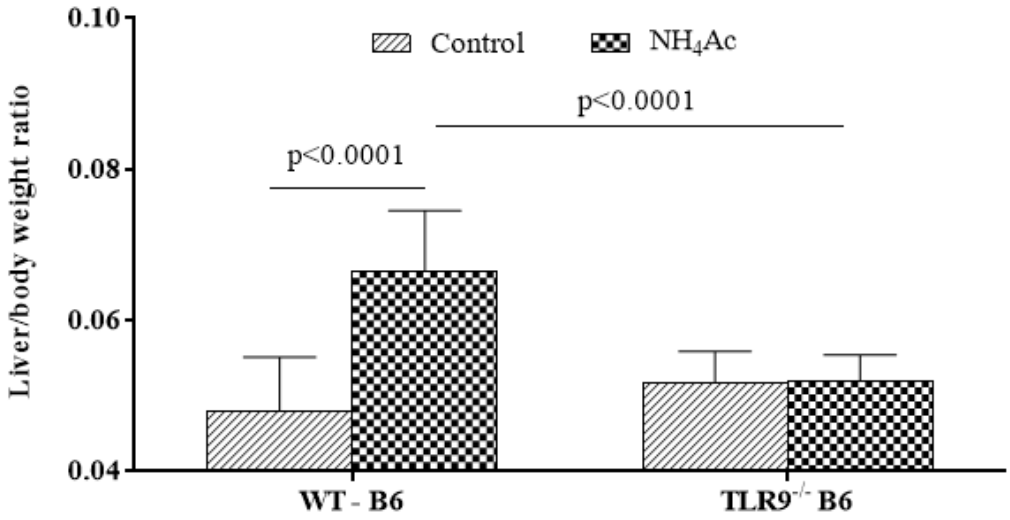

Figure 4.2: Liver bodyweight ratio in WT-B6 and TLR9$^{-/-}$ B6 mice following NH_4-Ac stimulation.

Following NH_4-Ac stimulation (4 mM), there was a significant increase in the liver bodyweight ratio in WT-B6 mice compared to controls ($p<0.0001$) [mean difference: 0.02; 95% C.I.: 0.013 to 0.026], which was ameliorated in TLR9$^{-/-}$ B6 mice compared to WT-B6 mice ($p<0.0001$) [mean difference: -0.015; 95% C.I.: -0.019 to 0.011]. [WT-B6 mice (n=16) & controls (n=13); TLR9$^{-/-}$ B6 mice (n=11) & controls (n=14)]. Normality assumptions were checked and the data are expressed as mean with S.D.; $p<0.05$ were considered statistically significant. Student t-test was used to analyse the differences between parametric data sets.

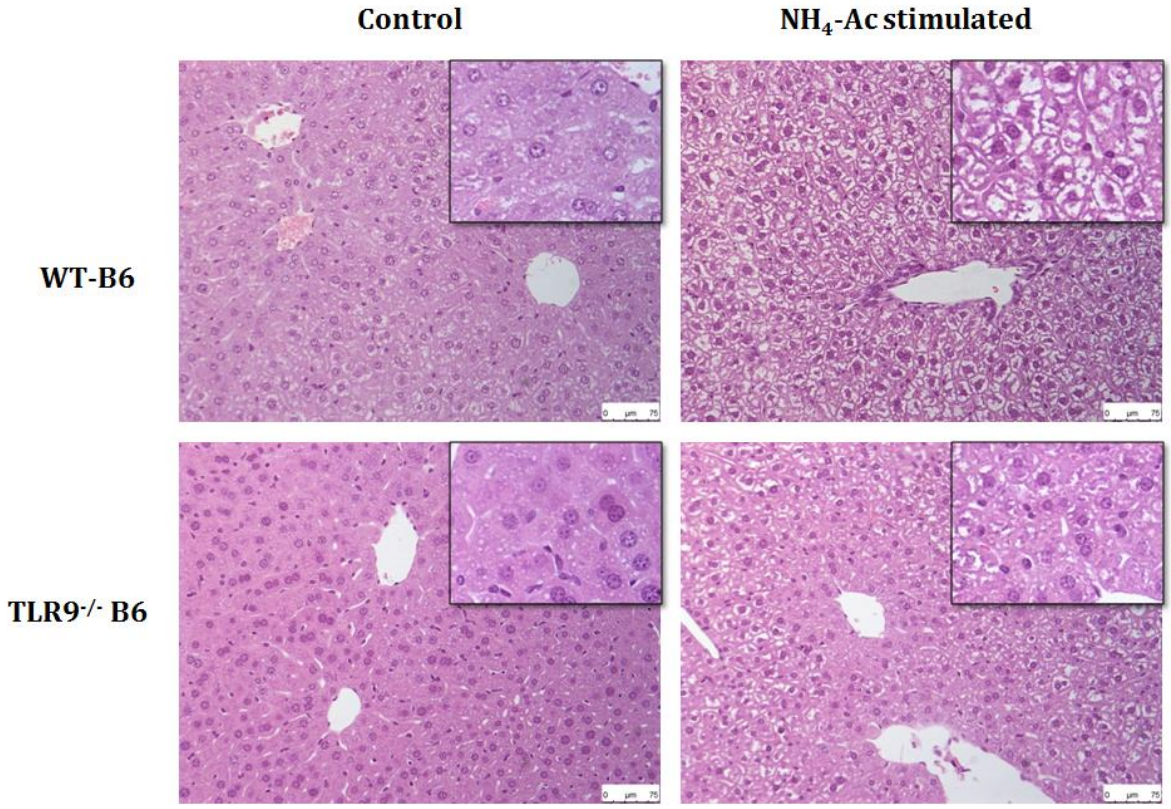

Figure 4.3: Liver histological changes in WT-B6 mice and TLR9$^{-/-}$ B6 mice following NH_4-Ac stimulation.

These light microscope images (200x magnification) are histological sections (H&E stained) of the liver representing four different mice groups. Following NH_4-Ac stimulation (4 mM), hepatocyte swelling was usually identified by the clearing of cytoplasm was increased in the histological sections of the liver in WT-B6 mice compared to controls, where the cytoplasm of cells remained intact. Following NH_4-Ac stimulation (4 mM), there was no difference in the hepatocyte morphology in TLR9$^{-/-}$ B6 mice compared to controls but the hepatocyte swelling was decreased compared to WT-B6 mice. The images in the black box inset are the same regions of the specimen captured at a higher magnification (400x).

4.2. Neutrophil function was unaltered following NH_4-Ac stimulation

Ammonia induces neutrophil dysfunction by decreasing neutrophil phagocytic activity and increasing the release of reactive oxygen species (ROS), which further contributes to the oxidative stress and systemic inflammation characteristic of PALF [139]. This exacerbates the cerebral effects of ammonia [140]. Therefore to determine whether ammonia altered the neutrophil phenotype and function through a TLR9-mediated pathway, NH_4-Ac (4 mM) was administered to WT-B6 mice (n=7) and TLR9$^{-/-}$ B6 mice (n=6) and compared to controls (NH_4-Ac untreated) [WT-B6 (n=10) & TLR9$^{-/-}$ B6 (n=10)]. Neutrophil phagocytosis was measured by incubating the whole blood with FITC dextran and myeloperoxidase expression was determined as a measure of spontaneous ROS production in the neutrophils (Lys6G and CD11b – positive cells) isolated from blood. Although there are many indirect methods employed to measure the ROS production in mice, there is no direct method to measure the neutrophil ROS production in mice. Moreover, the oxidative burst kit used to measure ROS production in humans is not compatible for mice, therefore this method was used.

Following NH_4-Ac stimulation (4 mM), there was no difference in the phagocytic activity of neutrophils from whole blood in WT-B6 mice and TLR9$^{-/-}$ B6 mice compared to controls [Figure 4.4a]. Also there was no difference in the expression of myeloperoxidase present on the surface of neutrophils isolated from whole blood in WT-B6 mice and TLR9$^{-/-}$ B6 mice following NH_4-Ac stimulation (4 mM) compared to controls [Figure 4.4b].

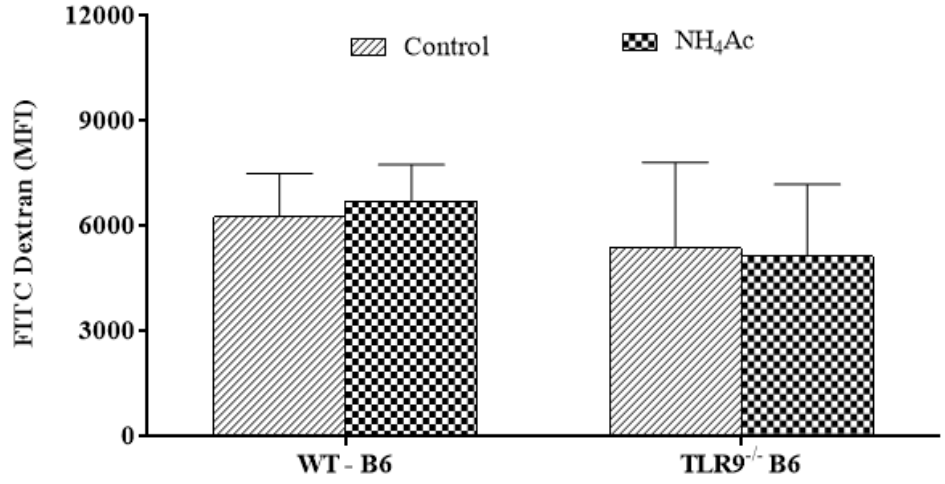

(a)

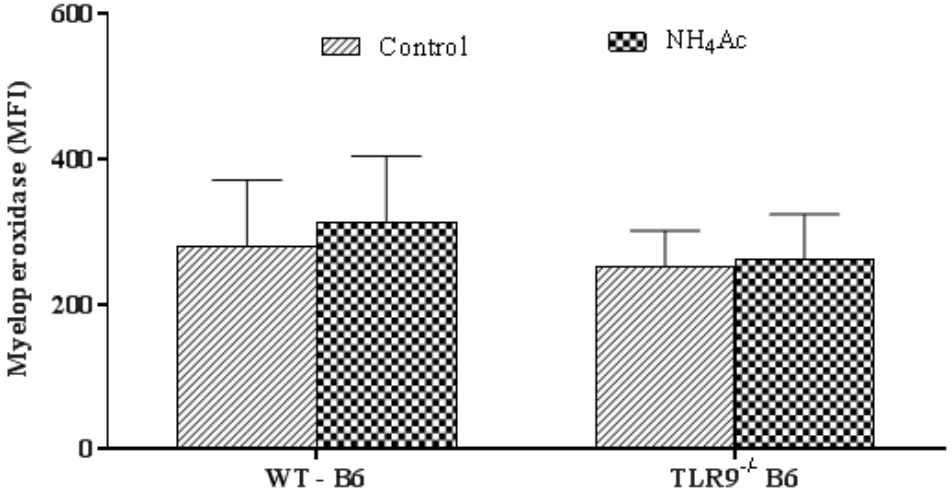

(b)

Figure 4.4: Circulating neutrophil function following NH_4-Ac stimulation

Following NH_4-Ac stimulation (4 mM), there was no difference in the phagocytic activity (a) or myeloperoxidase expression (b) of neutrophils in WT-B6 mice or TLR9$^{-/-}$ B6 mice compared to controls. Normality assumptions were checked and the data are expressed as mean with S.D.; $p<0.05$ were considered statistically significant. Student t-test was used to analyse the differences between parametric data sets.

4.3. Ammonia altered the function of T cells, macrophages and NK cells in a TLR9-dependent manner

It is well known that systemic inflammation exacerbates the development of ammonia-induced brain oedema [39, 103]. Astrocyte swelling was markedly increased in cultures pre-treated with ammonia and then exposed to the cytokines IFN-γ, TNF-α, IL-1 and IL-6 [191]. Immune cell subsets including T cells, NK cells and macrophages produce these cytokines and contribute to an inflammatory environment [118].

To understand whether inflammation contributes to the ammonia-induced brain water content through a TLR9-mediated pathway, the cytokine production of these cell subsets was determined in WT-B6 mice and TLR9$^{-/-}$ B6 following NH_4-Ac (4 mM) stimulation. The intracellular cytokine production of T cells, macrophages and NK cells was determined in those cells isolated from spleen using flow cytometry in WT-B6 mice and TLR9$^{-/-}$ B6 mice. Intracellular cytokine production of T cells was also determined in the immune cells isolated from liver [Method-2.13].

4.3.1. Decreased cytokine production in splenic T cells in TLR9$^{-/-}$ B6 mice

Intracellular cytokine production was determined in the CD4^{pos} T cells (CD3 & CD4 – positive cells) and CD8^{pos} T cells (CD3 & CD8 – positive cells) in WT-B6 mice (n=13) and TLR9$^{-/-}$ B6 mice (n=14) six hours following NH_4-Ac (4 mM) stimulation and compared to controls (NH_4-Ac untreated) [WT-B6 (n=13) & TLR9$^{-/-}$ B6 (n=10)] [Method-2.14.4.7].

4.3.1.1. Decreased cytokine production in splenic $CD4^{pos}$ T cells in $TLR9^{-/-}$ B6 mice

Following NH_4-Ac stimulation (4 mM), there was a significant increase in the intracellular cytokine IFN-γ produced by $CD4^{pos}$ T cells isolated from spleen in WT-B6 mice compared to controls ($p<0.0001$); there was no difference in the intracellular cytokine IFN-γ produced by $CD4^{pos}$ T cells isolated from spleen in $TLR9^{-/-}$ B6 mice compared to controls. There was a significant decrease in the intracellular cytokine IFN-γ produced by $CD4^{pos}$ T cells in $TLR9^{-/-}$ B6 mice compared to WT-B6 mice following NH_4-Ac stimulation (4 mM) ($p<0.001$) [Figure 4.5].

Following NH_4-Ac stimulation (4 mM), there was a significant increase in the intracellular cytokine TNF-α produced by $CD4^{pos}$ T cells isolated from spleen in WT-B6 mice compared to controls ($p<0.0001$). There was also a significant increase in the intracellular cytokine TNF-α produced by $CD4^{pos}$ T cells isolated from spleen in $TLR9^{-/-}$ B6 mice compared to controls ($p<0.0001$). However, there was a significant decrease in the intracellular cytokine TNF-α produced by $CD4^{pos}$ T cells in $TLR9^{-/-}$ B6 mice compared to WT-B6 mice following NH_4-Ac stimulation (4 mM) ($p<0.0001$) [Figure 4.6].

Following NH_4-Ac stimulation (4 mM), there was a significant increase in the intracellular cytokine IL-6 produced by $CD4^{pos}$ T cells isolated from spleen in WT-B6 mice compared to controls ($p<0.0001$) but there was no difference in the intracellular cytokine IL-6 produced by $CD4^{pos}$ T cells isolated from spleen in $TLR9^{-/-}$ B6 mice compared to controls. There was a significant decrease in the intracellular cytokine IL-6 produced by $CD4^{pos}$ T cells in $TLR9^{-/-}$ B6 mice compared to WT-B6 mice following NH_4-Ac stimulation (4 mM) ($p<0.01$) [Figure 4.7].

Following NH_4-Ac stimulation (4 mM), there was no difference in the intracellular cytokine IL-17 produced by $CD4^{pos}$ T cells isolated from spleen in WT-B6 mice and TLR9$^{-/-}$ B6 mice and compared to controls [Figure 4.8].

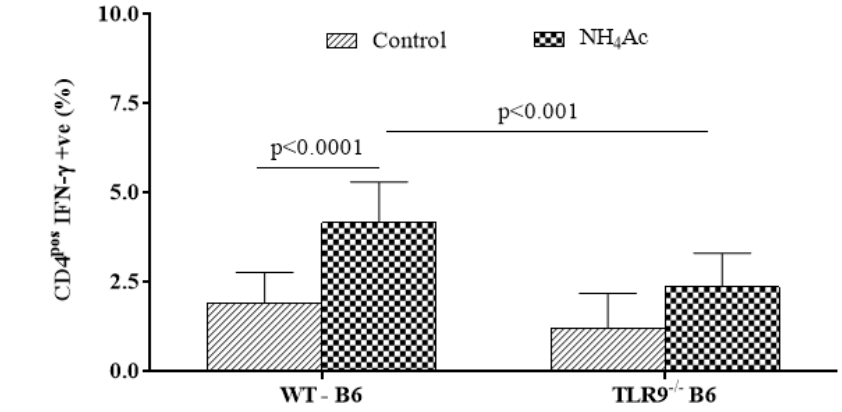

(A)

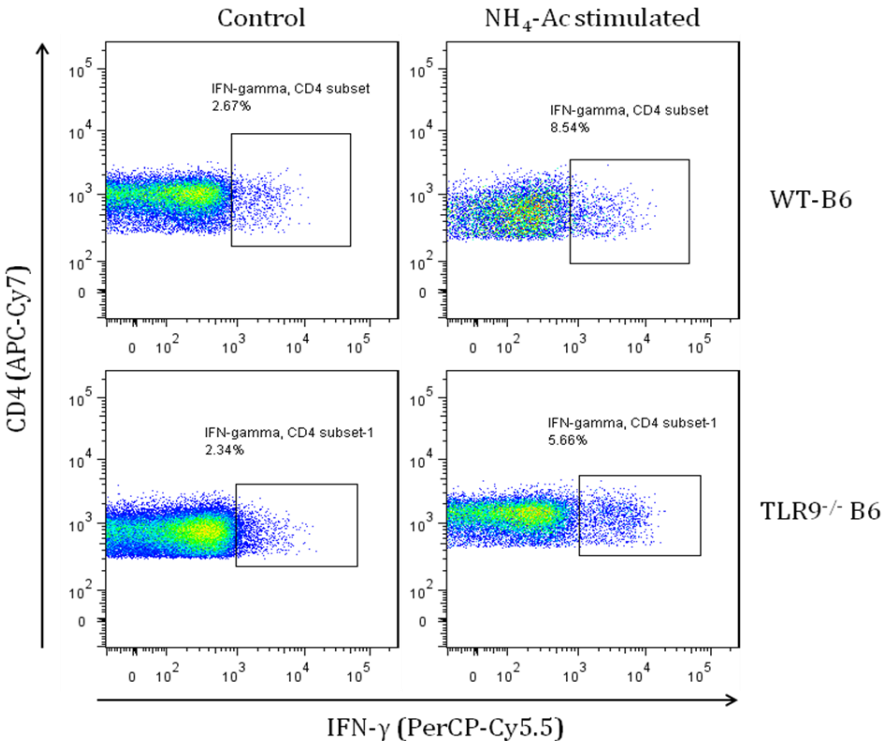

(B)

Figure 4.5: CD4^{pos} IFN-γ production in WT-B6 and TLR9$^{-/-}$ B6 mice splenocytes following NH_4-Ac stimulation.

The intracellular cytokine IFN-γ produced by splenic CD4^{pos} T cells was significantly increased in WT-B6 mice following NH_4-Ac stimulation (4 mM) compared to controls ($p<0.0001$) [median difference: 2.2; 95% C.I.: 1.5 to 3] (non-normal data). There was no difference in IFN-γ produced by splenic CD4^{pos} T cells in TLR9$^{-/-}$ B6 mice following NH_4-Ac stimulation (4 mM) compared to controls [median difference: 0.8; 95% C.I.: -0.1 to 1.7] (non-normal data), but it was significantly ameliorated compared to WT-B6 mice ($p<0.001$) [median difference: –1.9; 95% C.I.: -3 to -1.2] (non-normal data). [WT-B6 mice

(n=13) & controls (n=13); TLR9$^{-/-}$ B6 mice (n=14) & controls (n=10)]. Normality assumptions were checked and the data are expressed as mean with S.D.; $p<0.05$ were considered statistically significant. Mann-Whitney U test was used to analyse the differences between non-parametric data sets. (A) Graph and (B) FACS plots representing each group.

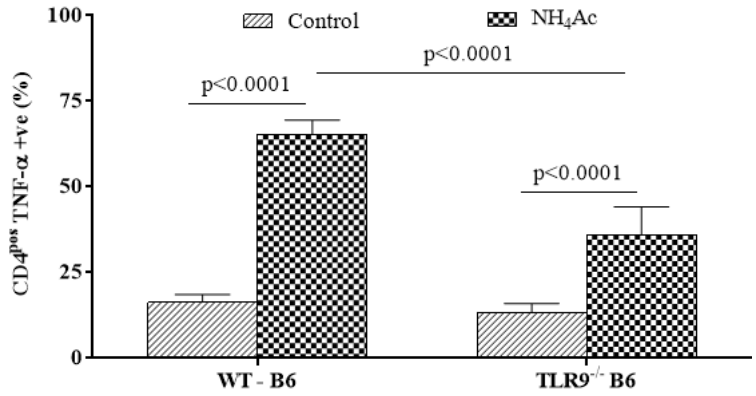

(A)

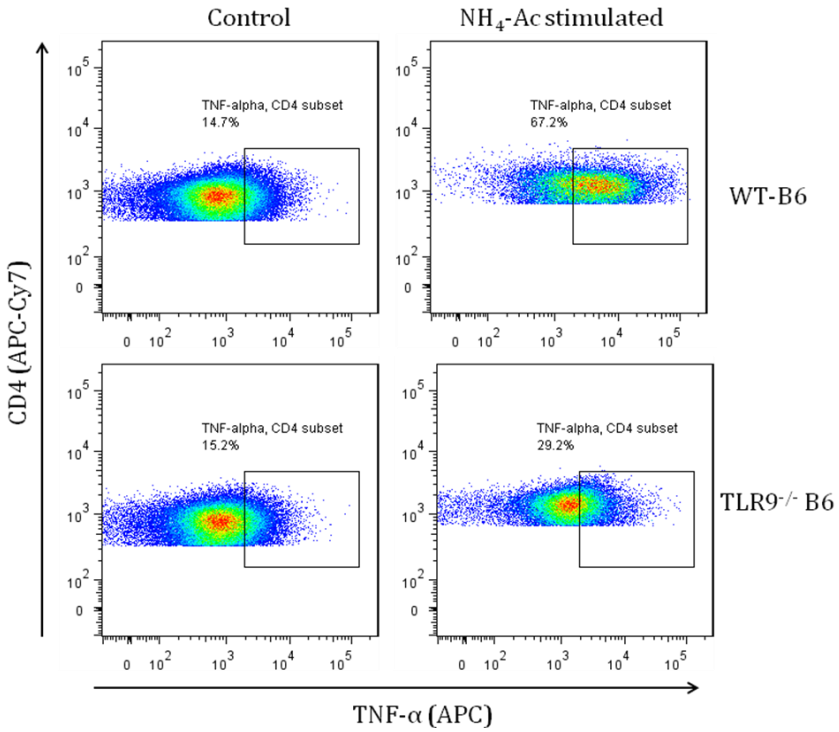

(B)

Figure 4.6: CD4^{pos} TNF-α production in WT-B6 and TLR9$^{-/-}$ B6 mice splenocytes following NH_4-Ac stimulation.

The intracellular cytokine TNF-α produced by splenic CD4^{pos} T cells was significantly increased in WT-B6 mice following NH_4-Ac stimulation (4 mM) compared to controls ($p<0.0001$) [median difference: 49.7; 95% C.I.: 47.4 to 51.7] (non-normal data). There was a significant increase in TNF-α produced by splenic CD4^{pos} T cells in TLR9$^{-/-}$ B6 mice following NH_4-Ac stimulation (4 mM) compared to controls ($p<0.0001$) [median difference: 25.2; 95% C.I.: 22.7 to 27.5] (non-normal data), but it was significantly

ameliorated compared to WT-B6 mice ($p<0.0001$) [median difference: –27.8; 95% C.I.: -30 to -25.3] (non-normal data). [WT-B6 mice (n=13) & controls (n=13); $TLR9^{-/-}$ B6 mice (n=14) & controls (n=10)]. Normality assumptions were checked and the data are expressed as mean with S.D.; $p<0.05$ were considered statistically significant. Mann-Whitney U test was used to analyse the differences between non-parametric data sets. (A) Graph and (B) FACS plots representing each group.

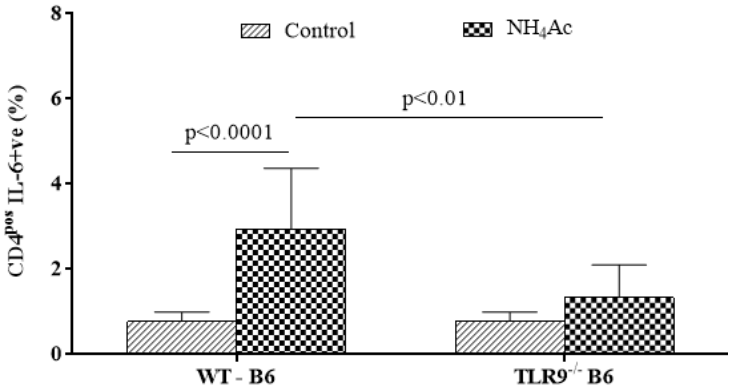

(A)

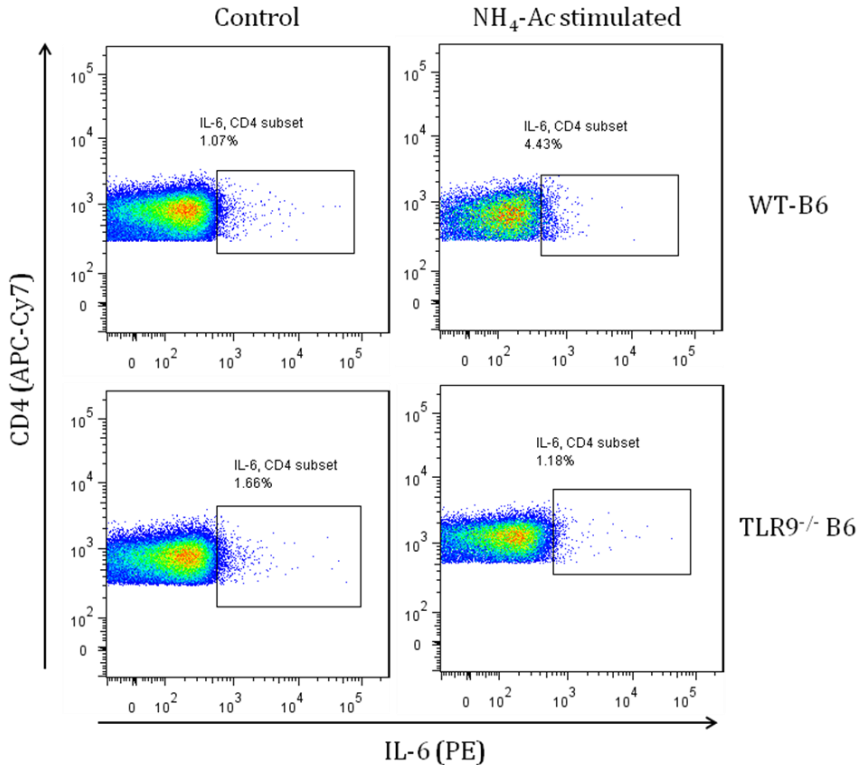

(B)

Figure 4.7: CD4^{pos} IL-6 production in WT-B6 and TLR9$^{-/-}$ B6 mice splenocytes following NH_4-Ac stimulation.

The intracellular cytokine IL-6 produced by splenic CD4^{pos} T cells was significantly increased in WT-B6 mice following NH_4-Ac stimulation (4 mM) compared to controls ($p<0.0001$) [mean difference: 2.1; 95% C.I.: 1.3 to 3] (normal data). There was no difference in IL-6 produced by splenic CD4^{pos} T cells in TLR9$^{-/-}$ B6 mice following NH_4-Ac stimulation (4 mM) compared to controls [mean difference: 0.5; 95% C.I.: 0.02 to 1.07] (normal data), but it was significantly ameliorated compared to WT-B6 mice ($p<0.01$)

[mean difference: –1.6; 95% C.I.: -2.6 to -0.6] (normal data). [WT-B6 mice (n=13) & controls (n=13); $TLR9^{-/-}$ B6 mice (n=14) & controls (n=10)]. Normality assumptions were checked and the data are expressed as mean with S.D.; $p<0.05$ were considered statistically significant. Student t-test was used to analyse the differences between parametric data sets. (A) Graph and (B) FACS plots representing each group.

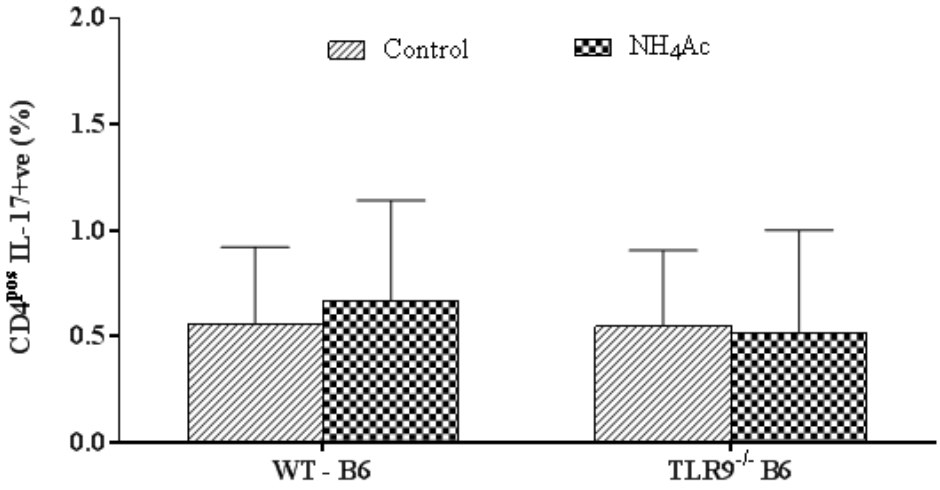

Figure 4.8: $CD4^{pos}$ IL-17 production in WT-B6 mice and $TLR9^{-/-}$ B6 mice splenocytes following NH_4-Ac stimulation.

There was no difference in the intracellular cytokine IL-17 produced by splenic $CD4^{pos}$ T cells in WT-B6 mice or TLR9-/- B6 mice following NH_4-Ac stimulation (4 mM) compared to controls. Normality assumptions were checked and the data are expressed as mean with S.D.; $p<0.05$ were considered statistically significant. Student t-test was used to analyse the differences between parametric data sets.

4.3.1.2. Decreased cytokine production in splenic $CD8^{pos}$ T cells in $TLR9^{-/-}$ B6 mice

Following NH_4-Ac stimulation (4 mM), there was a significant increase in the intracellular cytokine IFN-γ produced by $CD8^{pos}$ T cells isolated from spleen in WT-B6 mice compared to controls ($p<0.0001$). There was also a significant increase in the intracellular cytokine IFN-γ produced by $CD8^{pos}$ T cells isolated from spleen in $TLR9^{-/-}$ B6 mice compared to controls ($p<0.05$). There was however a significant decrease in the intracellular cytokine IFN-γ produced by $CD8^{pos}$ T cells in $TLR9^{-/-}$ B6 mice compared to WT-B6 mice following NH_4-Ac stimulation (4 mM) ($p<0.001$) [Figure 4.9].

Following NH_4-Ac stimulation (4 mM), there was a significant increase in the intracellular cytokine TNF-α produced by $CD8^{pos}$ T cells isolated from spleen in WT-B6 mice compared to controls ($p<0.0001$). There was also a significant increase in the intracellular cytokine TNF-α produced by $CD8^{pos}$ T cells isolated from spleen in $TLR9^{-/-}$ B6 mice compared to controls ($p<0.05$). There was a significant decrease in the intracellular cytokine TNF-α produced by $CD8^{pos}$ T cells in $TLR9^{-/-}$ B6 mice compared to WT-B6 mice following NH_4-Ac stimulation (4 mM) ($p<0.0001$) [Figure 4.10].

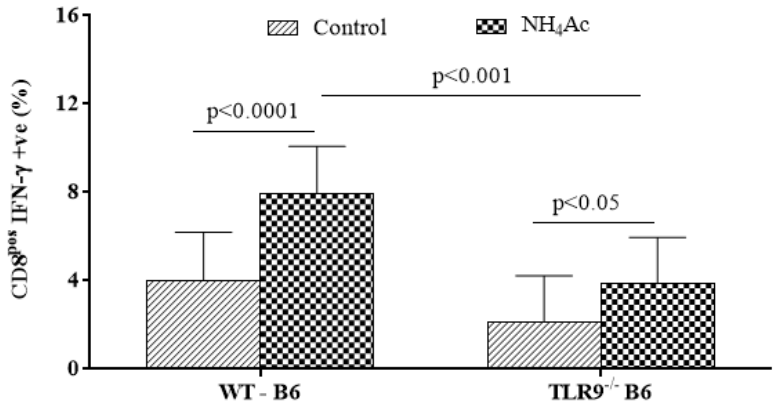

(A)

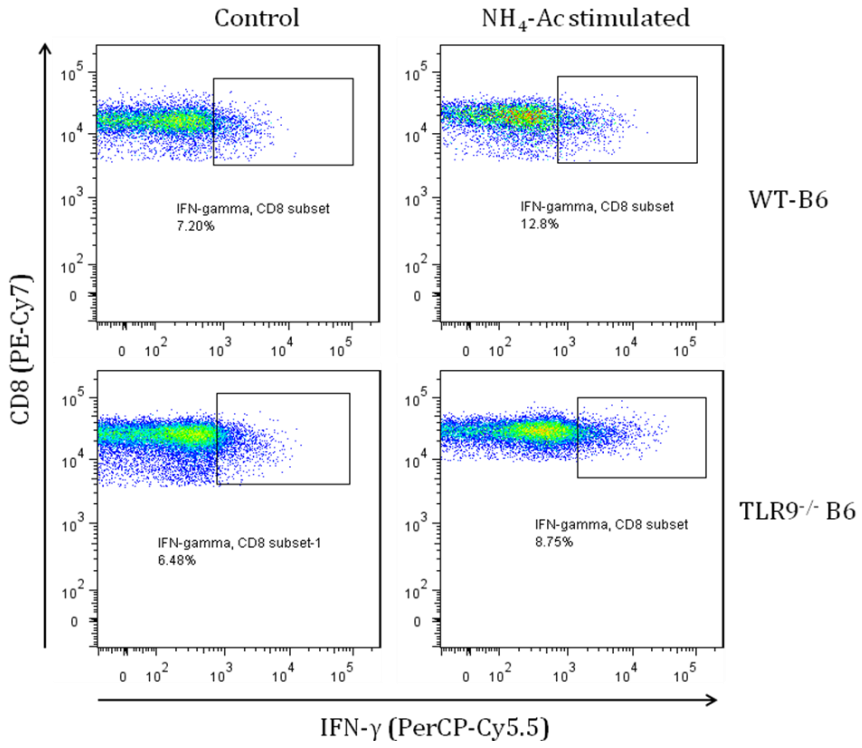

(B)

Figure 4.9: CD8^{pos} IFN-γ production in WT-B6 and TLR9$^{-/-}$ B6 mice splenocytes following NH_4-Ac stimulation.

The intracellular cytokine IFN-γ produced by splenic CD8^{pos} T cells was significantly increased in WT-B6 mice following NH_4-Ac stimulation (4 mM) compared to controls ($p<0.0001$) [mean difference: 3.9; 95% C.I.: 2.1 to 5.8] (normal data). There was no difference in IFN-γ produced by splenic CD8^{pos} T cells in TLR9$^{-/-}$ B6 mice following NH_4-Ac stimulation (4 mM) compared to controls [mean difference: 1.78; 95% C.I.: -0.4 to 4] (normal data), but it was significantly ameliorated compared to WT-B6 mice ($p<0.001$) [mean difference: –4; 95% C.I.: -6 to -2] (normal data). [WT-B6 mice (n=13) & controls

(n=13); TLR9$^{-/-}$ B6 mice (n=14) & controls (n=10)]. Normality assumptions were checked and the data are expressed as mean with S.D.; $p<0.05$ were considered statistically significant. Student t-test was used to analyse the differences between parametric data sets. (A) Graph and (B) FACS plots representing each group.

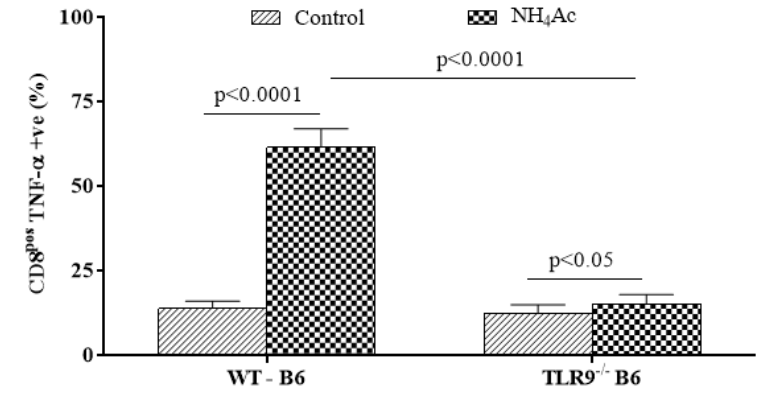

(A)

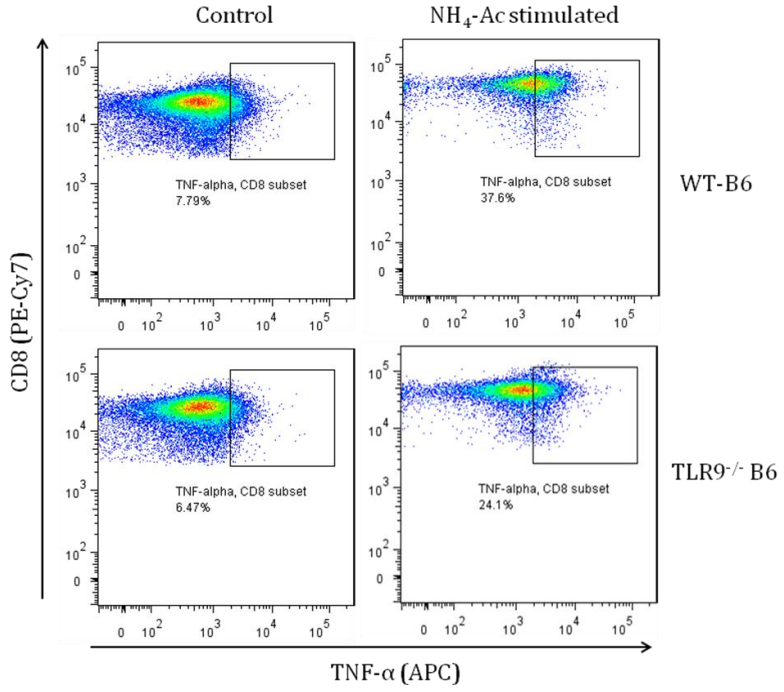

(B)

Figure 4.10: CD8^{pos} TNF-α production in WT-B6 and TLR9$^{-/-}$ B6 mice splenocytes following NH_4-Ac stimulation.

The intracellular cytokine TNF-α produced by splenic CD8^{pos} T cells was significantly increased in WT-B6 mice following NH_4-Ac stimulation (4 mM) compared to controls ($p<0.0001$) [mean difference: 47.6; 95% C.I.: 44.2 to 51] (normal data). There was a significant increase in TNF-α produced by splenic CD8^{pos} T cells in TLR9$^{-/-}$ B6 mice following NH_4-Ac stimulation (4 mM) compared to controls ($p<0.05$) [mean difference: 3; 95% C.I.: 0.8 to 5.4] (normal data), but it was significantly ameliorated compared to WT-B6 mice ($p<0.0001$) [mean difference: –46; 95% C.I.: -49.6 to -42.7] (normal data). [WT-B6 mice (n=13) & controls (n=13); TLR9$^{-/-}$ B6 mice (n=14) & controls (n=10)].

Normality assumptions were checked and the data are expressed as mean with S.D.; $p<0.05$ were considered statistically significant. Student t-test was used to analyse the differences between parametric data sets. (A) Graph and (B) FACS plots representing each group

4.3.1.3. Decreased cytokine production in hepatic $CD4^{pos}$ T cells in $TLR9^{-/-}$ B6 mice

Following NH_4-Ac stimulation (4 mM), there was a significant increase in the intracellular cytokine IFN-γ produced by $CD4^{pos}$ T cells isolated from the liver in WT-B6 mice compared to controls ($p<0.0001$). There was also a significant increase in the intracellular cytokine IFN-γ produced by $CD4^{pos}$ T cells isolated from liver in $TLR9^{-/-}$ B6 mice compared to controls ($p<0.001$). There was however a significant decrease in the intracellular cytokine IFN-γ produced by $CD4^{pos}$ T cells in $TLR9^{-/-}$ B6 mice compared to WT-B6 mice following NH_4-Ac stimulation (4 mM) ($p<0.0001$) [Figure 4.11].

Following NH_4-Ac stimulation (4 mM), there was a significant increase in the intracellular cytokine TNF-α produced by $CD4^{pos}$ T cells isolated from the liver in WT-B6 mice compared to controls ($p<0.0001$) but there was no difference in the intracellular cytokine TNF-α produced by $CD4^{pos}$ T cells isolated from liver in $TLR9^{-/-}$ B6 mice compared to controls. There was a significant decrease in the intracellular cytokine TNF-α produced by $CD4^{pos}$ T cells in $TLR9^{-/-}$ B6 mice compared to WT-B6 mice following NH_4-Ac stimulation (4 mM) ($p<0.0001$) [Figure 4.12].

Following NH_4-Ac stimulation (4 mM), there was a significant increase in the intracellular cytokine IL-6 produced by $CD4^{pos}$ T cells isolated from the liver in WT-B6 mice compared to controls ($p<0.0001$). There was also a significant increase in the intracellular cytokine IL-6 produced by $CD4^{pos}$ T cells isolated from liver in $TLR9^{-/-}$ B6 mice compared to controls ($p<0.05$). There was however a significant decrease in the intracellular cytokine IL-6 produced by $CD4^{pos}$ T cells in $TLR9^{-/-}$ B6 mice compared to WT-B6 mice following NH_4-Ac stimulation (4 mM) ($p<0.01$) [Figure 4.13].

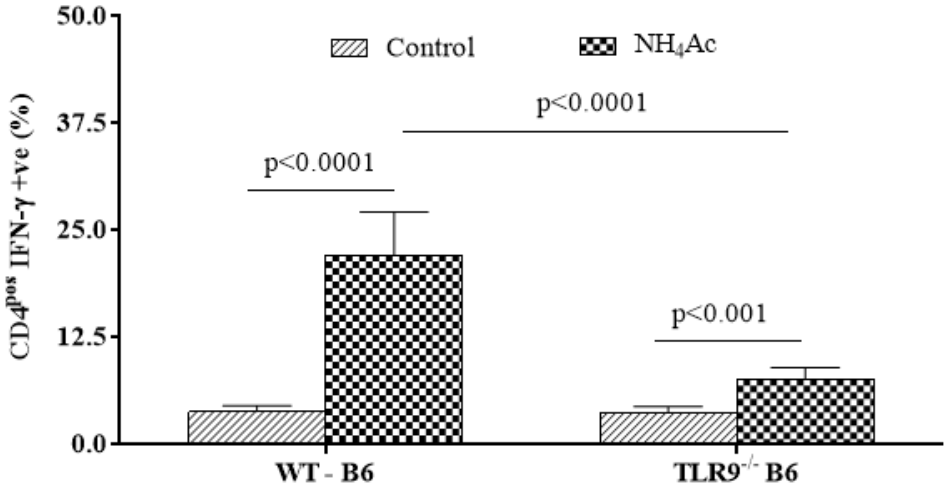

Figure 4.11: CD4^{pos} IFN-γ production in WT-B6 and TLR9$^{-/-}$ B6 mice hepatic T cells following NH_4-Ac stimulation.

The intracellular cytokine IFN-γ produced by hepatic CD4^{pos} T cells was significantly increased in WT-B6 mice following NH_4-Ac stimulation (4 mM) compared to controls ($p<0.0001$) [mean difference: 18.3; 95% C.I.: 15 to 21.7] (normal data). There was a significant increase in IFN-γ produced by hepatic CD4^{pos} T cells in TLR9$^{-/-}$ B6 mice following NH_4-Ac stimulation (4 mM) compared to controls ($p<0.001$) [mean difference: 3.9; 95% C.I.: 2.3 to 5.4] (normal data), but it was significantly ameliorated compared to WT-B6 mice ($p<0.0001$) [mean difference: –14.5; 95% C.I.: -18.6 to -10.4] (normal data). [WT-B6 mice (n=13) & controls (n=13); TLR9$^{-/-}$ B6 mice (n=14) & controls (n=10)]. Normality assumptions were checked and the data are expressed as mean with S.D.; $p<0.05$ were considered statistically significant. Student t-test was used to analyse the differences between parametric data sets.

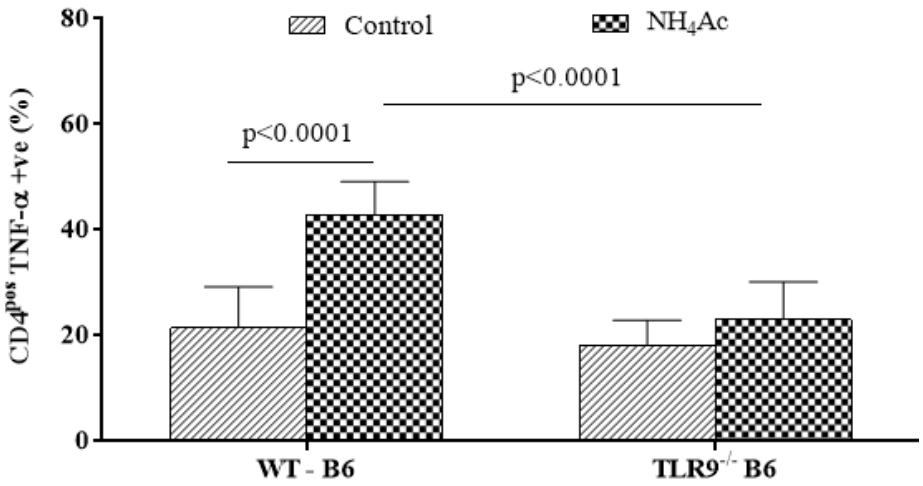

Figure 4.12: $CD4^{pos}$ TNF-α production in WT-B6 and $TLR9^{-/-}$ B6 mice hepatic T cells following NH_4-Ac stimulation.

The intracellular cytokine TNF-α produced by hepatic $CD4^{pos}$ T cells was significantly increased in WT-B6 mice following NH_4-Ac stimulation (4 mM) compared to controls ($p<0.0001$) [mean difference: 21.4; 95% C.I.: 14.5 to 28.2] (normal data). There was no difference in TNF-α produced by hepatic $CD4^{pos}$ T cells in $TLR9^{-/-}$ B6 mice following NH_4-Ac stimulation (4 mM) compared to controls [mean difference: 4.9; 95% C.I.: -4.1 to 14] (normal data), but it was significantly ameliorated compared to WT-B6 mice ($p<0.0001$) [mean difference: –19.9; 95% C.I.: -27 to -12.6] (normal data). [WT-B6 mice (n=13) & controls (n=13); $TLR9^{-/-}$ B6 mice (n=14) & controls (n=10)]. Normality assumptions were checked and the data are expressed as mean with S.D.; $p<0.05$ were considered statistically significant. Student t-test was used to analyse the differences between parametric data sets.

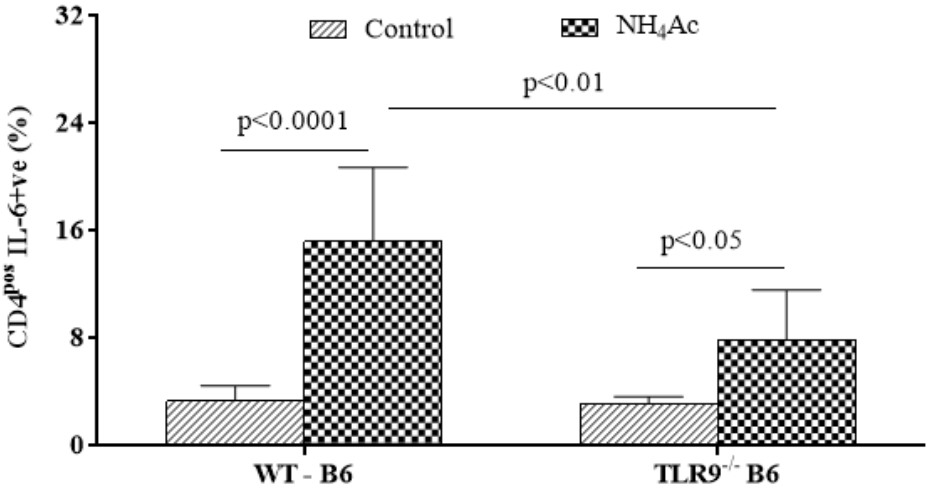

Figure 4.13: $CD4^{pos}$ IL-6 production in WT-B6 and $TLR9^{-/-}$ B6 mice hepatic T cells following NH_4-Ac stimulation.

The intracellular cytokine IL-6 produced by hepatic $CD4^{pos}$ T cells was significantly increased in WT-B6 mice following NH_4-Ac stimulation (4 mM) compared to controls ($p<0.0001$) [mean difference: 11.9; 95% C.I.: 8.1 to 15.6] (normal data). There was a significant increase in IL-6 produced by hepatic $CD4^{pos}$ T cells in $TLR9^{-/-}$ B6 mice following NH_4-Ac stimulation (4 mM) compared to controls ($p<0.05$) [mean difference: 4.8; 95% C.I.: 0.4 to 9] (normal data), but it was significantly ameliorated compared to WT-B6 mice ($p<0.01$) [mean difference: –7.2; 95% C.I.: -12.4 to -2.2] (normal data). [WT-B6 mice (n=13) & controls (n=13); $TLR9^{-/-}$ B6 mice (n=14) & controls (n=10)]. Normality assumptions were checked and the data are expressed as mean with S.D.; $p<0.05$ were considered statistically significant. Student t-test was used to analyse the differences between parametric data sets.

4.3.1.4. Decreased cytokine production in hepatic $CD8^{pos}$ T cells in $TLR9^{-/-}$ B6 mice

Following NH_4-Ac stimulation (4 mM), there was a significant increase in the intracellular cytokine IFN-γ produced by $CD8^{pos}$ T cells isolated from liver in WT-B6 mice compared to controls ($p<0.0001$). There was also a significant increase in the intracellular cytokine IFN-γ produced by $CD8^{pos}$ T cells isolated from liver in $TLR9^{-/-}$ B6 mice compared to controls ($p<0.05$). There was however a significant decrease in the intracellular cytokine IFN-γ produced by $CD8^{pos}$ T cells in $TLR9^{-/-}$ B6 mice compared to WT-B6 mice following NH_4-Ac stimulation (4 mM) ($p<0.0001$) [Figure 4.14].

Following NH_4-Ac stimulation (4 mM), there was a significant increase in the intracellular cytokine TNF-α produced by $CD8^{pos}$ T cells isolated from liver in WT-B6 mice compared to controls ($p<0.0001$) but there was no difference in the intracellular cytokine TNF-α produced by $CD8^{pos}$ T cells isolated from liver in $TLR9^{-/-}$ B6 mice compared to controls. There was however a significant decrease in the intracellular cytokine TNF-α produced by $CD8^{pos}$ T cells in $TLR9^{-/-}$ B6 mice compared to WT-B6 mice following NH_4-Ac stimulation (4 mM) ($p<0.0001$) [Figure 4.15].

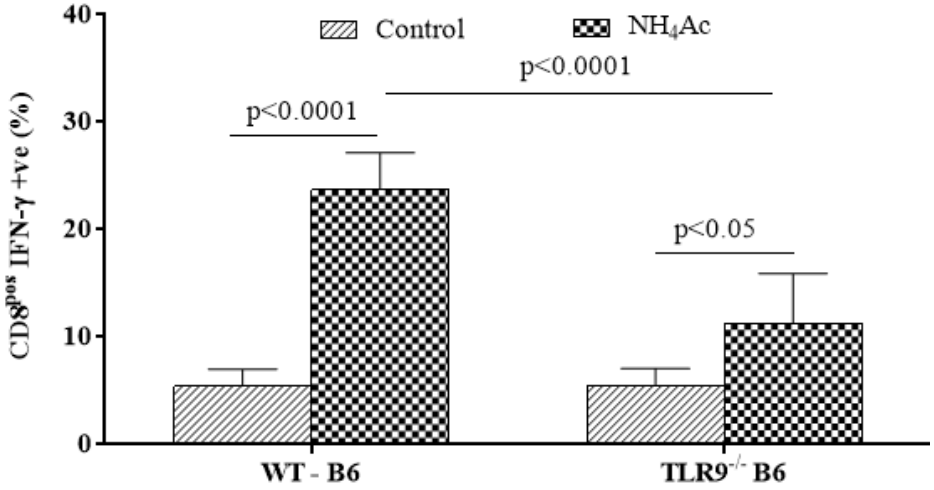

Figure 4.14: $CD8^{pos}$ IFN-γ production in WT-B6 and $TLR9^{-/-}$ B6 mice hepatic T cells following NH_4-Ac stimulation

The intracellular cytokine IFN-γ produced by hepatic $CD8^{pos}$ T cells was significantly increased in WT-B6 mice following NH_4-Ac stimulation (4 mM) compared to controls ($p<0.0001$) [mean difference: 18.3; 95% C.I.: 15.8 to 20.8] (normal data). There was a significant increase in IFN-γ produced by hepatic $CD8^{pos}$ T cells in $TLR9^{-/-}$ B6 mice following NH_4-Ac stimulation (4 mM) compared to controls ($p<0.05$) [mean difference: 5.8; 95% C.I.: 0.3 to 11.3] (normal data), but it was significantly ameliorated compared to WT-B6 mice ($p<0.0001$) [mean difference: –12.4; 95% C.I.: -16.7 to -8.1] (normal data). [WT-B6 mice (n=13) & controls (n=13); $TLR9^{-/-}$ B6 mice (n=14) & controls (n=10)]. Normality assumptions were checked and the data are expressed as mean with S.D.; $p<0.05$ were considered statistically significant. Student t-test was used to analyse the differences between parametric data sets.

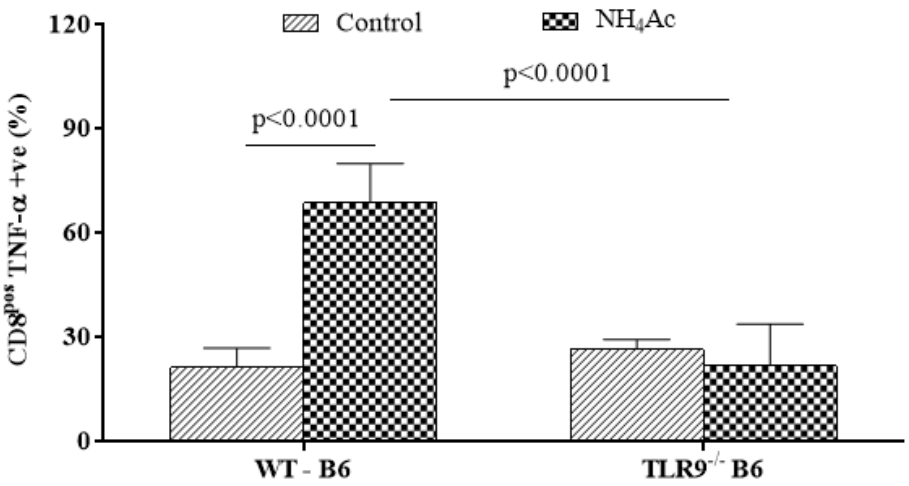

Figure 4.15: $CD8^{pos}$ TNF-α production in WT-B6 and $TLR9^{-/-}$ B6 mice hepatic T cells following NH_4-Ac stimulation.

The intracellular cytokine TNF-α produced by hepatic $CD8^{pos}$ T cells was significantly increased in WT-B6 mice following NH_4-Ac stimulation (4 mM) compared to controls ($p<0.0001$) [mean difference: 47.3; 95% C.I.: 38.8 to 55.8] (normal data). There was no difference in TNF-α produced by hepatic $CD8^{pos}$ T cells in $TLR9^{-/-}$ B6 mice following NH_4-Ac stimulation (4 mM) compared to controls [mean difference: -1; 95% C.I.: -14 to 10] (normal data), but it was significantly ameliorated compared to WT-B6 mice ($p<0.0001$) [mean difference: –44; 95% C.I.: -55 to -32] (normal data). [WT-B6 mice (n=13) & controls (n=13); $TLR9^{-/-}$ B6 mice (n=14) & controls (n=10)]. Normality assumptions were checked and the data are expressed as mean with S.D.; $p<0.05$ were considered statistically significant. Student t-test was used to analyse the difference between parametric data sets.

4.3.2. T cell phenotype was unaltered following NH_4-Ac stimulation

To determine whether ammonia altered the T cell phenotype, the frequency of naive (CD44+ and CD62L-); memory T cells (CD44- and CD62L+) and activation markers (CD69+) were determined in the $CD4^{pos}$ T cells (CD3 & CD4 – positive cells) and $CD8^{pos}$ T cells (CD3 & CD8 – positive cells) isolated from the spleen using flow cytometry [Method- 2.14.4.7].

There was no difference in the naive and memory subsets of the splenic $CD4^{pos}$ T cells in WT-B6 mice and $TLR9^{-/-}$ B6 mice following NH_4-Ac stimulation (4 mM) compared to controls [Figure 4.16a and b]. However, there was a significant increase in the splenic $CD4^{pos}$ CD69+ T cells in WT-B6 mice and $TLR9^{-/-}$ B6 mice following NH_4-Ac stimulation (4 mM) compared to controls [Figure 4.16c].

There was also no difference in the naive and memory subsets of the splenic $CD8^{pos}$ T cells in WT-B6 mice and $TLR9^{-/-}$ B6 mice following NH_4-Ac stimulation (4 mM) compared to controls [Figure 4.16d and e]. However, there was a significant increase in the splenic $CD8^{pos}$ CD69+ T cells in WT-B6 mice and $TLR9^{-/-}$ B6 mice following NH_4-Ac stimulation (4 mM) compared to controls ($p<0.05$) [Figure 4.16f].

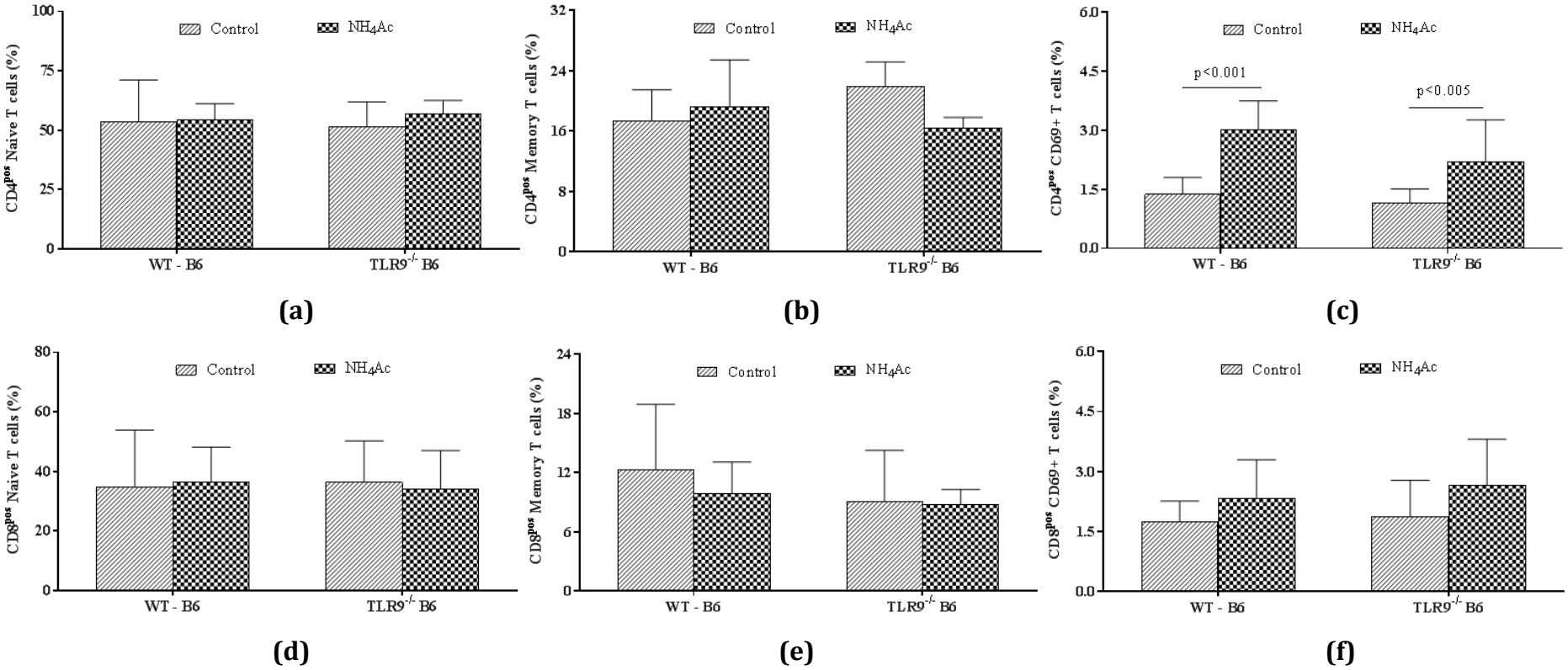

Figure 4.16: Phenotype of T cells following NH_4-Ac stimulation.

Following NH_4-Ac stimulation (4 mM), there was no difference in the frequency of $CD4^{pos}$ naive and memory T cells (a & b) and $CD8^{pos}$ naive and memory T cells (d & e) isolated from spleen in WT-B6 mice or $TLR9^{-/-}$ B6 mice compared to controls. Following NH_4-Ac stimulation (4 mM), there was a significant increase in the $CD4^{pos}$ CD69+ T cells but there was no difference in the $CD8^{pos}$ CD69+ T cells in WT-B6 mice or $TLR9^{-/-}$ B6 mice compared to controls. Normality assumptions were checked and the data are expressed as mean with S.D.; $p<0.05$ were considered statistically significant. Student t-test was used to analyse the differences between parametric data sets.

4.3.3. Decreased cytokine production in splenic macrophages in TLR9$^{-/-}$ B6 mice

The frequency of intracellular cytokines was determined in the macrophages (F4/80 & CD11b – positive cells) in WT-B6 mice (n=5) and TLR9$^{-/-}$ B6 mice (n=6) six hours following NH_4-Ac (4 mM) stimulation and compared to controls (NH_4-Ac untreated) [WT-B6 (n=5) & TLR9$^{-/-}$ B6 (n=7)] [Method-2.14.4.9].

Following NH_4-Ac stimulation (4 mM), there was a significant increase in the intracellular cytokine IFN-γ produced by macrophages isolated from the spleen in WT-B6 mice compared to controls ($p<0.01$) but there was no difference in the intracellular cytokine IFN-γ produced by macrophages isolated from spleen in TLR9$^{-/-}$ B6 mice and compared to controls. There was however a significant decrease in the intracellular cytokine IFN-γ produced by macrophages in TLR9$^{-/-}$ B6 mice compared to WT-B6 mice following NH_4-Ac stimulation (4 mM) ($p<0.001$) [Figure 4.17].

Following NH_4-Ac stimulation (4 mM), there was a significant increase in the intracellular cytokine TNF-α produced by macrophages isolated from spleen in WT-B6 mice compared to controls ($p<0.0001$). There was also a significant increase in the intracellular cytokine TNF-α produced by macrophages isolated from spleen in TLR9$^{-/-}$ B6 mice compared to controls ($p<0.001$). There was however a significant decrease in the intracellular cytokine TNF-α produced by macrophages in TLR9$^{-/-}$ B6 mice compared to WT-B6 mice following NH_4-Ac stimulation (4 mM) ($p<0.0001$) [Figure 4.18].

Following NH_4-Ac stimulation (4 mM), there was a significant increase in the intracellular cytokine IL-6 produced by macrophages isolated from spleen in WT-B6 mice compared to controls ($p<0.0001$) but there was no difference in the intracellular

cytokine IL-6 produced by macrophages isolated from spleen in TLR9$^{-/-}$ B6 mice compared to controls. There was a significant decrease in the intracellular cytokine IL-6 produced by macrophages in TLR9$^{-/-}$ B6 mice compared to WT-B6 mice following NH_4-Ac stimulation (4 mM) ($p<0.0001$) [Figure 4.19].

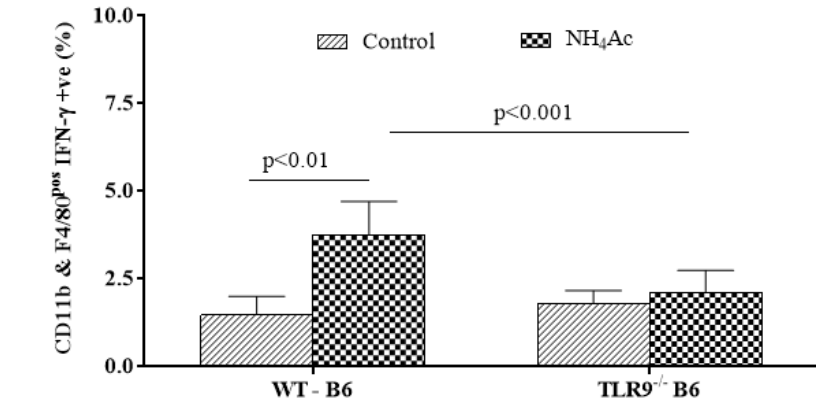

(A)

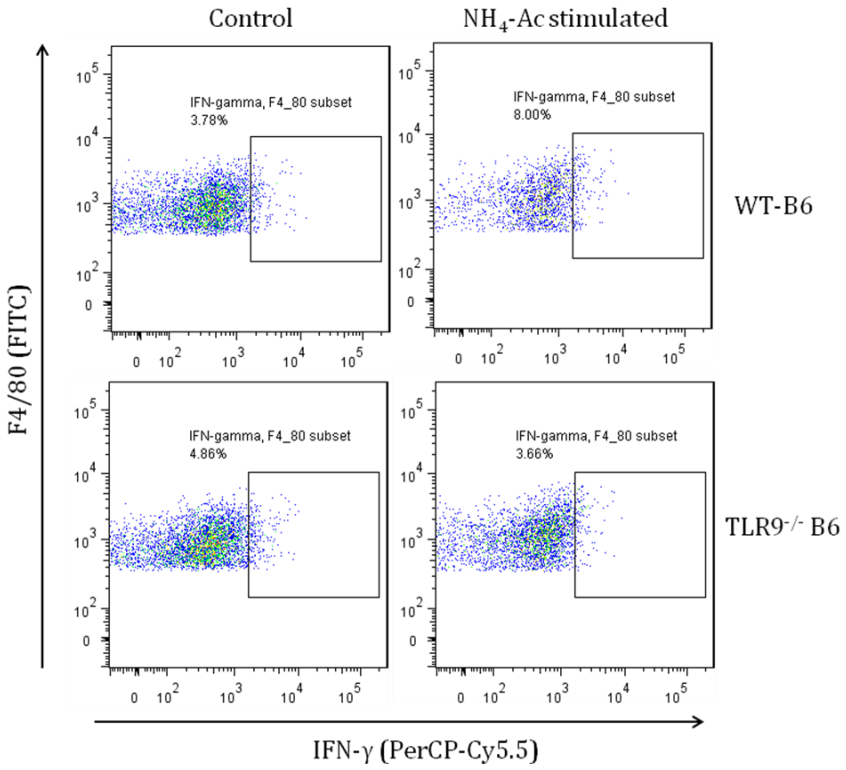

(B)

Figure 4.17: IFN-γ production by macrophages in WT-B6 and TLR9$^{-/-}$ B6 mice splenocytes following NH_4-Ac stimulation.

The intracellular cytokine IFN-γ produced by splenic macrophages was significantly increased in WT-B6 mice following NH_4-Ac stimulation (4 mM) compared to controls ($p<0.01$) [median difference: 2.4; 95% C.I.: 1.3 to 3.6] (non-normal data). There was no difference in IFN-γ produced by splenic macrophages in TLR9$^{-/-}$ B6 mice following NH_4-Ac stimulation (4 mM) compared to controls [mean difference: 0.3; 95% C.I.: -0.27 to 0.9] (normal data), but it was significantly ameliorated compared to WT-B6 mice ($p<0.001$) [mean difference: –1.6; 95% C.I.: -2.6 to -0.6] (normal data). [WT-B6 mice

(n=5) & controls (n=5); TLR9$^{-/-}$ B6 mice (n=6) & controls (n=7)]. Normality assumptions were checked and the data are expressed as mean with S.D.; $p<0.05$ were considered statistically significant. Student t-test was used to analyse the difference between parametric data sets and Mann-Whitney U test was used to analyse the difference between non-parametric data sets. (A) Graph and (B) FACS plots representing each group.

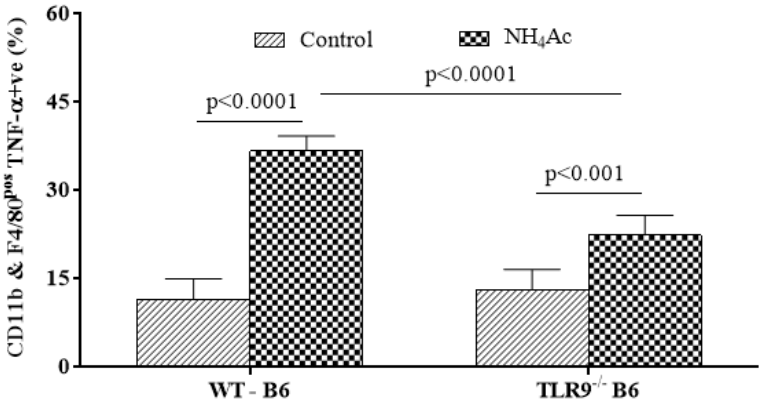

(A)

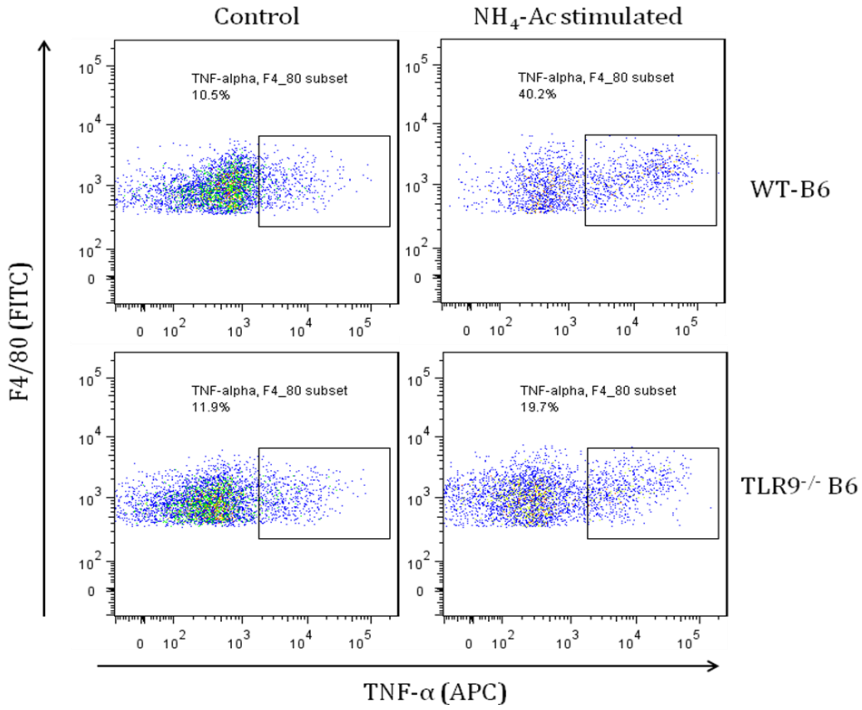

(B)

Figure 4.18: TNF-α production by macrophages in WT-B6 and TLR9$^{-/-}$ B6 mice splenocytes following NH_4-Ac stimulation.

The intracellular cytokine TNF-α produced by splenic macrophages was significantly increased in WT-B6 mice following NH_4-Ac stimulation (4 mM) compared to controls ($p<0.0001$) [mean difference: 25.1; 95% C.I.: 21.1 to 29.1] (normal data). There was a significant increase in TNF-α produced by splenic macrophages in TLR9$^{-/-}$ B6 mice following NH_4-Ac stimulation (4 mM) compared to controls ($p<0.001$) [mean difference: 9.3; 95% C.I.: 4.8 to 13.7] (normal data), but it was significantly ameliorated compared to WT-B6 mice ($p<0.0001$) [mean difference: –14.3; 95% C.I.: -18.3 to -10.3] (normal

data). [WT-B6 mice (n=5) & controls (n=5); TLR9$^{-/-}$ B6 mice (n=6) & controls (n=7)]. The data are normally distributed and expressed as mean with S.D.; $p<0.05$ were considered statistically significant. Student t-test was used to analyse the differences between parametric data sets. (A) Graph and (B) FACS plots representing each group.

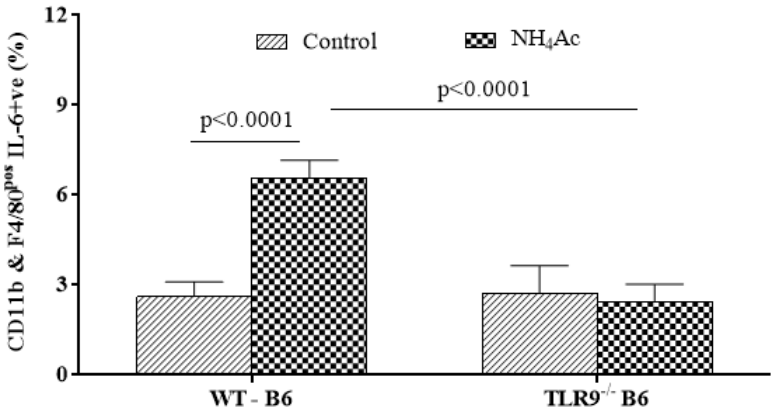

(A)

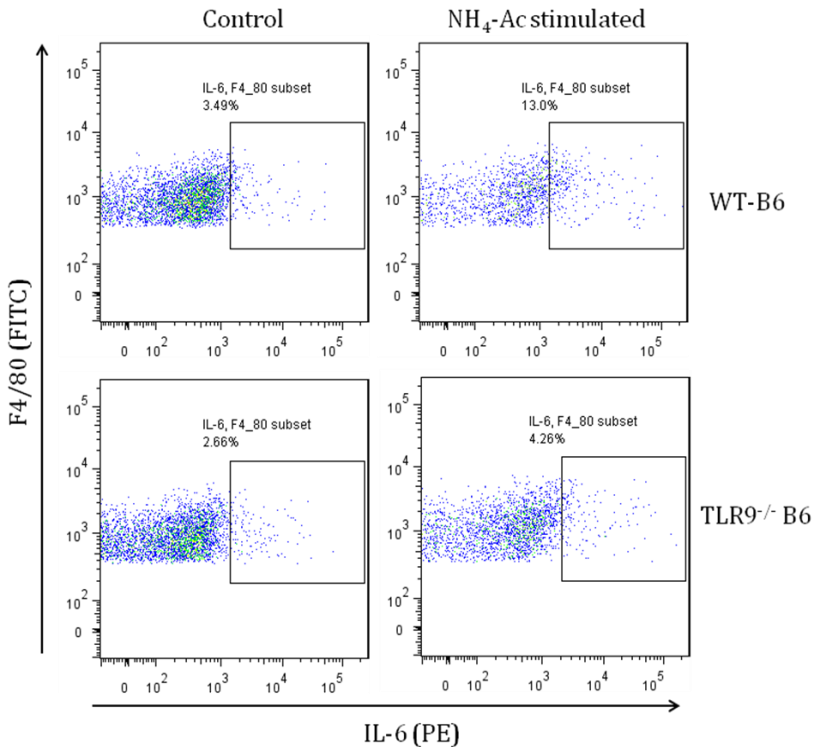

(B)

Figure 4.19: IL-6 production by macrophages in WT-B6 and TLR9$^{-/-}$ B6 mice splenocytes following NH_4-Ac stimulation.

The intracellular cytokine IL-6 produced by splenic macrophages was significantly increased in WT-B6 mice following NH_4-Ac stimulation (4 mM) compared to controls ($p<0.0001$) [mean difference: 4; 95% C.I.: 3.2 to 4.7] (normal data). There was no difference in IL-6 produced by splenic macrophages in TLR9$^{-/-}$ B6 mice following NH_4-Ac stimulation (4 mM) compared to controls [mean difference: -0.2; 95% C.I.: -1.1 to 0.5] (normal data), but it was significantly ameliorated compared to WT-B6 mice ($p<0.0001$)

[mean difference: –4.1; 95% C.I.: -4.7 to -3.4] (normal data). [WT-B6 mice (n=5) & controls (n=5); TLR9$^{-/-}$ B6 mice (n=6) & controls (n=7)]. Normality assumptions were checked and the data are expressed as mean with S.D.; $p<0.05$ were considered statistically significant. Student t-test was used to analyse the differences between parametric data sets. (A) Graph and (B) FACS plots representing each group.

4.3.4. Decreased cytokine production in splenic NK cells in TLR9$^{-/-}$ B6 mice

The phenotype and intracellular cytokine production was determined in the NK cells (DX-5 & CD122 – positive cells) in WT-B6 mice (n=5) and TLR9$^{-/-}$ B6 mice (n=6) six hours following NH_4-Ac (4 mM) stimulation and compared to controls (NH_4-Ac untreated) [WT-B6 (n=7) & TLR9$^{-/-}$ B6 (n=7)] [Methods-2.14.4.8].

NK cell phenotype

Among the controls, there was a significant decrease in the frequency of KLRG-1^{pos} NK cells isolated from spleen in TLR9$^{-/-}$ B6 mice compared to WT-B6 mice (p0.01). Following NH_4-Ac stimulation (4 mM), there was a significant increase in the frequency of KLRG-1^{pos} NK cells isolated from spleen in WT-B6 mice compared to controls ($p<0.05$) but there was no difference in the intracellular frequency of KLRG-1^{pos} NK cells isolated from spleen in TLR9$^{-/-}$ B6 mice compared to controls. There was however a significant decrease in the frequency of KLRG-1^{pos} NK cells in TLR9$^{-/-}$ B6 mice compared to WT-B6 mice following NH_4-Ac stimulation (4 mM) ($p<0.0001$) [Figure 4.20].

NK cell function

Following NH_4-Ac stimulation (4 mM), there was a significant increase in the intracellular cytokine IFN-γ produced by KLRG-1^{pos} NK cells isolated from spleen in WT-B6 mice compared to controls ($p<0.0001$), There was also a significant increase in the intracellular cytokine IFN-γ produced by KLRG-1^{pos} NK cells isolated from spleen in TLR9$^{-/-}$ B6 mice compared to controls ($p<0.01$). There was however a significant decrease in the intracellular cytokine IFN-γ produced by KLRG-1^{pos} NK cells in TLR9$^{-/-}$ B6 mice compared to WT-B6 mice following NH_4-Ac stimulation (4 mM) ($p<0.01$) [Figure 4.21].

Following NH_4-Ac stimulation (4 mM), there was a significant increase in the intracellular cytokine TNF-α produced by KLRG-1^{pos} NK cells isolated from spleen in WT-B6 mice compared to controls ($p<0.001$) but there was no difference in the intracellular cytokine TNF-α produced by KLRG-1^{pos} NK cells isolated from spleen in $TLR9^{-/-}$ B6 mice compared to controls. There was however a significant decrease in the intracellular cytokine TNF-α produced by KLRG-1^{pos} NK cells in $TLR9^{-/-}$ B6 mice compared to WT-B6 mice following NH_4-Ac stimulation (4 mM) ($p<0.01$) [Figure 4.22].

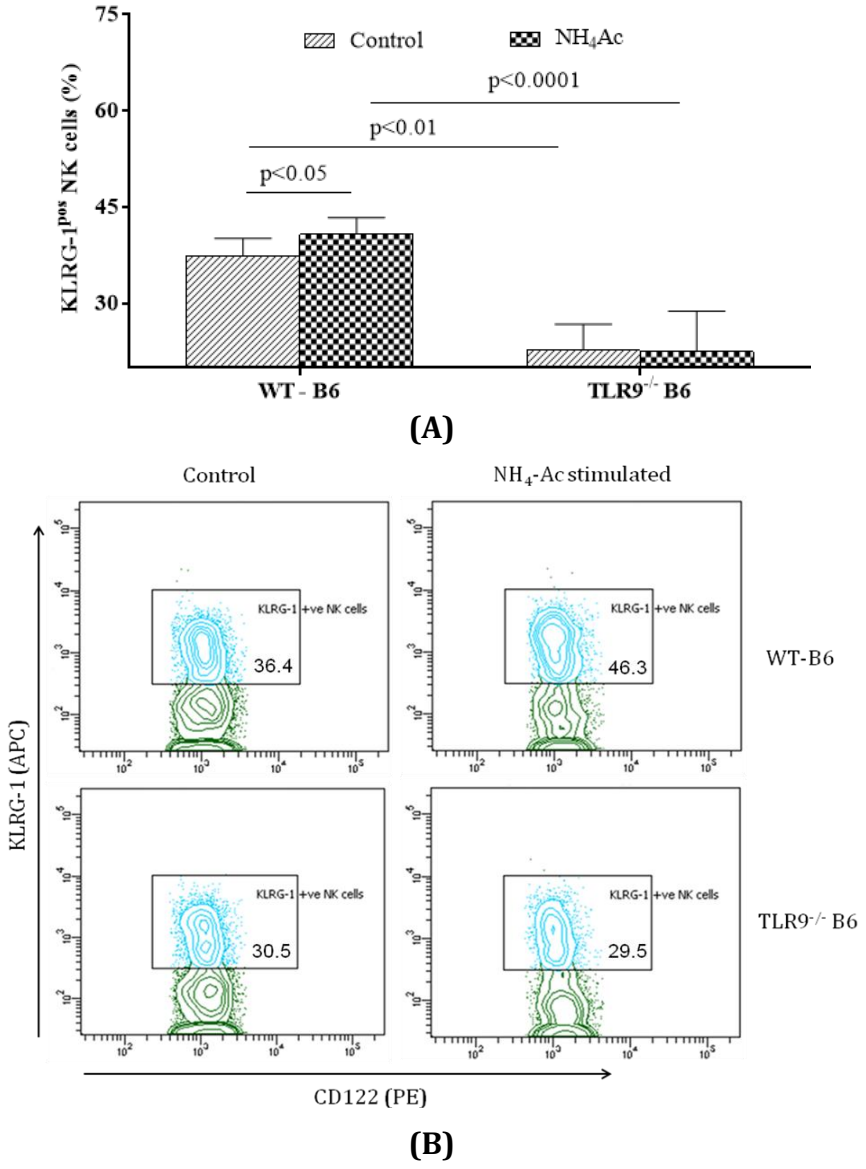

Figure 4.20: KLRG-1^{pos} NK cells in WT-B6 and TLR9$^{-/-}$ B6 mice splenocytes following NH_4-Ac stimulation.

Splenic KLRG-1^{pos} NK cells were significantly increased in WT-B6 mice following NH_4-Ac stimulation (4 mM) compared to controls ($p<0.05$) [mean difference: 3.4; 95% C.I.: 0.4 to 6.4] (normal data). There was no difference in splenic KLRG-1^{pos} NK cells in TLR9$^{-/-}$ B6 mice following NH_4-Ac stimulation (4 mM) compared to controls [median difference: -0.8; 95% C.I.: -6.3 to 7.6] (non-normal data), but they were significantly ameliorated compared to WT-B6 mice ($p<0.0001$) [mean difference: –18.3; 95% C.I.: -23.2 to -13.5] (normal data). Among the controls, there was a significant decrease in KLRG-1^{pos} NK cells in TLR9-/- B6 mice compared to WT-B6 mice ($p<0.01$) [median difference: -15.1; 95% C.I.: -20 to -9] (non-normal data). [WT-B6 mice (n=6) & controls (n=6); TLR9$^{-/-}$ B6

mice (n=7) & controls (n=7)]. Normality assumptions were checked and the data are expressed as mean with S.D.; $p<0.05$ were considered statistically significant. Student t-test was used to analyse the difference between parametric data sets and Mann-Whitney U test was used to analyse the difference between non-parametric data sets. (A) Graph and (B) FACS plots representing each group.

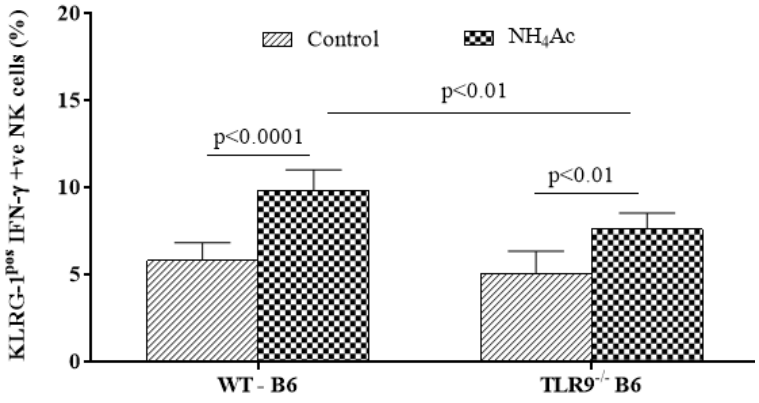

(A)

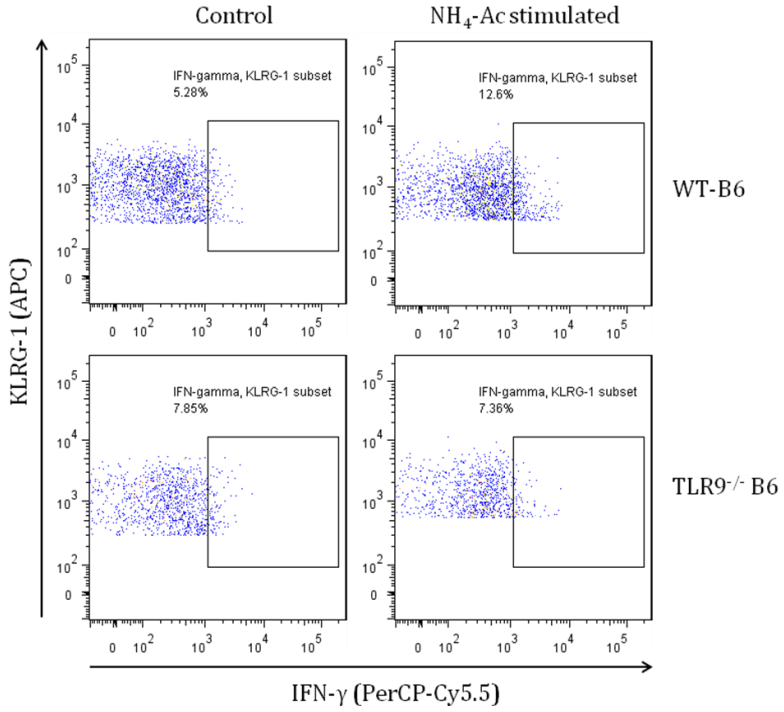

(B)

Figure 4.21: IFN-γ production by KLRG-1^{pos} NK cells in WT-B6 and TLR9$^{-/-}$ B6 mice splenocytes following NH_4-Ac stimulation.

The intracellular cytokine IFN-γ produced by splenic KLRG-1^{pos} NK cells was significantly increased in WT-B6 mice following NH_4-Ac stimulation (4 mM) compared to controls ($p<0.0001$) [mean difference: 4; 95% C.I.: 2.6 to 5.4] (normal data). There was a significant increase in IFN-γ produced by splenic KLRG-1^{pos} NK cells in TLR9$^{-/-}$ B6 mice following NH_4-Ac stimulation (4 mM) compared to controls ($p<0.01$) [mean difference: 2.5; 95% C.I.: 1.1 to 3.8] (normal data), but it was significantly ameliorated compared to WT-B6 mice ($p<0.01$) [median difference: –2.2; 95% C.I.: -3.6 to -0.8] (non-

normal data). [WT-B6 mice (n=6) & controls (n=6); TLR9$^{-/-}$ B6 mice (n=7) & controls (n=7)]. Normality assumptions were checked and the data are expressed as mean with S.D.; $p<0.05$ were considered statistically significant. Student t-test was used to analyse the difference between parametric data sets and Mann-Whitney U test was used to analyse the difference between non-parametric data sets. (A) Graph and (B) FACS plots representing each group.

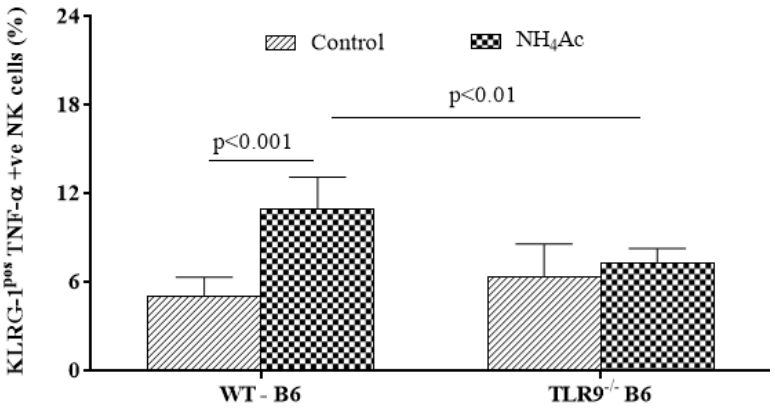

(A)

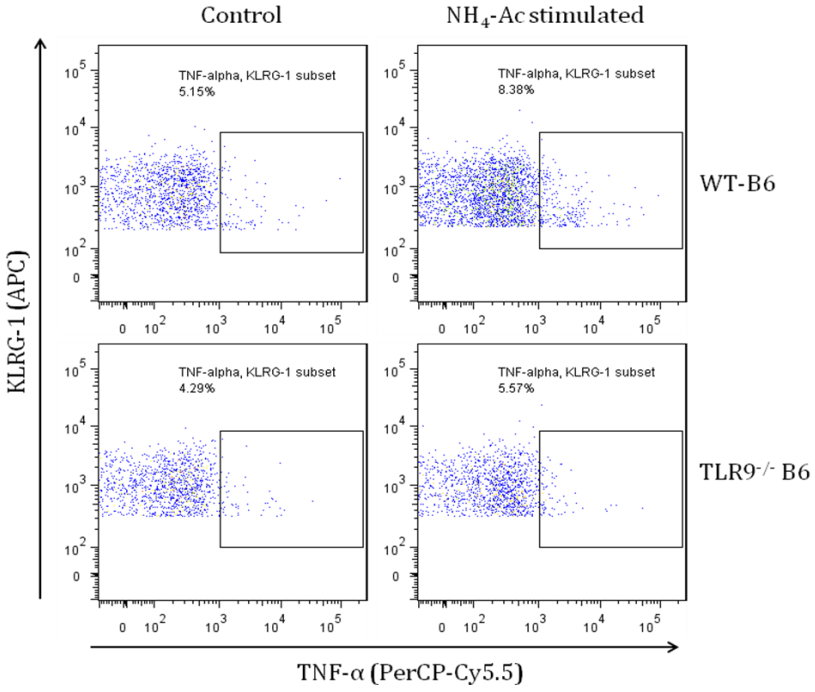

(B)

Figure 4.22: TNF-α production by KLRG-1^{pos} NK cells in WT-B6 and TLR9$^{-/-}$ B6 mice splenocytes following NH_4-Ac stimulation.

The intracellular cytokine TNF-α produced by splenic KLRG-1^{pos} NK cells was significantly increased in WT-B6 mice following NH_4-Ac stimulation (4 mM) compared to controls ($p<0.001$) [mean difference: 5.9; 95% C.I.: 3.7 to 8] (normal data). There was no difference in TNF-α produced by splenic KLRG-1^{pos} NK cells in TLR9$^{-/-}$ B6 mice following NH_4-Ac stimulation (4 mM) compared to controls [median difference: 0.75; 95% C.I.: -0.9 to 3.3] (non-normal data), but it was significantly ameliorated compared to WT-B6 mice ($p<0.01$) [median difference: –4.4; 95% C.I.: -5.7 to -0.6] (non-normal

data). [WT-B6 mice (n=6) & controls (n=6); TLR9$^{-/-}$ B6 mice (n=7) & controls (n=7)]. Normality assumptions were checked and the data are expressed as mean with S.D.; $p<0.05$ were considered statistically significant. Student t-test was used to analyse the difference between parametric data sets and Mann-Whitney U test was used to analyse the difference between non-parametric data sets. (A) Graph and (B) FACS plots representing each group.

4.4. Ammonia-induced mortality and inflammation were independent of acetate or pH

A recent study shows that acetate induces inflammation in acute alcoholic hepatitis [192]. In another study, it has been shown that the toxicity of ammonium salts was increased in relation to the rise in blood pH and the direct effect of pH (alkalinization) was responsible for promoting ammonium gas transfer across the blood brain barrier [71, 72]. Therefore to determine whether the TLR9-mediated mortality, brain oedema and inflammation were solely induced by ammonia and not by the acetate or change in pH, sodium acetate (Na-Ac), an alternate salt of acetate was injected in WT-B6 mice after adjusting for pH (same as NH_4-Ac).

4.4.1. Changes in immune function after 4 mM Na-Ac stimulation

Further, to determine whether it was acetate or pH that induced the systemic inflammation and subsequent brain oedema and changes in the liver in WT-B6 mice, Na-Ac (4 mM) was injected to WT-B6 mice (n=7) and compared to controls (n=13) and WT-B6 mice stimulated with NH_4-Ac (n=13).

4.4.1.1. Brain water content and liver bodyweight ratio after Na-Ac stimulation

There was no difference in the brain water content or liver bodyweight ratio in WT-B6 mice after Na-Ac (4 mM) stimulation compared to controls. The brain water content and liver bodyweight ratio was significantly decreased in WT-B6 mice treated with Na-Ac (4 mM) compared to WT-B6 mice treated with NH_4-Ac (4 mM) [Figure 4.23a and b].

4.4.1.2. $CD4^{pos}$ T cells and $CD8^{pos}$ T cells after Na-Ac stimulation

There was no difference in the intracellular cytokines (IFN-γ, TNF-α and IL-6) produced by splenic $CD4^{pos}$ T cells and CD8pos T cells in WT-B6 mice after Na-Ac stimulation (4 mM) compared to controls. The cytokine production was significantly decreased after Na-Ac stimulation compared to the group stimulated with NH_4-Ac ($p<0.001$) [Figures 4.24 and 25].

There was no difference in the intracellular cytokine production by hepatic $CD4^{pos}$ T cells and $CD8^{pos}$ T cells in WT-B6 mice after Na-Ac stimulation (4 mM) compared to controls [data not shown].

4.4.1.3. Macrophages and NK cells after Na-Ac stimulation

There was no difference in the intracellular cytokine production by splenic macrophages and KLRG-1^{pos} NK cells in WT-B6 mice after Na-Ac stimulation (4 mM) compared to controls. The cytokine production was significantly decreased after Na-Ac stimulation compared to the group stimulated with NH_4-Ac ($p<0.001$) [Figure 4.26].

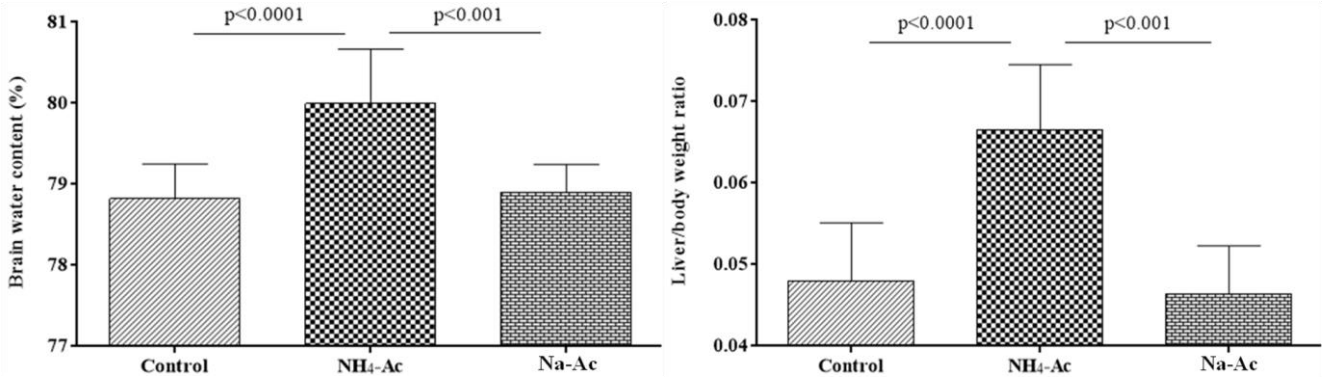

(a) **(b)**

Figure 4.23: Brain water content and liver bodyweight ratio in WT-B6 mice after Na-Ac stimulation.

(a) Brain water content and (b) liver bodyweight ratio were significantly increased in WT-B6 mice following NH_4-Ac stimulation (4 mM) compared to controls ($p<0.0001$) (normal data). There was no difference in brain water content (a) and liver bodyweight ratio (b) in WT-B6 mice after Na-Ac stimulation (4 mM) compared to controls, which were significantly ameliorated compared to those stimulated with NH_4-Ac ($p<0.001$) (normal data). [NH4-Ac treated mice (n=13), controls (n=13) and Na-Ac treated mice (n=7)]. Normality assumptions were checked and the data are expressed as mean with S.D.; $p<0.05$ were considered statistically significant. One-way ANOVA with Tukey's multiple comparisons test was used to analyse the differences between parametric data sets.

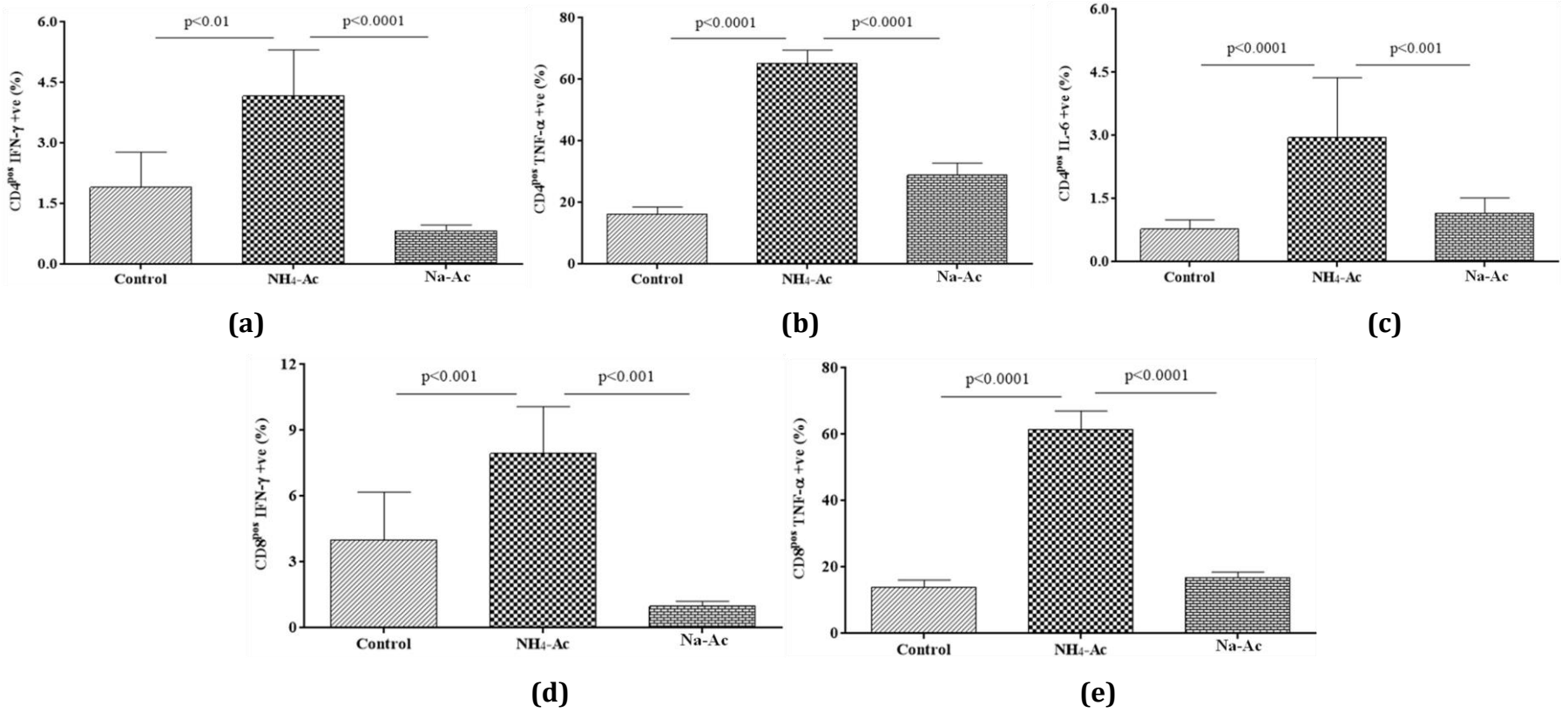

Figure 4.24: Intracellular cytokine production in splenic T cells after Na-Ac stimulation.

There was no difference in the intracellular cytokines (a) $CD4^{pos}$ IFN-γ, (b) $CD4^{pos}$ TNF-α, (c) $CD4^{pos}$ IL-6, (d) $CD8^{pos}$ IFN-γ and (e) $CD8^{pos}$ TNF-α in WT-B6 mice after Na-Ac stimulation (4 mM) compared to controls, which were significantly decreased compared to the NH_4-Ac stimulated group ($p<0.001$) (normal data). [NH_4-Ac treated mice (n=13), controls (n=13) and Na-Ac treated mice (n=7)]. Normality assumptions were checked and the data are expressed as mean with S.D.; $p<0.05$ were considered statistically significant. One-way ANOVA with Tukey's multiple comparisons test was used to analyse the differences between parametric data sets.

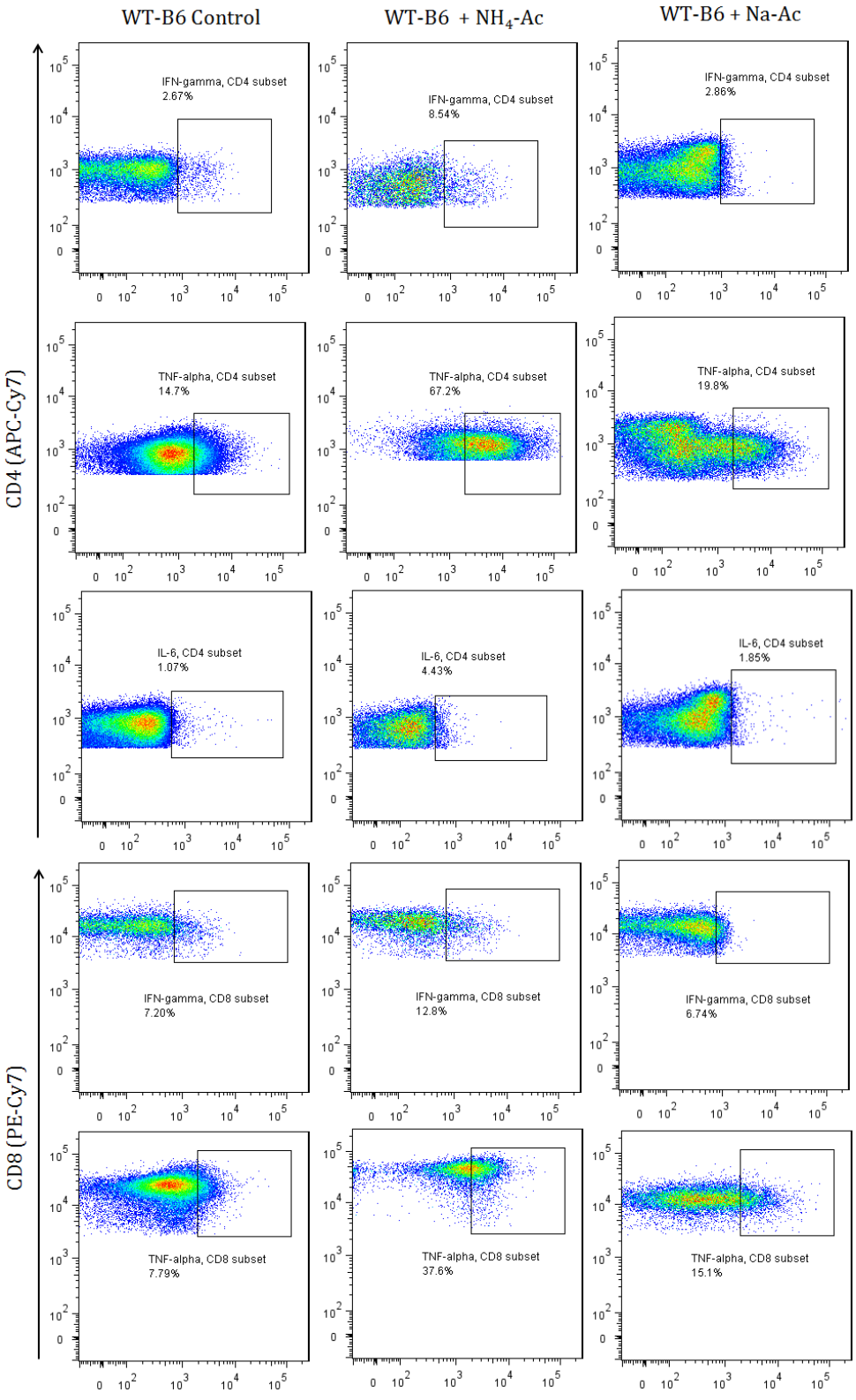

Figure 4.25: FACS plots of T cell cytokines after Na-Ac stimulation.

FACS plots of intracellular cytokines produced by $CD4^{pos}$ and $CD8^{pos}$ T cells in WT-B6 mice after Na-Ac stimulation compared to NH_4-Ac stimulation and control.

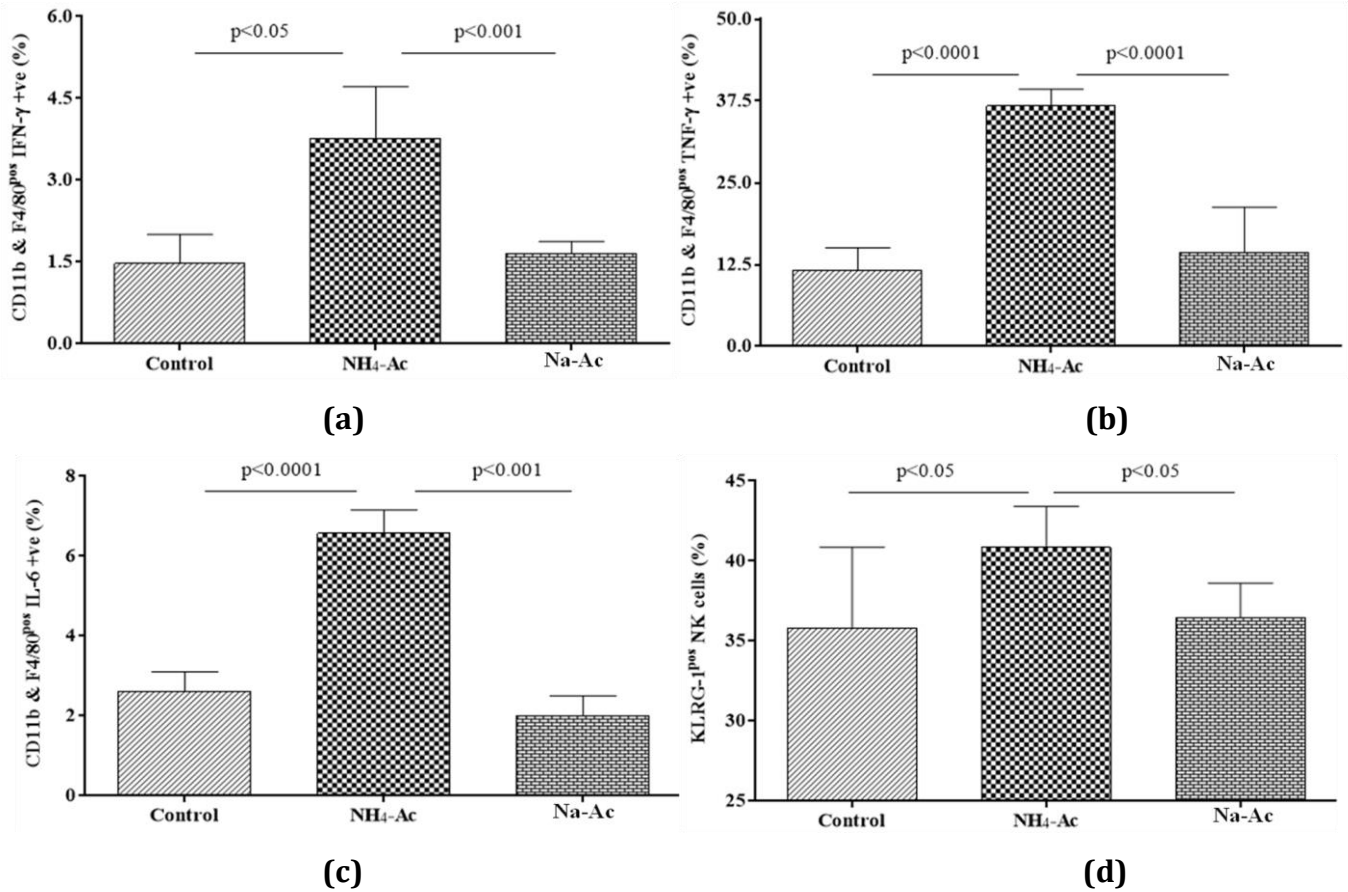

Figure 4.26: Cytokine production in macrophages and NK cells in WT-B6 mice after Na-Ac stimulation.

There was no difference in the intracellular cytokines produced by macrophages (a, b and c) and KLRG-1^{pos} NK cells (d) in WT-B6 mice after Na-Ac stimulation compared to controls, which were significantly ameliorated compared the NH_4-Ac stimulated group(normal data). [NH_4-Ac treated mice (n=13), controls (n=13) and Na-Ac treated mice (n=7)]. Normality assumptions were checked and the data are expressed as mean

with S.D.; $p<0.05$ were considered statistically significant. One-way ANOVA with Tukey's multiple comparison test was used to analyse the differences between parametric data sets.

4.5. Ammonia-induced TLR9 changes are activated by DNA

Since TLR9 is mainly activated by the CpG motif of the bacterial DNA and also as my human studies have shown that ammonia along with DNA activated neutrophil TLR9 expression, I sought to determine whether the ammonia-induced TLR9 changes were also mediated through DNA. To understand this mechanism, total dsDNA levels (pg/ml) were measured from plasma samples stored in -80°C from WT-B6 mice following NH_4-Ac (4 mM) stimulation (n=13) and controls (n=13); $TLR9^{-/-}$ B6 mice following NH_4-Ac (4 mM) stimulation (n=19) and controls (n=16); and WT-B6 mice after Na-Ac (4 mM) stimulation (n=7) [Method – 2.25].

Plasma dsDNA levels were significantly increased in WT-B6 mice and $TLR9^{-/-}$ B6 mice following NH_4-Ac stimulation (4 mM) compared to controls ($p<0.05$). There was no difference in plasma dsDNA level in $TLR9^{-/-}$ B6 mice compared to WT-B6 mice following NH_4-Ac stimulation (4 mM) [Figure 4.27].

Plasma dsDNA level was significantly increased in WT-B6 mice following NH_4-Ac stimulation (4 mM) compared to controls ($p<0.001$). There was no difference in plasma dsDNA level in WT-B6 mice after Na-Ac stimulation (4 mM) compared to controls, but it was significantly decreased compared to the NH_4-Ac stimulated group ($p<0.05$) [Figure 4.28].

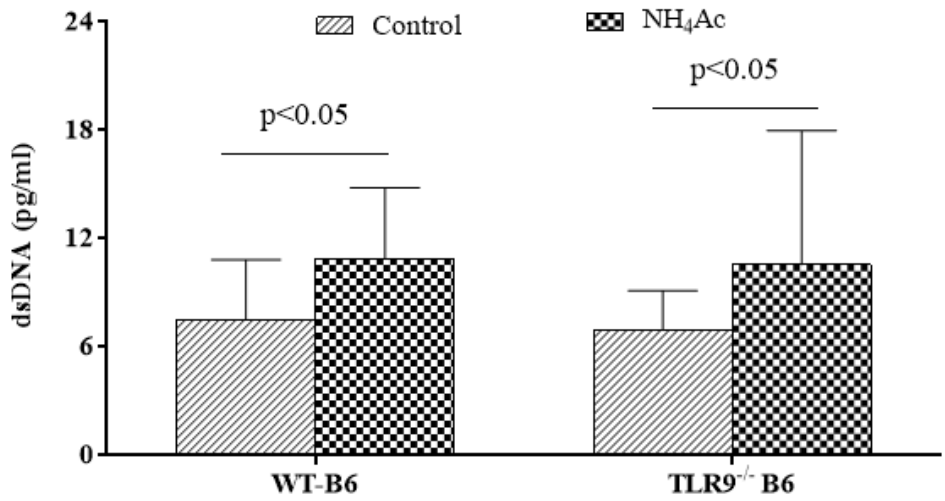

Figure 4.27: Plasma dsDNA level in WT-B6 and TLR9$^{-/-}$ B6 mice following NH_4-Ac stimulation.

Plasma dsDNA level was significantly increased in WT-B6 mice [median difference: 3.5; 95% C.I.: 0.3 to 5.7] (non-normal data) and TLR9$^{-/-}$ B6 mice [median difference: 1.9; 95% C.I.: 0.2 to 3.4] (non-normal data) following NH_4-Ac stimulation (4 mM) compared to controls ($p<0.05$). There was no difference in plasma dsDNA level in TLR9$^{-/-}$ B6 mice compared to WT-B6 mice following NH_4-Ac stimulation (4 mM) [median difference: –1.5; 95% C.I.: -3.2 to 0.1]. [WT-B6 mice (n=13) & controls (n=13); TLR9$^{-/-}$ B6 mice (n=19) & controls (n=16)].

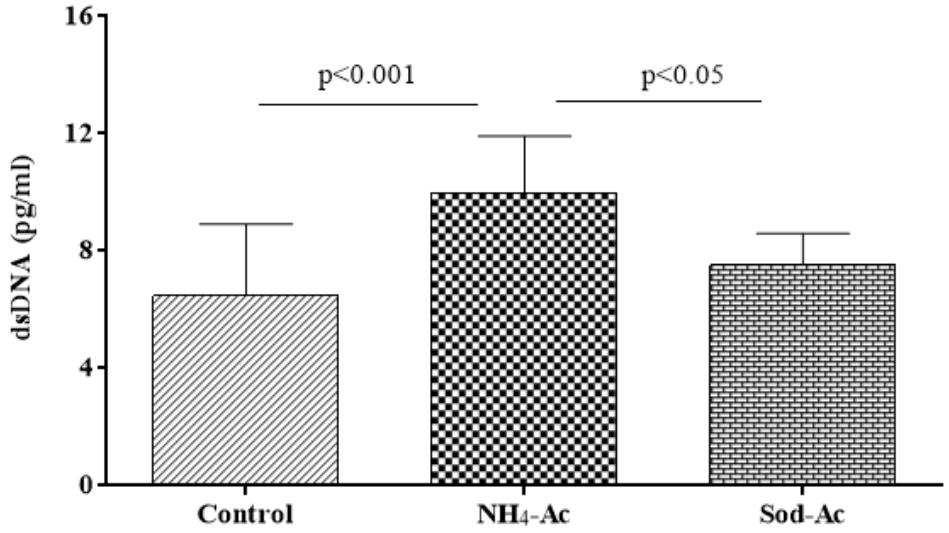

Figure 4.28: Plasma dsDNA level in WT-B6 mice after Na-Ac stimulation.

Plasma dsDNA level was significantly increased in WT-B6 mice following NH_4-Ac stimulation (4 mM) compared to controls ($p<0.001$) [mean difference: 3.5; 95% C.I.: 1.4 to 5.5] (normal data). There was no difference in plasma dsDNA level in WT-B6 mice after Na-Ac stimulation (4 mM) compared to controls [mean difference: 1.2; 95% C.I.: -1.8 to 3.6] (normal data), but it was significantly ameliorated compared to the NH_4-Ac stimulated group ($p<0.05$) [mean difference: –2.5; 95% C.I.: -4.8 to -0.11] (normal data). Normality assumptions were checked and the data are expressed as mean with S.D.; $p<0.05$ were considered statistically significant. One-way ANOVA with Tukey's multiple comparisons test was used to analyse the differences between parametric data sets.

4.6. Summary

The decreased survival rate in TLR9 deficient ($TLR9^{-/-}$) B6 mice following a high dose of NH_4-Ac stimulation indicates that TLR9 plays an important role in ammonia-induced mortality. The decreased cytokine production and brain water content in $TLR9^{-/-}$ B6 mice, following the stimulation of NH_4-Ac suggests that TLR9 plays an important role in the pathogenesis of inflammation and subsequent brain oedema in a DNA dependent fashion.

4.6.1. Ammonia-induced inflammation and brain oedema

In this study ammonia stimulation upregulated the production of the cytokines IFN-γ, TNF-α and IL-6. The observation of increased cytokine production from the hepatic infiltrated T cells indicates that the immune response originates from the liver. The cytokines IFN-γ, TNF-α and IL-6 produced by T_H1/T_H2 cells are predominantly responsible for mediating inflammation within the liver [193-195]. The cytokines IFN-γ and TNF-α play an important role in inducing the systemic inflammatory response in paracetamol toxicity [196-198], and NK cells play a particularly important role in this process by secreting IFN-γ [199] which induces the production of the chemokines that recruit neutrophils and macrophages to the site of injury which further propagates the inflammatory response [200, 201]. In this study ammonia also activated cytokine production in NK cells and macrophages indicating that those cells, along with effector and cytotoxic T cells, are responsible for inducing the proinflammatory environment. Together, ammonia and systemic inflammation induce brain oedema by inducing astrocyte swelling. This supports the previously published observation that astrocyte swelling can

be induced when astrocytes are exposed to pro-inflammatory cytokines after being exposed to ammonia [191].

4.6.2. Role of TLR9 in the inflammation and brain oedema

Activation of TLR9 results in the upregulation of cytokine production and increase in the brain water content, and the critical role of TLR9 in this mechanism have been demonstrated by using genetically modified mice. Furthermore, TLR9 is essential for the cytokines TNF-α and IL-6 to be produced by macrophages in response to CpG DNA, [158] and IFN-γ produced by $CD4^{pos}$ T cells in response to CpG DNA and Mycobacteria [158, 202].

Although the T cell cytokine production was reduced in $TLR9^{-/-}$ mice following ammonia stimulation, there was an increase in the production of TNF-α and an increasing trend in other pro-inflammatory cytokines was observed compared to the controls. However this was not observed in the macrophages isolated from spleen after ammonia stimulation. It is well known that stimulation of TLR4 induces the production of TNF-α in macrophages [203]. These findings taken together indicate that apart from TLR9 activation, other factors are also involved in stimulating the production of cytokines following ammonia-exposure.

4.6.3. Activation of TLR9 by ammonia is mediated by DNA

The increase in the liver weight could be due to the combined effect of hepatocyte swelling caused by ammonia [189] and the inflammation within the liver. DNA released by the swollen hepatocytes likely binds to TLR9 thereby activating the innate immune system. In paracetamol toxicity, DNA fragments released by apoptotic hepatocytes have been shown to be responsible for the activation of TLR9, inducing pro-inflammation [108, 179] and resulting in MOF by damaging the lungs [106]. These findings taken together with

the observations in my human studies that neutrophil TLR9 activated by ammonia, IL-8 and DNA induced SIRS and progression to HE in PALF [204] suggest that TLR9 mediates the ammonia-induced inflammation and subsequent brain oedema in a DNA dependent manner.

Chapter 5. TLR9 antagonism abrogates ammonia-induced inflammation and brain oedema

In the previous chapter, by using TLR9$^{-/-}$ B6 mice it has been established that TLR9 plays an important role inducing the cytokine production of T cells, NK cells and macrophages, increasing brain water content following ammonia stimulation and driving mortality. Since TLR9$^{-/-}$ B6 mice were protected against NH_4-Ac stimulation, the next aim was to determine whether an antagonist of TLR9 would inhibit the ammonia-induced pro-inflammatory changes and brain oedema seen in the WT-B6 mice [Method – 2.26].

5.1. Decreased brain water content and liver bodyweight ratio in WT-B6 mice after TLR9 inhibition

Following administration of the TLR9 antagonist, ODN2088 (50 μg) along with NH_4-Ac (4 mM), there was a significant decrease in the brain water content in WT-B6 mice (n=10) compared to the NH_4-Ac alone treated group ($p<0.001$) whereas there was a significant increase in the brain water content in WT- B6 mice treated with NH_4-Ac alone (n=11) compared to controls (n=12) ($p<0.0001$). There was no difference in the brain water content in WT-B6 mice treated with ODN2088 and NH_4-Ac (4 mM) compared to controls [Figure 5.1].

Administration of ODN2088 along with NH_4-Ac (4 mM), significantly decreased the liver bodyweight ratio in WT-B6 mice (n=15) compared to the NH_4-Ac alone treated group ($p<0.0001$) whereas there was a significant increase in the liver bodyweight ratio in WT-B6 mice treated with NH_4-Ac alone (n=16) compared to controls (n=13) ($p<0.0001$). There was no difference in the liver bodyweight ratio in WT-B6 mice treated with ODN2088 and NH_4-Ac (4 mM) compared to controls [Figure 5.2].

Administration of ODN2088 along with NH_4-Ac (4 mM), reduced the hepatocyte swelling observed in WT-B6 mice compared to the NH_4-Ac alone treated group whereas there

was an increase in the liver bodyweight ratio in WT- B6 mice treated with NH_4-Ac alone compared to controls. There was no difference in the liver bodyweight ratio in WT-B6 mice treated with ODN2088 and NH_4-Ac (4 mM) compared to controls [Figure 5.3].

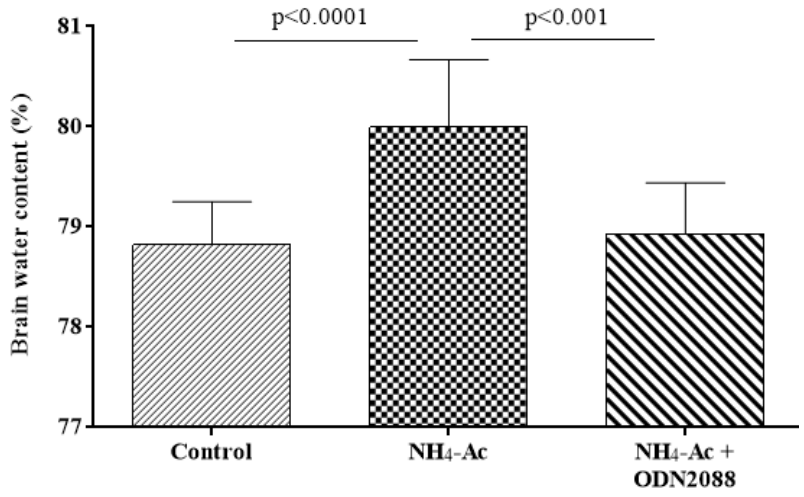

Figure 5.1: Decreased brain water content in WT-B6 mice after TLR9 inhibition.

Brain water content was significantly increased in WT-B6 mice following NH_4-Ac stimulation (4 mM) compared to controls ($p<0.0001$) [mean difference: 1.2; 95% C.I.: 0.64 to 1.7]. This was significantly inhibited when the TLR9 antagonist (ODN2088) was administered to WT-B6 mice along with NH_4-Ac (4 mM) ($p<0.001$) [mean difference: –1.1; 95% C.I.: -1.71 to -0.48] and there was no difference compared to controls [mean difference: 0.1; 95% C.I.: -0.46 to 0.68]. [NH_4-Ac (n=11); controls (n=12) & ODN2088 (n=10)] (normal data). Normality assumptions were checked and the data are expressed as mean with S.D.; $p<0.05$ were considered statistically significant. One-way ANOVA was used to analyse the differences between parametric data sets.

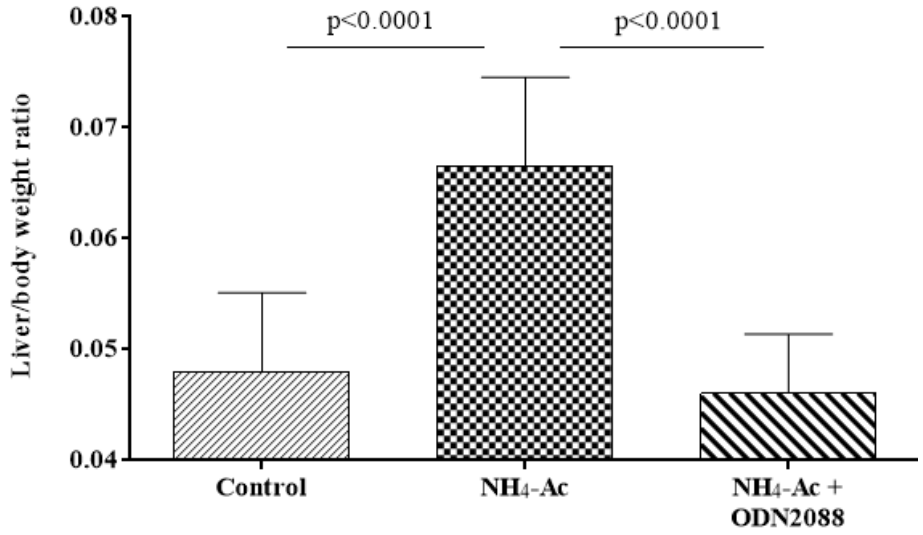

Figure 5.2: Decreased liver bodyweight ratio in WT-B6 mice after TLR9 inhibition.

Liver bodyweight ratio was significantly increased in WT-B6 mice following NH_4-Ac stimulation (4 mM) compared to controls ($p<0.0001$) [median difference: 0.018; 95% C.I.: 0.012 to 0.024]. The liver bodyweight ratio was significantly inhibited when TLR9 was inhibited using ODN2088 in WT-B6 mice following NH_4-Ac stimulation (4 mM) ($p<0.0001$) [median difference: –0.02; 95% C.I.: -0.025 to -0.016] and there was no difference compared to controls [median difference: -0.002; 95% C.I.: -0.008 to 0.004]. [NH_4-Ac (n=16); controls (n=13) & ODN2088 (n=15)] (non-normal data). Normality assumptions were checked and the data are expressed as mean with S.D.; $p<0.05$ were considered statistically significant. Kruskal-Wallis with Dunn's multiple comparison test was used to analyse the differences between non-parametric data sets.

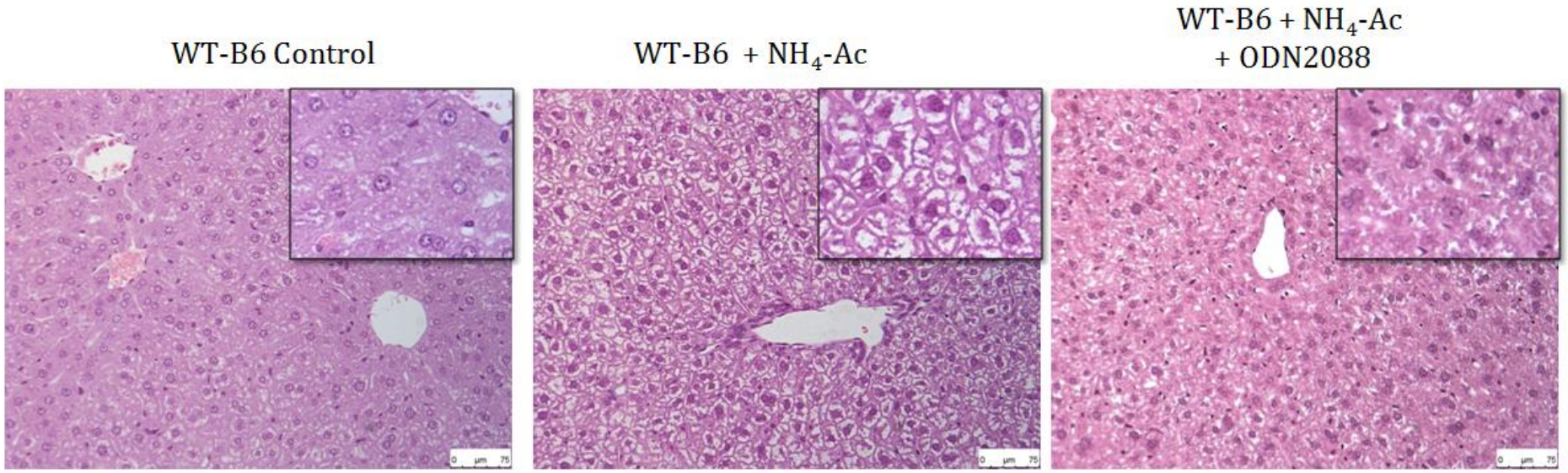

Figure 5.3: Liver histological changes in WT-B6 mice liver following NH_4-Ac stimulation after TLR9 inhibition.

These light microscope images (200x magnification) are histological sections (H&E stained) of the liver representing three different mice groups. Administration of ODN2088 along with NH_4-Ac (4 mM) inhibited the hepatocyte swelling in WT-B6 mice. The images in the black box inset are the same regions of the specimen captured at a higher magnification (400x).

5.2. Cytokine production of T cells, macrophages and NK cells function were reduced after using ODN2088

To determine whether the TLR9 antagonist inhibited the function of splenic or hepatic T cells, ODN2088 (50 µg) was administered to WT-B6 mice along with NH_4-Ac (4 mM) for 6 hours (n=14) and compared to controls (n=13) and WT-B6 mice stimulated with NH_4-Ac alone (n=13).

5.2.1. Decreased cytokine production in splenic $CD4^{pos}$ T cells

Following NH_4-Ac (4 mM) stimulation, intracellular cytokine IFN-γ produced by splenic $CD4^{pos}$ T cells in WT- B6 mice was significantly increased compared to controls ($p<0.0001$). When the TLR9 antagonist, ODN2088 was administered along with NH_4-Ac (4 mM), intracellular cytokine IFN-γ produced by splenic $CD4^{pos}$ T cells in WT-B6 mice was significantly decreased compared to NH_4-Ac alone treated group ($p<0.01$) and was not different compared to controls [Figure 5.4].

Following NH_4-Ac (4 mM) stimulation, the intracellular cytokine TNF-α produced by splenic $CD4^{pos}$ T cells in WT- B6 mice was significantly increased compared to controls ($p<0.0001$). When the TLR9 antagonist, ODN2088 was administered along with NH_4-Ac (4 mM), the intracellular cytokine TNF-α produced by splenic $CD4^{pos}$ T cells in WT-B6 mice was significantly decreased compared to the NH_4-Ac alone treated group ($p<0.05$) and significantly increased compared to controls ($p<0.001$) [Figure 5.5].

Following NH_4-Ac (4 mM) stimulation, the intracellular cytokine IL-6 produced by splenic $CD4^{pos}$ T cells in WT- B6 mice was significantly increased compared to controls ($p<0.0001$). When the TLR9 antagonist, ODN2088 was administered along with NH_4-Ac

(4 mM), the intracellular cytokine IL-6 produced by splenic $CD4^{pos}$ T cells in WT-B6 mice was significantly decreased compared to the NH_4-Ac alone treated group ($p<0.0001$) and was not different compared to controls [Figure 5.6].

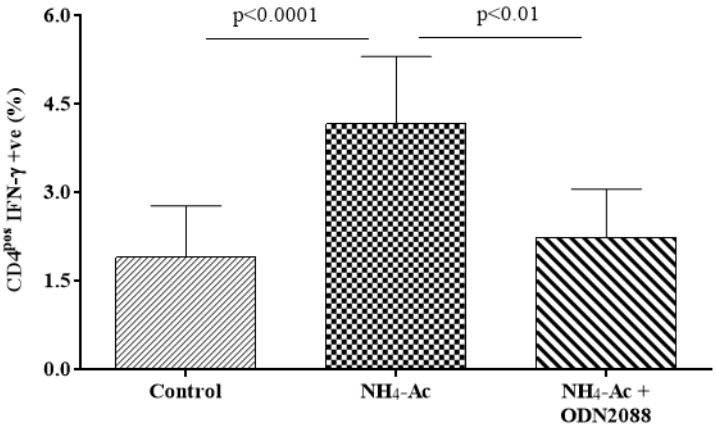

(A)

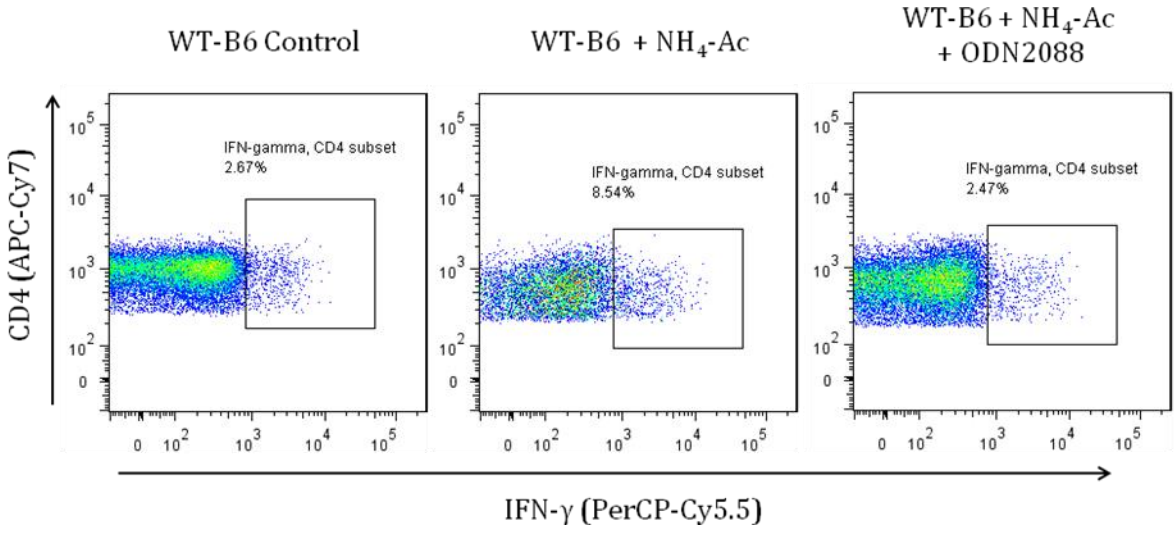

(B)

Figure 5.4: Decreased CD4^{pos} IFN-γ production in WT-B6 mice splenocytes after TLR9 inhibition.

The intracellular cytokine IFN-γ produced by splenic CD4^{pos} T cells was significantly increased in WT-B6 mice following NH_4-Ac stimulation (4 mM) compared to controls ($p<0.0001$) [median difference: 2.2; 95% C.I.: 1.5 to 3]. This was significantly inhibited when the TLR9 antagonist (ODN2088) was administered in WT-B6 mice along with NH_4-Ac (4 mM) ($p<0.01$) [median difference: –1.8; 95% C.I.: -2.5 to -1.1]; there was no difference compared to controls [median difference: 0.5; 95% C.I.: -0.3 to 1.1]. [NH_4-Ac (n=13); controls (n=13) & ODN2088 (n=14)] (non-normal data). Normality assumptions were checked and the data are expressed as mean with S.D.; $p<0.05$ were considered statistically significant. Kruskal-Wallis with Dunn's multiple comparisons test was used to analyse the differences between non-parametric data sets. (A) Graph and (B) FACS plots representing each group.

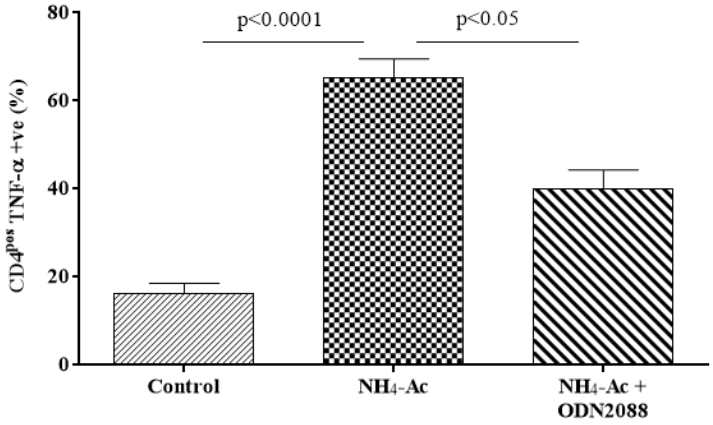

(A)

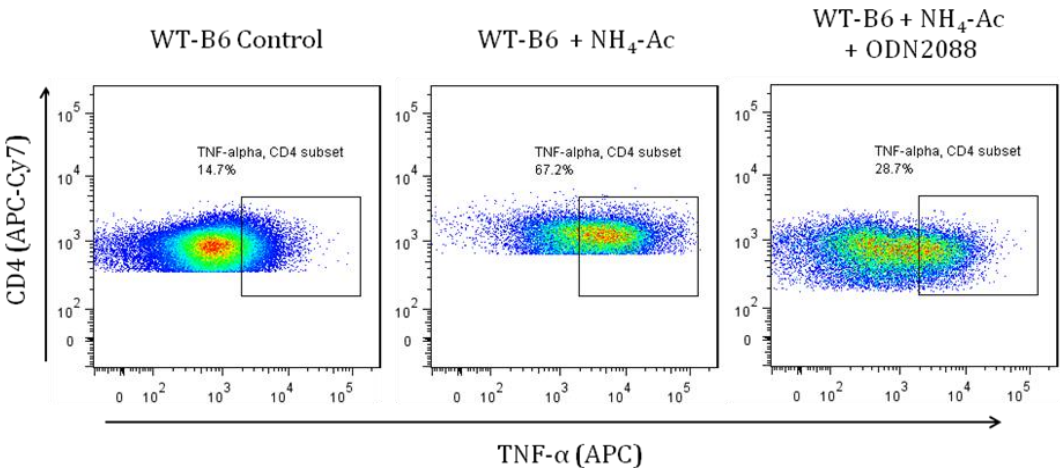

(B)

Figure 5.5: Decreased CD4^{pos} TNF-α production in WT-B6 mice splenocytes after TLR9 inhibition.

The intracellular cytokine TNF-α produced by splenic CD4^{pos} T cells was significantly increased in WT-B6 mice following NH_4-Ac stimulation (4 mM) compared to controls ($p<0.0001$) [median difference: 49.7; 95% C.I.: 47.4 to 51.7]. This was significantly inhibited when the TLR9 antagonist (ODN2088) was administered in WT-B6 mice along with NH_4-Ac (4 mM) ($p<0.05$) [median difference: –25.4; 95% C.I.: -28.8 to -22.2] although was significantly increased compared to controls [median difference: 24.1; 95% C.I.: 20.8 to 27.1]. [NH_4-Ac (n=13); controls (n=13) & ODN2088 (n=14)] (non-normal data). Normality assumptions were checked and the data are expressed as mean with S.D.; $p<0.05$ were considered statistically significant. Kruskal-Wallis with Dunn's multiple comparison test was used to analyse the differences between non-parametric data sets. (A) Graph and (B) FACS plots representing each group.

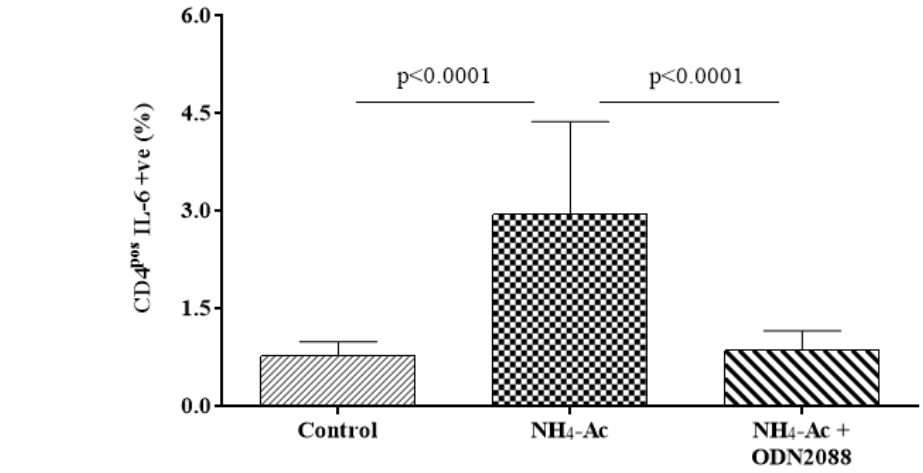

(A)

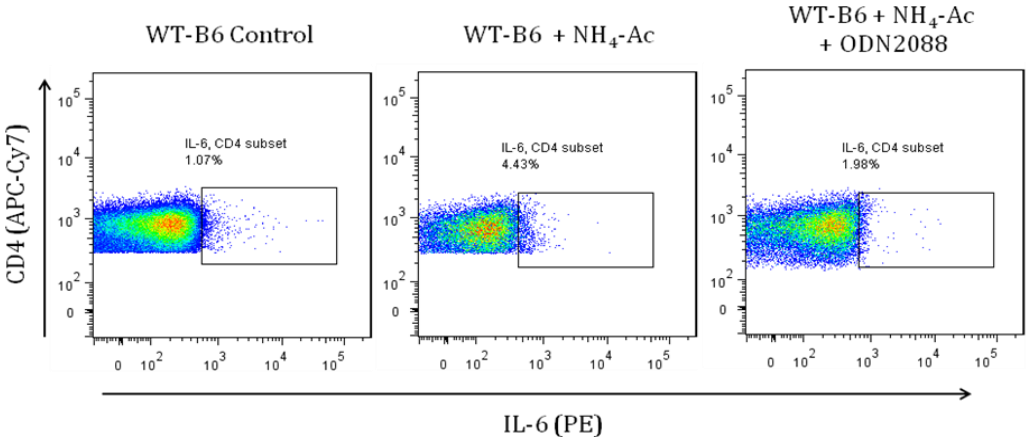

(B)

Figure 5.6: Decreased CD4^{pos} IL-6 production in WT-B6 mice splenocytes after TLR9 inhibition.

The intracellular cytokine IL-6 produced by splenic CD4^{pos} T cells was significantly increased in WT-B6 mice following NH_4-Ac stimulation (4 mM) compared to controls ($p<0.0001$) [mean difference: 2.1; 95% C.I.: 1.3 to 3]. This was significantly inhibited when the TLR9 antagonist (ODN2088) was administered in WT-B6 mice along with NH_4-Ac (4 mM) ($p<0.0001$) [mean difference: –2; 95% C.I.: -2.8 to -1.3] and there was no difference compared to controls [mean difference: 0.09; 95% C.I.: -0.6 to 0.8]. [NH_4-Ac (n=13); controls (n=13) & ODN2088 (n=14)] (normal data). Normality assumptions were checked and the data are expressed as mean with S.D.; $p<0.05$ were considered statistically significant. One-way ANOVA with Tukey's multiple comparisons test was used to analyse the differences between parametric data sets. (A) Graph and (B) FACS plots representing each group.

5.2.2. Decreased cytokine production in splenic $CD8^{pos}$ T cells

Following NH_4-Ac (4 mM) stimulation, the intracellular cytokine IFN-γ produced by splenic $CD8^{pos}$ T cells in WT- B6 mice was significantly increased compared to controls ($p<0.0001$). When the TLR9 antagonist, ODN2088 was administered along with NH_4-Ac (4 mM), the intracellular cytokine IFN-γ produced by splenic $CD8^{pos}$ T cells in WT-B6 mice was significantly decreased compared to the NH_4-Ac alone treated group ($p<0.0001$) and was not different compared to controls [Figure 5.7].

Following NH_4-Ac (4 mM) stimulation, the intracellular cytokine TNF-α produced by splenic $CD8^{pos}$ T cells in WT- B6 mice was significantly increased compared to controls ($p<0.0001$). When the TLR9 antagonist, ODN2088 was administered along with NH_4-Ac (4 mM), the intracellular cytokine TNF-α produced by splenic $CD8^{pos}$ T cells in WT-B6 mice was significantly decreased compared to NH_4-Ac alone treated group ($p<0.0001$) and was not different compared to controls [Figure 5.8].

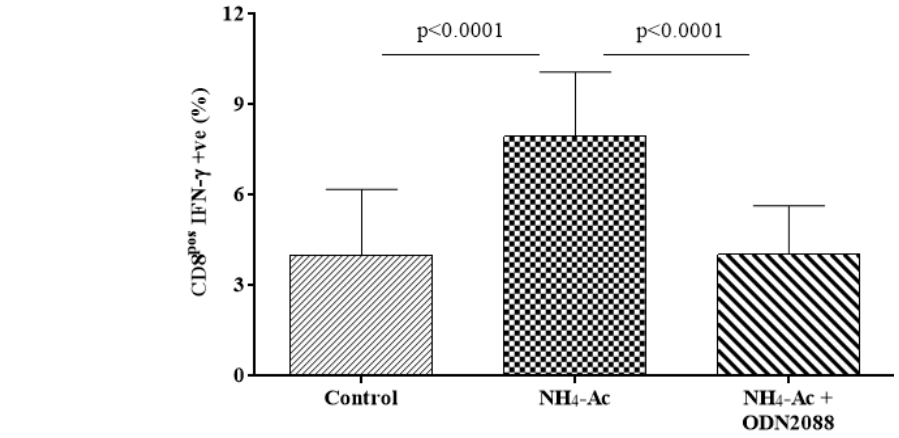

(A)

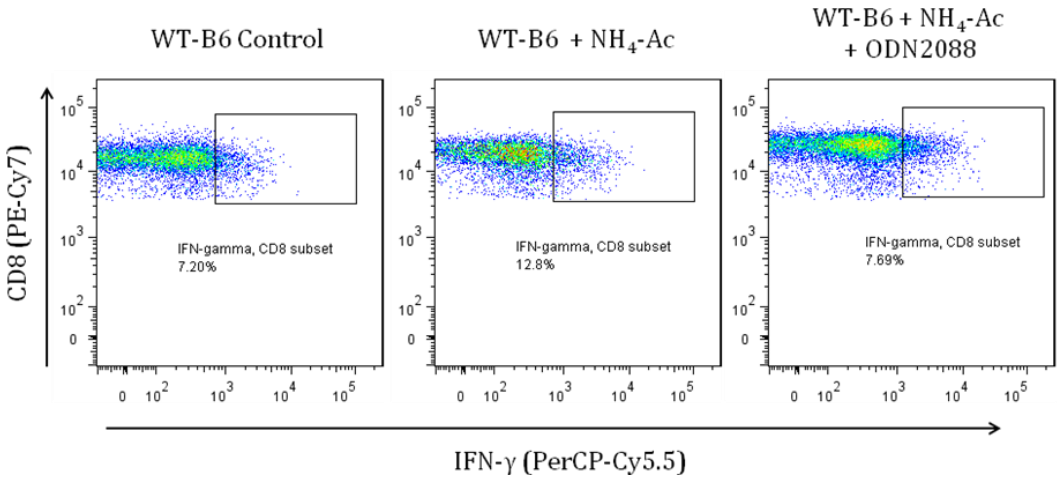

(B)

Figure 5.7: Decreased CD8^{pos} IFN-γ production in WT-B6 mice splenocytes after TLR9 inhibition.

The intracellular cytokine IFN-γ produced by splenic CD8^{pos} T cells was significantly increased in WT-B6 mice following NH_4-Ac stimulation (4 mM) compared to controls ($p<0.0001$) [mean difference: 3.9; 95% C.I.: 2 to 5.9]. This was significantly inhibited when the TLR9 antagonist (ODN2088) was administered in WT-B6 mice along with NH_4-Ac (4 mM) ($p<0.0001$) [mean difference: –3.9; 95% C.I.: -5.8 to -2]; there was no difference compared to controls [mean difference: 0.03; 95% C.I.: -1.7 to 1.8]. [NH_4-Ac (n=13); controls (n=13) & ODN2088 (n=14)] (normal data). Normality assumptions were checked and the data are expressed as mean with S.D.; $p<0.05$ were considered statistically significant. One-way ANOVA with Tukey's multiple comparisons test was used to analyse the differences between parametric data sets. (A) Graph and (B) FACS plots representing each group.

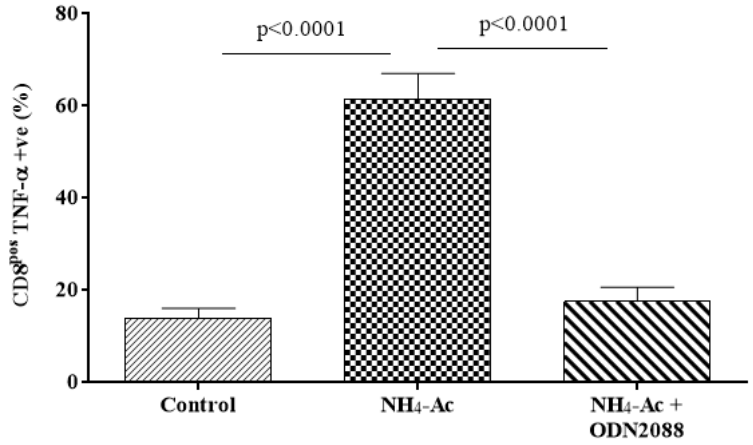

(A)

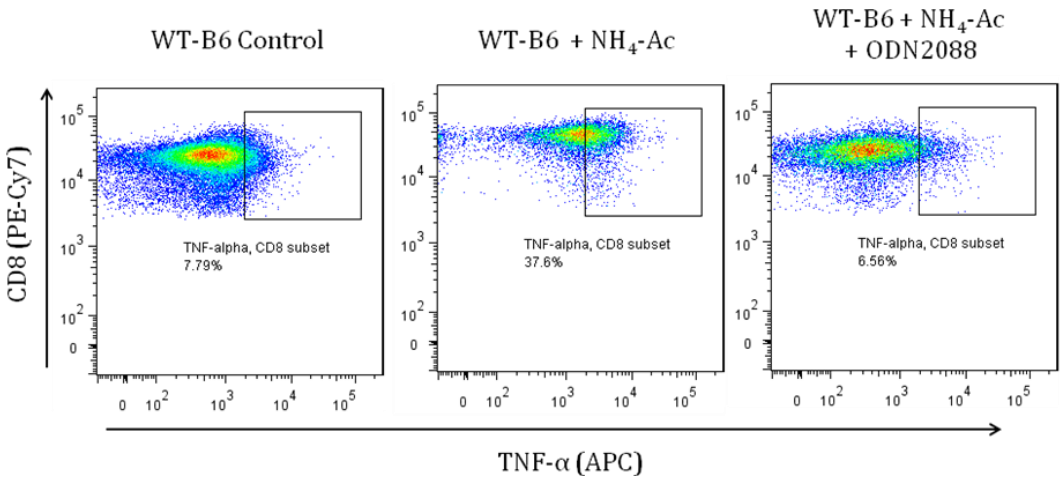

(B)

Figure 5.8: Decreased CD8^{pos} TNF-α production in WT-B6 mice splenocytes after TLR9 inhibition.

The intracellular cytokine TNF-α produced by splenic CD8^{pos} T cells was significantly increased in WT-B6 mice following NH_4-Ac stimulation (4 mM) compared to controls ($p<0.0001$) [mean difference: 47.6; 95% C.I.: 44.2 to 51]. This was significantly inhibited when the TLR9 antagonist (ODN2088) was administered in WT-B6 mice along with NH_4-Ac (4 mM) ($p<0.0001$) [mean difference: –44; 95% C.I.: -47.8 to -40.1]; there was no difference compared to controls [mean difference: 3.5; 95% C.I.: -0.2 to 7.4]. [NH_4-Ac (n=13); controls (n=13) & ODN2088 (n=14)] (normal data). Normality assumptions were checked and the data are expressed as mean with S.D.; $p<0.05$ were considered statistically significant. One-way ANOVA with Tukey's multiple comparisons test was used to analyse the differences between parametric data sets. (A) Graph and (B) FACS plots representing each group.

5.2.3. Decreased cytokine production in hepatic $CD4^{pos}$ T cells

Following NH_4-Ac (4 mM) stimulation, the intracellular cytokine IFN-γ produced by hepatic $CD4^{pos}$ T cells in WT- B6 mice was significantly increased compared to controls ($p<0.0001$). When the TLR9 antagonist, ODN2088 was administered along with NH_4-Ac (4 mM), the intracellular cytokine IFN-γ produced by hepatic $CD4^{pos}$ T cells in WT-B6 mice was significantly decreased compared to the NH_4-Ac alone treated group ($p<0.0001$) and was not different compared to controls [Figure 5.9].

Following NH_4-Ac (4 mM) stimulation, the intracellular cytokine TNF-α produced by hepatic $CD4^{pos}$ T cells in WT- B6 mice was significantly increased compared to controls ($p<0.0001$). When the TLR9 antagonist, ODN2088 was administered along with NH_4-Ac (4 mM),the intracellular cytokine TNF-α produced by hepatic $CD4^{pos}$ T cells in WT-B6 mice was significantly decreased compared to the NH_4-Ac alone treated group ($p<0.001$) and was not different compared to controls [Figure 5.10].

Following NH_4-Ac (4 mM) stimulation, the intracellular cytokine IL-6 produced by hepatic $CD4^{pos}$ T cells in WT- B6 mice was significantly increased compared to controls ($p<0.0001$). When the TLR9 antagonist, ODN2088 was administered along with NH_4-Ac (4 mM), the intracellular cytokine IL-6 produced by hepatic $CD4^{pos}$ T cells in WT-B6 mice was significantly decreased compared to the NH_4-Ac alone treated group ($p<0.0001$) and was not different compared to controls [Figure 5.11].

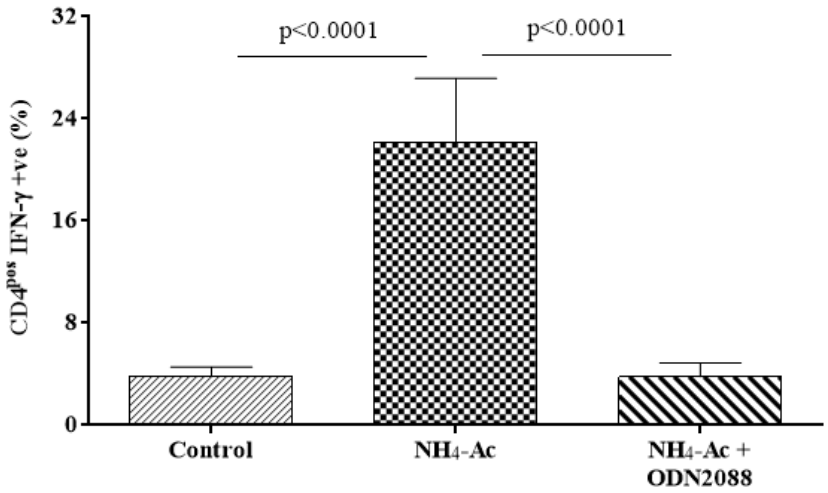

Figure 5.9: Decreased $CD4^{pos}$ IFN-γ production in WT-B6 mice hepatic T cells after TLR9 inhibition.

The intracellular cytokine IFN-γ produced by hepatic $CD4^{pos}$ T cells was significantly increased in WT-B6 mice following NH_4-Ac stimulation (4 mM) compared to controls ($p<0.0001$) [mean difference: 18.3; 95% C.I.: 15.1 to 21.6]. This was significantly inhibited when the TLR9 antagonist (ODN2088) was administered in WT-B6 mice along with NH_4-Ac (4 mM) ($p<0.0001$) [mean difference: –18.4; 95% C.I.: -21.54 to -15.2]; there was no difference compared to controls [mean difference: -0.05; 95% C.I.: -3.2 to 3.1]. [NH_4-Ac (n=13); controls (n=13) & ODN2088 (n=14)] (normal data). Normality assumptions were checked and the data are expressed as mean with S.D.; $p<0.05$ were considered statistically significant. One-way ANOVA with Tukey's multiple comparisons test was used to analyse the differences between parametric data sets.

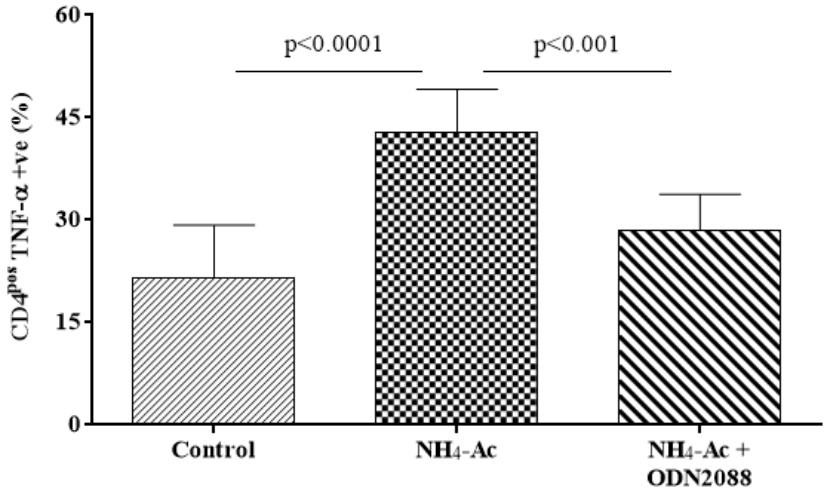

Figure 5.10: Decreased $CD4^{pos}$ TNF-α production in WT-B6 mice hepatic T cells after TLR9 inhibition.

The intracellular cytokine TNF-α produced by hepatic $CD4^{pos}$ T cells was significantly increased in WT-B6 mice following NH_4-Ac stimulation (4 mM) compared to controls ($p<0.0001$) [median difference: 21.4; 95% C.I.: 13.8 to 28.9]. This was significantly inhibited when the TLR9 antagonist (ODN2088) was administered in WT-B6 mice along with NH_4-Ac (4 mM) ($p<0.001$) [median difference: –14.3; 95% C.I.: -22.3 to -6.3]; there was no difference compared to controls [median difference: 7; 95% C.I.: -0.7 to 14.8]. [NH_4-Ac (n=13); controls (n=13) & ODN2088 (n=14)] (non-normal data). Normality assumptions were checked and the data are expressed as mean with S.D.; $p<0.05$ were considered statistically significant. Kruskal-Wallis with Dunn's multiple comparisons test was used to analyse the differences between non-parametric data sets.

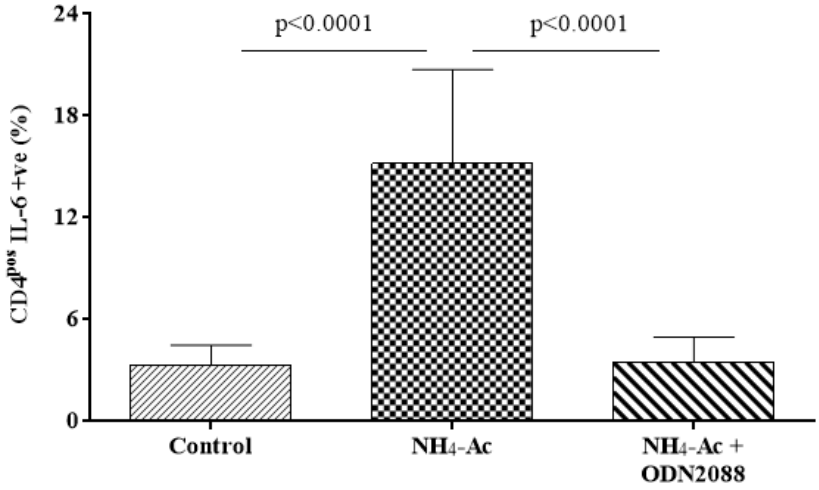

Figure 5.11: Decreased $CD4^{pos}$ IL-6 production in WT-B6 mice hepatic T cells after TLR9 inhibition.

The intracellular cytokine IL-6 produced by hepatic $CD4^{pos}$ T cells was significantly increased in WT-B6 mice following NH_4-Ac stimulation (4 mM) compared to controls ($p<0.0001$) [mean difference: 11.9; 95% C.I.: 18.2 to 15.6]. This was significantly inhibited when the TLR9 antagonist (ODN2088) was administered in WT-B6 mice along with NH_4-Ac (4 mM) ($p<0.0001$) [mean difference: –11.7; 95% C.I.: -15.3 to -8.1]; there was no difference compared to controls [mean difference: 0.1; 95% C.I.: -3.4 to 3.7]. [NH_4-Ac (n=13); controls (n=13) & ODN2088 (n=14)] (normal data). Normality assumptions were checked and the data are expressed as mean with S.D.; $p<0.05$ were considered statistically significant. One-way ANOVA with Tukey's multiple comparisons test was used to analyse the differences between parametric data sets.

5.2.4. Decreased cytokine production in hepatic $CD8^{pos}$ T cells

Following NH_4-Ac (4 mM) stimulation, the intracellular cytokine IFN-γ produced by hepatic $CD8^{pos}$ T cells in WT- B6 mice was significantly increased compared to controls ($p<0.0001$). When the TLR9 antagonist, ODN2088 was administered along with NH_4-Ac (4 mM), the intracellular cytokine IFN-γ produced by hepatic $CD8^{pos}$ T cells in WT-B6 mice was significantly decreased compared to the NH_4-Ac alone treated group ($p<0.0001$); there was no difference compared to controls [Figure 5.12].

Following NH_4-Ac (4 mM) stimulation, the intracellular cytokine TNF-α produced by hepatic $CD8^{pos}$ T cells in WT- B6 mice was significantly increased compared to controls ($p<0.0001$). When the TLR9 antagonist, ODN2088 was administered along with NH_4-Ac (4 mM), the intracellular cytokine TNF-α produced by hepatic $CD8^{pos}$ T cells in WT-B6 mice was significantly decreased compared to the NH_4-Ac alone treated group ($p<0.0001$); there was no difference compared to controls [Figure 5.13].

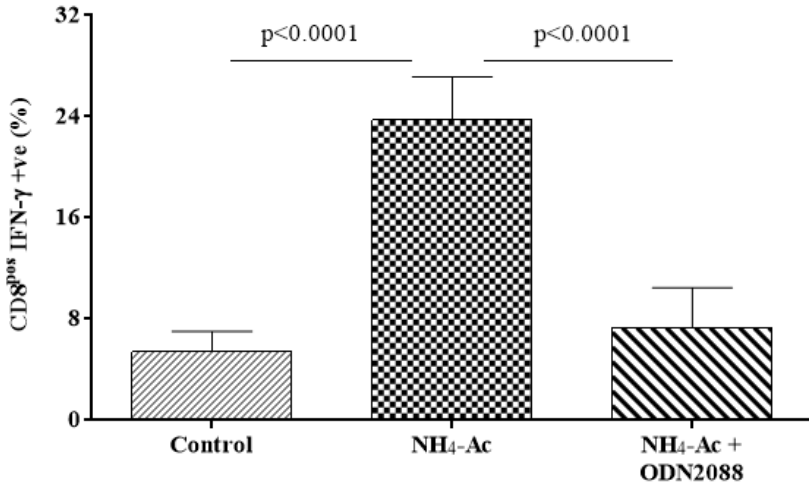

Figure 5.12: Decreased $CD8^{pos}$ IFN-γ production in WT-B6 mice hepatic T cells after TLR9 inhibition.

The intracellular cytokine IFN-γ produced by hepatic $CD8^{pos}$ T cells was significantly increased in WT-B6 mice following NH_4-Ac stimulation (4 mM) compared to controls ($p<0.0001$) [mean difference: 18.3; 95% C.I.: 15.1 to 21.5]. This was significantly inhibited when the TLR9 antagonist (ODN2088) was administered in WT-B6 mice along with NH_4-Ac (4 mM) ($p<0.0001$) [mean difference: –16.4; 95% C.I.: -19.58 to -13.3]; there was no difference compared to controls [mean difference: 4.9; 95% C.I.: -1.1 to 4.9]. [NH_4-Ac (n=13); controls (n=13) & ODN2088 (n=14)] (normal data). Normality assumptions were checked and the data are expressed as mean with S.D.; $p<0.05$ were considered statistically significant. One-way ANOVA with Tukey's multiple comparisons test was used to analyse the differences between parametric data sets.

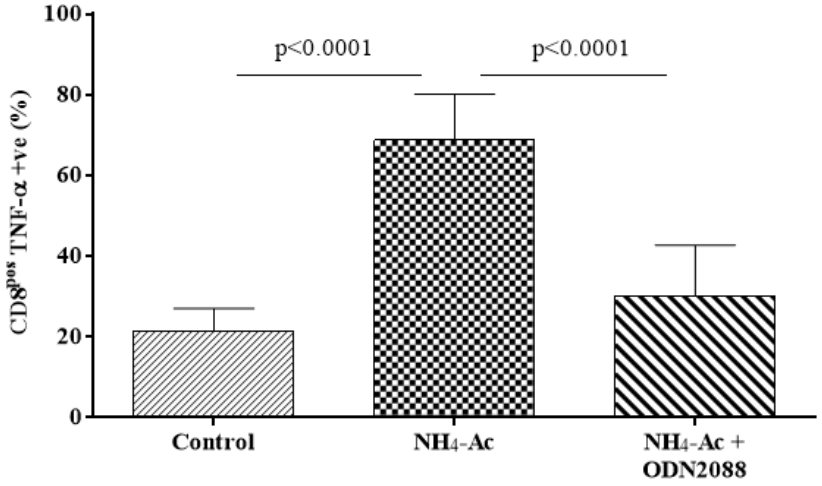

Figure 5.13: Decreased $CD8^{pos}$ TNF-α production in WT-B6 mice hepatic T cells after TLR9 inhibition.

The intracellular cytokine TNF-α produced by hepatic $CD8^{pos}$ T cells was significantly increased in WT-B6 mice following NH_4-Ac stimulation (4 mM) compared to controls ($p<0.0001$) [mean difference: 47.3; 95% C.I.: 35.6 to 59]. This was significantly inhibited when the TLR9 antagonist (ODN2088) was administered in WT-B6 mice along with NH_4-Ac (4 mM) ($p<0.0001$) [mean difference: –38.5; 95% C.I.: -50 to -27]; there was no difference compared to controls [mean difference: 8.8; 95% C.I.: -2.3 to 19.9]. [NH_4-Ac (n=13); controls (n=13) & ODN2088 (n=14)] (normal data). Normality assumptions were checked and the data are expressed as mean with S.D.; $p<0.05$ were considered statistically significant. One-way ANOVA with Tukey's multiple comparisons test was used to analyse the differences between parametric data sets.

5.2.5. Decreased cytokine production in macrophages

To determine whether the TLR9 antagonist inhibited the function of macrophages, ODN2088 (50 μg) was administered to WT-B6 mice along with NH_4-Ac (4 mM) for 6 hours (n=13) and compared to controls (n=5) and WT-B6 mice stimulated with NH_4-Ac alone (n=6).

Following NH_4-Ac (4 mM) stimulation, the intracellular cytokine IFN-γ produced by macrophages in WT-B6 mice was significantly increased compared to controls ($p<0.0001$). When the TLR9 antagonist, ODN2088 was administered along with NH_4-Ac (4 mM), the intracellular cytokine IFN-γ produced by macrophages in WT-B6 mice was significantly decreased compared to the NH_4-Ac alone treated group ($p<0.01$) and was not different compared to controls [Figure 5.14].

Following NH_4-Ac (4 mM) stimulation, the intracellular cytokine TNF-α produced by macrophages in WT-B6 mice was significantly increased compared to controls ($p<0.0001$). When the TLR9 antagonist, ODN2088 was administered along with NH_4-Ac (4 mM), the intracellular cytokine TNF-α produced by macrophages in WT-B6 mice was significantly decreased compared to the NH_4-Ac alone treated group ($p<0.05$) and was not different compared to controls [Figure 5.15].

Following NH_4-Ac (4 mM) stimulation, the intracellular cytokine IL-6 produced by macrophages in WT- B6 mice was significantly increased compared to controls ($p<0.0001$). When the TLR9 antagonist, ODN2088 was administered along with NH_4-Ac (4 mM), the intracellular cytokine IL-6 produced by macrophages in WT-B6 mice was significantly decreased compared to the NH_4-Ac alone treated group ($p<0.0001$) and was not different compared to controls [Figure 5.16].

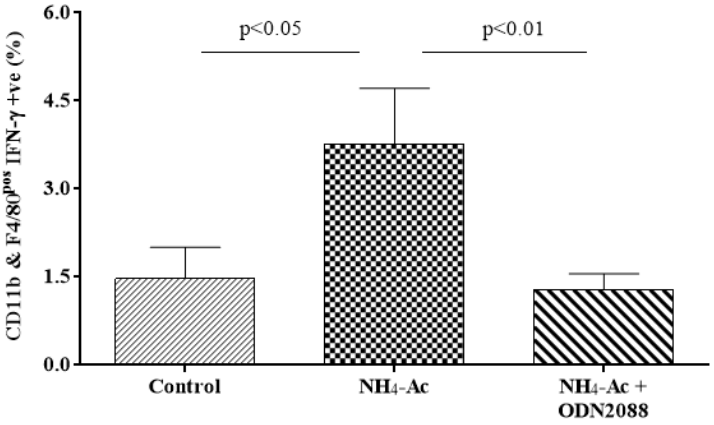

(A)

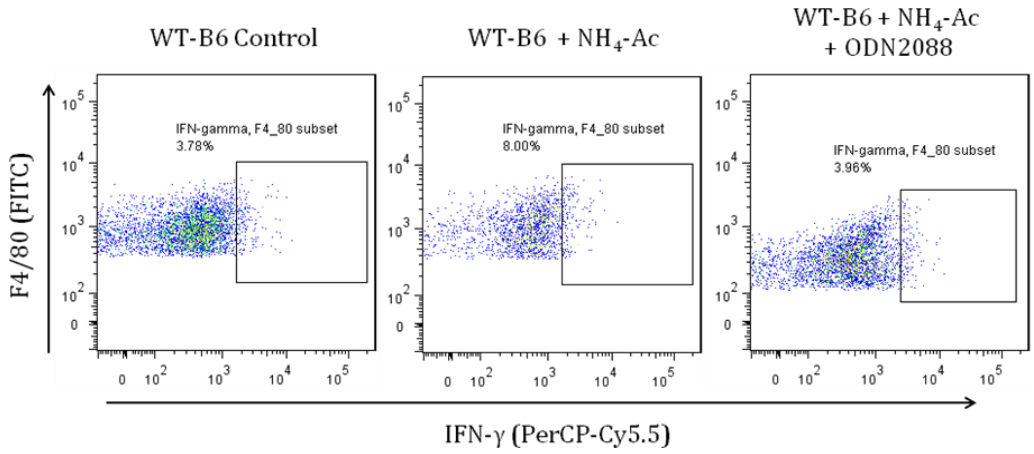

(B)

Figure 5.14: Decreased IFN-γ production by macrophages in WT-B6 mice splenocytes after TLR9 inhibition.

The intracellular cytokine IFN-γ produced by splenic macrophages was significantly increased in WT-B6 mice following NH_4-Ac stimulation (4 mM) compared to controls ($p<0.05$) [median difference: 2.4; 95% C.I.: 1.3 to 3.6]. This was significantly inhibited when the TLR9 antagonist (ODN2088) was administered in WT-B6 mice along with NH_4-Ac (4 mM) ($p<0.01$) [median difference: -2.4; 95% C.I.: -3.4 to -1.6]; there was no difference compared to controls [median difference: –0.1; 95% C.I.: -0.7 to 0.3]. [NH_4-Ac (n=6); controls (n=5) & ODN2088 (n=13)] (non-normal data). Normality assumptions were checked and the data are expressed as mean with S.D.; $p<0.05$ were considered statistically significant. Kruskal-Wallis with Dunn's multiple comparisons test was used to analyse the differences between non-parametric data sets. (A) Graph and (B) FACS plots representing each group.

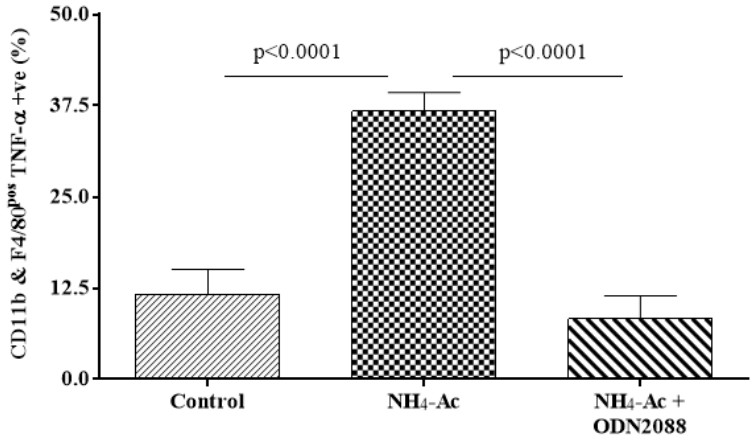

(A)

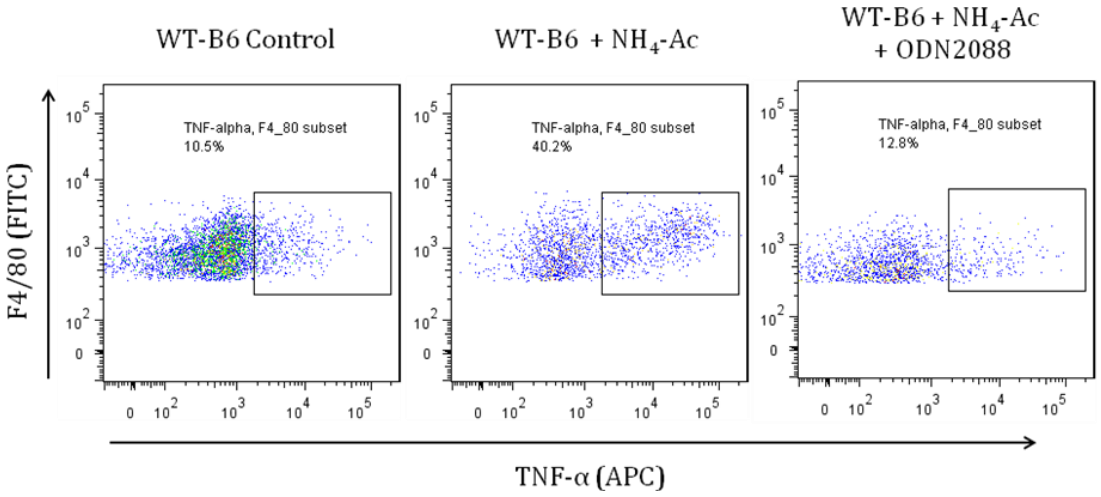

(B)

Figure 5.15: Decreased TNF-α production by macrophages in WT-B6 mice splenocytes after TLR9 inhibition.

The intracellular cytokine TNF-α produced by splenic macrophages was significantly increased in WT-B6 mice following NH_4-Ac stimulation (4 mM) compared to controls ($p<0.0001$) [mean difference: 25.1; 95% C.I.: 20.49 to 29.76]. This was significantly inhibited when the TLR9 antagonist (ODN2088) was administered in WT-B6 mice along with NH_4-Ac (4 mM) ($p<0.0001$) [mean difference: -28.4; 95% C.I.: -32.2 to -24.7]; there was no difference compared to controls [mean difference: –3.3; 95% C.I.: -7.3 to 0.6]. [NH_4-Ac (n=6); controls (n=5) & ODN2088 (n=13)] (normal data). Normality assumptions were checked and the data are expressed as mean with S.D.; $p<0.05$ were considered statistically significant. One-way ANOVA with Tukey's multiple comparisons test was used to analyse the differences between parametric data sets. (A) Graph and (B) FACS plots representing each group.

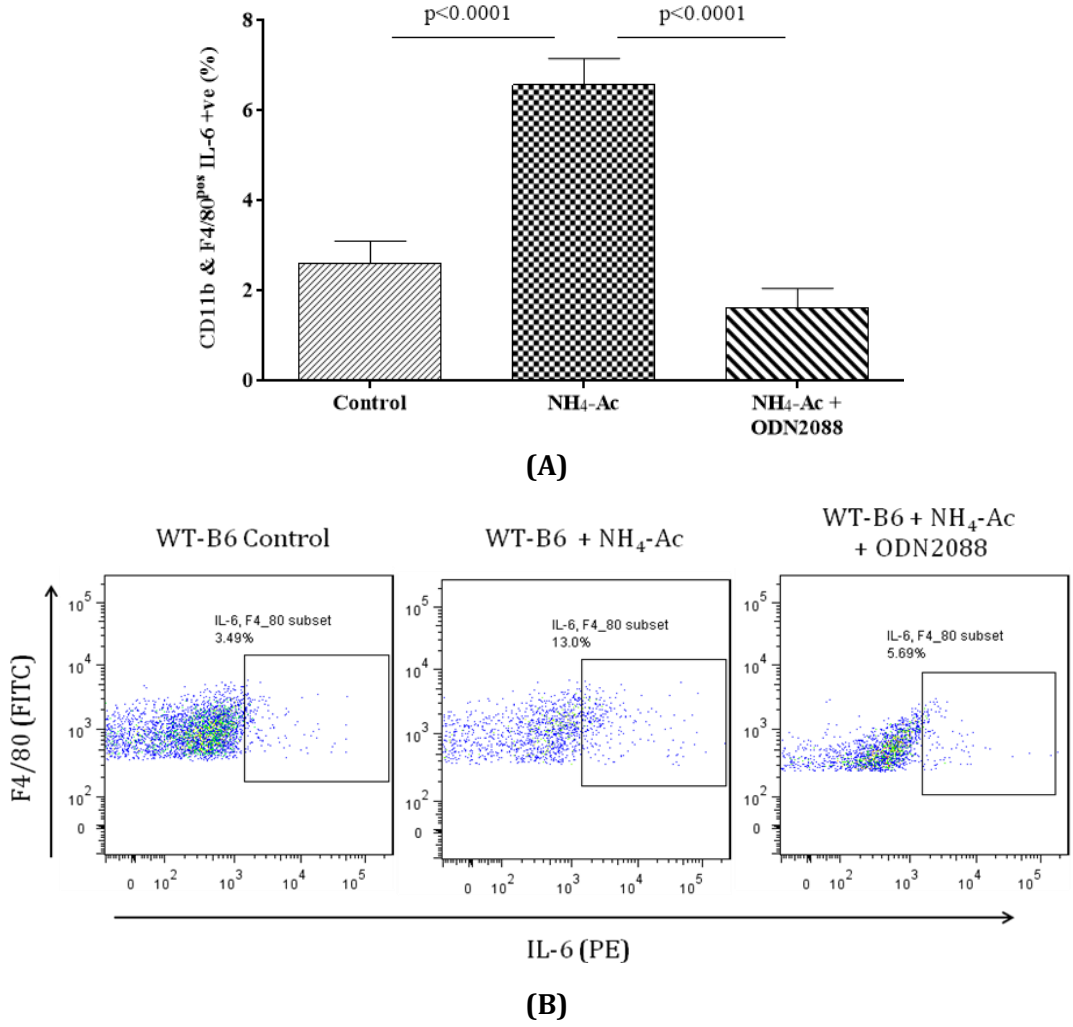

Figure 5.16: Decreased IL-6 production by macrophages in WT-B6 mice splenocytes after TLR9 inhibition.

The intracellular cytokine IL-6 produced by splenic macrophages was significantly increased in WT-B6 mice following NH_4-Ac stimulation (4 mM) compared to controls ($p<0.0001$) [mean difference: 3.9; 95% C.I.: 3.2 to 4.7]. This was significantly inhibited when the TLR9 antagonist (ODN2088) was administered in WT-B6 mice along with NH_4-Ac (4 mM) ($p<0.0001$) [mean difference: -4.9; 95% C.I.: -5.5 to -4.3]; there was no difference compared to controls [mean difference: –1; 95% C.I.: -1.6 to -0.3]. [NH_4-Ac (n=6); controls (n=5) & ODN2088 (n=13)] (normal data). Normality assumptions were checked and the data are expressed as mean with S.D.; $p<0.05$ were considered statistically significant. One-way ANOVA with Tukey's multiple comparisons test was used to analyse the differences between parametric data sets. (A) Graph and (B) FACS plots representing each group.

5.2.6. Decreased cytokine production in KLRG-1^{pos} NK cells

To determine whether the TLR9 antagonist inhibited the phenotype and function of KLRG-1^{pos} NK cells, ODN2088 (50 μg) was administered to WT-B6 mice along with NH_4-Ac (4 mM) for 6 hours (n=10) and compared to controls (n=7) and WT-B6 mice stimulated with NH_4-Ac alone (n=5).

Following NH_4-Ac (4 mM) stimulation, the frequency of KLRG-1^{pos} NK cells in WT-B6 mice was significantly increased compared to controls ($p<0.05$). When theTLR9 antagonist, ODN2088 was administered along with NH_4-Ac (4 mM), the frequency of KLRG-1^{high} NK cells in WT-B6 mice was significantly decreased compared to the NH_4-Ac alone treated group ($p<0.0001$) and was not different compared to controls [Figure 5.17].

Following NH_4-Ac (4 mM) stimulation, the intracellular cytokine IFN-γ produced by KLRG-1^{pos} NK cells in WT-B6 mice was significantly increased compared to controls ($p<0.001$). When the TLR9 antagonist, ODN2088 was administered along with NH_4-Ac (4 mM), the intracellular cytokine IFN-γ produced by KLRG-1^{pos} NK cells in WT-B6 mice was significantly decreased compared to the NH_4-Ac alone treated group ($p<0.0001$) and was not different compared to controls [Figure 5.18].

Following NH_4-Ac (4 mM) stimulation, the intracellular cytokine TNF-α produced by KLRG-1^{pos} NK cells in WT-B6 mice was significantly increased compared to controls ($p<0.0001$). When the TLR9 antagonist, ODN2088 was administered along with NH_4-Ac (4 mM), the intracellular cytokine TNF-α produced by KLRG-1^{pos} NK cells in WT-B6 mice was significantly decreased compared to the NH_4-Ac alone treated group ($p<0.0001$) and was not different compared to controls [Figure 5.19].

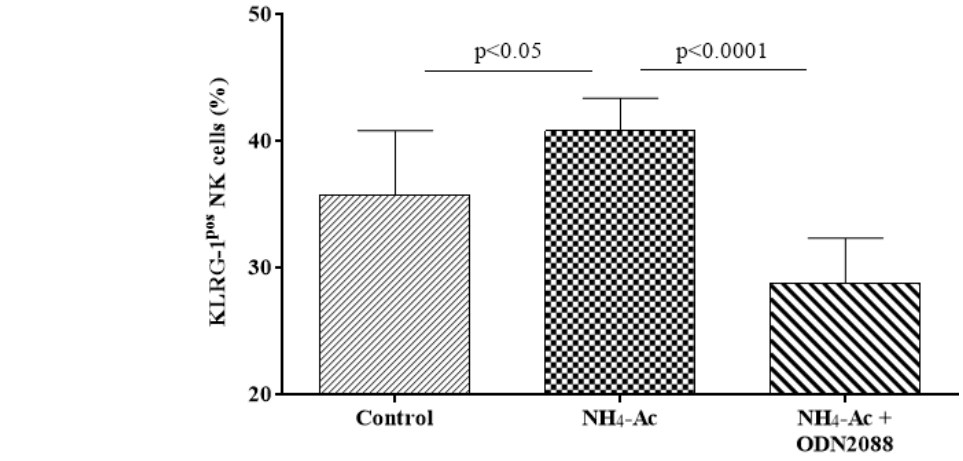

(A)

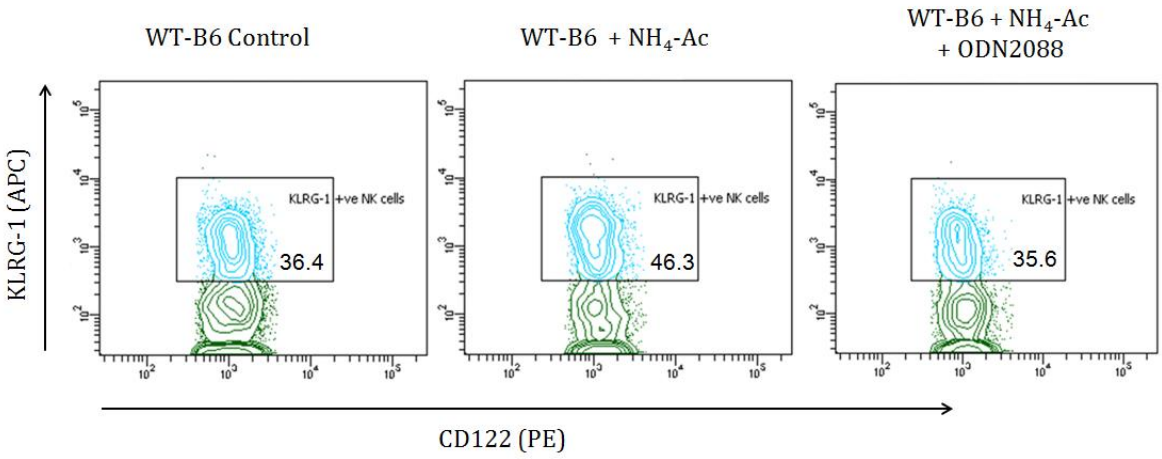

(B)

Figure 5.17: Decreased KLRG-1^{pos} NK cells in WT-B6 mice splenocytes after TLR9 inhibition.

Splenic KLRG-1^{pos} NK cells were significantly increased in WT-B6 mice following NH_4-Ac stimulation (4 mM) compared to controls ($p<0.05$) [mean difference: 5; 95% C.I.: 0.37 to 9.7]. This was significantly inhibited when the TLR9 antagonist (ODN2088) was administered in WT-B6 mice along with NH_4-Ac (4 mM) ($p<0.0001$) [mean difference: -12; 95% C.I.: -16.3 to -7.7]; there was no difference compared to controls [mean difference: –7; 95% C.I.: -11.6 to -2.3]. [NH_4-Ac (n=5); controls (n=7) & ODN2088 (n=10)] (normal data). Normality assumptions were checked and the data are expressed as mean with S.D.; $p<0.05$ were considered statistically significant. One-way ANOVA with Tukey's multiple comparisons test was used to analyse the differences between parametric data sets. (A) Graph and (B) FACS plots representing each group.

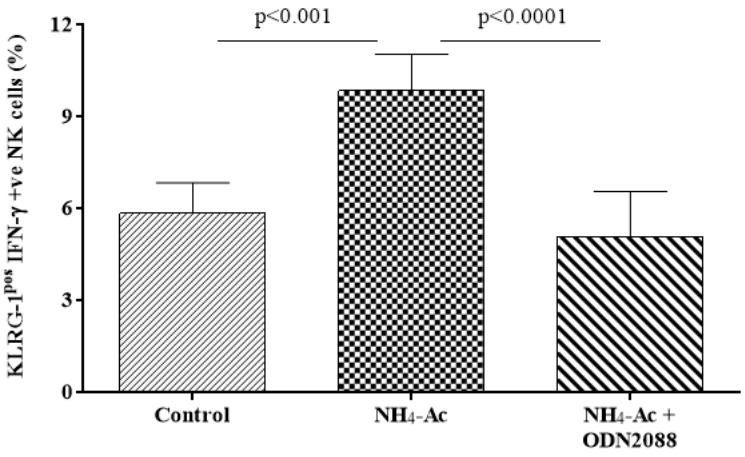

(A)

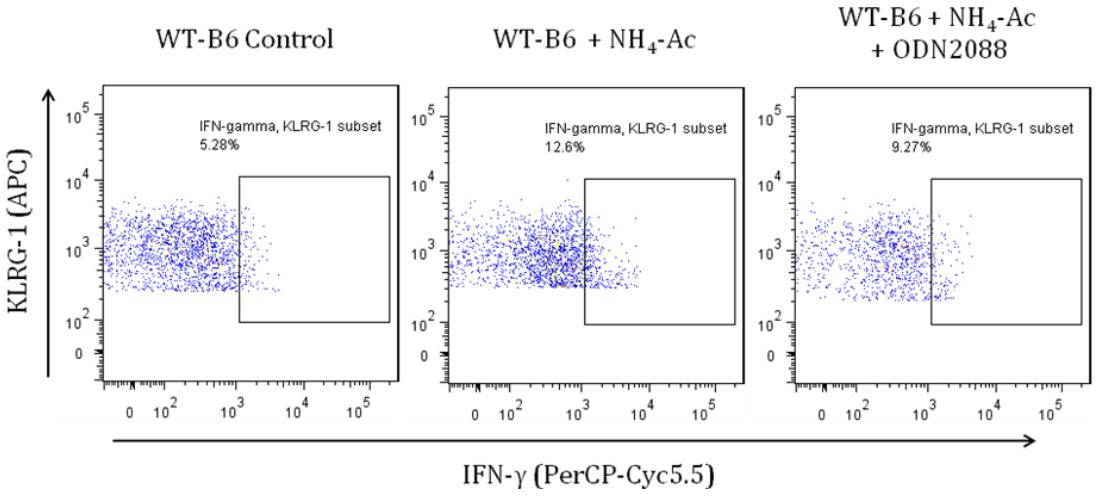

(B)

Figure 5.18: Decreased IFN-γ production by KLRG-1^{pos} NK cells in WT-B6 mice splenocytes after TLR9 inhibition.

The intracellular cytokine IFN-γ produced by splenic KLRG-1^{pos} NK cells was significantly increased in WT-B6 mice following NH_4-Ac stimulation (4 mM) compared to controls ($p<0.001$) [mean difference: 4; 95% C.I.: 2.1 to 5.9]. This was significantly inhibited when the TLR9 antagonist (ODN2088) was administered in WT-B6 mice along with NH_4-Ac (4 mM) ($p<0.0001$) [mean difference: -4.8; 95% C.I.: -6.5 to -3]; there was no difference compared to controls [mean difference: –0.7; 95% C.I.: -2.3 to 0.8]. [NH_4-Ac (n=5); controls (n=7) & ODN2088 (n=10)] (normal data). Normality assumptions were checked and the data are expressed as mean with S.D.; $p<0.05$ were considered statistically significant. One-way ANOVA with Tukey's multiple comparisons test was used to analyse the differences between parametric data sets. (A) Graph and (B) FACS plots representing each group.

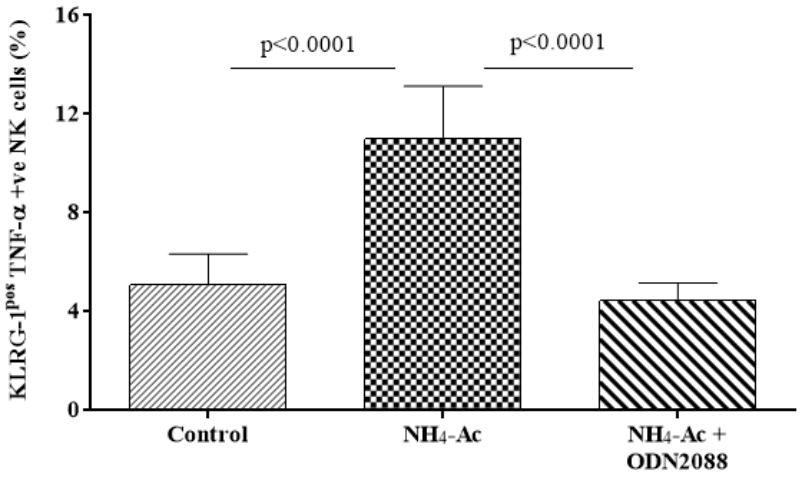

(A)

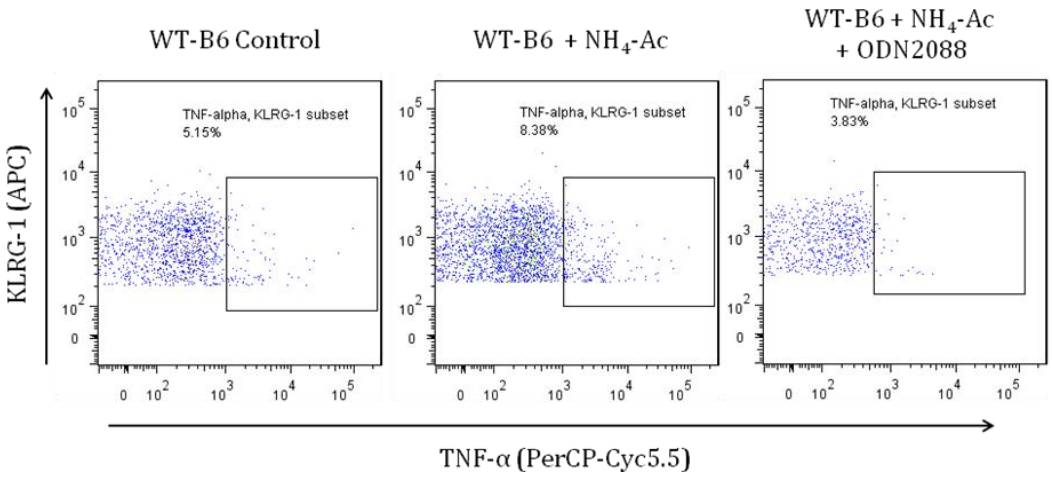

(B)

Figure 5.19: Decreased TNF-α produced by KLRG-1^{pos} NK cells in WT-B6 mice splenocytes after TLR9 inhibition.

The intracellular cytokine TNF-α produced by splenic KLRG-1^{pos} NK cells was significantly increased in WT-B6 mice following NH_4-Ac stimulation (4 mM) compared to controls ($p<0.0001$) [mean difference: 5.9; 95% C.I.: 4 to 7.8]. This was significantly inhibited when the TLR9 antagonist (ODN2088) was administered in WT-B6 mice along with NH_4-Ac (4 mM) ($p<0.0001$) [mean difference: -6.5; 95% C.I.: -8.3 to -4.8]; there was no difference compared to controls [mean difference: –0.6; 95% C.I.: -2.2 to 0.9]. [NH_4-Ac (n=5); controls (n=7) & ODN2088 (n=10)] (normal data). Normality assumptions were checked and the data are expressed as mean with S.D.; $p<0.05$ were considered statistically significant. One-way ANOVA with Tukey's multiple comparisons test was used to analyse the differences between parametric data sets. (A) Graph and (B) FACS plots representing each group.

To determine whether the TLR9 antagonist inhibited the dsDNA released into the circulation, ODN2088 (50 μg) was administered to WT-B6 mice along with NH_4-Ac (4 mM) for 6 hours (n=15) and compared to controls (n=13) and WT-B6 mice stimulated with NH_4-Ac alone (n=13).

Following NH_4-Ac (4 mM) stimulation, the plasma dsDNA level in WT-B6 mice was significantly increased compared to controls ($p<0.001$). When the TLR9 antagonist, ODN2088 was administered along with NH_4-Ac (4 mM), the plasma dsDNA level in WT-B6 mice was not different compared to NH_4-Ac alone treated group but was significantly increased compared to controls ($p<0.01$) [Figure 5.20].

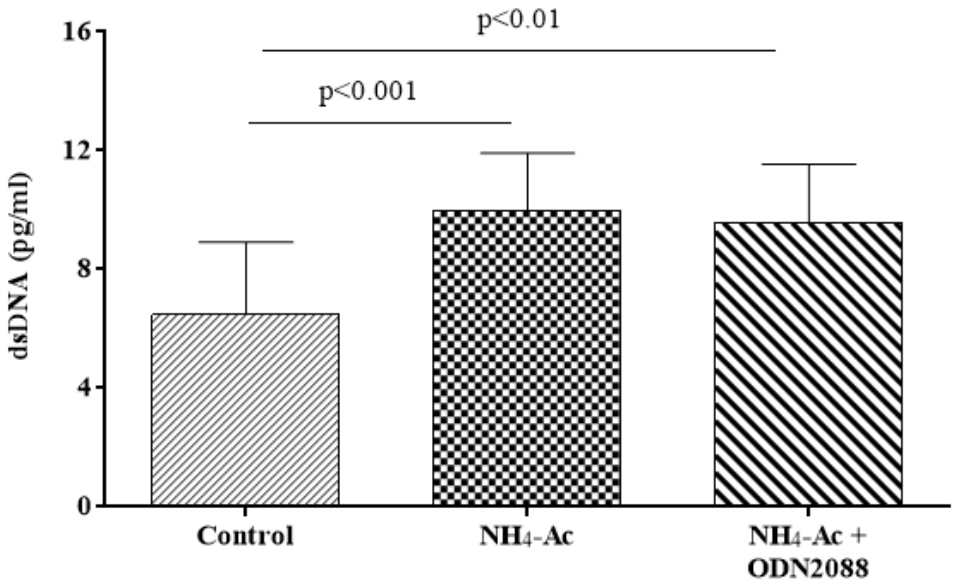

Figure 5.20: Unchanged plasma dsDNA level in WT-B6 mice after TLR9 inhibition.

Plasma dsDNA level was significantly increased in WT-B6 mice following NH_4-Ac (4 mM) stimulation compared to controls ($p<0.001$) [mean difference: 3.5; 95% C.I.: 1.3 to 5.6]. This was unchanged when the TLR9 antagonist (ODN2088) was administered in WT-B6 mice along with NH_4-Ac (4 mM) [mean difference: 3.5; 95% C.I.: 1.3 to 5.6] and remained significantly increased compared to controls ($p<0.01$) [mean difference: -0.4; 95% C.I.: -2.4 to 1.5].

5.3. Summary

In this chapter, it has been demonstrated that the TLR9 antagonist ODN2088 abrogates the cytokine production of T cells, macrophages and NK cells in WT-B6 mice and protects against the development of brain oedema in WT-B6 mice induced by 4 mM ammonia challenge. These data are well supported by the findings of Imaeda et al who in a paracetamol toxicity model, established that inhibition of TLR9 using ODN2088 and IRS954, a TLR7/9 antagonist, protected against the development of pro-inflammation and mortality [108]. Furthermore it has been shown that inhibition of TLR9 reduced the resultant inflammation induced by *Legionella pneumophila,* [205] and is an effective anti-hypertensive in rats [206].

Usually the TLR9 antagonist, ODN2088, acts by disrupting the co-localization of the CpG motif of the ODN with TLR9 without affecting cellular binding and uptake [207], therefore it could be assumed a similar mechanism would have been involved in this study as the TLR9 activated by ammonia-induced inflammation is dependent on DNA. The reactivity of the compound ODN2088 is specific for murine TLR9, but a study on systemic lupus erythematosus, an autoimmune disease, demonstrated that IRS954, a similar compound, inhibited both TLR7 and 9 [208], therefore it is unclear whether this compound cross reacts with other TLRs. Although ammonia was not measured in the brain or in other regions in the animals, the upregulation of TLR9 expression was reversed at the 8 hour-time point after the injection of ammonia, therefore it could be assumed that ammonia starts clearing from the body 6 hours after the injection.

There was no change in the DNA release when the TLR9 antagonist was injected along with NH_4-Ac. This is mainly because the ODN2088 disrupts the co-localization of the

DNA with TLR9 and as discussed previously the DNA release could be a result of ammonia stimulation [189]. There is no clear information about the duration it takes for this compound to get activated or whether it is able to cross the blood brain barrier.

It is clearly evident from this study that administration of ODN2088 prevents the ammonia-induced brain oedema in WT mice. However, the current understanding of ammonia-induced brain oedema in relation to ALF is that it is mainly caused by accumulation of glutamine in the astrocytes and the possible mechanisms for this include increased synthesis of glutamine and decreased clearance of glutamine from the astrocyte as a result of impaired transport [88, 89]. This raises the question as to whether the TLR9 antagonist might have influenced the glutamine system in the brain, but there is no existing literature that supports or validates the impact of TLR9 antagonism on the brain and/or the glutamine system. This also leads us to postulate that the ammonia-induced brain oedema in ALF is mainly driven by systemic inflammation mediated by the activation of TLR9.

Chapter 6. Neutrophil and/or Kupffer cell TLR9 expression mediates the ammonia-induced inflammation and brain oedema

In chapters 4 and 5, it has been shown that TLR9$^{-/-}$ B6 mice were protected against the deleterious effects of ammonia on the immune system and brain. The use of a TLR9 antagonist tempered the pro-inflammatory state and abrogated the development of brain oedema following ammonia stimulation. Furthermore, it has also been shown that T cells, macrophages and NK cells were the immune cell sub-sets involved in this ammonia-induced TLR9-mediated systemic inflammatory response. However, it remains unclear as to which innate immune cell type(s) were activated by the ammonia and triggered the adaptive immune response. Although there was no difference in the neutrophil function between WT-B6 mice and TLR9$^{-/-}$ B6 mice following NH_4-Ac stimulation, neutrophil TLR9 expression was synergistically upregulated by ammonia, IL-8 and DNA in the human study.

Therefore to determine whether neutrophils play an important role in the ammonia-induced inflammatory response, NH_4-Ac was injected into another transgenic mouse model, TLR9$^{fl/fl}$ LysCre B6 mice whereby TLR9 is only deficient in neutrophils and Kupffer cells, and compared to controls and TLR9$^{fl/fl}$ B6 mice. The TLR9$^{fl/fl}$ LysCre B6 mice results were also compared to WT-B6 mice and TLR9$^{-/-}$ B6 mice [Method – 2.24.1].

6.1. Ammonia-induced brain oedema and changes in the liver were dependent on neutrophils and/or Kupffer cell TLR9

6.1.1. Brain water content

To determine whether neutrophils and/or Kupffer cell TLR9 expression influenced the ammonia-induced brain oedema, the differences in the brain water content of TLR9$^{fl/fl}$ B6 mice and TLR9$^{fl/fl}$ LysCre B6 mice was determined six hours after a single low dose of NH_4-Ac administration (I.P., 4 mM) and compared to controls (untreated).

Following NH_4-Ac stimulation (4 mM), there was a significant increase in the brain water content in $TLR9^{fl/fl}$ B6 mice (n=11) compared to controls (n=8) (NH_4-Ac untreated) ($p<0.001$); there was no difference in the brain water content in $TLR9^{fl/fl}$ LysCre B6 mice (n=9) compared to controls (n=9). There was a significant decrease in the brain water content in $TLR9^{fl/fl}$ LysCre B6 mice compared to $TLR9^{fl/fl}$ B6 mice ($p<0.05$) following NH_4-Ac stimulation (4 mM) [Figure 6.1].

When compared between three groups, brain water content was significantly decreased in $TLR9^{-/-}$ B6 mice (n=8) ($p<0.05$) and $TLR9^{fl/fl}$ LysCre B6 mice (n=9) ($p<0.001$) compared to WT-B6 mice (n=9) following NH_4-Ac stimulation (4 mM). There was no difference in the brain water content between $TLR9^{-/-}$ B6 mice and $TLR9^{fl/fl}$ LysCre B6 mice [Figure 6.2].

6.1.2. Changes in the liver bodyweight ratio

Following NH_4-Ac stimulation (4 mM), there was a significant increase in the liver bodyweight ratio in $TLR9^{fl/fl}$ B6 mice (n=15) compared to controls (n=8) (NH_4-Ac untreated) ($p<0.05$); there was no difference in the liver bodyweight ratio in $TLR9^{fl/fl}$ LysCre B6 mice (n=10) compared to controls (n=10). There was a significant decrease in the liver bodyweight ratio in $TLR9^{fl/fl}$ LysCre B6 mice compared to $TLR9^{fl/fl}$ B6 mice ($p<0.05$) following NH_4-Ac stimulation (4 mM) [Figure 6.3].

When compared between three groups, liver bodyweight ratio was significantly decreased in $TLR9^{-/-}$ B6 mice (n=11) ($p<0.0001$) and $TLR9^{fl/fl}$ LysCre B6 mice (n=10) ($p<0.0001$) compared to WT-B6 mice (n=16) following NH_4-Ac stimulation (4 mM). There was no difference in the liver bodyweight ratio between $TLR9^{-/-}$ B6 mice and $TLR9^{fl/fl}$ LysCre B6 mice [Figure 6.4].

6.1.3. Changes in the liver histology

Hepatocyte swelling was decreased in $TLR9^{-/-}$ B6 mice and $TLR9^{fl/fl}$ LysCre B6 mice compared to WT-B6 mice following NH_4-Ac stimulation (4 mM). There was no difference in the hepatocyte morphology between $TLR9^{-/-}$ B6 mice and $TLR9^{fl/fl}$ LysCre B6 mice [Figure 6. 5].

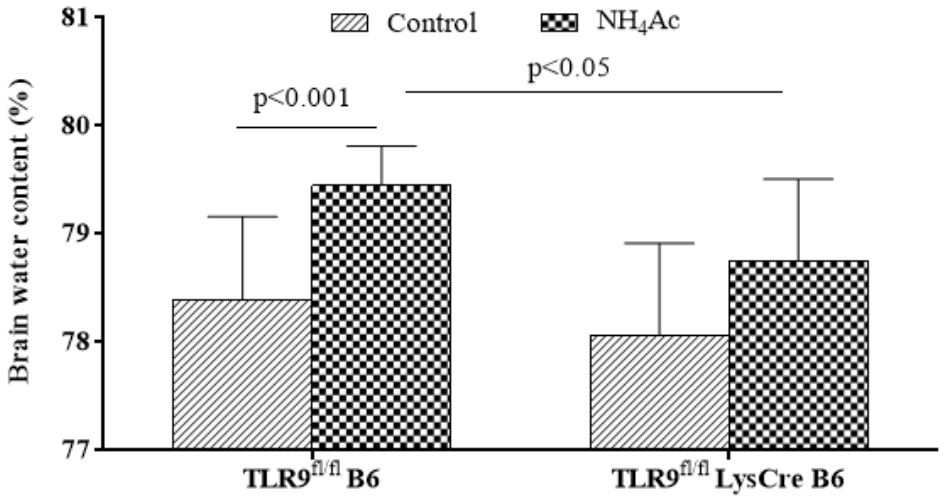

Figure 6.1: Brain water content in TLR9$^{fl/fl}$ B6 mice and TLR9$^{fl/fl}$ LysCre B6 mice following NH_4-Ac stimulation.

Following NH_4-Ac stimulation (4 mM), there was a significant increase in the brain water content in TLR9$^{fl/fl}$ B6 mice compared to controls ($p<0.001$) [mean difference: 1.1; 95% C.I.: 0.5 to 1.6] (normal data). The increase in brain water was significantly ameliorated in TLR9$^{fl/fl}$ LysCre B6 mice compared to TLR9$^{fl/fl}$ B6 mice ($p<0.05$) [mean difference: -0.7; 95% C.I.: -1.2 to -0.15] (normal data). [TLR9$^{fl/fl}$ B6 mice (n=11) & controls (n=8); TLR9$^{fl/fl}$ LysCre B6 mice (n=9) & controls (n=9)]. Normality assumptions were checked and the data are expressed as mean with S.D.; $p<0.05$ were considered statistically significant. Student t-test was used to analyse the difference between parametric data sets.

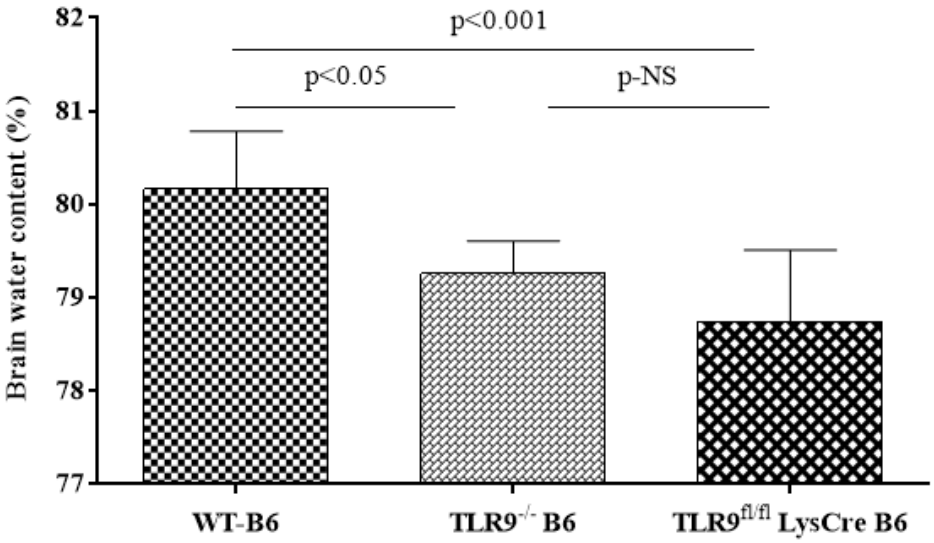

Figure 6.2: Brain water content in WT-B6 mice, TLR9$^{-/-}$ B6 mice and TLR9$^{fl/fl}$ LysCre B6 mice following NH_4-Ac stimulation.

Following NH_4-Ac stimulation (4 mM), there was a significant decrease in the brain water content in TLR9$^{-/-}$ B6 mice ($p<0.05$) [mean difference: -0.91; 95% C.I.: -1.6 to -0.17] and TLR9$^{fl/fl}$ LysCre B6 mice ($p<0.001$) [mean difference: -1.4; 95% C.I.: -2.1 to -0.7] compared to WT-B6 mice. There was no difference between the brain water content in TLR9$^{fl/fl}$ LysCre B6 mice and TLR9$^{-/-}$ B6 mice [mean difference: -0.5; 95% C.I.: -1.2 to 0.2]. [WT-B6 mice (n=9); TLR9$^{-/-}$ B6 mice (n=8) and TLR9$^{fl/fl}$ LysCre B6 mice (n=9)] (normal data). Normality assumptions were checked and the data are expressed as mean with S.D.; $p<0.05$ were considered statistically significant. One-way ANOVA with Tukey's multiple comparisons test was used to analyse the differences between parametric data sets.

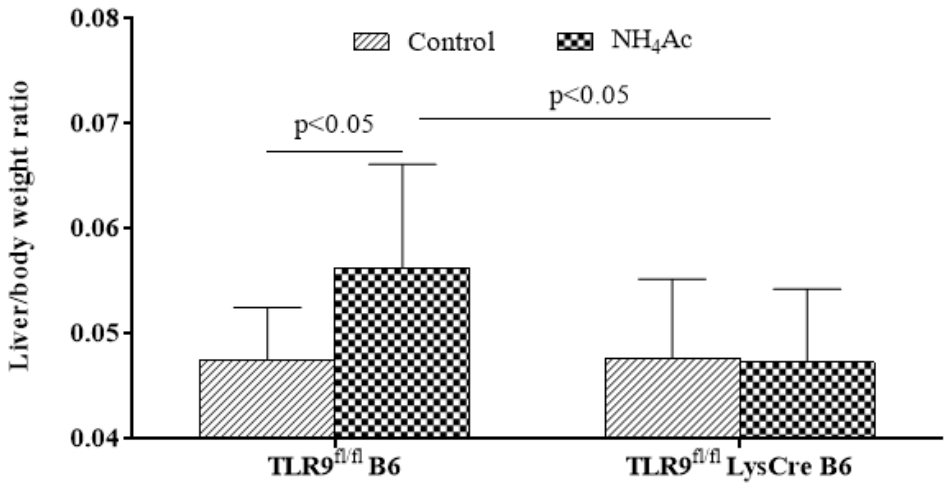

Figure 6.3: Liver bodyweight ratio in $TLR9^{fl/fl}$ B6 mice and $TLR9^{fl/fl}$ LysCre B6 mice following NH_4-Ac stimulation.

Following NH_4-Ac stimulation (4 mM), there was a significant increase in the brain water content in $TLR9^{fl/fl}$ B6 mice compared to controls ($p<0.05$) [median difference: 0.007; 95% C.I.: 0.001 to 0.01] (non-normal data), which was abrogated in the $TLR9^{fl/fl}$ LysCre B6 mice ($p<0.05$) [mean difference: -0.006; 95% C.I.: -0.015 to -0.001] (normal data). [$TLR9^{fl/fl}$ B6 mice (n=11) & controls (n=8); $TLR9^{fl/fl}$ LysCre B6 mice (n=9) & controls (n=9)]. Normality assumptions were checked and the data are expressed as mean with S.D.; $p<0.05$ were considered statistically significant. Student t-test was used to analyse the difference between parametric data sets and Mann-Whitney U test was used to analyse the difference between non-parametric data sets.

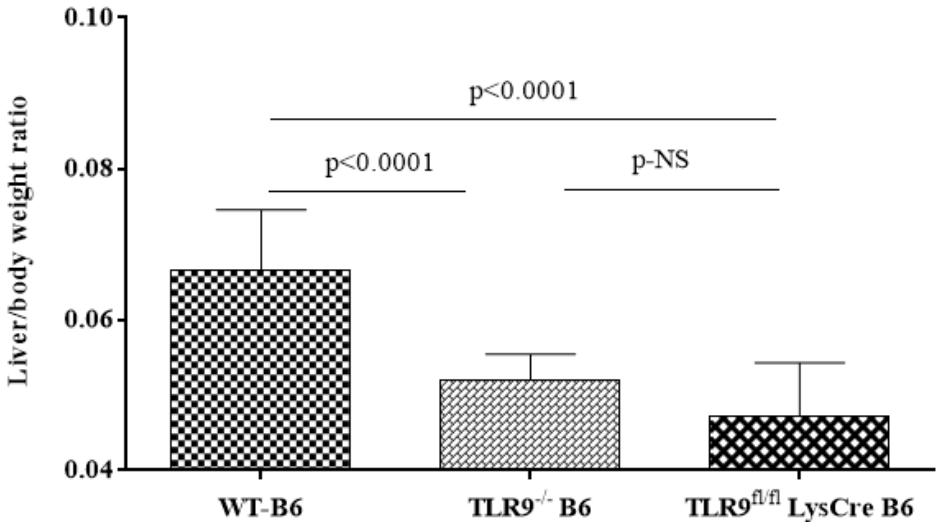

Figure 6.4: Liver bodyweight ratio in WT-B6 mice, $TLR9^{-/-}$ B6 mice and $TLR9^{fl/fl}$ LysCre B6 mice following NH_4-Ac stimulation.

Following NH_4-Ac stimulation (4 mM), there was a significant decrease in the liver bodyweight ratio in $TLR9^{-/-}$ B6 mice ($p<0.0001$) [mean difference: -0.015; 95% C.I.: -0.02 to -0.008] and $TLR9^{fl/fl}$ LysCre B6 mice ($p<0.0001$) [mean difference: -0.019; 95% C.I.: -026 to -0.013] compared to WT-B6 mice. There was no difference between $TLR9^{fl/fl}$ LysCre B6 mice compared to $TLR9^{-/-}$ B6 mice [mean difference: -0.005; 95% C.I.: -0.01 to -0.002]. [WT-B6 mice (n=16); $TLR9^{-/-}$ B6 mice (n=11) and $TLR9^{fl/fl}$ LysCre B6 mice (n=10)] (normal data). Normality assumptions were checked and the data are expressed as mean with S.D.; $p<0.05$ were considered statistically significant. One-way ANOVA with Tukey's multiple comparisons test was used to analyse the differences between parametric data sets.

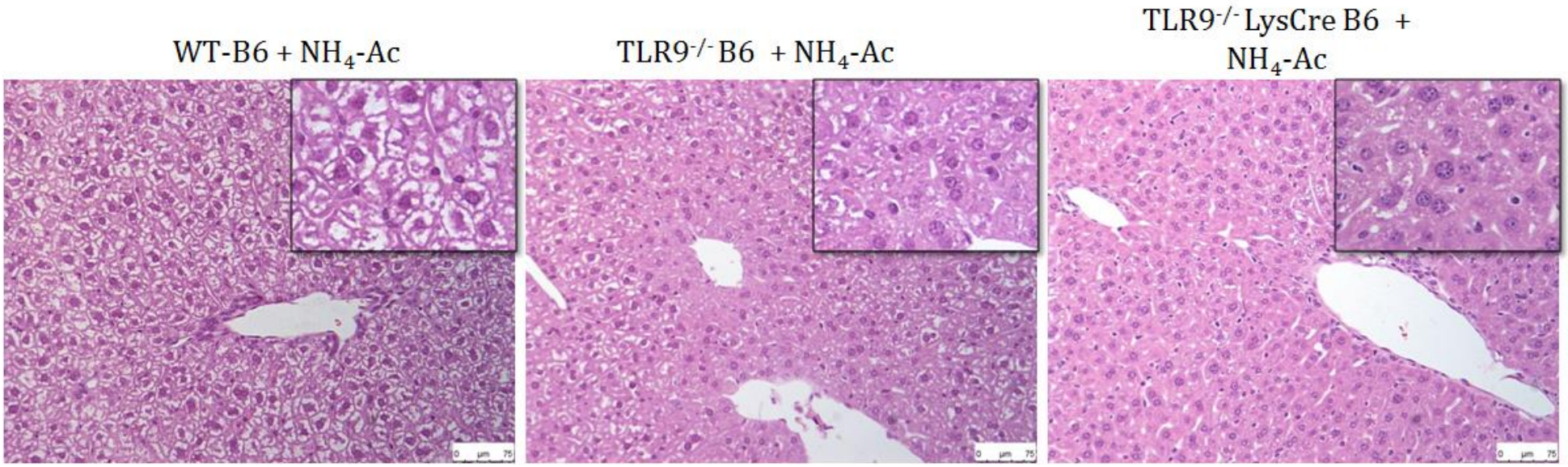

Figure 6.5: Liver histological changes following NH_4-Ac stimulation.

These light microscope images (200x magnification) are sections (H&E stained) of the liver representing three different mice groups. Following NH_4-Ac stimulation (4 mM), hepatocyte swelling was increased in the sections of the liver in WT-B6 mice compared to $TLR9^{-/-}$ B6 mice and $TLR9^{fl/fl}$ LysCre B6 mice. There was no difference in the hepatocyte morphology between $TLR9^{-/-}$ B6 mice and $TLR9^{fl/fl}$ LysCre B6 mice. The images in the black box inset are the same regions of the specimen captured at a higher magnification (400x).

6.2. Ammonia-induced macrophage dysfunction was mediated by TLR9 expressed on neutrophils and/or Kupffer cells

To determine whether TLR9 expressed on neutrophils and Kupffer cells influenced the ammonia-induced inflammation, the differences in the intracellular cytokine production of macrophages in $TLR9^{fl/fl}$ B6 mice (n=13) and $TLR9^{fl/fl}$ LysCre B6 mice (n=9) was determined six hours after the administration of a single low dose of NH_4-Ac (I.P., 4 mM) and compared to controls (untreated) [$TLR9^{fl/fl}$ B6 mice (n=8) and $TLR9^{fl/fl}$ LysCre B6 mice (n=10)] (Method-2).

6.2.1. IFN-γ produced by macrophages

Following NH_4-Ac stimulation (4 mM), there was a significant increase in the intracellular cytokine IFN-γ produced by macrophages in $TLR9^{fl/fl}$ B6 mice compared to controls (NH_4-Ac untreated) ($p<0.0001$); there was no difference in the intracellular cytokine IFN-γ produced by macrophages in $TLR9^{fl/fl}$ LysCre B6 mice compared to controls. There was a significant decrease in the intracellular cytokine IFN-γ produced by macrophages in $TLR9^{fl/fl}$ LysCre B6 mice compared to $TLR9^{fl/fl}$ B6 mice ($p<0.0001$) following NH_4-Ac stimulation (4 mM) [Figure 6.6].

When compared between three groups, the intracellular cytokine IFN-γ produced by macrophages was significantly decreased in $TLR9^{-/-}$ B6 mice (n=7) ($p<0.01$) and $TLR9^{fl/fl}$ LysCre B6 mice (n=9) ($p<0.05$) compared to WT-B6 mice (n=5) following NH_4-Ac stimulation (4 mM). There was no difference in the intracellular cytokine IFN-γ produced by macrophages of $TLR9^{-/-}$ B6 mice and $TLR9^{fl/fl}$ LysCre B6 mice [Figure 6.7].

6.2.2. TNF-α produced by macrophages

Following NH_4-Ac stimulation (4 mM), there was a significant increase in the intracellular cytokine TNF-α produced by macrophages in $TLR9^{fl/fl}$ B6 mice compared to controls (NH_4-Ac untreated) ($p<0.0001$); there was also a significant increase in the intracellular cytokine TNF-α produced by macrophages in $TLR9^{fl/fl}$ LysCre B6 mice compared to controls ($p<0.05$). There was however, a significant decrease in the intracellular cytokine TNF-α produced by macrophages in $TLR9^{fl/fl}$ LysCre B6 mice compared to $TLR9^{fl/fl}$ B6 mice ($p<0.0001$) following NH_4-Ac stimulation (4 mM) [Figure 6.8].

When compared between three groups, the intracellular cytokine TNF-α produced by macrophages was significantly decreased in $TLR9^{-/-}$ B6 mice (n=7) ($p<0.01$) and $TLR9^{fl/fl}$ LysCre B6 mice (n=9) ($p<0.01$) compared to WT-B6 mice (n=5) following NH_4-Ac stimulation (4 mM). There was no difference in the production of the intracellular cytokine TNF-α by macrophages between $TLR9^{-/-}$ B6 mice and $TLR9^{fl/fl}$ LysCre B6 mice [Figure 6.9].

6.2.3. IL-6 produced by macrophages

Following NH_4-Ac stimulation (4 mM), there was a significant increase in the intracellular cytokine IL-6 produced by macrophages in $TLR9^{fl/fl}$ B6 mice compared to controls (NH_4-Ac untreated) ($p<0.0001$); there was no difference in the intracellular cytokine IL-6 produced by macrophages in $TLR9^{fl/fl}$ LysCre B6 mice compared to controls. There was however a significant decrease in the intracellular cytokine IL-6 produced by macrophages in $TLR9^{fl/fl}$ LysCre B6 mice compared to $TLR9^{fl/fl}$ B6 mice ($p<0.0001$) following NH_4-Ac stimulation (4 mM) [Figure 6.10].

When compared between three groups, the intracellular cytokine IL-6 produced by macrophages was significantly decreased in $TLR9^{-/-}$ B6 mice (n=7) ($p<0.0001$) and $TLR9^{fl/fl}$ LysCre B6 mice (n=10) ($p<0.0001$) compared to WT-B6 mice (n=5) following NH_4-Ac stimulation (4 mM). There was no difference in the production of the intracellular cytokine IFN-γ by macrophages between $TLR9^{-/-}$ B6 mice and $TLR9^{fl/fl}$ LysCre B6 mice [Figure 6.11].

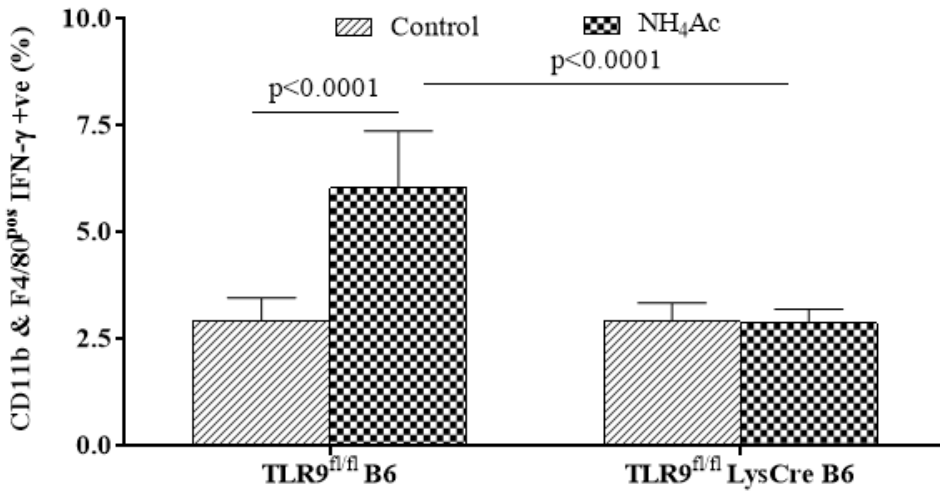

Figure 6.6: IFN-γ production by macrophages in TLR9$^{fl/fl}$ B6 mice and TLR9$^{fl/fl}$ LysCre B6 mice splenocytes following NH_4-Ac stimulation.

The intracellular cytokine IFN-γ produced by splenic macrophages was significantly increased in TLR9$^{fl/fl}$ B6 mice following NH_4-Ac stimulation (4 mM) compared to controls ($p<0.0001$) [mean difference: 3.1; 95% C.I.: 2 to 4.2] (normal data). There was no difference in IFN-γ produced by splenic macrophages in TLR9$^{fl/fl}$ LysCre B6 mice following NH_4-Ac stimulation (4 mM) compared to controls [mean difference: -0.04; 95% C.I.: -0.4 to 0.3] (normal data), but it was significantly decreased compared to TLR9$^{fl/fl}$ B6 mice ($p<0.0001$) [mean difference: –3.1; 95% C.I.: -4.1 to -2.2] (normal data). [TLR9$^{fl/fl}$ B6 mice (n=13) & controls (n=9); TLR9$^{fl/fl}$ LysCre B6 mice (n=8) & controls (n=10)]. Normality assumptions were checked and the data are expressed as mean with S.D.; $p<0.05$ were considered statistically significant. Student t-test was used to analyse the difference between parametric data sets.

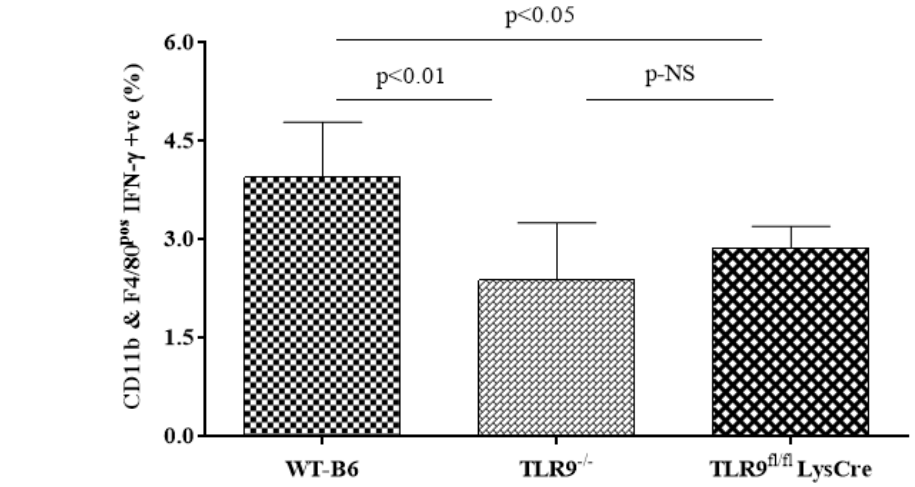

(A)

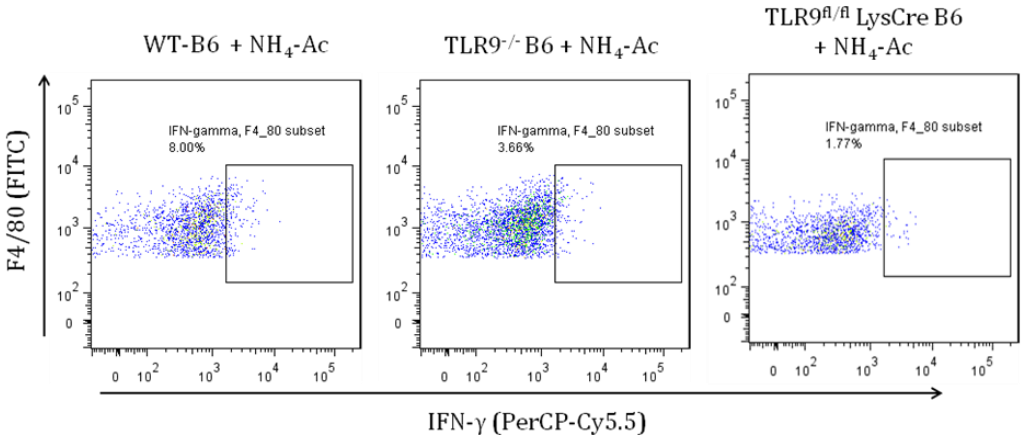

(B)

Figure 6.7: IFN-γ production by macrophages in WT-B6 mice, TLR9$^{-/-}$ B6 mice and TLR9$^{fl/fl}$ LysCre B6 mice following NH_4-Ac stimulation.

Following NH_4-Ac stimulation (4 mM), there was a significant decrease in the IFN-γ production by macrophages in TLR9$^{-/-}$ B6 mice ($p<0.01$) [mean difference: -1.5; 95% C.I.: -2.6 to -0.6] and TLR9$^{fl/fl}$ LysCre B6 mice ($p<0.05$) [mean difference: -1.1; 95% C.I.: -2 to -0.12] compared to WT-B6 mice. There was no difference between TLR9$^{fl/fl}$ LysCre B6 mice compared to TLR9$^{-/-}$ B6 mice [mean difference: 0.5; 95% C.I.: -0.3 to 1.3]. [WT-B6 mice (n=5); TLR9$^{-/-}$ B6 mice (n=7) and TLR9$^{fl/fl}$ LysCre B6 mice (n=9)] (normal data). Normality assumptions were checked and the data are expressed as mean with S.D.; $p<0.05$ were considered statistically significant. One-way ANOVA with Tukey's multiple comparisons test was used to analyse the differences between parametric data. (A) Graph and (B) FACS plots representing each group.

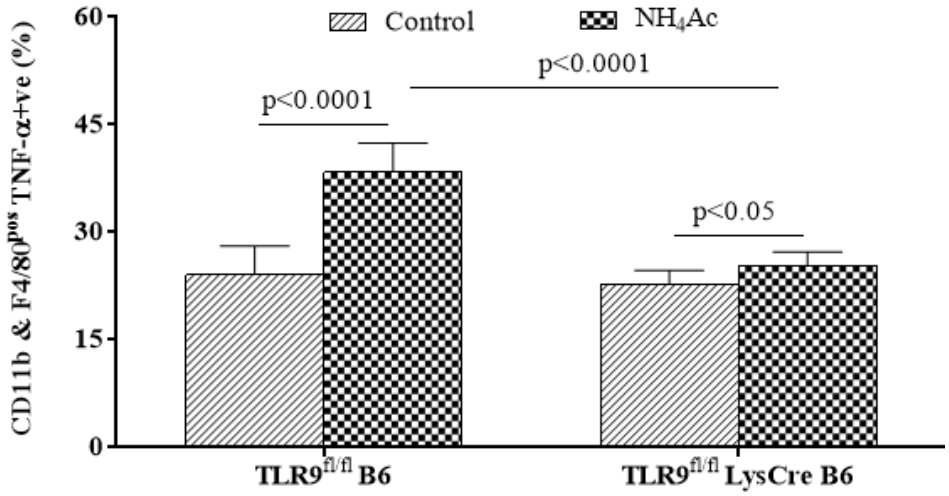

Figure 6.8: TNF-α production by macrophages in TLR9$^{fl/fl}$ B6 mice and TLR9$^{fl/fl}$ LysCre B6 mice following NH_4-Ac stimulation.

The intracellular cytokine TNF-α produced by splenic macrophages was significantly increased in TLR9$^{fl/fl}$ B6 mice following NH_4-Ac stimulation (4 mM) compared to controls ($p<0.0001$) [mean difference: 14.3; 95% C.I.: 10.2 to 18.3] (normal data). There was a significant increase in the TNF-α produced by splenic macrophages in TLR9$^{fl/fl}$ LysCre B6 mice following NH_4-Ac stimulation (4 mM) compared to controls ($p<0.05$) [median difference: 2.9; 95% C.I.: 0.5 to 4.5] (normal data), but it was significantly decreased compared to TLR9$^{fl/fl}$ B6 mice ($p<0.0001$) [mean difference: –13; 95% C.I.: -16.3 to -9.7] (normal data). [TLR9$^{fl/fl}$ B6 mice (n=13) & controls (n=9); TLR9$^{fl/fl}$ LysCre B6 mice (n=8) & controls (n=10)]. Normality assumptions were checked and the data are expressed as mean with S.D.; $p<0.05$ were considered statistically significant. Student t-test was used to analyse the difference between parametric data sets.

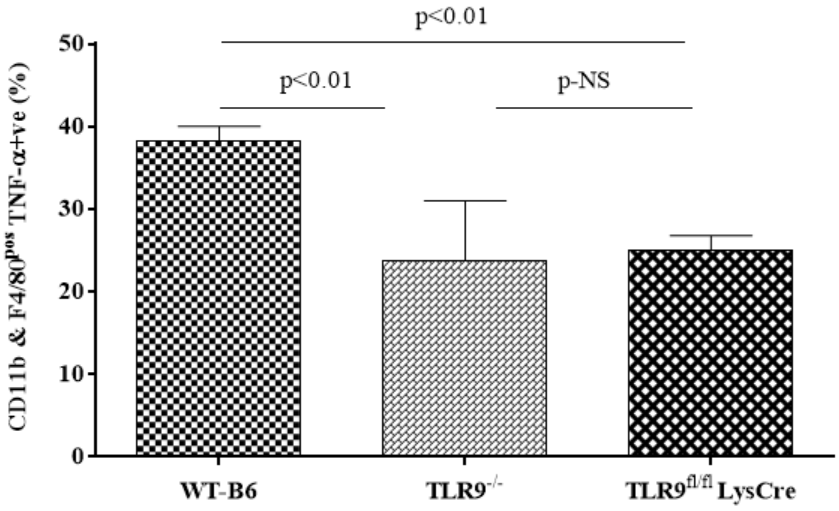

(A)

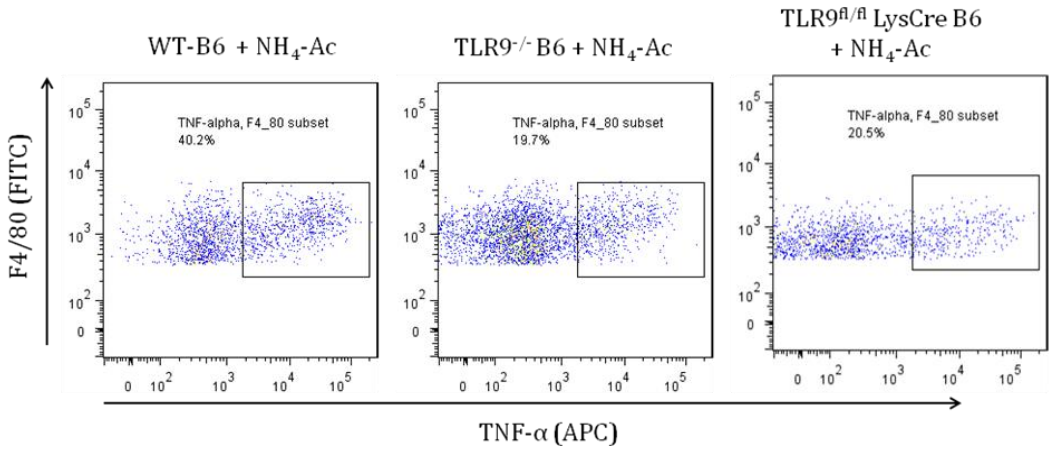

(B)

Figure 6.9: TNF-α production by macrophages in WT-B6 mice, TLR9$^{-/-}$ B6 mice and TLR9$^{fl/fl}$ LysCre B6 mice following NH_4-Ac stimulation.

Following NH_4-Ac stimulation (4 mM), there was a significant decrease in the TNF-α production by macrophages in TLR9$^{-/-}$ B6 mice ($p<0.01$) [median difference: -15.9; 95% C.I.: -20.6 to -9.3] and TLR9$^{fl/fl}$ LysCre B6 mice ($p<0.01$) [median difference: -13.5; 95% C.I.: -15 to -10.8] compared to WT-B6 mice. There was no difference between TLR9$^{fl/fl}$ LysCre B6 mice compared to TLR9$^{-/-}$ B6 mice [median difference: 3.7; 95% C.I.: -4.4 to 6.9]. [WT-B6 mice (n=5); TLR9$^{-/-}$ B6 mice (n=7) and TLR9$^{fl/fl}$ LysCre B6 mice (n=9)] (non-normal data). Normality assumptions were checked and the data are expressed as mean with S.D.; $p<0.05$ were considered statistically significant. Kruskal-Wallis with Dunn's multiple comparisons test was used to analyse the differences between non-parametric data sets. (A) Graph and (B) FACS plots representing each group.

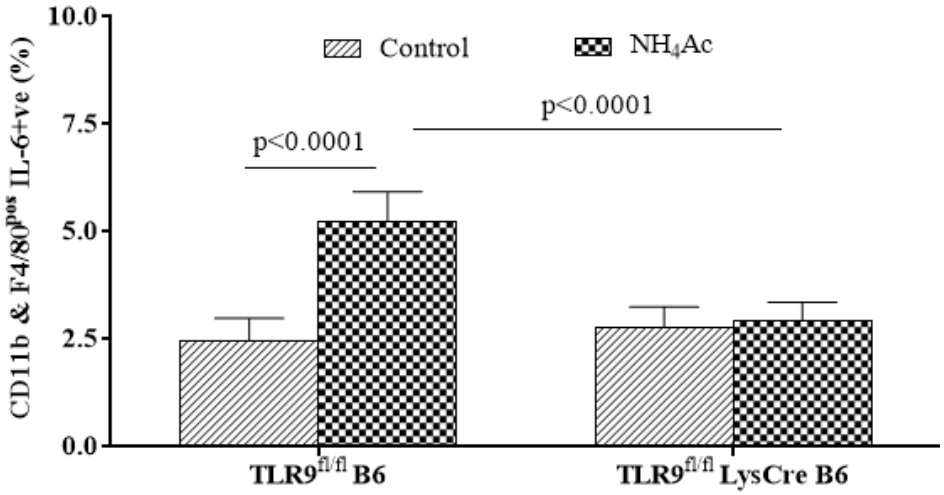

Figure 6.10: IL-6 production by macrophages in TLR9$^{fl/fl}$ B6 mice and TLR9$^{fl/fl}$ LysCre B6 mice splenocytes following NH_4-Ac stimulation.

The intracellular cytokine IL-6 produced by splenic macrophages was significantly increased in TLR9$^{fl/fl}$ B6 mice following NH_4-Ac stimulation (4 mM) compared to controls ($p<0.0001$) [mean difference: 2.7; 95% C.I.: 2.2 to 3.4] (normal data). There was no difference in the IL-6 produced by splenic macrophages in TLR9$^{fl/fl}$ LysCre B6 mice following NH_4-Ac stimulation (4 mM) compared to controls [mean difference: 0.17; 95% C.I.: -0.25 to 0.6] (normal data), but it was significantly decreased compared to TLR9$^{fl/fl}$ B6 mice ($p<0.0001$) [mean difference: –2.3; 95% C.I.: -2.8 to -1.8] (normal data). [TLR9$^{fl/fl}$ B6 mice (n=13) & controls (n=9); TLR9$^{fl/fl}$ LysCre B6 mice (n=8) & controls (n=10)]. Normality assumptions were checked and the data are expressed as mean with S.D.; $p<0.05$ were considered statistically significant. Student t-test was used to analyse the difference between parametric data sets.

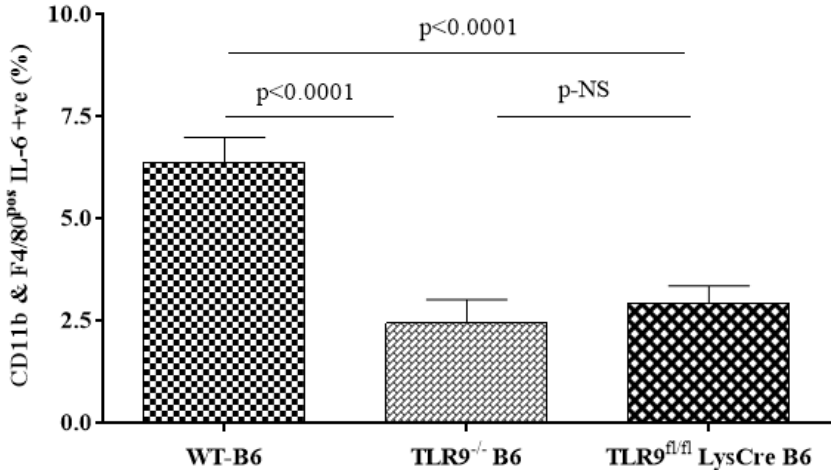

(A)

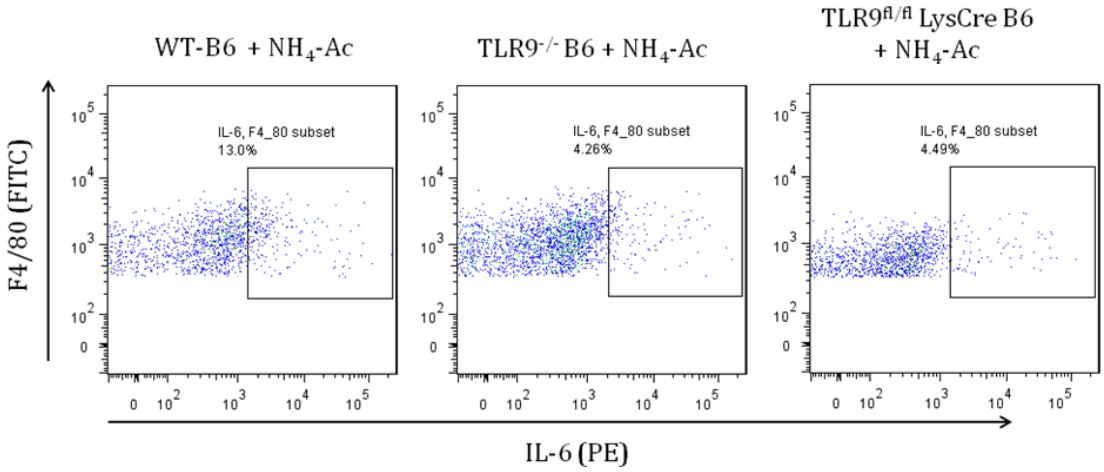

(B)

Figure 6.11: IL-6 production by macrophages in WT-B6 mice, TLR9$^{-/-}$ B6 mice and TLR9$^{fl/fl}$ LysCre B6 mice following NH_4-Ac stimulation.

Following NH_4-Ac stimulation (4 mM), there was a significant decrease in the IL-6 production by macrophages in TLR9$^{-/-}$ B6 mice ($p<0.0001$) [mean difference: -4; 95% C.I.: -4.7 to -3.2] and TLR9$^{fl/fl}$ LysCre B6 mice ($p<0.0001$) [mean difference: -3.5; 95% C.I.: -4.1 to -2.7] compared to WT-B6 mice. There was no difference between TLR9$^{fl/fl}$ LysCre B6 mice compared to TLR9$^{-/-}$ B6 mice [mean difference: 0.5; 95% C.I.: -0.13 to 1.1]. [WT-B6 mice (n=5); TLR9$^{-/-}$ B6 mice (n=7) and TLR9$^{fl/fl}$ LysCre B6 mice (n=9)] (normal data). Normality assumptions were checked and the data are expressed as mean with S.D.; $p<0.05$ were considered statistically significant. One-way ANOVA with Tukey's multiple comparisons test was used to analyse the differences between parametric data sets. (A) Graph and (B) FACS plots representing each group.

6.3. Ammonia-induced T cell dysfunction was independent of TLR9 expressed on neutrophils and/or Kupffer cells

To determine whether TLR9 expression on neutrophils and Kupffer cells influenced the ammonia-induced inflammatory response, the differences in the intracellular cytokine production of T cells in $TLR9^{fl/fl}$ B6 mice (n=13) and $TLR9^{fl/fl}$ LysCre B6 mice (n=9) was determined six hours after a single low dose of NH_4-Ac administration (I.P., 4 mM) and compared to controls (untreated) [$TLR9^{fl/fl}$ B6 mice (n=8) and $TLR9^{fl/fl}$ LysCre B6 mice (n=10)] (Method-2).

Intracellular cytokine production by T cells

Following NH_4-Ac stimulation (4 mM), there was a significant increase in the production of the intracellular cytokines (IFN-γ, TNF-α and IL-6) by $CD4^{pos}$ T cells and $CD8^{pos}$ T cells in $TLR9^{fl/fl}$ B6 mice compared to controls (NH_4-Ac untreated) ($p<0.0001$). In contrast, there was a significant increase in the production of the intracellular cytokines (IFN-γ, TNF-α and IL-6) by $CD4^{pos}$ T cells and $CD8^{pos}$ T cells in $TLR9^{fl/fl}$ LysCre B6 mice compared to controls ($p<0.0001$). There was no difference in the production of the intracellular cytokines (IFN-γ, TNF-α and IL-6) by $CD4^{pos}$ T cells and $CD8^{pos}$ T cells in $TLR9^{fl/fl}$ LysCre B6 mice compared to $TLR9^{fl/fl}$ B6 mice following NH_4-Ac stimulation (4 mM) [data not shown].

When compared between three groups, the production of the intracellular cytokines (IFN-γ, TNF-α and IL-6) by $CD4^{pos}$ T cells and $CD8^{pos}$ T cells was significantly decreased in $TLR9^{-/-}$ B6 mice (n=10) compared to WT-B6 mice (n=11) ($p<0.05$) and $TLR9^{fl/fl}$ LysCre B6 mice (n=7) ($p<0.01$) following NH_4-Ac stimulation (4 mM). There was no difference in the production of the intracellular cytokines (IFN-γ, TNF-α and IL-6) by $CD4^{pos}$ T cells

and $CD8^{pos}$ T cells between WT-B6 mice and $TLR9^{fl/fl}$ LysCre B6 mice [Figures 6.12 and 6.13].

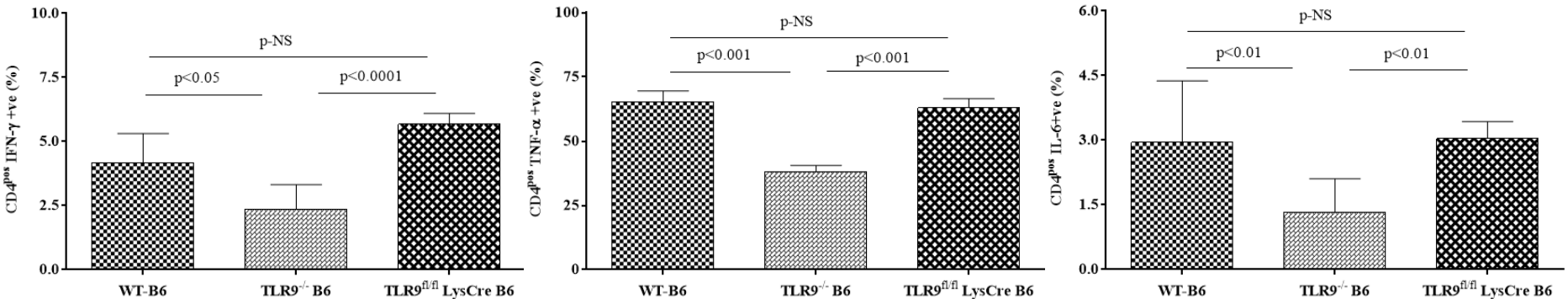

Figure 6.12: Intracellular cytokine production by $CD4^{pos}$ T cells in WT-B6 mice, $TLR9^{-/-}$ B6 mice and $TLR9^{fl/fl}$ LysCre B6 mice following NH_4-Ac stimulation.

Following NH_4-Ac stimulation (4 mM), the production of the intracellular cytokines (IFN-γ, TNF-α and IL-6) by $CD4^{pos}$ T cells in $TLR9^{-/-}$ B6 mice was significantly decreased compared to WT-B6 mice ($p<0.05$) and $TLR9^{fl/fl}$ LysCre B6 mice ($p<0.01$). There was no difference in the production of the intracellular cytokines (IFN-γ, TNF-α and IL-6) by $CD4^{pos}$ T cells of WT-B6 mice and $TLR9^{fl/fl}$ LysCre B6 mice. Normality assumptions were checked and the data are expressed as mean with S.D.; $p<0.05$ were considered statistically significant. One-way ANOVA with Tukey's multiple comparisons test was used to analyse the differences between parametric data sets and Kruskal-Wallis with Dunn's multiple comparisons test was used to analyse the differences between non-parametric data sets.

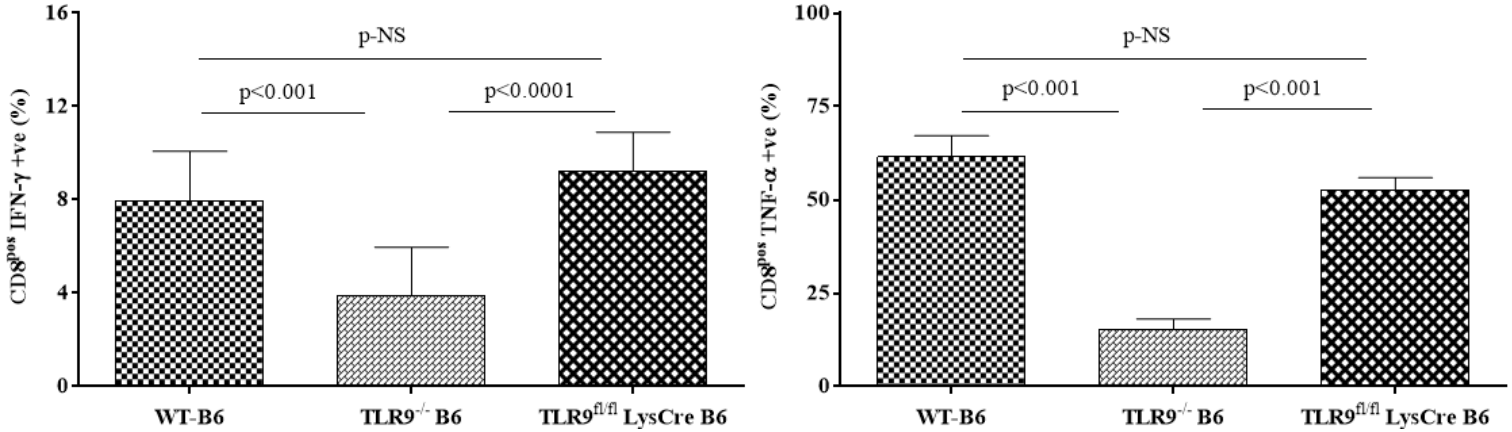

Figure 6.13: Intracellular cytokine production by $CD8^{pos}$ T cells in WT-B6 mice, $TLR9^{-/-}$ B6 mice and $TLR9^{fl/fl}$ LysCre B6 mice following NH_4-Ac stimulation.

Following NH_4-Ac stimulation (4 mM), the production of the intracellular cytokines (IFN-γ, TNF-α and IL-6) by $CD8^{pos}$ T cells in $TLR9^{-/-}$ B6 mice was significantly decreased compared to WT-B6 mice ($p<0.001$) and $TLR9^{fl/fl}$ LysCre B6 mice ($p<0.001$). There was no difference in the production of the intracellular cytokines (IFN-γ, TNF-α and IL-6) by $CD8^{pos}$ T cells of WT-B6 mice and $TLR9^{fl/fl}$ LysCre B6 mice. Normality assumptions were checked and the data are expressed as mean with S.D.; $p<0.05$ were considered statistically significant. One-way ANOVA with Tukey's multiple comparisons test was used to analyse the differences between parametric data sets and Kruskal-Wallis with Dunn's multiple comparisons test was used to analyse the differences between non-parametric data sets.

6.4. Ammonia-induced NK cell dysfunction was independent of TLR9 expressed on neutrophils and/or Kupffer cells

To determine whether TLR9 expressed on neutrophils and Kupffer cells influenced the ammonia-induced inflammation, the differences in the phenotype of NK cells in $TLR9^{fl/fl}$ B6 mice (n=13) and $TLR9^{fl/fl}$ LysCre B6 mice (n=9) was determined six hours after a single low dose of NH_4-Ac administration (I.P., 4 mM) and compared to controls (untreated) [$TLR9^{fl/fl}$ B6 mice (n=8) and $TLR9^{fl/fl}$ LysCre B6 mice (n=10)] (Method-2).

Intracellular cytokine production by NK cells

Following NH_4-Ac stimulation (4 mM), there was a significant increase in the KLRG-1^{pos} NK cells in $TLR9^{fl/fl}$ B6 mice compared to controls (NH_4-Ac untreated) ($p<0.01$); there was also a significant increase in the KLRG-1^{pos} NK cells in $TLR9^{fl/fl}$ LysCre B6 mice compared to controls ($p<0.01$). There was no difference however in the KLRG-1^{pos} NK cells in $TLR9^{fl/fl}$ LysCre B6 mice compared to $TLR9^{fl/fl}$ B6 mice following NH_4-Ac stimulation (4 mM) [data not shown].

When compared between three groups, the frequency of KLRG-1^{pos} NK cells was significantly decreased in $TLR9^{-/-}$ B6 mice (n=10) compared to WT-B6 mice (n=11) ($p<0.0001$) and $TLR9^{fl/fl}$ LysCre B6 mice (n=7) ($p<0.01$) following NH_4-Ac stimulation (4 mM). There was also a significant decrease in the frequency of KLRG-1^{pos} NK cells in $TLR9^{fl/fl}$ LysCre B6 mice compared to WT-B6 mice ($p<0.01$) [Figure 6.14].

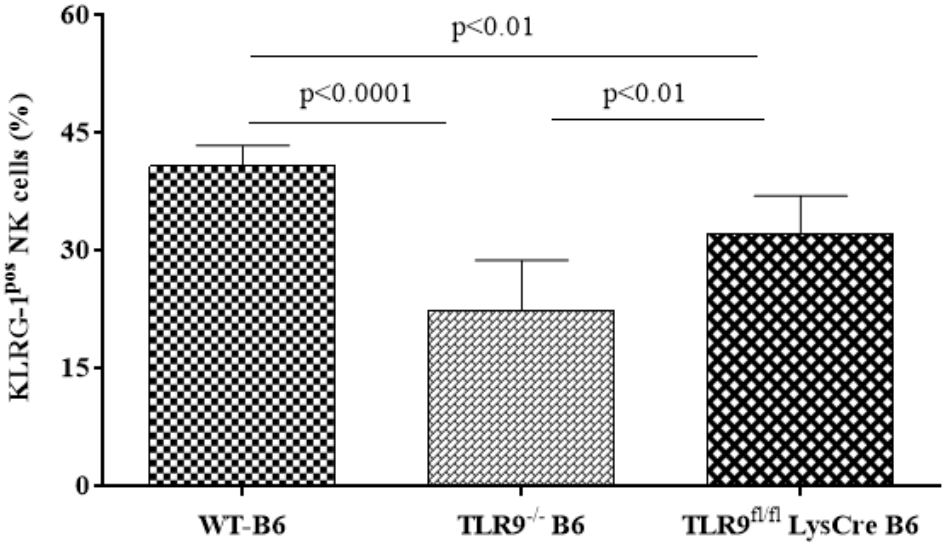

Figure 6.14: KLRG-1^{pos} NK cells in WT-B6 mice, TLR9$^{-/-}$ B6 mice and TLR9$^{fl/fl}$ LysCre B6 mice following NH_4-Ac stimulation.

Following NH_4-Ac stimulation (4 mM), the frequency of KLRG-1^{pos} NK cells in TLR9$^{-/-}$ B6 mice was significantly decreased compared to WT-B6 mice ($p<0.0001$) and TLR9$^{fl/fl}$ LysCre B6 mice ($p<0.01$). There was also a significant decrease in the frequency of KLRG-1^{pos} NK cells in TLR9$^{fl/fl}$ LysCre B6 mice compared to WT-B6 mice ($p<0.01$). Normality assumptions were checked and the data are expressed as mean with S.D.; $p<0.05$ were considered statistically significant. One-way ANOVA with Tukey's multiple comparisons test was used to analyse the differences between parametric data sets and Kruskal-Wallis with Dunn's multiple comparisons test was used to analyse the differences between non-parametric data sets.

6.5. Summary

In this chapter the most important finding is that there was decreased cytokine production from macrophages and a reduction in liver bodyweight ratio and brain water content in $TLR9^{fl/fl}$ LysCre B6 mice following NH_4-Ac stimulation; and surprisingly, they exhibited no difference compared to $TLR9^{-/-}$ B6 mice.

Macrophages are liver resident Kupffer cells and infiltrating monocytes, and are one of the important proinflammatory cell subsets that were induced by ammonia stimulation. Neutrophil function although seemingly unaffected by ammonia in mice has been reported to be abnormal in hyperammonemic conditions in rats [140] and ALF patients [139]. Although neutrophils have a definitive role in amplifying the liver injury in paracetamol and cholestasis mice models [106, 107, 209, 210], the phenotype and function of neutrophils in normal mice has not been characterised so far. Thus neutrophils may behave differently in mice and humans in response to ammonia. Moreover the ratio of neutrophils in mice is reduced compared to the humans [199].

In this study, deletion of TLR9 in Kupffer cells and neutrophils reduced macrophage-induced inflammation and prevented an increase in brain water content following ammonia stimulation indicating that TLR9 expressed in those cells plays an important role in sensing the DNA released by the hepatocytes in the circulation. Marques et al recently demonstrated that neutrophils are the key innate immune cells, but not the Kupffer cells, that sense DNA through the TLR9/NF-κB pathway and induce proinflammation in paracetamol toxicity [107]. These data are well supported by the strong correlation demonstrated between neutrophil TLR9, ammonia and IL-8 in PALF and the abrogation of neutrophil TLR9 upregulation and cytokine production to PALF

plasma by DNAse-I. Taken together these data suggest that although neutrophil function remains unaffected by ammonia in this mouse model, neutrophils may still play an important role in the development of brain oedema as suggested by the human PALF study by sensing DNA released by ammonia and the necrotic liver mediated through TLR9. The downstream consequences of neutrophil TLR9 activation then results in the recruitment of other adaptive immune cell sub-sets, to produce a pro-inflammatory milieu. However, this postulated mechanism can only be tested in the future by depleting the neutrophils in normal mice and performing adoptive transfer.

Chapter 7. General discussion

Hypothesis 1: Circulating neutrophil TLR9 expression is increased in PALF patients with advanced hepatic encephalopathy and SIRS resulting from the release of necrotic hepatocyte products, ammonia, DNA and IL-8 into the circulation [Chapter 3].

The importance of neutrophil TLR9 expression in human PALF has been demonstrated by characterising neutrophil phenotype and function, although the role of neutrophils in the development of liver injury and importance of TLR4 and -9 have been previously studied extensively in paracetamol-induced murine models. *Ex-vivo* studies revealing robust correlations demonstrate that ammonia and IL-8 synergistically upregulate neutrophil TLR9 and induce systemic inflammation. Incubation of healthy neutrophils with and without DNAse-I demonstrates that necrotic hepatocyte products upregulate neutrophil TLR9 expression. Moreover, following stimulation with various stimuli and undertaking further functional studies it has been demonstrated that neutrophil function varied in PALF. Neutrophils were pre-primed in patients with low SIRS scores and HE grade, but exhausted in patients with high SIRS scores and advanced HE. Taken together these data demonstrate that circulating neutrophil TLR9 expression is increased in PALF as a result of necrotic hepatocyte products released in the circulation and thereby induces systemic inflammation and advanced coma grades .

Hypothesis 2: TLR9 is central in the development of ammonia-induced cerebral oedema [Chapters 4 and 5].

Brain water content, a measure of brain oedema was increased in WT-B6 mice six hours following stimulation with NH_4-Ac (4mM). The importance of TLR9 in the development of ammonia-induced brain oedema was demonstrated by the observation that any

increase in ammonia-induced brain water content could be abrogated using a mouse model deficient of TLR9 or by inhibiting TLR9 using the antagonist ODN2035.

Hypothesis 3: Ammonia induces inflammation by activating neutrophils and adaptive immune cell sub-sets through a TLR9-mediated mechanism [chapters 3, 4 and 5].

In the human PALF study, *ex-vivo* stimulation with NH_4Cl resulted in the upregulation of TLR9 and cytokine production in neutrophils in HC and PALF patients. In the animal study, intraperitoneal injection of NH_4-Ac resulted in the upregulation of pro-inflammatory cytokine production by T cells, NK cells and macrophages which was abrogated in mice deficient of TLR9 or by inhibiting TLR9 using the antagonist ODN2035. Taken together these results indicate that ammonia induces inflammation by activating circulating neutrophils and adaptive immune cells through a TLR9 mediated mechanism.

Hypothesis 4: Activation of TLR9 is a DNA dependent mechanism [Chapters 3 and 4].

In the human study, TLR9 and intracellular IL-8 expression was upregulated in healthy neutrophils following the exposure to PALF plasma, which could be decreased when the plasma was pre-treated with DNAse-I. In the animal study, total DNA was increased in the plasma samples of WT-B6 mice and $TLR9^{-/-}$ B6 mice following NH_4-Ac stimulation but not after Na-Ac stimulation indicating that ammonia influenced the release of DNA into the circulation in both the groups. Taken together these results indicate that ammonia activates TLR9 through a DNA dependent mechanism.

In this thesis, a novel link between ammonia-induced inflammation and the subsequent development of hepatic encephalopathy in PALF mediated by neutrophil TLR9 activation has been demonstrated using two different models, human and mouse. In patients with PALF, a strong correlation between neutrophil TLR9 expression and ammonia and IL-8 was observed with the highest values of neutrophil TLR9 expression and IL-8 production observed in PALF patients with severe SIRS and advanced HE. Moreover, it was observed that necrotic by products such as ammonia, IL-8 and DNA released into the circulation upregulate neutrophil TLR9 expression in PALF. In the mouse model, a low dose of ammonia induced systemic inflammation and subsequent brain oedema through a TLR9-mediated mechanism in a DNA dependent manner with the importance of TLR9 being unequivocally demonstrated by using antagonists and genetically modified mice. In concordance with the human study, neutrophil and/or Kupffer cell TLR9 expression played an important role in inducing brain oedema and this was observed in the mouse model by deleting the TLR9 gene only in lysozyme expressing cells. Furthermore, the improved survival following a high dose of ammonia in the absence of TLR9 demonstrates the central role of TLR9 in the pathophysiology of ammonia-induced death. In addition to the existing literature base that demonstrates the importance of TLR9 in binding to DNA and inducing inflammation in PALF, I have demonstrated that TLR9 also plays an important role in the development of brain oedema in PALF [106-108].

This novel observation that activation of TLR9 by ammonia induces systemic inflammation and subsequently leads to the development of brain oedema is well supported by recently published studies that show TLR9 induces inflammation in paracetamol overdose and non-alcoholic steatohepatitis [108, 211]. This study further

expands our understanding of the role of TLR9 in liver failure by demonstrating that it plays an important role in the development of brain oedema. It has been already been established that pre-treatment with ammonia and then incubation with a mixture of pro-inflammatory cytokines exacerbates astrocyte swelling through the NF-κB pathway [191]. Furthermore, it has been demonstrated that mitochondrial permeability transition induces astrocyte swelling when cultured astrocytes were exposed to ammonia [212, 213] or a mixture of cytokines IFN-γ, TNF-α, IL-6 and IL-1β [214]. Consistent with these published findings, increased cytokine production and brain water content in response to ammonia stimulation were observed in the animal study. The abrogation of cytokine production and protection against the development of brain oedema following administration of a specific TLR9 antagonist and in mice deficient of TLR9 indicates that TLR9 has an important role in the development of HE. This finding also supports the observation that increased cerebral hyperemia and systemic inflammation are responsible for inducing ICH [215].

In this study, TLR9 has been shown to have a central role in the development of brain oedema in HE. It has also been previously reported that reduced astrocyte swelling can be seen in TLR4 silenced brain endothelium exposed to ammonia, cytokines and LPS [180] and an increase in brain water content can be prevented following the administration of a TLR4 antagonist or in mice deficient of TLR4 in paracetamol hepatotoxicity [165] implicating TLR4 as also playing a major role in the development of brain oedema. In spite of these data, the mechanism behind the activation of TLR4 remains unclear in the pathogenesis of HE. The observation of decreased circulating neutrophil TLR4 expression in PALF in the context of no detectable systemic endotoxin in my human study suggests that neutrophil TLR4 does not play as significant a role as TLR9 in the

development of systemic inflammation or HE in PALF. These findings are corroborated by the animal study as neutrophil TLR4 expression was showing a trend towards downregulation during the optimization of ammonia in contrast to the upregulation of TLR9. The observation of increased necrotic byproducts such as high mobility group box – 1 (HMGB-1), a ligand of TLR4, in paracetamol overdose [216] and its role in the activation of TLR4 and guiding the neutrophils towards the liver [217] supports my postulation that TLR4 is not responsible for the ammonia-induced inflammation and subsequent brain oedema, rather other factors could be responsible for the activation of TLR4.

Another important point to consider would be the route by which paracetamol is administered in human and mouse. In an animal model of paracetamol overdose, it has been demonstrated that oral administration of paracetamol developed clinical features similar to that of humans, but those administered paracetamol through the intraperitoneal route developed respiratory distress which was associated with a reduction in the arterial partial pressure of oxygen [218]. These findings taken together suggest that the route of administration plays an important role in determining the mechanism by which paracetamol causes acute liver injury and subsequent development of multiple organ failure in those animals.

In this study, deletion of TLR9 in Kupffer cells and neutrophils abrogated the inflammation induced by macrophages and increase in brain water content following ammonia stimulation. The decrease in the liver weight, brain water content and macrophage cytokine production after ammonia stimulation in $TLR9^{fl/fl}$ LysCre mice indicates that Kupffer cells and neutrophils sense the DNA induced by ammonia via a TLR9 mediated pathway. Recently it has been demonstrated that neutrophils, but not Kupffer cells, mainly sense the DNA through the TLR9 and NF-κB pathways in

paracetamol toxicity [107] supporting my earlier finding in human PALF that ammonia, IL-8 and DNA upregulate neutrophil TLR9 expression, induce inflammation and exacerbate the severity of hepatic encephalopathy. Although neutrophil function remains unaffected by ammonia in the mouse model, it has been demonstrated that ammonia impairs neutrophil phagocytosis and increases the production of ROS in patients with liver cirrhosis [140]. Furthermore, it has been demonstrated that neutrophil TLR9 collaborates with chemokines and mitochondrial products to amplify the liver injury and systemic inflammation in paracetamol toxicity [106]. These data taken together with the human study suggest that neutrophils may still play an important role in the development of brain oedema by sensing DNA released by ammonia and the necrotic liver mediated through TLR9. The downstream signalling of neutrophil TLR9 activation then results in the recruitment of other adaptive immune cell sub-sets, which then leads to the production of pro-inflammatory cytokines. However, this postulated mechanism can only be tested in the future by performing an adoptive transfer in neutrophil depleted mice.

It has been previously reported that acetylation induces inflammation in acute alcoholic hepatitis [192] and the toxicity of ammonium salts was due to the rise in blood pH and alkalinization was responsible for the transfer of ammonium gas across the blood brain barrier [71, 72]. Since the pH of mice is different compared to humans, infusion of fluids might affect the buffer reserve in the system. In the animal study, stimulation with 4 mM of Na-Ac did not alter the cytokine production of the immune cells or change the water content in the brain. Furthermore, the volume of NH_4-Ac injected in this experiment was less than 5% of the total volume of blood. Taken together these results suggest that

inflammation and brain oedema was not influenced by acetate or change in the pH and this effect was solely induced by ammonia.

This study for the first time demonstrates the central role of innate immunity as a driver of acute ammonia toxicity. When TLR9 gets activated by DNA, pro-inflammatory cytokines are produced by a number of innate immune cell sub-sets [158] and this normally takes about 5 hours. In a model of paracetamol hepatotoxicity, after sensing the DNA through TLR9, neutrophil infiltration was increased in the DNA-rich areas of the necrotic liver 6 hours after the administration of paracetamol and increased the production of proinflammatory cytokines [107]. Based on these findings it can be assumed that ammonia-induced systemic inflammation within 5 hours and the subsequent development of brain oedema occurred shortly thereafter. This concept is supported by the acute ammonia toxicity model, where it has been demonstrated that animals develop brain oedema within minutes rather than hours [73]. Taken together with the optimisation experiments, these results indicate that ammonia induces systemic inflammation and brain oedema within a span of 6 hours.

The compensatory anti-inflammatory response syndrome (CARS) is a pattern of immunological responses that are responsible for deactivation of an over-exuberant SIRS restoring homeostasis [219]. It has been previously reported that early changes in the anti-inflammatory cytokine IL-10 can predict outcomes thereby highlighting the importance of CARS in the pathophysiology of PALF [220]. In this study, although the production of the anti-inflammatory cytokine, IL-10 was observed in PALF patients, the levels of the pro-inflammatory cytokines, IL-6 and IL-8 were markedly increased in comparison.

Conclusion

Ammonia plays a central role in the pathogenesis of HE and brain oedema in ALF, with up to 25% of patients developing ICH and succumbing to brain herniation [32, 33, 51, 62]. Infection and systemic inflammation are common in ALF, drive the development of HE and are major prognosticators [37, 38]. Experimental models have unequivocally associated ammonia exposure with astrocyte swelling in the brain, an important finding of ALF, where ammonia is converted to glutamine and exerts an osmotic effect and induces oedema [47, 49, 191]. This study provides new insights into ammonia, inflammation and brain oedema in PALF. In the animal study, I have demonstrated that ammonia-induced brain oedema is mediated through TLR9, dependent on DNA and is driven by the innate immune system. These findings taken along with the important observations in the human study that neutrophil TLR9 expression in PALF is mediated both by circulating endogenous DNA as well as ammonia and IL-8 in a synergistic manner inducing systemic inflammation and exacerbating HE implies that neutrophil TLR9 plays an important role in the development of HE. These data are well supported by the recently published observation that DNA deposition within the hepatocytes triggers inflammation in PALF through neutrophil TLR9 [107]. The amelioration of brain oedema and cytokine production by ODN2088 supports exploration of TLR9 antagonism as a therapeutic modality in early ALF to prevent the progression to advanced stages of HE and the development of ICH.

Chapter 8. Drawbacks and perspectives for the future

In this thesis, the role that TLR9 plays in the development of ammonia-induced inflammation and HE in the context of PALF has been explored. The importance of the role of ammonia has been highlighted previously with respect to both inflammation and on brain swelling through its detoxification in the astrocyte, the cell most often associated with the pathogenesis of HE. This thesis still represents just the tip of the iceberg in terms of understanding the mechanisms involved in the pathogenesis of HE, however it was not possible for me to answer or demonstrate certain aspects due to the limitations of time and funding inherent in undertaking a PhD. Therefore I will summarise the drawbacks and briefly outline the future directions of travel for this study on which I look forward to continuing to work on over the coming years.

One of the most important observations in this thesis is the role of TLR9 in the development of brain oedema following ammonia challenge, with astrocyte swelling most often associated with HE and quantified by measuring the brain water content. The observation of astrocyte swelling under an electron microscope remains the best method in terms of analysing it qualitatively. However this was not possible in the animal study due to the restriction in funding. Alternatively, immunofluorescence was tried on the brain sections by staining them for TLR9 expressed by astrocytes. This was not successful since most of the commercially available TLR9 antibodies were raised from mouse and had high background when they were tested on my samples. The availability of TLR9 antibodies raised from other species, which are reactive with mouse and could be used for immunohistochemistry/immunofluorescence, were limited. The mouse-on-mouse protocol provided by Abcam, for which the Fc region of the antigen was blocked, also yielded negative results.

Future studies which could include immunohistochemistry and electron microscopy techniques with specific labels to detect astrocytes, TLR9 and other brain organelles such as mitochondria in WT-B6 mice and TLR9$^{-/-}$ B6 mice brain sections would allow the investigation of TLR9 expressed within those cells and the effect of ammonia on brain energy metabolism.

The influence of gut bacteria on TLR9 and the ammonia-induced inflammation and subsequent brain oedema has not yet been examined. It is well established that TLR9 has ligands to bacterial DNA [158] and intestinal bacteria produce ammonia by splitting urea and other amino acids [77], while PAG present in the enterocytes of germ-free mice breaks down glutamine to produce ammonia [78]. Furthermore, it has also been observed that engineering the gut microbes decreased the urease activity, thereby reducing the morbidity and mortality in a murine model of hepatic injury [81]. Therefore it can also be argued/postulated that the ammonia produced by the intestines along with the injected ammonia could have exacerbated the inflammation and brain oedema.

Future studies involving the alteration of gut microbiota by inoculation of bacteria and/or treatment with antibiotics would allow investigation of the influence intestinal bacteria have on ammonia and TLR9. In fact, I have also measured the cytokine production from mesenteric lymph nodes and Peyer's patches and have stored the gut flush samples of all the mice studied. Analysis of these samples in the future with RNAseq would allow me to determine the influence of gut bacteria on ammonia and TLR9.

Neutrophil TLR9 expression has been shown to play an important role in inducing brain oedema in this study. Future studies involving neutrophil depletion and adoptive

transfer of neutrophils from TLR9$^{-/-}$ B6 mice to WT-B6 mice and vice versa would allow us to investigate the role of neutrophils in ammonia-induced inflammation. Furthermore, inflammasomes such as Nalp3 and Caspase-1, along with TLR9 induce pro-inflammation. Therefore future studies involving mouse models deficient of these inflammasomes would allow us to identify whether they are involved and essential in this process.

In this thesis it has been shown that neutrophils are the key innate cells that amplify the acute liver injury and induce inflammation and brain oedema. However, the mechanism by which neutrophils interplay with the adaptive immune cells and induce systemic inflammation is unknown. NK cells promote the activation and recruitment of macrophages and T cells to the injury site thereby inducing inflammation. Preliminary experiments on PALF samples in our lab indicate that NK cells become effector cells and produce cytokines on interaction with activated neutrophils. Therefore further studies in PALF patients that could involve co-culture of neutrophils with effector T cells in the presence and absence of NK cells, along with methods or molecules that can inhibit the interaction of neutrophils with lymphocytes would allow us to investigate the mechanism behind the activation of the adaptive immune system and also identify whether NK cells serve as the bridging cells between the innate and adaptive immune systems.

Another main drawback to the human study is that we were only first able to analyze plasma arterial ammonia and IL-8 concentrations on day 1 of the ICU admission. We therefore were unable to determine how these variables might influence neutrophil TLR9 expression and the severity of SIRS and HE during the early onset of PALF preceding ICU admission. Furthermore, we were unable to interrogate how neutrophil

TLR9 expression and intracellular cytokine production in response to LPS, ammonia or oligodinucleotides related to the eventual development (or not) of sepsis due to the limited number of patients that could be studied and due to the fact that the sickest patients with advanced HE were transplanted early on during their admission, died before transplantation could be performed or underwent plasmapheresis.

References

1. Chapman RW, J.D. C, Hayes PC. Liver and biliary tract disease. In: Boon A.N. et al (20th edition) Davidson's Principles & Practice of Medicine. Churchill Livingstone India. 2006:p.935-98.

2. Jungermann K, Katz N. Metabolism of Carbohydrates. In: Thurman RG, Kauffman FC, Jungermann K, editors. Regulation of Hepatic Metabolism: Intra- and Intercellular Compartmentation. Boston, MA: Springer US; 1986. p. 211-35.

3. Billing BH, Lathe GH. Bilirubin metabolism in jaundice. The American Journal of Medicine. 1958;24(1):111-21.

4. Forrest JA, Clements J, Prescott L. Clinical pharmacokinetics of paracetamol. Clinical pharmacokinetics. 1982;7(2):93-107.

5. Fauci AS. Harrison's principles of internal medicine: McGraw-Hill, Medical Publishing Division; 2008.

6. Walker BR, Colledge NR. Davidson's principles and practice of medicine: Elsevier Health Sciences; 2013.

7. Adapted from Dr Debbie Shawcross's presentation slides. 2013.

8. Adapted from Dr Ragai Mitry's presentation. 2015.

9. Adapted from Dr Debbie Shawcross's presentation. 2012.

10. Trey C, Davidson CS. The management of fulminant hepatic failure. Prog Liver Dis. 1970;3::282-98.

11. O'Grady JG. Acute liver failure. Postgraduate Medical Journal. 2005;81(953):148-54.

12. Bernal W, Wendon J. Acute liver failure. New England Journal of Medicine. 2013;369(26):2525-34.

13. Bernal W, Auzinger G, Dhawan A, Wendon J. Acute liver failure. The Lancet. 2010;376(9736):190-201.

14. Ostapowicz G, Fontana RJ, Schiødt FV, Larson A, Davern TJ, Han SHB, McCashland TM, Shakil AO, Hay JE, Hynan L, Crippin JS, Blei AT, Samuel G, Reisch J, Lee WM. Results of a Prospective Study of Acute Liver Failure at 17 Tertiary Care Centers in the United States. Annals of Internal Medicine. 2002;137(12):947-54.

15. Larson AM, Polson J, Fontana RJ, Davern TJ, Lalani E, Hynan LS, Reisch JS, Schiødt FV, Ostapowicz G, Shakil AO. Acetaminophen-induced acute liver failure: results of a United States multicenter, prospective study. Hepatology. 2005;42(6):1364-72.

16. Bernal W, Auzinger G, Wendon J. Prognostic utility of the bilirubin lactate and etiology score. Clinical gastroenterology and hepatology. 2009;7(2):249.

17. Hawton K, Simkin S, Deeks J, Cooper J, Johnston A, Waters K, Arundel M, Bernal W, Gunson B, Hudson M. UK legislation on analgesic packs: before and after study of long term effect on poisonings. Bmj. 2004;329(7474):1076.

18. Bernal W, editor Changing patterns of causation and the use of transplantation in the United kingdom. Seminars in liver disease; 2003.

19. Sheen CL, Dillon JF, Bateman DN, Simpson KJ, MacDonald TM. Paracetamol pack size restriction: the impact on paracetamol poisoning and the over-the-counter supply of paracetamol, aspirin and ibuprofen. Pharmacoepidemiology and drug safety. 2002;11(4):329-31.

20. Moynihan R. FDA fails to reduce accessibility of paracetamol despite 450 deaths a year: confidential documents from the US Food and Drug Administration suggest that the agency has avoided a debate on tough new measures to reduce overdoses from painkillers--to avoid offending the pharmaceutical industry.(News). British Medical Journal. 2002;325(7366):678-9.

21. Dart RC, Bailey E. Does therapeutic use of acetaminophen cause acute liver failure? Pharmacotherapy. 2007;27(9):1219-30.

22. Whitcomb DC, Block GD. Association of acetaminophen hepatotoxicity with fasting and ethanol use. Jama. 1994;272(23):1845-50.

23. Zimmerman HJ, Maddrey WC. Acetaminophen (paracetamol) hepatotoxicity with regular intake of alcohol: analysis of instances of therapeutic misadventure. Hepatology. 1995;22(3):767-73.

24. Maddrey WC. Hepatic effects of acetaminophen. Enhanced toxicity in alcoholics. Journal of clinical gastroenterology. 1987;9(2):180-5.

25. Benson GD, Koff RS, Tolman KG. The Therapeutic Use of Acetaminophen in Patients with Liver Disease. American Journal of Therapeutics. 2005;12(2):133-41.

26. Manyike PT, Kharasch ED, Kalhorn TF, Slattery JT. Contribution of CYP2E1 and CYP3A to acetaminophen reactive metabolite formation. Clinical Pharmacology & Therapeutics. 2000;67(3):275-82.

27. Mitchell J, Jollow D, Potter W, Davis D, Gillette J, Brodie B. Acetaminophen-induced hepatic necrosis. I. Role of drug metabolism. Journal of Pharmacology and Experimental Therapeutics. 1973;187(1):185-94.

28. Villeneuve J, Raymond G, Bruneau J, Colpron L, Pomier-Layrargues G. [Pharmacokinetics and metabolism of acetaminophen in normal, alcoholic and cirrhotic subjects]. Gastroenterologie clinique et biologique. 1983;7(11):898-902.

29. Pessayre D, Larrey D. Drug-induced liver injury. In: Rhodes J. et al (3rd edition) Textbook of Hepatology From Basic Science to Clinical Practice. Blackwell Publishing Limited. 2007;2:p. 1211-68.

30. Mitchell JR, Thorgeirsson SS, Potter WZ, Jollow D, Keiser H. Acetaminophen-induced hepatic injury: protective role of glutathione in man and rationale for therapy. Clinical pharmacology and therapeutics. 1974;16(4):676-84.

31. O'Riordan A, Brummell Z, Sizer E, Auzinger G, Heaton N, O'Grady JG, Bernal W, Hendry BM, Wendon JA. Acute kidney injury in patients admitted to a liver intensive therapy unit with paracetamol-induced hepatotoxicity. Nephrology, dialysis, transplantation : official publication of the European Dialysis and Transplant Association - European Renal Association. 2011;26(11):3501-8.

32. Butterworth RF. Pathogenesis of Hepatic Encephalopathy and Brain Edema in Acute Liver Failure. Journal of Clinical and Experimental Hepatology. 2015;5, Supplement 1:S96-S103.

33. Bernal W, Hall C, Karvellas CJ, Auzinger G, Sizer E, Wendon J. Arterial ammonia and clinical risk factors for encephalopathy and intracranial hypertension in acute liver failure. Hepatology. 2007;46(6):1844-52.

34. Larsen FS, editor Cerebral circulation in liver failure: Ohm's law in force. Seminars in liver disease; 1996: © 1996 by Thieme Medical Publishers, Inc.

35. Bernal W, Wendon J. Acute liver failure. N Engl J Med. 2013;369(26):2525-34.

36. Bone RC, Balk RA, Cerra FB, Dellinger RP, Fein AM, Knaus WA, Schein RM, Sibbald WJ. Definitions for sepsis and organ failure and guidelines for the use of innovative therapies in sepsis. The ACCP/SCCM Consensus Conference Committee. American College of Chest Physicians/Society of Critical Care Medicine. CHEST Journal. 1992;101(6):1644-55.

37. Vaquero J, Polson J, Chung C, Helenowski I, Schiodt FV, Reisch J, Lee WM, Blei AT. Infection and the progression of hepatic encephalopathy in acute liver failure. Gastroenterology. 2003;125(3):755-64.

38. Rolando N, Wade J, Davalos M, Wendon J, Philpott-Howard J, Williams R. The systemic inflammatory response syndrome in acute liver failure. Hepatology. 2000;32(4):734-9.

39. Jalan R, Damink SWO, Hayes PC, Deutz NE, Lee A. Pathogenesis of intracranial hypertension in acute liver failure: inflammation, ammonia and cerebral blood flow. Journal of hepatology. 2004;41(4):613-20.

40. Butterworth RF. Hepatic encephalopathy: a central neuroinflammatory disorder? Hepatology. 2011;53(4):1372-6.

41. Butterworth RF. Pathogenesis of hepatic encephalopathy: new insights from neuroimaging and molecular studies. Journal of Hepatology. 2003;39(2):278-85.

42. Conn HOL. The hepatic coma syndromes and lactulose. 1979.

43. Hahn M, Massen O, Nencki M, Pawlow J. Die Eck'sche Fistel zwischen der unteren Hohlvene und der Pfortader und ihre Folgen für den Organismus. Archiv für experimentelle Pathologie und Pharmakologie. 1893;32(3):161-210.

44. Nance FC, Kaufman HJ, Kline DG. Role of urea in the hyperammonemia of germ-free Eck fistula dogs. Gastroenterology. 1974;66(1):108-12.

45. Nencki M, Pawlow JP, Zaleski J. Ueber den Ammoniakgehalt des Blutes und der Organe und die Harnstoffbildung bei den Säugethieren. Archiv für experimentelle Pathologie und Pharmakologie. 1895;37(1):26-51.

46. Szerb JC, Butterworth RF. Effect of ammonium ions on synaptic transmission in the mammalian central nervous system. Progress in neurobiology. 1992;39(2):135-53.

47. Kato M, Hughes RD, Keays RT, Williams R. Electron microscopic study of brain capillaries in cerebral edema from fulminant hepatic failure. Hepatology. 1992;15(6):1060-6.

48. Norenberg M. Hepatic encephalopathy: studies with astrocyte cultures. The Biochemical Pathology of Astrocytes New York: Alan R Liss. 1988:451-64.

49. Shawcross D, Jalan R. The pathophysiologic basis of hepatic encephalopathy: central role for ammonia and inflammation. Cell Mol Life Sci. 2005;62(19-20):2295-304.

50. Olde Damink SWM, Deutz NEP, Dejong CHC, Soeters PB, Jalan R. Interorgan ammonia metabolism in liver failure. Neurochemistry International. 2002;41(2–3):177-88.

51. Clemmesen JO, Larsen FS, Kondrup J, Hansen BA, Ott P. Cerebral herniation in patients with acute liver failure is correlated with arterial ammonia concentration. Hepatology. 1999;29(3):648-53.

52. Butterworth RF. Pathophysiology of Hepatic Encephalopathy: A New Look at Ammonia. Metab Brain Dis. 2002;17(4):221-7.

53. Cooper AJ, Plum F. Biochemistry and physiology of brain ammonia. Physiological Reviews. 1987;67(2):440-519.

54. Vasudevan DM, Sreekumari S, Vaidhyanathan K. General Amino Acid metabolism (Urea cycle, One Carbon Metabolism). In: Vasudevan et al's (6th edition) Textbook of Biochemistry for Medical Students. Jaypee Brothers Medical Publishers (P) Ltd, India. 2011:p.170-82.

55. Munro HN. Mammalian protein metabolism: Elsevier; 2012.

56. van Hall G, van der Vusse GJ, Söderlund K, Wagenmakers AJ. Deamination of amino acids as a source for ammonia production in human skeletal muscle during prolonged exercise. The Journal of Physiology. 1995;489(Pt 1):251-61.

57. Lowenstein JM. Ammonia production in muscle and other tissues: the purine nucleotide cycle. Physiological Reviews. 1972;52(2):382-414.

58. Holmes FL, editor Hans Krebs and the discovery of the ornithine cycle. Federation proceedings; 1980.

59. Krebs HA. The discovery of the ornithine cycle of urea synthesis. Trends in Biochemical Sciences. 1982;7(2):76-8.

60. Burcham PC, Harman AW. Mitochondrial dysfunction in paracetamol hepatotoxicity: In vitro studies in isolated mouse hepatocytes. Toxicology Letters. 1990;50(1):37-48.

61. Traeger H, Gabzuda S, Ballou A, Davidson C. Blood ammonia concentration in liver disease and liver coma. Metabolism. 1954;3:99-109.

62. Phear E, Sherlock S, Summerskill W. Blood ammonia levels in liver disease and hepatic coma. Lancet. 1955;7:836-40.

63. Zwingmann C, Chatauret N, Leibfritz D, Butterworth RF. Selective increase of brain lactate synthesis in experimental acute liver failure: Results of a [1H-13C] nuclear magnetic resonance study. Hepatology. 2003;37(2):420-8.

64. Lai JC, Cooper AJ. Brian alpha-ketoglutarate dehydrogenase complex: kinetic properties, regional distribution and effects of inhibitors. J Neurochem. 1986;47(5):1376-86.

65. Hindfelt B, Plum F, Duffy T. Effect of acute ammonia intoxication on cerebral metabolism in rats with portacaval shunts. J Clin invest. 1977;59(3):386-9.

66. Yao H, Sadoshima S, Fujii K, Kusuda K, Ishitsuka T, Tamaki K. Cerebrospinal fluid lactate in patients with hepatic encephalopathy. Eur Neurol. 1987;27(3):182-7.

67. Desjardins P, Bélanger M, Butterworth RF. Alterations in expression of genes coding for key astrocytic proteins in acute liver failure. Journal of Neuroscience Research. 2001;66(5):967-71.

68. Rama Rao KV, Chen M, Simard JM, Norenberg MD. Increased aquaporin-4 expression in ammonia-treated cultured astrocytes. Neuroreport. 2003;14(18):2379-82.

69. Larsen FS, Strauss G, Møller K, Hansen BA. Regional cerebral blood flow autoregulation in patients with fulminant hepatic failure. Liver Transplantation. 2000;6(6):795-800.

70. Kato M, Hughes R, Keays R, Williams R. Electron microscopic studies of brain capillaries in cerebral oedema from fulminant hepatic failure. Hepatology. 1992;15:1060-6.

71. Warren KS. DIFFERENTIAL TOXICITY OF AMMONIUM SALTS. J Clin Invest. 1958;37(4):497-501.

72. Warren KS, Nathan DG. The Passage of Ammonia Across the Blood-Brain-Barrier and its Relation to Blood pH. J Clin Invest. 1958;37(12):1724-8.

73. Marcaida G, Felipo V, Hermenegildo C, Miñana M-D, Grisolia S. Acute ammonia toxicity is mediated by the NMDA type of glutamate receptors. FEBS letters. 1992;296(1):67-8.

74. Kosenko E, Kaminsky Y, Grau E, Miñana M-D, Marcaida G, Grisolía S, Felipo V. Brain ATP Depletion Induced by Acute Ammonia Intoxication in Rats Is Mediated by Activation of the NMDA Receptor and Na+, K+-ATPase. Journal of Neurochemistry. 1994;63(6):2172-8.

75. Kosenko E, Kaminsky Y, Lopata O, Muravyov N, Kaminsky A, Hermenegildo C, Felipo V. Nitroarginine, an Inhibitor of Nitric Oxide Synthase, Prevents Changes in Superoxide Radical and Antioxidant Enzymes Induced by Ammonia Intoxication. Metab Brain Dis. 1998;13(1):29-41.

76. Kosenko E, Kaminski Y, Lopata O, Muravyov N, Felipo V. Blocking NMDA receptors prevents the oxidative stress induced by acute ammonia intoxication. Free Radical Biology and Medicine. 1999;26(11):1369-74.

77. Windmueller HG. Glutamine utilization by the small intestine. Adv Enzymol Relat Areas Mol Biol. 1982;53(201):37.

78. Floch MH, Katz J, Conn HO. Qualitative and quantitative relationships of the fecal flora in cirrhotic patients with portal systemic encephalopathy and following portacaval anastomosis. Gastroenterology. 1970;59(1):70-5.

79. Riordan SM, Williams R. Treatment of hepatic encephalopathy. New England Journal of Medicine. 1997;337(7):473-9.

80. Saudubray J, Narcy C, Lyonnet L, Bonnefont J, Munnich A. Clinical approach to inherited metabolic disorders in neonates. Neonatology. 1990;58(Suppl. 1):44-53.

81. Shen T-CD, Albenberg L, Bittinger K, Chehoud C, Chen Y-Y, Judge CA, Chau L, Ni J, Sheng M, Lin A, Wilkins BJ, Buza EL, Lewis JD, Daikhin Y, Nissim I, Yudkoff M, Bushman FD, Wu GD. Engineering the gut microbiota to treat hyperammonemia. The Journal of Clinical Investigation. 2015;125(7):2841-50.

82. Dejong CH, Deutz NE, Soeters PB. Intestinal glutamine and ammonia metabolism during chronic hyperammonaemia induced by liver insufficiency. Gut. 1993;34(8):1112-9.

83. Dejong CH, Deutz NE, Soeters PB. Renal ammonia and glutamine metabolism during liver insufficiency-induced hyperammonemia in the rat. J Clin Invest. 1993;92(6):2834-40.

84. McCarty JH. Cell biology of the neurovascular unit: implications for drug delivery across the blood-brain barrier. Assay and drug development technologies. 2005;3(1):89-95.

85. Scott TR, Kronsten VT, Hughes RD, Shawcross DL. Pathophysiology of cerebral oedema in acute liver failure. World J Gastroenterol. 2013;19(48):9240-55.

86. Rangroo Thrane V, Thrane AS, Wang F, Cotrina ML, Smith NA, Chen M, Xu Q, Kang N, Fujita T, Nagelhus EA, Nedergaard M. Ammonia triggers neuronal disinhibition and seizures by impairing astrocyte potassium buffering. Nat Med. 2013;19(12):1643-8.

87. Shawcross DL, Wendon JA. The neurological manifestations of acute liver failure. Neurochemistry International. 2012;60(7):662-71.

88. Albrecht J, Norenberg MD. Glutamine: a Trojan horse in ammonia neurotoxicity. Hepatology. 2006;44(4):788-94.

89. Butterworth RF. Glutamate transporters in hyperammonemia. Neurochemistry International. 2002;41(2–3):81-5.

90. Strange K. Regulation of solute and water balance and cell volume in the central nervous system. Journal of the American Society of Nephrology : JASN. 1992;3(1):12-27.

91. Shawcross DL, Balata S, Olde Damink SWM, Hayes PC, Wardlaw J, Marshall I, Deutz NEP, Williams R, Jalan R. Low myo-inositol and high glutamine levels in brain are associated with neuropsychological deterioration after induced hyperammonemia. American Journal of Physiology - Gastrointestinal and Liver Physiology. 2004;287(3):G503.

92. Bluml S, Zuckerman E, Tan J, Ross BD. Proton-decoupled 31P magnetic resonance spectroscopy reveals osmotic and metabolic disturbances in human hepatic encephalopathy. J Neurochem. 1998;71(4):1564-76.

93. Häussinger D, Laubenberger J, Vom Dahl S, Ernst T, Bayer S, Langer M, Gerok W, Hennig J. Proton magnetic resonance spectroscopy studies on human brain Myo-inositol

in hypo-osmolarity and hepatic encephalopathy. Gastroenterology. 1994;107(5):1475-80.

94. Butterworth RF. Taurine in Hepatic Encephalopathy. In: Huxtable RJ, Azuma J, Kuriyama K, Nakagawa M, Baba A, editors. Taurine 2: Basic and Clinical Aspects. Boston, MA: Springer US; 1996. p. 601-6.

95. Rosen HM, Yoshimura N, Hodgman JM, Fischer JE. Plasma amino acid patterns in hepatic encephalopathy of differing etiology. Gastroenterology. 1977;72(3):483-7.

96. Record CO, Buxton B, Chase RA, Curzon G, Murray-Lyon IM, Williams R. Plasma and brain amino acids in fulminant hepatic failure and their relationship to hepatic encephalopathy. European journal of clinical investigation. 1976;6(5):387-94.

97. de Vries HE, Blom-Roosemalen MC, van Oosten M, de Boer AG, van Berkel TJ, Breimer DD, Kuiper J. The influence of cytokines on the integrity of the blood-brain barrier in vitro. Journal of neuroimmunology. 1996;64(1):37-43.

98. Falsig J, Latta M, Leist M. Defined inflammatory states in astrocyte cultures: Correlation with susceptibility towards CD95-driven apoptosis. Journal of neurochemistry. 2004;88(1):181-93.

99. Didier N, Romero IA, Creminon C, Wijkhuisen A, Grassi J, Mabondzo A. Secretion of interleukin-1β by astrocytes mediates endothelin-1 and tumour necrosis factor-α effects on human brain microvascular endothelial cell permeability. Journal of neurochemistry. 2003;86(1):246-54.

100. Olson JK, Miller SD. Microglia Initiate Central Nervous System Innate and Adaptive Immune Responses through Multiple TLRs. The Journal of Immunology. 2004;173(6):3916.

101. Andersson AK, Rönnbäck L, Hansson E. Lactate induces tumour necrosis factor-α, interleukin-6 and interleukin-1β release in microglial-and astroglial-enriched primary cultures. Journal of neurochemistry. 2005;93(5):1327-33.

102. Sen S, Rose C, Ytrebo LM, Davies NA, Nedredal GI, Drevland SS, Kjonno M, Williams R, Butterworth RF, Revhaug A. Albumin dialysis reduces brain water and intracranial pressure in acute liver failure: a randomised controlled study in a pig model. Hepatology. 2003;38:540.

103. Wright G, Shawcross D, Olde Damink SWM, Jalan R. Brain cytokine flux in acute liver failure and its relationship with intracranial hypertension. Metab Brain Dis. 2007;22(3):375-88.

104. Vale J, Proudfoot A. Paracetamol (acetaminophen) poisoning. The Lancet. 1995;346(8974):547-52.

105. Schiødt FV, Bondesen S, Tygstrup N, Christensen E. Prediction of hepatic encephalopathy in paracetamol overdose: a prospective and validated study. Scandinavian journal of gastroenterology. 1999;34(7):723-8.

106. Marques PE, Amaral SS, Pires DA, Nogueira LL, Soriani FM, Lima BHF, Lopes GAO, Russo RC, Ávila TV, Melgaço JG, Oliveira AG, Pinto MA, Lima CX, De Paula AM, Cara DC, Leite MF, Teixeira MM, Menezes GB. Chemokines and mitochondrial products activate

neutrophils to amplify organ injury during mouse acute liver failure. Hepatology. 2012;56(5):1971-82.

107. Marques PE, Oliveira AG, Pereira RV, David BA, Gomides LF, Saraiva AM, Pires DA, Novaes JT, Patricio DO, Cisalpino D, Menezes-Garcia Z, Leevy WM, Chapman SE, Mahecha GA, Marques RE, Guabiraba R, Martins VP, Souza DG, Mansur DS, Teixeira MM, Leite MF, Menezes GB. Hepatic DNA deposition drives drug-induced liver injury and inflammation in mice. Hepatology. 2014:n/a-n/a.

108. Imaeda AB, Watanabe A, Sohail MA, Mahmood S, Mohamadnejad M, Sutterwala FS, Flavell RA, Mehal WZ. Acetaminophen-induced hepatotoxicity in mice is dependent on Tlr9 and the Nalp3 inflammasome. The Journal of Clinical Investigation. 2009;119(2):305-14.

109. Larsen FS, Schmidt LE, Bernsmeier C, Rasmussen A, Isoniemi H, Patel VC, Triantafyllou E, Bernal W, Auzinger G, Shawcross D. High-volume plasma exchange in patients with acute liver failure: An open randomised controlled trial. Journal of hepatology. 2016;64(1):69-78.

110. Clemmesen JO, Kondrup J, Nielsen LB, Larsen FS, Ott P. Effects of high-volume plasmapheresis on ammonia, urea, and amino acids in patients with acute liver failure. Am J Gastroenterol. 2001;96(4):1217-23.

111. **Schenker S**, **Warren KS**. **Effect of temperature variation on toxicity and metabolism of ammonia in mice**. **The Journal of Laboratory and Clinical Medicine**. **1962**;**60**(**2**):**291-301**.

112. Córdoba J, Crespin J, Gottstein J, Blei AT. Mild hypothermia modifies ammonia-induced brain edema in rats after portacaval anastomosis. Gastroenterology. 1999;116(3):686-93.

113. Jalan R, Davies NA, Olde Damink SWM. Hypothermia for the Management of Intracranial Hypertension in Acute Liver Failure. Metab Brain Dis. 2002;17(4):437-44.

114. Vaquero J, Bélanger M, James L, Herrero R, Desjardins P, Côté J, Blei AT, Butterworth RF. Mild Hypothermia Attenuates Liver Injury and Improves Survival in Mice With Acetaminophen Toxicity. Gastroenterology. 2007;132(1):372-83.

115. Jalan R, Olde Damink SW, Deutz NE, Hayes PC, Lee A. Restoration of cerebral blood flow autoregulation and reactivity to carbon dioxide in acute liver failure by moderate hypothermia. Hepatology. 2001;34(1):50-4.

116. Jalan R, Damink SWO, Deutz NE, Davies NA, Garden OJ, Madhavan KK, Hayes PC, Lee A. Moderate hypothermia prevents cerebral hyperemia and increase in intracranial pressure in patients undergoing liver transplantation for acute liver failure. Transplantation. 2003;75(12):2034-9.

117. Bernal W, Murphy N, Brown S, Whitehouse T, Bjerring PN, Hauerberg J, Frederiksen HJ, Auzinger G, Wendon J, Larsen FS. A multicentre randomized controlled trial of moderate hypothermia to prevent intracranial hypertension in acute liver failure. Journal of Hepatology. 2016.

118. Murphy KM. Janeway's immunobiology: Garland Science; 2011.

119. Johnson RM, Brown EJ. Innate (General or Nonspecific) Host Defense Mechanisms. In: Mandell G. et al (5th edition) Mandell, Douglas, and Bennett's Principles and Practice of Infectious Diseases. churchill Livingstone Philadelphia. 2000;1:p.112-44.

120. Dieffenbach CW, Tramont EC. Innate (General or Nonspecific) Host Defense Mechanisms. In: Mandell G. et al (6th edition) Mandell, Douglas, and Bennett's Principles and Practice of Infectious Diseases. Churchill Livingstone Philadelphia. 2005;1:p.34-41.

121. http://faculty.ccbcmd.edu/courses/bio141/lecguide/unit4/innate/bloodcells.html. online. Accessed on 27th July 2011. 2011.

122. Tramont EC, Hoover DL. Innate (General or Nonspecific) Host Defense Mechanisms. In: Mandell G. et al (5th edition) Mandell, Douglas, and Bennett's Principles and Practice of Infectious Diseases. churchill Livingstone Philadelphia. 2000;1:p.31-8.

123. Tayal V, Kalra BS. Cytokines and anti-cytokines as therapeutics — An update. European Journal of Pharmacology. 2008;579(1–3):1-12.

124. Dinarello CA. Proinflammatory cytokines. Chest. 2000;118(2):503-8.

125. Opal SM, DePalo VA. Anti-inflammatory cytokines. Chest. 2000;117(4):1162-72.

126. Guo H, Callaway JB, Ting JPY. Inflammasomes: mechanism of action, role in disease, and therapeutics. Nat Med. 2015;21(7):677-87.

127. http://people.eku.edu/ritchisong/301notes4b.html. Online. Accessed on 5th August 2011. 2011.

128. Lewis SM, Bain BJ, Bates I, Dacie JV. Dacie and Lewis practical haematology: Elsevier Health Sciences; 2006.

129. Witko-Sarsat V, Rieu P, Descamps-Latscha B, Lesavre P, Halbwachs-Mecarelli L. Neutrophils: Molecules, Functions and Pathophysiological Aspects. Lab Invest. 0000;80(5):617-53.

130. Pillay J, den Braber I, Vrisekoop N, Kwast LM, de Boer RJ, Borghans JAM, Tesselaar K, Koenderman L. In vivo labeling with 2H2O reveals a human neutrophil lifespan of 5.4 days. Blood. 2010;116(4):625-7.

131. Ravetech JV, Perussia B. Alternative membrane forms of FcyRIII(CD16) On Human Natural Killer Cells and Neutrophils Cell Type-Specific Expression of Two Genes That Differ in Single Nucleotide Substitutions. J ExpMed. 1989;170:481-97.

132. Solovjov DA, Pluskota E, Plow EF. Distinct Roles for the α and β Subunits in the Functions of Integrin αMβ2. Journal of Biological Chemistry. 2005;280(2):1336-45.

133. Segal AW. HOW NEUTROPHILS KILL MICROBES. Annual Review of Immunology. 2005;23(1):197-223.

134. Watts RG. Neutropenia. In: Greer. J.P. et al (12th edition) Wintrobe's Cllinical Hematology. Lippincott William & Wilkins, a Wolters Kluwer business, Philadelphia. 2009;2:p.1527-47.

135. Jaeschke H, Hasegawa T. Role of neutrophils in acute inflammatory liver injury. Liver international : official journal of the International Association for the Study of the Liver. 2006;26(8):912-9.

136. Damme JV, Decock B, Conings R, Lenaerts J-P, Opdenakker G, Billiau A. The chemotactic activity for granulocytes produced by virally infected fibroblasts is identical to monocyte-derived interleukin 8. European Journal of Immunology. 1989;19(7):1189-94.

137. Jaeschke H, Williams CD, Ramachandran A, Bajt ML. Acetaminophen hepatotoxicity and repair: the role of sterile inflammation and innate immunity. Liver International. 2012;32(1):8-20.

138. Liu ZX, Han D, Gunawan B, Kaplowitz N. Neutrophil depletion protects against murine acetaminophen hepatotoxicity. Hepatology. 2006;43(6):1220-30.

139. Taylor NJ, Nishtala A, Manakkat Vijay GK, Abeles RD, Auzinger G, Bernal W, Ma Y, Wendon JA, Shawcross DL. Circulating neutrophil dysfunction in acute liver failure. Hepatology. 2013;57(3):1142-52.

140. Shawcross DL, Wright GAK, Stadlbauer V, Hodges SJ, Davies NA, Wheeler-Jones C, Pitsillides AA, Jalan R. Ammonia impairs neutrophil phagocytic function in liver disease. Hepatology. 2008;48(4):1202-12.

141. Manakkat Vijay GK, Kronsten VT, Bain BJ, Shawcross DL. Neutrophil vacuolation in acetaminophen-induced acute liver failure. American Journal of Hematology. 2015:n/a-n/a.

142. Schwarz BA, Bhandoola A. Trafficking from the bone marrow to the thymus: a prerequisite for thymopoiesis. Immunological Reviews. 2006;209(1):47-57.

143. Ahmed R, Gray D. Immunological memory and protective immunity: understanding their relation. Science. 1996;272(5258):54-60.

144. Sanders ME, Makgoba MW, Shaw S. Human naive and memory T cells. Immunology Today. 1988;9(7):195-9.

145. Sakaguchi S, Yamaguchi T, Nomura T, Ono M. Regulatory T Cells and Immune Tolerance. Cell. 2008;133(5):775-87.

146. Medzhitov R. Toll-like receptors and innate immunity. Nat Rev Immunol. 2001;1(2):135-45.

147. Janeway CA, editor Approaching the asymptote? Evolution and revolution in immunology. Cold Spring Harbor symposia on quantitative biology; 1989: Cold Spring Harbor Laboratory Press.

148. Medzhitov R. Approaching the Asymptote: 20 Years Later. Immunity. 2009;30(6):766-75.

149. Braun A, Hoffmann JA, Meister M. Analysis of the Drosophila host defense in domino mutant larvae, which are devoid of hemocytes. Proceedings of the National Academy of Sciences. 1998;95(24):14337-42.

150. Medzhitov R, Preston-Hurlburt P, Janeway CA, Jr. A human homologue of the Drosophila Toll protein signals activation of adaptive immunity. Nature. 1997;388(6640):394-7.

151. Medzhitov R, Janeway CA, Jr. Innate immune induction of the adaptive immune response. Cold Spring Harbor symposia on quantitative biology. 1999;64:429-35.

152. Poltorak A, He X, Smirnova I, Liu M-Y, Van Huffel C, Du X, Birdwell D, Alejos E, Silva M, Galanos C. Defective LPS signaling in C3H/HeJ and C57BL/10ScCr mice: mutations in Tlr4 gene. Science. 1998;282(5396):2085-8.

153. Hayashi F, Means TK, Luster AD. Toll-like receptors stimulate human neutrophil function. Blood. 2003;102(7):2660-9.

154. Parker LC, Whyte MKB, Dower SK, Sabroe I. The expression and roles of Toll-like receptors in the biology of the human neutrophil. Journal of Leukocyte Biology. 2005;77(6):886-92.

155. Takeda K, Akira S. Toll-like receptors in innate immunity. International Immunology. 2005;17(1):1-14.

156. Underhill DM, Ozinsky A. Toll-like receptors: key mediators of microbe detection. Current Opinion in Immunology. 2002;14(1):103-10.

157. Medzhitov R. Toll-like receptors and innate immunity. Nat Rev Immunol. 2001;1(2):135-45.

158. Hemmi H, Takeuchi O, Kawai T, Kaisho T, Sato S, Sanjo H, Matsumoto M, Hoshino K, Wagner H, Takeda K, Akira S. A Toll-like receptor recognizes bacterial DNA. Nature. 2000;408(6813):740-5.

159. Tai N, Wong FS, Wen L. TLR9 deficiency promotes CD73 expression in T cells and diabetes protection in nonobese diabetic mice. The Journal of Immunology. 2013;191(6):2926-37.

160. Piccinini A, Midwood K. DAMPening inflammation by modulating TLR signalling. Mediators of inflammation. 2010;2010.

161. Prince LR, Whyte MK, Sabroe I, Parker LC. The role of TLRs in neutrophil activation. Current Opinion in Pharmacology. 2011;In Press, Corrected Proof.

162. Alvarez-Arellano L, Camorlinga-Ponce M, Maldonado-Bernal C, Torres J. Activation of human neutrophils with Helicobacter pylori and the role of Toll-like receptors 2 and 4 in the response. FEMS Immunology & Medical Microbiology. 2007;51(3):473-9.

163. Chen Y, Sun R. Toll-like receptors in acute liver injury and regeneration. International Immunopharmacology. 2011;In Press, Corrected Proof.

164. Yi A-K, Yoon H, Park J-E, Kim B-S, Kim HJ, Martinez-Hernandez A. CpG DNA-mediated Induction of Acute Liver Injury in d-Galactosamine-sensitized Mice. Journal of Biological Chemistry. 2006;281(21):15001-12.

165. Shah N, Montes de Oca M, Jover-Cobos M, Tanamoto K-i, Muroi M, Sugiyama K-i, Davies NA, Mookerjee RP, Dhar DK, Jalan R. Role of Toll-Like Receptor 4 in Mediating Multiorgan Dysfunction in Mice With Acetaminophen Induced Acute Liver Failure. Liver Transplantation. 2013;19(7):751-61.

166. Rama Rao K, Jayakumar A, Norenberg M. Brain edema in acute liver failure: mechanisms and concepts. Metab Brain Dis. 2014:1-10.

167. Williams R, Schalm SW, O'Grady JG. Acute liver failure: redefining the syndromes. The Lancet. 1993;342(8866):273-5.

168. Vincent JL, Moreno R, Takala J, Willatts S, Mendonça A, Bruining H, Reinhart CK, Suter PM, Thijs LG. The SOFA (Sepsis-related Organ Failure Assessment) score to describe organ dysfunction/failure. Intensive Care Med. 1996;22(7):707-10.

169. Knaus WA, Draper EA, Wagner DP, Zimmerman JE. Prognosis in acute organ-system failure. Annals of surgery. 1985;202(6):685-93.

170. Shawcross DL, Sharifi Y, Canavan JB, Yeoman AD, Abeles RD, Taylor NJ, Auzinger G, Bernal W, Wendon JA. Infection and systemic inflammation, not ammonia, are associated with Grade 3/4 hepatic encephalopathy, but not mortality in cirrhosis. Journal of Hepatology. 2011;54(4):640-9.

171. Brown M, Wittwer C. Flow Cytometry: Principles and Clinical Applications in Hematology. Clin Chem. 2000;46(8):1221-9.

172. Shapiro HM. Practical flow cytometry: John Wiley & Sons; 2005.

173. Paraskevas F. Clinical Flow Cytometry. In: Greer J.P. et al (12th edition) Wintrobe's Clinical Hematology. Lippincott William & Wilkins, a Wolters Kluwer business, Philadelphia. 2009;1:p.21-49.

174. O'Grady JG, Alexander GJ, Hayllar KM, Williams R. Early indicators of prognosis in fulminant hepatic failure. Gastroenterology. 1989;97(2):439-45.

175. Bernal W, Auzinger G, Sizer E, Wendon J. Intensive care management of acute liver failure. Seminars in liver disease. 2008;28(2):188-200.

176. Kamath PS, Wiesner RH, Malinchoc M, Kremers W, Therneau TM, Kosberg CL, D'Amico G, Dickson ER, Kim WR. A model to predict survival in patients with end-stage liver disease. Hepatology. 2001;33(2):464-70.

177. Li J, Ma Z, Tang Z-L, Stevens T, Pitt B, Li S. CpG DNA-mediated immune response in pulmonary endothelial cells. American Journal of Physiology - Lung Cellular and Molecular Physiology. 2004;287(3):L552-L8.

178. Kim JM, Kim NI, Oh Y-K, Kim Y-J, Youn J, Ahn M-J. CpG oligodeoxynucleotides induce IL-8 expression in CD34+ cells via mitogen-activated protein kinase-dependent and NF-κB-independent pathways. International Immunology. 2005;17(12):1525-31.

179. McGill MR, Sharpe MR, Williams CD, Taha M, Curry SC, Jaeschke H. The mechanism underlying acetaminophen-induced hepatotoxicity in humans and mice involves mitochondrial damage and nuclear DNA fragmentation. J Clin Invest. 2012;122(4):1574-83.

180. Jayakumar AR, Tong XY, Curtis KM, Ruiz-Cordero R, Abreu MT, Norenberg MD. Increased toll-like receptor 4 in cerebral endothelial cells contributes to the astrocyte swelling and brain edema in acute hepatic encephalopathy. Journal of Neurochemistry. 2014;128(6):890-903.

181. Rolando N, Harvey F, Brahm J, Philpott-Howard J, Alexander G, Gimson A, Casewell M, Fagan E, Williams R. Prospective study of bacterial infection in acute liver failure: An analysis of fifty patients. Hepatology. 1990;11(1):49-53.

182. Altstaedt J, Kirchner H, Rink L. Cytokine production of neutrophils is limited to interleukin-8. Immunology. 1996;89(4):563-8.

183. Hou HS, Liao CL, Sytwu HK, Liao NS, Huang TY, Hsieh TY, Chu HC. Deficiency of interleukin-15 enhances susceptibility to acetaminophen-induced liver injury in mice. PloS one. 2012;7(9):e44880.

184. Ferret PJ, Hammoud R, Tulliez M, Tran A, TRebeden H, Jaffray P, Malassagne B, Calmus Y, Weill B, Batteux F. Detoxification of reactive oxygen species by a nonpeptidyl mimic of superoxide dismutase cures acetaminophen-induced acute liver failure in the mouse. Hepatology. 2001;33(5):1173-80.

185. Chastre A, Bélanger M, Beauchesne E, Nguyen BN, Desjardins P, Butterworth RF. Inflammatory cascades driven by tumor necrosis factor-alpha play a major role in the progression of acute liver failure and its neurological complications. PloS one. 2012;7(11):e49670.

186. Eash KJ, Means JM, White DW, Link DC. CXCR4 is a key regulator of neutrophil release from the bone marrow under basal and stress granulopoiesis conditions. Blood. 2009;113(19):4711-9.

187. Eash KJ, Greenbaum AM, Gopalan PK, Link DC. CXCR2 and CXCR4 antagonistically regulate neutrophil trafficking from murine bone marrow. J Clin Invest. 2010;120(7):2423-31.

188. Blei AT, Olafsson S, Therrien G, Butterworth RF. Ammonia-induced brain edema and intracranial hypertension in rats after portacaval anastomosis. Hepatology. 1994;19.

189. Baquet A, Hue L, Meijer AJ, van Woerkom GM, Plomp P. Swelling of rat hepatocytes stimulates glycogen synthesis. Journal of Biological Chemistry. 1990;265(2):955-9.

190. Häussinger D, Schliess F, Dombrowski F, Vom Dahl S. Involvement of p38MAPK in the regulation of proteolysis by liver cell hydration. Gastroenterology. 1999;116(4):921-35.

191. Rama Rao KV, Jayakumar AR, Tong X, Alvarez VM, Norenberg MD. Marked potentiation of cell swelling by cytokines in ammonia-sensitized cultured astrocytes. Journal of Neuroinflammation. 2010;7(1):1-8.

192. Kendrick SF, O'Boyle G, Mann J, Zeybel M, Palmer J, Jones DE, Day CP. Acetate, the key modulator of inflammatory responses in acute alcoholic hepatitis. Hepatology. 2010;51(6):1988-97.

193. Lin F, Taylor NJ, Su H, Huang X, Hussain MJ, Abeles RD, Blackmore L, Zhou Y, Ikbal MM, Heaton N, Jassem W, Shawcross DL, Vergani D, Ma Y. Alcohol dehydrogenase-specific T-cell responses are associated with alcohol consumption in patients with alcohol-related cirrhosis. Hepatology. 2013;58(1):314-24.

194. Blackmore LJ, Ryan JM, Huang X, Hussain M, Triantafyllou E, Vergis N, Vijay GM, Antoniades CG, Thursz MR, Jassem W, Vergani D, Shawcross DL, Ma Y. Acute alcoholic hepatitis and cellular Th1 immune responses to alcohol dehydrogenase. Lancet. 2015;385 Suppl 1:S22.

195. Yuksel M, Wang Y, Tai N, Peng J, Guo J, Beland K, Lapierre P, David C, Alvarez F, Colle I, Yan H, Mieli-Vergani G, Vergani D, Ma Y, Wen L. A novel "humanized mouse" model for autoimmune hepatitis and the association of gut microbiota with liver inflammation. Hepatology. 2015;62(5):1536-50.

196. ISHIDA Y, KONDO T, OHSHIMA T, FUJIWARA H, IWAKURA Y, MUKAIDA N. A pivotal involvement of IFN-γ in the pathogenesis of acetaminophen-induced acute liver injury. The FASEB Journal. 2002;16(10):1227-36.

197. Blazka ME, Wilmer JL, Holladay SD, Wilson RE, Luster MI. Role of Proinflammatory Cytokines in Acetaminophen Hepatotoxicity. Toxicology and Applied Pharmacology. 1995;133(1):43-52.

198. Blazka ME, Elwell MR, Holladay SD, Wilson RE, Luster MI. Histopathology of Acetaminophen-Induced Liver Changes: Role of Interleukin 1α and Tumor Necrosis Factor α. Toxicologic Pathology. 1996;24(2):181-9.

199. Liu Z-X, Govindarajan S, Kaplowitz N. Innate immune system plays a critical role in determining the progression and severity of acetaminophen hepatotoxicity. Gastroenterology. 2004;127(6):1760-74.

200. Laskin DL, Gardner CR, Price VF, Jollow DJ. Modulation of macrophage functioning abrogates the acute hepatotoxicity of acetaminophen. Hepatology. 1995;21(4):1045-50.

201. Dambach DM, Watson LM, Gray KR, Durham SK, Laskin DL. Role of CCR2 in macrophage migration into the liver during acetaminophen-induced hepatotoxicity in the mouse. Hepatology. 2002;35(5):1093-103.

202. Bafica A, Scanga CA, Feng CG, Leifer C, Cheever A, Sher A. TLR9 regulates Th1 responses and cooperates with TLR2 in mediating optimal resistance to Mycobacterium tuberculosis. The Journal of experimental medicine. 2005;202(12):1715-24.

203. Beutler B. Tlr4: central component of the sole mammalian LPS sensor. Current Opinion in Immunology. 2000;12(1):20-6.

204. Manakkat Vijay GK, Ryan JM, Abeles RD, Ramage S, Patel V, Bernsmeier C, Riva A, McPhail MJ, Tranah TH, Markwick LJ, Taylor NJ, Bernal W, Auzinger G, Willars C, Chokshi S, Wendon JA, Ma Y, Shawcross DL. Neutrophil Toll-Like Receptor 9 Expression and the Systemic Inflammatory Response in Acetaminophen-Induced Acute Liver Failure. Crit Care Med. 2016;44(1):43-53.

205. Newton CA, Perkins I, Widen RH, Friedman H, Klein TW. Role of Toll-Like Receptor 9 in Legionella pneumophila-Induced Interleukin-12 p40 Production in Bone Marrow-Derived Dendritic Cells and Macrophages from Permissive and Nonpermissive Mice. Infection and Immunity. 2007;75(1):146-51.

206. McCarthy CG, Wenceslau CF, Goulopoulou S, Ogbi S, Baban B, Sullivan JC, Matsumoto T, Webb RC. Circulating mitochondrial DNA and Toll-like receptor 9 are associated with vascular dysfunction in spontaneously hypertensive rats. Cardiovascular Research. 2015;107(1):119.

207. Krieg AM, Wu T, Weeratna R, Efler SM, Love-Homan L, Yang L, Yi A-K, Short D, Davis HL. Sequence motifs in adenoviral DNA block immune activation by stimulatory CpG motifs. Proceedings of the National Academy of Sciences. 1998;95(21):12631-6.

208. Barrat FJ, Meeker T, Chan JH, Guiducci C, Coffman RL. Treatment of lupus-prone mice with a dual inhibitor of TLR7 and TLR9 leads to reduction of autoantibody production and amelioration of disease symptoms. European Journal of Immunology. 2007;37(12):3582-6.

209. Gujral JS, Farhood A, Bajt ML, Jaeschke H. Neutrophils aggravate acute liver injury during obstructive cholestasis in bile duct-ligated mice. Hepatology. 2003;38(2):355-63.

210. Liu ZX, Han D, Gunawan B, Kaplowitz N. Neutrophil depletion protects against murine acetaminophen hepatotoxicity. Hepatology. 2006;43(6):1220-30.

211. Garcia-Martinez I, Santoro N, Chen Y, Hoque R, Ouyang X, Caprio S, Shlomchik MJ, Coffman RL, Candia A, Mehal WZ. Hepatocyte mitochondrial DNA drives nonalcoholic steatohepatitis by activation of TLR9. J Clin Invest. 2016;126(3):859-64.

212. Rama Rao KV, Chen M, Simard JM, Norenberg MD. Suppression of ammonia-induced astrocyte swelling by cyclosporin A. J Neurosci Res. 2003;74(6):891-7.

213. Rama Rao KV, Jayakumar AR, Norenberg DM. Ammonia neurotoxicity: role of the mitochondrial permeability transition. Metab Brain Dis. 2003;18(2):113-27.

214. Alvarez VM, Rama Rao KV, Brahmbhatt M, Norenberg MD. Interaction between cytokines and ammonia in the mitochondrial permeability transition in cultured astrocytes. Journal of neuroscience research. 2011;89(12):2028-40.

215. Jalan R, Olde Damink SW, Hayes PC, Deutz NE, Lee A. Pathogenesis of intracranial hypertension in acute liver failure: inflammation, ammonia and cerebral blood flow. J Hepatol. 2004;41.

216. Antoine DJ, Jenkins RE, Dear JW, Williams DP, McGill MR, Sharpe MR, Craig DG, Simpson KJ, Jaeschke H, Park BK. Molecular forms of HMGB1 and keratin-18 as mechanistic biomarkers for mode of cell death and prognosis during clinical acetaminophen hepatotoxicity. Journal of Hepatology. 2012;56(5):1070-9.

217. Wang X, Sun R, Wei H, Tian Z. High-mobility group box 1 (HMGB1)-toll-like receptor (TLR) 4-interleukin (IL)-23-IL-17A axis in drug-induced damage-associated lethal hepatitis: Interaction of γδ T cells with macrophages. Hepatology. 2013;57(1):373-84.

218. Gazzard BG, Hughes RD, Mellon PJ, Portmann B, Williams R. A dog model of fulminant hepatic failure produced by paracetamol administration. British Journal of Experimental Pathology. 1975;56(5):408-11.

219. Ward NS, Casserly B, Ayala A. The Compensatory Anti-inflammatory Response Syndrome (CARS) in Critically Ill Patients. Clinics in Chest Medicine. 2008;29(4):617-25.

220. Berry PA, Antoniades CG, Hussain MJ, McPhail MJW, Bernal W, Vergani D, Wendon JA. Admission levels and early changes in serum interleukin-10 are predictive of poor outcome in acute liver failure and decompensated cirrhosis. Liver International. 2010;30(5):733-40.

Appendices

Table – 1: Antibodies used for characterisation of neutrophil phenotype at baseline

Antibody (Fluorochromes)	Clone	Reactivity	Supplier	Concentration	Dilution
CD16 (PE)	3G8	Human	BD Biosciences, UK	100 Tests	1:500
CD11b (APC-Cy7)	ICRF44	Human	BD Biosciences, UK	100 Tests	1:500
CD282 (Alexafluor 488)	11G7	Human	BD Biosciences, UK	100 Tests	1:500
TLR4 (Biotin-conjugated)	HTA125	Human	BD Biosciences, UK	100 Tests	1:500
Streptavidin (PE-Cy7)	--	Human	BD Biosciences, UK	0.2 mg/mL	1:500
TLR9 (APC)	eB72-1665	Human	BD Biosciences, UK	100 Tests	1:500

Table – 2: Antibodies used for characterisation of neutrophil phenotype and IL-8

Antibody (Fluorochromes)	Clone	Reactivity	Supplier	Concentration	Dilution
CD16 (PerCP-Cy5.5)	3G8	Human	BD Biosciences, UK	50 Tests	1:500
CD11b (APC-Cy7)	ICRF44	Human	BD Biosciences, UK	100 Tests	1:500
CD62L (FITC)	DREG-56	Human	BD Biosciences, UK	100 Tests	1:500
TLR9 (APC)	eB72-1665	Human	BD Biosciences, UK	100 Tests	1:500
IL-8 (PE)	G265-8	Human	BD Biosciences, UK	0.2 mg/mL	1:500

Table – 3: Antibodies used for characterisation of neutrophil phenotype in mice

Antibody (Fluorochromes)	Clone	Reactivity	Supplier	Concentration	Dilution
CD11b (PerCP-Cy5.5)	M1/70	Mouse	Biolegend, USA	0.2 mg/mL	1:1000
MPO (Biotin)	--	Mouse	Hycult, USA	0.2 mg/mL	1:1000
Streptavidin (PE)	11-26C.2a	Mouse	Biolegend, USA	0.2 mg/mL	1:1000
Ly6G (APC)	1A8	Mouse	Biolegend, USA	0.2 mg/mL	1:1000

Table – 4: Antibodies used for characterisation of T cells phenotype

Antibody (Fluorochromes)	Clone	Reactivity	Supplier	Concentration	Dilution
CD4 (APC-Cy7)	GK1.5	Mouse	Biolegend, USA	0.2 mg/mL	1:1000
CD8 (PE-Cy7)	53-6.7	Mouse	Biolegend, USA	0.2 mg/mL	1:1000
CD44 (PE)	IM7	Mouse	Biolegend, USA	0.2 mg/mL	1:8000
CD62L (FITC)	MEL-14	Mouse	Biolegend, USA	0.5 mg/mL	1:1000
CD69 (PerCP-Cy5.5)	7E9	Mouse	Biolegend, USA	0.2 mg/mL	1:1000
CD3 (APC)	145-2C11	Mouse	Biolegend, USA	0.2 mg/mL	1:1000

Table – 5: Antibodies used for characterisation of T cells cytokine - 1

Antibody (Fluorochromes)	Clone	Reactivity	Supplier	Concentration	Dilution
CD3 (FITC)	17A2	Mouse	Biolegend, USA	0.5 mg/mL	1:1000
CD4 (APC-Cy7)	GK1.5	Mouse	Biolegend, USA	0.2 mg/mL	1:1000
CD8 (PE-Cy7)	53-6.7	Mouse	Biolegend, USA	0.2 mg/mL	1:1000
TNF-α (APC)	MP6-XT22	Mouse	Biolegend, USA	0.2 mg/mL	1:1000
IFN-γ (PerCP-Cy5.5)	XMG1.2	Mouse	Biolegend, USA	0.2 mg/mL	1:1000
IL-6 (PE)	MP5-20F3	Mouse	Biolegend, USA	0.2 mg/mL	1:1000

Table – 6: Antibodies used for characterisation of T cells cytokine - 2

Antibody (Fluorochromes)	Clone	Reactivity	Supplier	Concentration	Dilution
CD3 (FITC)	17A2	Mouse	Biolegend, USA	0.5 mg/mL	1:1000
CD4 (APC-Cy7)	GK1.5	Mouse	Biolegend, USA	0.2 mg/mL	1:1000
CD8 (PE-Cy7)	53-6.7	Mouse	Biolegend, USA	0.2 mg/mL	1:1000
IL-17A (PerCP-Cy5.5)	TC11-18H10.1	Mouse	Biolegend, USA	0.2 mg/mL	1:1000

Table – 7: Antibodies used for characterisation of NK cell phenotype

Antibody (Fluorochromes)	Clone	Reactivity	Supplier	Concentration	Dilution
CD122 (PE)	TM-b1	Mouse	ebioscience, USA	0.2 mg/mL	1:1000
DX-5 (FITC)	DX-5	Mouse	Biolegend, USA	0.5 mg/mL	1:1000
KLRG-1(APC)	2F2/KLRG-1	Mouse	Biolegend, USA	0.2 mg/mL	1:1000
NKG2D (PE-Cy7)	CX5	Mouse	ebioscience, USA	0.2 mg/mL	1:1000

Table – 8: Antibodies used for characterisation of NK-cells cytokine

Antibody (Fluorochromes)	Clone	Reactivity	Supplier	Concentration	Dilution
CD122 (PE)	TM-b1	Mouse	ebioscience, USA	0.2 mg/mL	1:1000
DX-5 (FITC)	DX-5	Mouse	Biolegend, USA	0.5 mg/mL	1:1000
KLRG-1 (APC)	2F2/KLRG-1	Mouse	Biolegend, USA	0.2 mg/mL	1:1000
IFN-γ (PerCP-Cy5.5)	XMG1.2	Mouse	Biolegend, USA	0.2 mg/mL	1:1000

Table – 9: Antibodies used for characterisation of NK cells cytokine

Antibody (Fluorochromes)	Clone	Reactivity	Supplier	Concentration	Dilution
CD122 (PE)	TM-b1	Mouse	ebioscience, USA	0.2 mg/mL	1:1000
DX-5 (FITC)	DX-5	Mouse	Biolegend, USA	0.5 mg/mL	1:1000
KLRG-1 (APC)	2F2/KLRG-1	Mouse	Biolegend, USA	0.2 mg/mL	1:1000
TNF-α (PerCP-Cy5.5)	MP6-XT22	Mouse	Biolegend, USA	0.2 mg/mL	1:1000

Table – 10: Antibodies used for characterisation of Macrophages cytokine

Antibody (Fluorochromes)	Clone	Reactivity	Supplier	Concentration	Dilution
F4/80 (FITC)	BM8	Mouse	Biolegend, USA	0.2 mg/mL	1:1000
CD11b (PE-Cy7)	M1/70	Mouse	Biolegend, USA	0.2 mg/mL	1:1000
TNF-α (APC)	MP6-XT22	Mouse	Biolegend, USA	0.2 mg/mL	1:1000
IFN-γ (PerCP-Cy5.5)	XMG1.2	Mouse	Biolegend, USA	0.2 mg/mL	1:1000
IL-6 (PE)	MP5-20F3	Mouse	Biolegend, USA	0.2 mg/mL	1:1000

Table –11: Preparation of in-house reagents

Reagent Name	Contents
Ammonium acetate solution (1M)	Dissolved 0.77 gm of ammonium acetate in 10 mL of de-ionised water
Anaesthesia solution	Mixed 1 part of iso-fluorane with 3 parts of 1, 2 – Propanediol
Complete media	Freshly prepared by adding Foetal bovine serum (FBS) [10%] and antibiotics [1%] in RPMI 1640 and stored in 4°C
Cytofix solution	Dissolved 5 g of p-formaldehyde in 100 mL of de-ionised water
Phosphate Buffered Saline (PBS) (1x)	Dissolved five PBS tablets in one litre of de-ionised water
Phosphate Buffered Saline (PBS) (10x)	Dissolved five PBS tablets in 100 mL of de-ionised water
30% Polymorphprep™ solution	Mixed 3 parts of Polymorphprep™ solution with 7 parts of RPMI 1640
70% Polymorphprep™ solution	Mixed 7 parts of Polymorphprep™ solution was mixed with 3 parts of 10x PBS
Digestion solution for liver	Dissolved collagenase-IV [0.05%] and DNAse-I [0.005%] in 10 mL of RPMI

Acknowledgements

It would have been impossible for me to write this thesis and complete my PhD, without the guidance and encouragement of a large number of people who I would like to thank sincerely. Firstly I thank God for enabling me to do a PhD and complete this work successfully. For without His grace it would have been impossible for me to start and complete this work.

I would like to thank my supervisor Dr Debbie Shawcross who during her PhD at UCL, laid down the foundation stones on which I've based much of my studies and consequently this thesis. In fact it is the common interest on 'Ammonia and Neutrophils' that led me to do my research under her. Since the first day I began working for her at the King's College Hospital in 2011, she has continuously supported me in my research and has been a constant source of ideas and laboratory-based technical help. She has been brilliant in giving comments and suggestions, as well as proof-reading this thesis several times over.

I would also like thank Dr Yun Ma who has been unfailing in her support as a second supervisor, have been constant source of ideas and laboratory-based technical help. Apart from being a second supervisor she has been instrumental in the collaboration with Dr Li Wen, Yale School of Medicine for the animal studies. I thank her for facilitating this collaboration.

I also thank my third supervisor Dr Li Wen, School of Medicine, Yale University for kindly inviting me to perform the animal studies in her laboratory and giving me the opportunity to work in a great atmosphere at a world class institution. Whilst she has

diabetes background she has been very constructive during my stint at Yale by having frequent meetings with me and being very critical on my animal study.

I also thank Dr Wajahat Z Mehal, faculty in the liver unit at Yale University for being very supportive and guiding me at various stages of the animal study. It is his publications on paracetamol and TLR9 that motivated me to specialise in this area of research. He also kindly provided me with the special $TLR9^{fl/fl}$ LysCre mice type that was required for my research and gave me the insights for using that model. I also thank Irma Garcia, Yonglin Li and Rafaz Hoque, members in Dr Mehal's lab, who gave various inputs during my stay at Yale.

I thank Changyun Hu and Muhamed Yuksel, Dr Li Wen's lab for teaching me the basics of handling the animals. I thank Lucy Zhang for teaching me the important techniques in handling the animals and for her help in the animal house in taking special care of the animals required for my study. I also thank my other colleagues Jian Peng, Youjia Hu, Ningwen Tai, Jake Carrion and Michael Carrion at Yale University without whom it would have been impossible to complete the animal studies.

I thank Dr Daniel Abeles, Institute of Liver Studies, KCL, for teaching me the basics of flow cytometry and helping me with the recruitment of patients. I also thank Antonio Riva and Shilpa Chokshi, Foundation for Liver Research, London UK for helping me with the cytometric bead array experiments.

I thank the clinicians, Jennifer Ryan, Laura Blackmore, Vishal Patel and Christine Bernsmeier who helped me in recruiting the patients and collecting the samples required for my study. I also thank the clinicians, Thomas Tranah and Stephen Ramage who helped me with the data collection. I also thank the liver intensive care unit

consultants Drs William Bernal, Georg Auzinger, Christopher Willars and Julia Wendon who were in charge of the unit and helped me approach the patients and gave me all the required information about the patients recruited for my study. I also thank the patients and their family for their co-operation in this study.

I would also like to mention Mrs Rejina Mariam Vergis, The Royal Hospitals, Belfast, Northern Ireland and Dr Mark McPhail, Imperial College London for their help on statistical analysis.

Most importantly I thank King's College London for providing me with the international scholarship King's International Graduate Scholarship, King's Alumni bursary and King's Continuation scholarship during my PhD. It would have been impossible for me to pursue this research without this scholarship as it paid my tuition fees and living expenses here and in USA. I also sincerely thank King's College Hospital charity for awarding me a research grant worth £10,000 to pursue my research here at King's College Hospital and Yale University, USA.

Lastly and most importantly I'd like to thank my family and friends without whom I could not have done this research. Words cannot express how grateful I am to my mom and my wife, Princey, who have never stopped believing in me and encouraged me always and managed the household chores and cooking throughout the last eight months.

Publications related to this work

1. **Manakkat Vijay GK,** Ryan J, Abeles RD et al., *Neutrophil toll-like receptor 9 expression and the systemic inflammatory response in acetaminophen-induced acute liver failure.* **Critical Care Medicine**, 2016. **44** (1): p. 43-53.

2. **Manakkat Vijay GK**, Kronsten et al., *Neutrophil vacuolation in acetaminophen-induced acute liver failure.* **American Journal of Hematology**, 2015. **90** (5) p.461.